

# **TOWARDS A CLINICALLY PRACTICAL BRAIN-COMPUTER INTERFACE**

By

Gerwin Schalk

A Thesis Submitted to the Graduate

Faculty of Rensselaer Polytechnic Institute

in Partial Fulfillment of the

Requirements for the Degree of

**DOCTOR OF PHILOSOPHY**

Major Subject: Computer and Systems Engineering

Approved by the  
Examining Committee:

---

Lester A. Gerhardt, PhD, Thesis Adviser

---

Selmer Bringsjord, PhD, Member

---

Shivkumar Kalyanaraman, PhD, Member

---

Badrinath Roysam, DSc, Member

Rensselaer Polytechnic Institute  
Troy, New York

December 2006  
(For Graduation December 2006)

**TOWARDS A CLINICALLY PRACTICAL  
BRAIN-COMPUTER INTERFACE**

By

Gerwin Schalk

An Abstract of a Thesis Submitted to the Graduate

Faculty of Rensselaer Polytechnic Institute

in Partial Fulfillment of the

Requirements for the Degree of

**DOCTOR OF PHILOSOPHY**

Major Subject: Computer and Systems Engineering

The original of the complete thesis is on file  
in the Rensselaer Polytechnic Institute Library

Examining Committee:

Lester A. Gerhardt, PhD, Thesis Adviser

Selmer Bringsjord, PhD, Member

Shivkumar Kalyanaraman, PhD, Member

Badrinath Roysam, DSc, Member

Rensselaer Polytechnic Institute  
Troy, New York

December 2006  
(For Graduation December 2006)

© Copyright 2006  
by  
Gerwin Schalk  
All Rights Reserved

# CONTENTS

LIST OF TABLES . . . . .	viii
LIST OF FIGURES . . . . .	ix
ACKNOWLEDGMENT . . . . .	xiii
ABSTRACT . . . . .	xiv
1. BACKGROUND . . . . .	1
1.1 Communication Options For The Paralyzed . . . . .	1
1.2 Brain-Computer Interfaces (BCIs) . . . . .	3
1.3 Recent Interest in BCI Systems . . . . .	6
1.4 Sensorimotor Cortex Rhythms . . . . .	8
1.5 The Wadsworth BCI System . . . . .	9
1.6 BCI2000: A General-Purpose BCI System . . . . .	11
1.7 Relevant Issues of BCI Technology . . . . .	14
1.8 The Three Themes in this Dissertation . . . . .	16
1.9 Overview of Contributions . . . . .	17
2. THEME I: BETTER SIGNALS . . . . .	20
2.1 Summary of Contributions and Approach . . . . .	20
2.2 Introduction . . . . .	21
2.3 Electrocorticography (ECoG) . . . . .	25
2.4 Aim 1: Real-Time Access to ECoG Signals . . . . .	28
2.4.1 Site 1: St. Louis . . . . .	28
2.4.2 Site 2: Seattle . . . . .	30
2.4.3 Recording from Patients . . . . .	32
2.5 Aim 2: Analysis and Visualization Techniques . . . . .	34
2.5.1 Frequency Analysis . . . . .	34
2.5.2 Statistical Evaluation . . . . .	35
2.5.3 Visualization of ECoG Signals . . . . .	36
2.6 Aim 3: Use of ECoG Signals for Real-Time BCI Control . . . . .	42
2.6.1 Introduction . . . . .	43

2.6.2	Methods . . . . .	44
2.6.2.1	Subjects and Experimental Paradigms . . . . .	44
2.6.2.2	Data Collection . . . . .	45
2.6.2.3	Identification of ECoG Features to be Used for On-line Cursor Control . . . . .	45
2.6.2.4	ECoG Control of Vertical Cursor Movement Online . . . . .	47
2.6.2.5	Anatomical and Functional Mapping . . . . .	49
2.6.3	Results: ECoG Control of 1D Cursor Movements . . . . .	50
2.6.4	Discussion . . . . .	52
2.7	Conclusions . . . . .	53
2.8	Recommendations . . . . .	55
3.	THEME II: BETTER SIGNAL PROCESSING . . . . .	57
3.1	Summary of Contributions and Approach . . . . .	57
3.2	Introduction . . . . .	58
3.2.1	The Signal Identification Problem . . . . .	59
3.2.2	Relevant Signal Processing Issues . . . . .	62
3.2.3	A Novel Approach to BCI Signal Processing . . . . .	63
3.3	Overview of Traditional BCI Signal Processing . . . . .	64
3.3.1	Feature Extraction . . . . .	65
3.3.2	Translation Algorithm . . . . .	71
3.4	Feature Translation Using a Detection Approach . . . . .	73
3.4.1	Overview . . . . .	73
3.4.2	Gaussian Mixture Models . . . . .	74
3.4.3	Parameterization of Gaussian Mixture Models . . . . .	79
3.4.4	Algorithmic Improvements . . . . .	80
3.4.4.1	Automatic Model Selection . . . . .	81
3.4.4.2	Robustness . . . . .	84
3.4.4.3	Model Adaptation . . . . .	85
3.4.5	Using Signal Detection for BCI Signal Translation . . . . .	86
3.5	Method Validation . . . . .	87
3.5.1	Summary . . . . .	87
3.5.2	Methods . . . . .	88
3.5.2.1	Dataset . . . . .	88
3.5.2.2	The Present Analyses . . . . .	88

3.5.2.3	Feature Extraction and Selection . . . . .	89
3.5.2.4	Performance Metric . . . . .	90
3.5.3	Results . . . . .	91
3.5.3.1	Effect of Parameters on Classification Performance .	91
3.5.3.2	Comparing Signal Detection to Linear Regression .	95
3.5.3.3	Characteristics of BCI Control Signals . . . . .	96
3.6	Discussion and Interpretation . . . . .	98
3.7	Other Important Applications of Signal Detection . . . . .	102
3.7.1	Introduction . . . . .	102
3.7.2	Methods . . . . .	104
3.7.2.1	Subjects . . . . .	104
3.7.2.2	Data Collection . . . . .	104
3.7.3	Results . . . . .	105
3.7.3.1	Example 1: Real-Time Visualization . . . . .	105
3.7.3.2	Example 2: Localization of Face Motor/Language Function . . . . .	106
3.7.3.3	Example 3: Localization of Motor Function . . . . .	108
3.8	Conclusions . . . . .	109
4.	<b>THEME III: MORE INTUITIVE TASKS</b> . . . . .	111
4.1	Summary of Contributions and Approach . . . . .	111
4.2	Introduction . . . . .	113
4.3	Decoding Discrete 2D Joystick Movements . . . . .	116
4.3.1	Data Collection and Analysis . . . . .	116
4.3.2	Results . . . . .	118
4.3.3	Discussion and Interpretation . . . . .	121
4.4	Decoding Real-Time Continuous 2D Joystick Movements . . . . .	123
4.4.1	Methods: Data Acquisition and Result Presentation . . . . .	123
4.4.1.1	Subjects . . . . .	123
4.4.1.2	Experimental Paradigm . . . . .	124
4.4.1.3	Data Collection . . . . .	126
4.4.1.4	3D Cortical Mapping . . . . .	128
4.4.2	Methods: Signal Processing . . . . .	128
4.4.2.1	The Decoding Problem . . . . .	128
4.4.2.2	Signal Pre-Processing . . . . .	129
4.4.2.3	Feature Extraction . . . . .	131

4.4.2.4	Feature Processing . . . . .	132
4.4.2.5	Feature Selection . . . . .	134
4.4.2.6	Decoding . . . . .	134
4.4.2.7	Definition of Kinematic Parameters . . . . .	136
4.4.2.8	Evaluation . . . . .	137
4.4.3	Results: Decoding Procedure . . . . .	138
4.4.3.1	Selection of Datasets and Kinematic Parameters . . . . .	138
4.4.3.2	Spatial Filtering . . . . .	140
4.4.3.3	Feature Transformation . . . . .	140
4.4.3.4	Feature Smoothing . . . . .	141
4.4.3.5	Optimal Filtering . . . . .	142
4.4.3.6	Feature Whitening . . . . .	143
4.4.3.7	Parametric/Nonparametric Methods . . . . .	144
4.4.3.8	Conclusions: Decoding Procedure . . . . .	144
4.4.3.9	Additional Evaluations . . . . .	146
4.4.4	Results: Neuroscience . . . . .	149
4.4.4.1	Relative Importance of Different Features . . . . .	149
4.4.4.2	Significance of the LMP Component . . . . .	155
4.4.4.3	Topography of Locations Implicated in the Decoding	155
4.4.4.4	Decoding Cursor and Target Kinematics . . . . .	156
4.4.4.5	Decoded Movement Trajectories . . . . .	156
4.4.4.6	Directional Tuning . . . . .	161
4.4.4.7	Tracking vs. Decoding Performance . . . . .	165
4.4.5	Summary of Results . . . . .	165
4.4.5.1	Accurate Decoding of Movement Parameters . . . . .	165
4.4.5.2	The Local Motor Potential (LMP) . . . . .	167
4.4.5.3	Anatomical Relevance of Sites Involved in Predictions	170
4.4.5.4	Directional Tuning . . . . .	172
4.4.6	Discussion and Interpretation . . . . .	172
4.5	Conclusions . . . . .	179
5.	INTEGRATION . . . . .	180
5.1	Use of Signal Detection With Other Brain Signals . . . . .	180
5.2	P300-Based BCIs Using ECoG . . . . .	182
5.3	Decoding Hand Movements Using Signal Detection . . . . .	183

6. CONCLUSIONS AND RECOMMENDATIONS . . . . .	185
6.1 Conclusions . . . . .	185
6.2 Recommendations . . . . .	186
6.2.1 Real-Time Experiments Using Signal Detection . . . . .	187
6.2.2 Decoding of Hand Movements: Further Studies . . . . .	188
6.2.3 ECoG for BCI Purposes: Recommendations . . . . .	188
6.3 Potential Impact of Brain-Computer Interface Technologies . . . . .	193
6.3.1 Introduction . . . . .	193
6.3.1.1 The Communication Problem . . . . .	193
6.3.1.2 Feasibility . . . . .	197
6.3.2 Expected Development . . . . .	201
6.3.2.1 Towards the Limit . . . . .	201
6.3.2.2 Expected Performance and Price Development . . . . .	202
6.3.2.3 Expected Adoption and Impact . . . . .	205
6.3.3 Brain-Computer Symbiosis . . . . .	207
APPENDICES	
A. NOTATION . . . . .	239

## LIST OF TABLES

2.1	Clinical profiles . . . . .	45
2.2	Details of ECoG control of cursor movement . . . . .	52
3.1	Statistic moments for control signals derived using signal detection . . .	101
4.1	Performance of decoding average 2D hand movement velocity . . . . .	121
4.2	List of joystick datasets collected from 10 patients . . . . .	127
4.3	Clinical profiles of Seattle patients . . . . .	166
4.4	Summary of performance decoding 2D continuous movement parameters	168
4.5	Comparison of the present joystick movement decoding results to results achieved previously using intracortical microelectrodes . . . . .	168

## LIST OF FIGURES

1.1	Communication options for the paralyzed . . . . .	2
1.2	Basic design and operation of any BCI system . . . . .	4
1.3	Examples of mu/beta rhythm signals . . . . .	9
1.4	BCI2000 system design . . . . .	12
2.1	Overview of <b>THEME I</b> . . . . .	21
2.2	Compatibility of current BCI signal acquisition methods with requirements of clinical BCI systems . . . . .	24
2.3	Three possible sensor locations for BCI devices . . . . .	26
2.4	Sample ECoG electrode placement . . . . .	27
2.5	St. Louis Architecture . . . . .	30
2.6	St. Louis BCI System . . . . .	31
2.7	Seattle Architecture . . . . .	32
2.8	Example of 2D topographical mapping . . . . .	37
2.9	3D brain template . . . . .	38
2.10	Flow chart of the visualization procedure . . . . .	39
2.11	Projection and activation procedure . . . . .	40
2.12	Example of ECoG signals during a task and rest . . . . .	46
2.13	Analysis comparing right hand movement and rest . . . . .	48
2.14	One-dimensional BCI task . . . . .	50
2.15	Electrode locations activation using passive and active mapping . . . . .	51
2.16	ECoG control of vertical cursor movement . . . . .	53
2.17	Learning curves for ECoG control of vertical cursor movement . . . . .	54
2.18	Recommendations resulting from <b>THEME I</b> of this dissertation . . . . .	56
3.1	Overview of <b>THEME II</b> . . . . .	58

3.2	Signal processing in BCI2000 . . . . .	65
3.3	Example of locations involved in different spatial filters . . . . .	67
3.4	Electrode designations . . . . .	68
3.5	Example of application of a Common Average Reference spatial filter .	69
3.6	Example analyses of the temporal filter . . . . .	71
3.7	Example of a classification approach . . . . .	74
3.8	Contribution of the proposed new signal processing procedure . . . . .	75
3.9	Example of signal detection . . . . .	75
3.10	Classification vs. detection approach . . . . .	77
3.11	Gaussian Mixture Model (GMM) . . . . .	78
3.12	Illustration of clustering with automated model selection . . . . .	83
3.13	Effect of feature transformation . . . . .	92
3.14	Effect of full/diagonal covariance matrices . . . . .	93
3.15	Effect of AIC/BIC penalty scores . . . . .	94
3.16	Effect of the number of seed clusters . . . . .	95
3.17	Effect of training time and the number of features . . . . .	96
3.18	Comparison of the detection approach to linear regression . . . . .	97
3.19	Distribution of trial averages of control signal values derived using signal detection . . . . .	99
3.20	Averages and standard deviations of control signal values derived using signal detection . . . . .	100
3.21	Real-time visualization of brain function . . . . .	107
3.22	Language and face motor mapping without electrical stimulation . . . . .	108
3.23	Motor mapping without electrical stimulation . . . . .	110
4.1	Overview of THEME III . . . . .	112
4.2	Design of the 2D center-out task . . . . .	117
4.3	ECoG correlations with direction of discrete movements . . . . .	119

4.4	Electrode locations in the five Seattle patients . . . . .	124
4.5	Electrode numbering in the five Seattle patients . . . . .	124
4.6	The tracking task and its parameters. . . . .	125
4.7	Overview of the decoding procedure . . . . .	130
4.8	Effect of spatial filtering . . . . .	141
4.9	Effect of feature transformations . . . . .	141
4.10	Effect of feature smoothing . . . . .	142
4.11	Effect of optimal filtering . . . . .	143
4.12	Influence of feature whitening . . . . .	143
4.13	Comparison of linear and kNN methods . . . . .	144
4.14	Overview of the final decoding procedure . . . . .	145
4.15	Effect of the number of cross-validation folds . . . . .	146
4.16	Effect of feature offset . . . . .	147
4.17	Effect of smoothing pre/postprocessing . . . . .	148
4.18	Effect of data randomization . . . . .	149
4.19	Relative feature importance for predicting horizontal cursor position . .	151
4.20	Relative feature importance for predicting vertical cursor position . .	152
4.21	Relative feature importance for predicting horizontal cursor velocity . .	153
4.22	Relative feature importance for predicting vertical cursor velocity . . .	154
4.23	Significance of the LMP component . . . . .	155
4.24	Electrode locations holding information in the LMP about movement parameters . . . . .	157
4.25	Decoding kinematics of the user's cursor and target . . . . .	157
4.26	Actual and decoded trajectories for subject A (joystick) . . . . .	158
4.27	Actual and decoded trajectories for subject A (mouse) . . . . .	159
4.28	Actual and decoded trajectories for subject B . . . . .	159
4.29	Actual and decoded trajectories for subject C . . . . .	160

4.30	Actual and decoded trajectories for subject D . . . . .	160
4.31	Directional tuning results for subject A . . . . .	162
4.32	Directional tuning results for subject B . . . . .	162
4.33	Directional tuning results for subject C . . . . .	163
4.34	Directional tuning results for subject D . . . . .	163
4.35	Directional tuning results for subject A (mouse dataset) . . . . .	164
4.36	Tracking performance vs. decoding performance . . . . .	166
4.37	Example of actual and predicted movement trajectories . . . . .	169
4.38	Example of the relative importance of different frequency bands . . . . .	170
4.39	Electrode locations holding information about movement parameters . .	171
4.40	LMP Tuning Curves . . . . .	173
4.41	LMP in other subjects and tasks . . . . .	175
5.1	A P300-based spelling application . . . . .	181
5.2	The use of P300 potentials in the EEG for spelling . . . . .	182
5.3	P300 potentials can also be detected in the electrocorticogram . . . . .	184
6.1	Initial test using SIGFRIED in real time . . . . .	187
6.2	Potential role of ECoG in BCI and neuroscience research . . . . .	192
6.3	The systems problem . . . . .	194
6.4	Comparison of communication rates between humans and the external world . . . . .	197
6.5	The communication problem solved . . . . .	200
6.6	Expected performance/price development and associated technology diffusion . . . . .	203
6.7	Increasing research activity in Brain-Computer Interface (BCI) research	204

## **ACKNOWLEDGMENT**

I would like to thank Dr. Lester Gerhardt for all mentoring, support, and patience throughout the work for this dissertation. I would also like to thank the members of my doctoral committee, Drs. Selmer Bringsjord, Shiv Kalyanaraman, and Badri-nath Roysam, for their suggestions and support; as well as Dr. Greg Hughes for his support and the numerous enlightening conversations. In addition, I feel tremen-dous gratitude towards my colleagues at the Wadsworth Center, in particular to Dr. Jonathan Wolpaw for his tenacious efforts to teach me scientific writing and the differences between science and engineering. Furthermore, the work in this thesis would have been impossible without the support of my collaborators at other insti-tutions, most notably Dr. Eric Leuthardt, Dr. Dan Moran, and Dr. Jeff Ojemann, as well as Kai Miller, Nick Anderson, Peter Brunner, and Jan Kubanek. My pro-fessional successes would have been impossible without the lasting support from my parents and without the many conversations with my friends at the Graz Giants, in particular Paul Kujawa and Bill Christensen, who showed me the value of hard work in a competitive environment. Finally, I thank my wife for putting up with me.

## ABSTRACT

Nearly two million people in the United States have degenerative diseases that impair the neural pathways that control muscles. The most severely affected people lose all voluntary muscle control and become completely "locked in" to their bodies, unable to communicate in any way. Brain-computer interfaces (BCIs) can allow these individuals to communicate again by creating a new communication channel directly from the brain to an output device. Recent studies have shown that BCI technology can allow paralyzed people to share their intent with others, and thereby demonstrate that direct communication from the brain to the external world is possible and that it might serve useful functions.

While these technical demonstrations are encouraging, practical applications of BCI technology to the needs of people with severe disabilities are significantly impeded primarily by three issues. These are the limitations of current sensor technologies, the requirements implied by traditional signal processing approaches, and the non-intuitive tasks that have been used for BCI communication. Mainly due to these three issues have current BCI systems produced impressive laboratory demonstrations but no device of appreciable clinical value.

This dissertation set out to address these problems to work towards a BCI system that can leave the confines of laboratory research to address the actual communication and control needs of the severely paralyzed. The principal results demonstrate that the use of sensors placed on the surface of the brain has favorable characteristics compared to existing non-invasive and highly invasive sensors, that application of a novel signal processing procedure can reduce the substantial expert supervision that is currently required, and disprove the widespread assumption that the use of intuitive tasks requires electrodes that are implanted within the brain.

In summary, the results presented in this dissertation encompass three advances that are critical to the successful translation of brain-computer interface from their current state of primarily laboratory demonstrations into clinically practical communication and control devices for the paralyzed.

# CHAPTER 1

## BACKGROUND

### 1.1 Communication Options For The Paralyzed

Many different disorders can disrupt the channels through which the brain normally communicates with and controls its external environment. Amyotrophic lateral sclerosis, brainstem stroke, brain or spinal cord injury, cerebral palsy, muscular dystrophies, multiple sclerosis, and numerous other degenerative diseases impair the neural pathways that control muscles or impair the muscles themselves. They affect nearly two million people in the United States alone, and far more around the world (Ficke [1991], National Advisory Board on Medical Rehabilitation Research [1992], Carter [1997], Murray and Lopez [1996]). Those most severely affected may lose all voluntary muscle control, including eye movements and respiration, and may become completely locked in to their bodies, unable to communicate in any way. Modern life-support technology can allow most individuals, even those who are locked-in, to live long lives, so that the personal, social, and economic burdens of their disabilities are prolonged and severe. In the absence of methods for repairing the damage done by these disorders, there are three options for restoring function.

The first option is to substitute the disrupted communication pathways and paralyzed muscles with nerves and muscles that remain under voluntary control (Figure 1.1-B). This substitution is often awkward and limited, but can still be useful. Patients largely paralyzed by massive brainstem lesions can often use eye movements detected by a variety of means (Gerhardt and Sabolcik [1996], Grauman et al. [2001]) to answer questions, give simple commands, or even operate a word processing program; and severely dysarthric patients can use hand movements to produce synthetic speech (e.g., Damper et al. [1987], LaCourse and F. C. Hludik [1990], Chen et al. [1999], Kubota et al. [2000]).

The second option is to restore function by detouring around breaks in the neural pathways that control muscles (Figure 1.1-C). In patients with spinal cord injury, electromyographic activity (EMG) from muscles above the level of the lesion

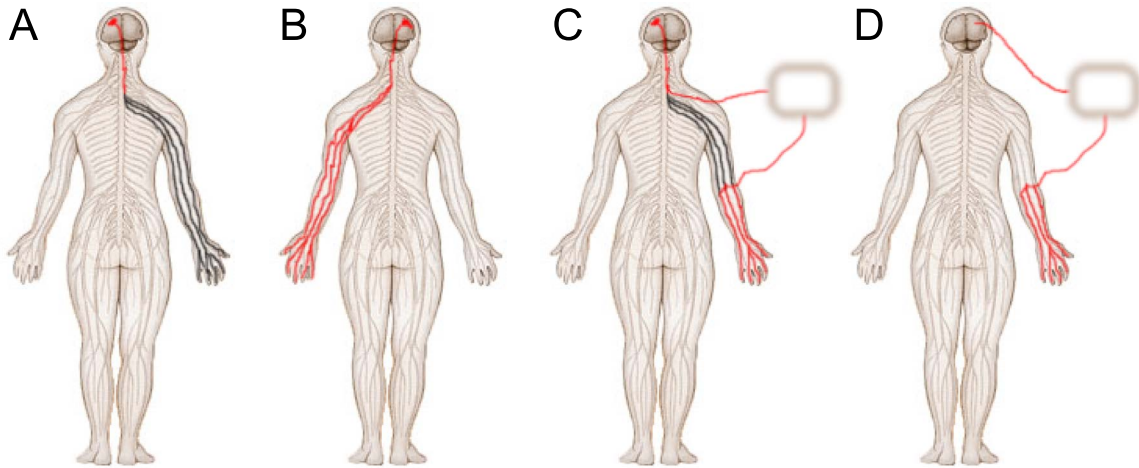


Figure 1.1: Communication options for the paralyzed. A: Normal output communication channels from the brain to the periphery (e.g., the right hand) are disrupted. B: Option 1: Communication by substitution with other options. C: Option 2: Communication by circumventing the impaired pathway. D: Option 3: Adding a new communication channel directly from the brain to an output device or an existing limb – a Brain-Computer Interface (BCI).

can control direct electrical stimulation of paralyzed muscles, and thereby restore useful movement. One current implementation of this functional electrical stimulation (FES) technology is restoring hand function to patients with cervical spinal cord injuries (Hoffer et al. [1996], Kilgore et al. [1997], Ferguson et al. [1999]).

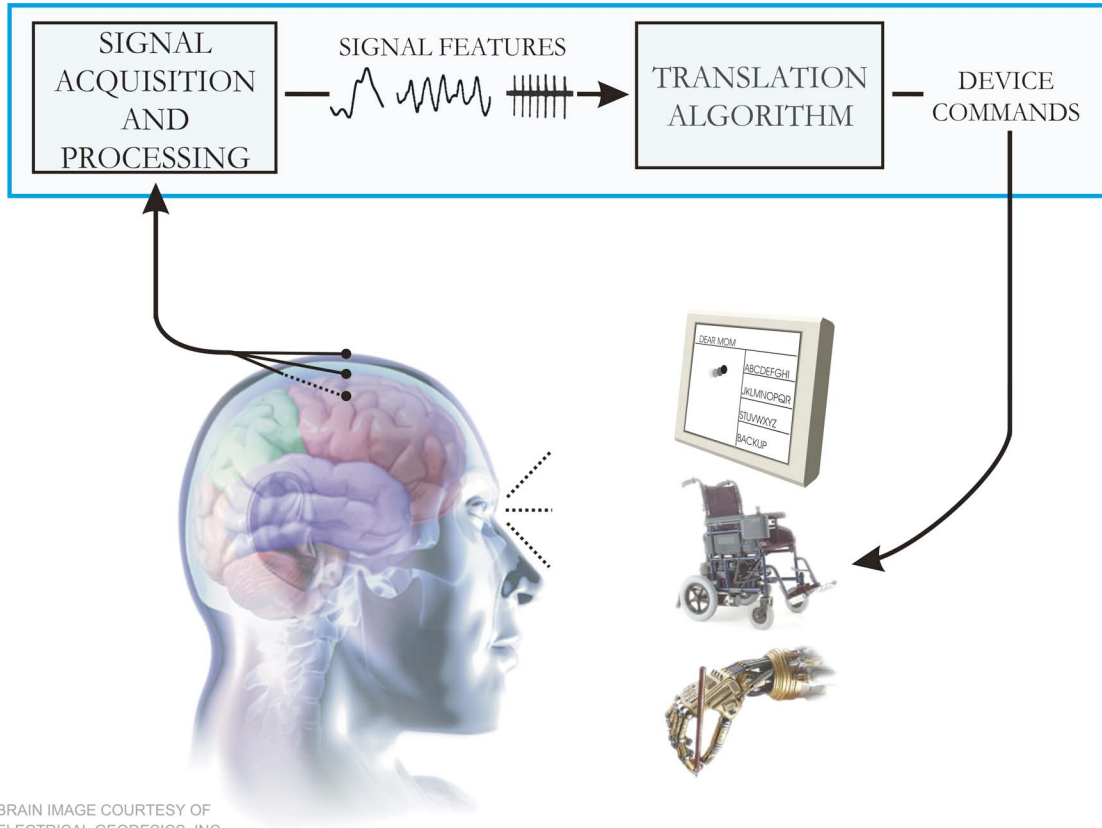
The final option for restoring function to those with motor impairments is to provide the brain with a new, non-muscular communication and control channel, a direct brain-computer interface (BCI) for conveying messages and commands to the external world (Figure 1.1-D). A variety of methods for monitoring brain activity exist, and could in principle provide the basis for a BCI. These include, besides electroencephalography (EEG) and more invasive electrophysiological methods such as electrocorticography (ECoG) and recordings from individual neurons within the brain, magnetoencephalography (MEG), positron emission tomography (PET), functional magnetic resonance imaging (fMRI), and optical imaging (i.e., functional Near InfraRed (fNIR)). However, MEG, PET, fMRI, and fNIR are still technically demanding and expensive. Furthermore, PET, fMRI, and fNIR, which depend on metabolic processes, have long time constants and thus seem to be less amenable to

rapid communication. Non-invasive and invasive electrophysiological methods (i.e., EEG, ECoG, and single-neuron recordings) are the only methods that use relatively simple and inexpensive equipment, have high temporal resolution, and can function in most environments. Thus, they are at present the only methods that can offer the possibility of a new nonmuscular communication and control channel – a practical brain-computer interface.

## 1.2 Brain-Computer Interfaces (BCIs)

A brain-computer interface (BCI) is a communication system in which messages or commands that a person sends to the external world do not depend on the brain's normal output pathways of peripheral nerves and muscles (Wolpaw et al. [2002]). The message is not carried by peripheral nerves and muscles, and, furthermore, activity in these pathways is not needed to generate the activity that does carry the message. A BCI replaces nerves and muscles and the movements they produce with physiological signals from the brain and the hardware and software that translate those signals into actions. Since a BCI system attaches function to what is usually just brain signal noise, it thus creates a new communication channel between the brain and a computer. The *language* of this communication is in part imposed on the brain (by the particular features that the signal processing component of a BCI system extracts from brain signals) and in part negotiated (by the continuous and mutual adaptations of both the user and the system). Like any communication and control system, a BCI has an input (i.e., brain signals from the user), an output (i.e., device commands), components that translate the former into the latter, and an operating protocol that determines the onset, offset, and timing of operation. Any BCI system can thus be described by four components, i.e., signal acquisition, which acquires signals from the brain; signal processing, which extracts signal features from brain signals and translates those into device commands; an output device, which acts upon these device commands and thereby effects the user's intent; and an operating protocol that guides operation (see Figure 1.2). The following paragraphs outline the function and possible realizations of these components.

The first component is signal acquisition. In current BCIs, the input is usually



BRAIN IMAGE COURTESY OF  
ELECTRICAL GEODESICS, INC.

Figure 1.2: Basic design and operation of any BCI system. Signals from the brain can be acquired by electrodes on the scalp, the cortical surface, or from within the cortex, and processed to extract specific signal features (e.g., time- or frequency-domain features) that reflect the user's intent. These features are translated into commands that operate a device (e.g., a simple word processing program, a wheelchair, or a neuroprosthesis).

either field potential activity recorded from the scalp or neuronal activity recorded from within the brain. In the signal acquisition part of BCI operation, this input is acquired by recording electrodes, amplified, and digitized.

The second component is signal processing, which is comprised of two stages: feature extraction and classification (i.e., the *translation algorithm*). In the first stage, the digitized signal is subjected to one or more of a variety of procedures, such as spatial filtering (i.e., application of different referencing methods), voltage amplitude measurements, spectral analyses, or single-neuron separation (e.g., detection of action-potentials of individual neurons using pattern recognition methods). This operation reveals the brain signal features that can be modulated by the user.

The second stage of signal processing is the translation algorithm. It takes these signal features and translates them into device commands – orders that carry out the user’s wishes. This algorithm might use linear methods (e.g., linear classification) or nonlinear methods (e.g., neural networks). Whatever its nature, each algorithm translates device-independent signal features into device control commands. For example, the translation algorithm could be a functional relationship that converts signal amplitudes, measured in  $\mu V$ , into cursor movement, measured in pixels. Effective translation algorithms adjust to each user by adapting to the particular signal features that the user can control, by adapting to spontaneous or permanent changes in those features, and by adapting so as to encourage the brain to learn and thus to improve performance. In sum, BCI operation depends on the effective interaction of two adaptive controllers – the user and the BCI system. This results in probably the most complex and difficult issue in BCI research and development.

The third component is the output device. For present-day BCIs, the output device is usually a computer screen and the output consists of the selection of targets, letters, or icons presented on it (e.g., Farwell and Donchin [1988], Wolpaw et al. [1991], Perelmouter et al. [1999], Pfurtscheller et al. [2000b], Kennedy et al. [2000]). Selection is indicated in various ways (e.g., the letter flashes). Some BCIs also give interim output, such as cursor movement toward the item prior to its selection (e.g., Wolpaw et al. [1991], Pfurtscheller et al. [2000b]). In addition to being the intended product of BCI operation, this output, both interim and final, is the feedback that the brain uses to maintain and improve the accuracy and speed of communication.

The fourth component of any BCI is a protocol that guides its operation. This protocol defines how the system is turned on and off, the sequence and speed of interactions between user and system, what feedback is provided to the user, and whether the user or the system chooses the message to be communicated. The protocols used in research differ in some respects from those likely to be suitable for actual application to the needs of people with disabilities (for further discussion: Wolpaw et al. [2000], Birch and Mason [2000], Kaiser et al. [2001]).

### 1.3 Recent Interest in BCI Systems

In the 70 years since Hans Berger's discovery of the electroencephalogram (Berger [1929]), the EEG or other signals from the brain have been used mainly to evaluate neurological disorders in the clinic and to investigate brain function in the laboratory; and a few studies have explored therapeutic possibilities (e.g., Travis et al. [1975], Kuhlman [1978], Elbert et al. [1980], Rice et al. [1993], Rockstroh et al. [1989], Sterman [2000]). Over this time, people have also theorized that brain signals could have another application, that it might be used to decipher intentions, so that a person could communicate with others or control devices directly by means of brain activity, without using the normal channels of peripheral nerves and muscles. They proposed that signals from the brain could serve as the basis for a brain-computer interface (BCI), a direct, non-muscular channel for communication and control. This idea has appeared often in popular fiction and fantasy (such as the book and subsequent movie "Firefox" in which an airplane is controlled in part by the pilot's EEG (Thomas [1977])). However, BCI systems have attracted little serious scientific attention until recently, for at least three reasons.

First, while signals recorded from the brain reflect brain activity, so that a person's intentions could in theory be detected in them, effective decoding was impeded by the vast number of electrically active neuronal elements, the complicated geometry of the head, and the disconcerting trial-to-trial variability of brain function. Until recently, the possibility of reliably recognizing a single message or command amidst this complexity, distortion, and variability appeared to be extremely remote.

Second, BCI communication requires the capacity to analyze brain signals in detail in real-time, and until recently the requisite technology either did not exist or was extremely expensive.

Third, there was in the past little interest in the very simple and limited communication capacity that a first-generation BCI was likely to offer.

Scientific, technological, and societal events of the past several decades have changed this situation. First, basic and clinical research has produced an impressively detailed and reasonably sophisticated knowledge of particular brain signals and their relationship to normal behavior. For example, numerous studies have

demonstrated correlations between EEG signals and actual or imagined movements and between EEG signals and mental tasks (Keirn and Aunon [1990], Lang et al. [1996], Pfurtscheller and Neuper [1997], Anderson et al. [1998], Altenmueller and Gerloff [1999], McFarland et al. [2000]). Recent studies that recorded signals in monkeys and rats from within the brain also showed highly specific correlations between firing rates of an appropriate selection of cortical neurons and concurrent voluntary movement (e.g., Georgopoulos et al. [1986], Schwartz [1993], Chapin and Nicolelis [1996], Chapin and Nicolelis [1999], Wessberg et al. [2000]). Furthermore, a variety of studies suggested that people might learn to control certain features of the EEG and use them for communication (Wyrwicka and Sterman [1968], Dalton [1969], Black et al. [1970], Nowles and Kamiya [1970], Black [1973], Black [1971], Travis et al. [1975], Kuhlman [1978], Rockstroh et al. [1989]) (reviewed in Niedermeyer [1999]). Invasive studies have shown that monkeys can be trained to modulate the firing rates of single cortical neurons to perform specific tasks (Fetz and Finocchio [1975], Wyler and Burchiel [1978], Wyler et al. [1979], Schmidt [1980]). Thus, present-day researchers are in a much better position to decide which signal features might be used for communication and control, and how they might best be used.

Second, the extremely rapid and continuing development of inexpensive computer hardware and software supports highly sophisticated online analyses of many signal channels at high digitization rates.

Third, greatly increased societal recognition of the needs and potential contributions of people with severe neuromuscular disorders such as spinal cord injury or cerebral palsy has generated clinical, scientific, and commercial interest in better augmentative communication and control technology. Development of such technology is both the principal impetus and the principal justification for current BCI research using non-invasive methods. Invasive recordings using penetrating micro-electrodes are usually done in monkeys. Because of the significant clinical risk and limited long-term stability of these electrodes, these studies typically address basic neuroscience research questions.

## 1.4 Sensorimotor Cortex Rhythms

In awake people, primary sensory or motor cortical areas typically display 8-12 Hz EEG activity when they are not engaged in processing sensory input or producing motor output (Gastault [1952], Kozelka and Pedley [1990], Fisch [1991], reviewed in Niedermeyer [1999]). This idling activity, called mu rhythm when recorded over sensorimotor cortex and visual alpha rhythm when recorded over visual cortex, is thought to be produced by thalamocortical circuits (Niedermeyer [1999]). Unlike the visual alpha rhythm, which is obvious in a large majority of normal people, the mu rhythm was until quite recently thought to occur in only a minority of people (Chatrian [1976]). However, computer-based analyses have shown that the mu rhythm is present in a large majority of adults (Pfurtscheller and Berghold [1989], Pfurtscheller [1999a]). Such analyses have also shown that mu rhythm activity comprises a variety of different 8-12 Hz rhythms, distinguished from each other by precise location, precise frequency, and/or typical relationship to concurrent sensory input or motor output. These mu rhythms are usually associated with 18-26 Hz beta rhythms. While some of these beta rhythms are harmonics of mu rhythms, some are separable by topography and/or timing from mu rhythms, and thus are independent EEG features (Pfurtscheller and Berghold [1989], Pfurtscheller [1999a], McFarland et al. [2000]).

Several factors suggest that mu and/or beta rhythms could be good signal features for BCI-based communication. These rhythms are associated with those cortical areas that are most directly connected to the brain's normal motor output channels. Movement or preparation for movement is typically accompanied by a decrease in mu and beta activity over sensorimotor cortex, particularly contralateral to the movement. This decrease has been labeled "event-related desynchronization" or ERD by Pfurtscheller (reviewed in Pfurtscheller [1999a]). Its opposite, rhythm increase, or "event-related synchronization" (ERS) occurs in the post-movement period and with relaxation Pfurtscheller [1999a]. Furthermore, and most relevant for BCI application, ERD and ERS occur also with motor imagery (i.e., imagined movement); they do not require actual movement (McFarland et al. [2000], Pfurtscheller and Neuper [1997]). Thus, they can occur independent of activity in the brain's

normal output channels of peripheral nerves and muscles, and could serve as the basis for a BCI. Since the mid 1980's, several mu/beta rhythm-based BCI research programs have been set up – one of them at the Wadsworth Center of the New York State Department of Health in Albany, New York.

## 1.5 The Wadsworth BCI System

With the BCI system developed by Dr. Jonathan Wolpaw's group in Albany (Wolpaw et al. [1986], Wolpaw et al. [1991], McFarland et al. [1997a], Wolpaw et al. [2000]), people with or without motor disabilities can learn, over periods of weeks to months, to control mu or beta rhythm amplitude and use that control to move a cursor in one or two dimensions to targets on a computer screen. Figure 1.3 shows the basic phenomenon of mu/beta-rhythm modulations.

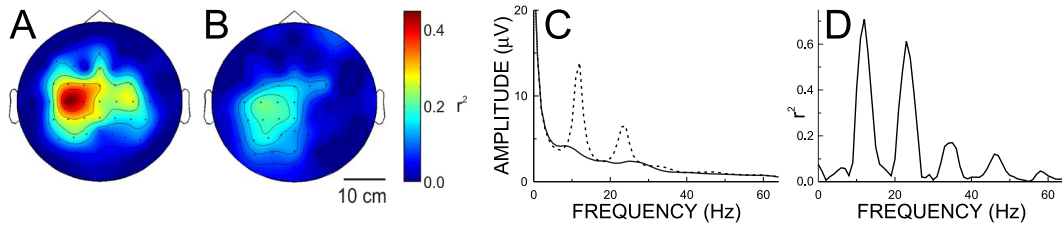


Figure 1.3: Examples of mu/beta rhythm signals (modified from Schalk et al. [2004]). A,B: Topographical distribution on the scalp of the difference (measured as  $r^2$  (the proportion of the single-trial variance that is due to the task)), calculated for actual (A) and imagined (B) right-hand movements and rest for a 3-Hz band centered at 12 Hz. C: Example voltage spectra for a different subject and a location over left sensorimotor cortex (i.e., C3 (see Sharbrough et al. [1991])) for comparing rest (dashed line) and imagery (solid line). D: Corresponding  $r^2$  spectrum for rest vs. imagery. Signal modulations are focused over sensorimotor cortex and in the mu- and beta-rhythm frequency bands.

For each dimension, a linear equation translates mu rhythm or beta rhythm amplitude from one or several scalp locations into cursor movement. This translation and the resulting cursor movement typically occur 30 times/sec. BCI users learn over a series of 40-min sessions to control cursor movement. They participate in 2-3 sessions per week, and most (i.e., about 80%) acquire some degree of one-dimensional control after prolonged, i.e., 4-6 weeks, training. Some of these individuals even

achieve two-dimensional control after additional training. In their initial sessions, most users employ motor imagery (e.g., imagination of hand movements, whole body activities, relaxation, etc.) to control the cursor. As training proceeds, imagery usually becomes less important, and users move the cursor in the same way that they perform conventional motor acts, that is, without thinking about the details of performance. While EEG from only one or two scalp locations is used to control cursor movement online, data from 64 locations covering the entire scalp are gathered for later offline analysis. This offline analysis defines the full topography of EEG changes associated with target position and helps develop improvements in online operation. Figure 1.3 uses the statistical measure  $r^2$  (Wonnacott and Wonnacott [1977]) to illustrate the topographical and spectral specificity and magnitude of the mu or beta rhythm control achieved by a representative user. The measure  $r^2$  is the proportion of the total variance in mu or beta rhythm amplitude that is accounted for by target position, and thus indicates the user's level of EEG control. In this user, control is sharply focused over sensorimotor cortex and in the mu and/or beta rhythm frequency bands. With this control, users can move the cursor to answer spoken yes/no questions with accuracies greater than 95% (Miner et al. [1998], Wolpaw et al. [1998]). Users can also achieve independent control of two different mu or beta rhythm channels and use that control to move a cursor in two dimensions (Wolpaw and McFarland [1994, 2004]).

One of the main characteristics of these studies, which at the same time represents the reason for the substantial difficulty and thus cost for engaging in this research, is that offline signal analyses are only of limited value. This is because during real-time control of the BCI system, both the user as well as the system continuously adapt to each other so as to improve performance. In consequence, any proposed improvement to the system has to ultimately be validated in online experiments. This requirement implies the need for empirical studies that systematically evaluate the impact of the various factors that determine BCI performance. To facilitate the implementation of these studies, I initiated a project to develop general-purpose software for BCI research and development, called BCI2000. While BCI2000 has been developed in advance and independently of this dissertation, I

utilized this system for the studies described in this dissertation in two ways. First, as described in Chapter 2, I extended BCI2000 so that it supported signal acquisition from different hardware. Second, I used this extended BCI2000 system to realize the experiments described in Chapters 2 and 4. To provide the reader with an overview of this system's capabilities, I summarized its general concepts below.

## 1.6 BCI2000: A General-Purpose BCI System

Brain-computer interface (BCI) systems measure specific features of brain activity and translate them into device control signals (see Figure 1.2 (modified from Wolpaw et al. [2002])). Many factors determine the performance of a BCI system. These factors include the brain signals measured, the signal processing methods that extract signal features, the algorithms that translate these features into device commands, the output devices that execute these commands, the feedback provided to the user, and the characteristics of the user. Thus, systematic studies that evaluate and compare alternative methods require software and associated tools that facilitate this process. Because existing BCI systems did not readily support such systematic research and development, BCI research consisted mainly of demonstrations of the feasibility of one particular method (Wolpaw et al. [2002]). Since 1999, I have been leading the development and testing of a general-purpose BCI research and development system, called BCI2000, that facilitates implementation of any BCI method (Schalk et al. [2004]). This system is rapidly becoming the standard in the field of BCI research and is currently in use by more than 90 laboratories around the world. Because the development and maintenance of this system has been my main responsibility at the Wadsworth Center, it was only natural to extend and utilize this system to conduct the work in this dissertation.

BCI2000 is based on a model that can describe any BCI system and that is similar to the one described in Mason and Birch [2003]. This model, shown in Figure 1.4, consists of four modules that communicate with each other: Source (Data Acquisition and Storage), Signal Processing, User Application, and Operator Interface. To date, my colleagues and I have used BCI2000 to implement BCI systems that support different data acquisition devices, signal processing algorithms, and

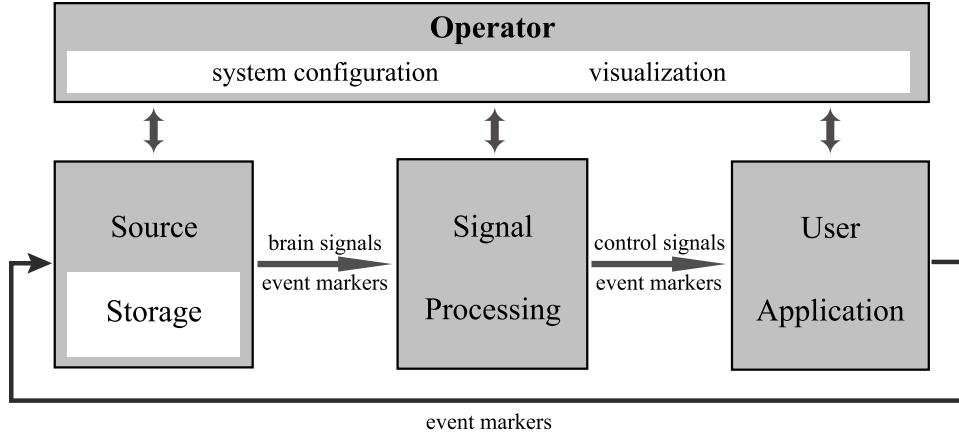


Figure 1.4: BCI2000 system design. BCI2000 consists of four modules: Operator, Source, Signal Processing, and Application. The operator module acts as a central relay for system configuration and defines onset and offset of operation. During operation, information (i.e., signals, parameters, or event markers) is communicated from Source to Signal Processing to User Application and back to Source.

user applications. The following paragraphs briefly describe these implementations.

Eleven Source module implementations have been created to date. Eight of them control data acquisition hardware (i.e., A/D converter boards) from different manufacturers (Measurement Computing, Inc.; Data Translation, Inc.; National Instruments, Inc.; g.USBamp and g.MOBILab devices from g.tec, Inc.; Modular-EEG systems; Biosemi, Inc., Tucker-Davis, Inc.), two provide support for different EEG recording systems (Brainproducts, Inc., Micromed, Inc.), and the last is a signal generator for use in system development and testing.

There are also a number of implementations of the signal processing module, whose processing capabilities consist of two stages. The first stage of signal processing, *feature extraction*, extracts features from the digitized brain signals. In all implementations to date, feature extraction consists of a series of three filters. The first filter is a calibration routine that performs a linear transformation of the input matrix (i.e., sample block) so that the n-bit digital input signal is converted to an analog output signal that is measured in  $\mu\text{V}$ . The second filter is a spatial filter that performs a linear transformation (i.e., a matrix multiplication of weights with the output of the calibration module) so that each output channel is a linear combination of all input channels. This signal operator can accommodate any linear spatial

filter operation (e.g., Laplacian derivation or common average reference (McFarland et al. [1997b]), independent components (Makeig et al. [1997]), or common spatial patterns (Ramoser et al. [2000])). The third signal operator is a temporal filter. To date, we have implemented five variations: a slow wave filter (see Kotchoubey et al. [1996], Kübler et al. [1999], Hinterberger [1999]), autoregressive spectral estimation McFarland et al. [1997a], a finite impulse response filter (FIR) (e.g., Haykin [1997]), a peak detection routine that extracts firing rates from neuronal action potentials, and a filter that averages evoked responses. The second stage of signal processing, the translation algorithm<sup>1</sup>, translates the signal features into control signals to be used by the User Application. In all implementations to date, it is comprised of two filters. The first filter is a classifier that performs a linear transformation (i.e., a matrix multiplication of a classification matrix with the output of the temporal filtering module) so that each output channel is a linear combination of all input channels. The second filter is a normalizer that performs a linear transformation on each output channel in order to create signals that have zero mean and a specific value range. This creates a signal with defined characteristics so that the User Application becomes invariant to the details of Signal Processing. An additional statistics component can be enabled to estimate in real-time certain parameters of the signal processing components such as the slope (i.e., gain) and intercept (i.e., baseline) of the linear equation the normalizer applies to each output channel so as to compensate for spontaneous or adaptive changes in the distribution of the control signal values (e.g., see Ramoser et al. [1997], McFarland and Wolpaw [2003]).

Finally, we have created seven different implementations of the user application module: four cursor movement applications (see Birbaumer et al. [2000], Vaughan et al. [2001], McFarland et al. [2003], Wolpaw and McFarland [2004]), an application for evaluating prospective users (McFarland et al. [2000]), an application that can present auditory and visual stimuli, and a spelling application based on evoked potentials as described by Farwell and Donchin [1988] and Donchin et al. [2000].

---

<sup>1</sup>I use the term *translation algorithm* instead of *classification* throughout this dissertation, because the typically continuous nature of the device control signals produced by BCI signal processing is better expressed by translation algorithm rather than the discrete output that is typically implied by the term classification.

## 1.7 Relevant Issues of BCI Technology

Nonmuscular communication and control is no longer merely speculation. Direct communication from the brain to the external world is possible and might serve useful functions. At the same time, practical applications of BCI technology to the needs of people with severe disabilities are impeded by primarily three limitations and requirements of current BCI methodologies.

First, current non-invasive or invasive sensor modalities do not facilitate widespread use of BCI technology in humans. Non-invasive BCIs use EEG activity (Vidal [1977], Sutter [1992], Elbert et al. [1980], Farwell and Donchin [1988], Wolpaw et al. [1991], Pfurtscheller et al. [1993]) recorded from the scalp. They are convenient, safe, and inexpensive, but they have relatively low spatial resolution (Freeman et al. [2003], Srinivasan et al. [1998]) that limits the maximum number of independent communication channels (i.e., degrees of freedom) that can be practically extracted, and are susceptible to muscle artifacts (i.e., electromyographic activity (EMG)) and artifacts from other sources. Systems using EEG will thus ultimately be limited in their capacities and cannot easily be used in noisy clinical environments. Most importantly, while EEG-based systems have been shown to support accurate non-muscular control, including 2D movement that can achieve a speed and accuracy similar to those reported for invasive studies in monkeys (Wolpaw and McFarland [2004]), they often require extensive user training over weeks or months (Wolpaw et al. [2002]). Invasive BCIs use single-neuron activity recorded within the brain (Georgopoulos et al. [1986], Kennedy and Bakay [1998], Laubach and Wessberg [2000], Taylor et al. [2002]). While they have higher spatial resolution, can provide control signals with many degrees of freedom, and appear to require less user training than EEG-based systems, BCIs that depend on electrodes within the cortex face substantial problems in achieving and maintaining stable long-term recordings. The small, high-impedance recording sites make penetrating electrodes susceptible to signal degradation due to encapsulation (Shain et al. [2003]). These issues are crucial obstacles that strongly impede their clinical use in humans (Donoghue et al. [2004]). In summary, a sensor that could detect signals from the brain safely and with high fidelity might reduce the substantial training requirements of current EEG-based

systems, and would thus facilitate the creation of clinically practical BCI devices.

Second, current signal processing algorithms do not facilitate use by non-experts. In all current BCI systems, the BCI signal processing problem is formulated as a classification problem. In this approach, an initial procedure first identifies, out of all possible signals, the set of specific brain signals features that can be modulated by the user using a particular task (typically motor imagery). These brain signal features are then extracted in real time and are translated into an output, which can be a discrete decision or a continuous control signal. This output is used to provide feedback to the user. While this approach is effective in the laboratory, its use in clinical environments is problematic and that mainly because the initial identification and continuous tracking of the signals that express the user's intent is laborious, difficult, and thus necessitates substantial expert supervision. Initial signal identification procedures suggest the brain signal features and the (imagery) task that best modulates them. This signal identification procedure can be time-consuming (because all possible tasks have to be executed by the user) and unreliable (because a user might not be able to repeatedly reproduce the same task with the requisite specificity). In addition to initial expert oversight, continuous expert supervision is currently required. This is because over the course of BCI use, the user's control strategy, which is expressed in the modulation of brain signal features, will change as the user adapts to the BCI system. Thus, the translation algorithm (e.g., linear classifier) that translates the features into device control has to be adaptive, which cannot always be automated. In summary, a signal processing procedure that does not require the initial and continuous expert judgments would facilitate the creation of clinically practical BCI systems.

The third impediment of current approaches is that the tasks that are used by BCI users to control the system are non-intuitive. In a typical EEG-based setup, brain signals associated with imagined limb movements are first identified. These signals, i.e., modulations in the mu or beta rhythm frequency bands (i.e., 8-12 Hz or 18-25 Hz, respectively), are then used alone or in combination to provide one- or two-dimensional control. While the origin of these rhythms remains unclear (da Silva [1991]), mu and beta rhythm oscillations usually do not correspond to the direction

of limb movements (Toro et al. [1994]) and thus their modulation in the context of directional movement control might require considerable cortical plasticity. In consequence, the use of mu and beta rhythms, and the motor imagery tasks that modulate them, is thus not immediately intuitive which impedes their utility as a practical communication device.

In sum, mainly due to these three issues have current BCI systems produced impressive laboratory demonstrations but no device of appreciable clinical value. The goal of this dissertation was to address these specific issues to work towards a system that can leave the confines of laboratory research to address the actual communication and control needs of the severely paralyzed.

## 1.8 The Three Themes in this Dissertation

This dissertation is focused on three themes that address these three critical issues of current BCI methodologies. They are: *Better Sensors, Better Signal Processing, and More Intuitive Tasks*.

The first theme, *Better Sensors*, focuses on an intermediate BCI methodology, i.e., using electrocorticographic activity (ECoG) recorded from the cortical surface. This signal acquisition methodology, which has been used in humans for the diagnosis of intractable epilepsy for decades and also sometimes for research purposes (e.g., Levine et al. [2000], Freeman et al. [2003]), but never for real-time BCI experiments, could be a powerful and practical alternative to the non-invasive and intracortical methods described in Section 1.7. This first theme is initially concerned with development of the experimental setups that allow real-time access to ECoG signals and with the development of methods to effectively analyze these signals offline. I then use these methods to conduct BCI experiments in humans using ECoG signals. The results demonstrate that humans can rapidly achieve one-dimensional BCI control, which is in contrast to the many weeks or months that were previously required. This could lead to more practical deployment of BCI systems to severely paralyzed individuals who often cannot be subjected to the substantial training procedures that current EEG-based methods require.

The second theme, *Better Signal Processing*, focuses on the development of a

BCI signal processing methodology using a detection approach. While signal detection has played a large role in image processing (Radke et al. [2005] for review), all current BCI methods rely on signal classification instead. The approach described in this theme uses methods that have been applied before in other domains, i.e., a Gaussian Mixture Model (GMM) that is parameterized using the Competitive-EM (CEM) algorithm, and extends them with robust processing and automatic model selection (i.e., automatic definition of the number of Gaussian mixtures). In this second theme, I describe this method and validate it by applying it to a comprehensive BCI dataset and comparing the results to results achieved using a traditional regression-based approach. These results demonstrate that BCI control could be achieved without the tedious signal identification procedures that are currently required.

The third theme, *More Intuitive Tasks*, focuses on the possibility that the direction of joystick movements could be decoded from ECoG signals in humans. This could lead to BCI systems that are more intuitive to use than the current EEG-based approaches that require non-intuitive movements or imagery. While it has been shown before that a number of kinematic movement parameters relating to arm movements can be extracted from brain signals, it has been widely assumed that this requires intracortical implants of microelectrodes<sup>2</sup>. For this theme, we asked patients with ECoG electrodes to use a joystick to move a joystick so as to track a target to a computer screen. The principal results show that joystick movement trajectories can be faithfully decoded using ECoG signals in humans using relatively simple methods that can readily be implemented to function in real time.

## 1.9 Overview of Contributions

The work on the three themes described in this dissertation produced a number of important contributions to applied Brain-Computer Interface research, as well as to basic and applied neuroscience. These contributions are described in detail in Chapters 2, 3, and 4, and are briefly summarized here.

---

<sup>2</sup>"EEG has nowhere near the coding capacity," Nature Neuroscience, 1999. "Movement control requires recordings from neurons," Current Opinion in Neurology, 2000. "Scalp EEG lacks the resolution needed," Nature, 2001.

**THEME I: Better Signals** The work described in THEME I provided three contributions. First, I developed the methodology for the real-time use and offline analysis of electrocorticographic (ECoG) signals recorded from the surface of the brain. Second, I used these methods to realize the first real-time BCI experiments using ECoG signals. Third, in these experiments I show for the first time that the higher fidelity of ECoG signals results in a significant reduction of the substantial training requirements that are currently necessary with EEG-based methods. This has direct and major implications for the development of clinically relevant BCI systems. In addition, these experiments also produced data utilized later in THEME II and THEME III. The methods developed in THEME I have been provided to a number of laboratories in the USA and in Europe. The importance of this contribution is evident in the rapid adoption of these methods, which are now being used to replicate and extend the results of this dissertation.

**THEME II: Better Signal Processing** At present, translation of BCI technology demonstrations into widespread clinical practice is impeded by the initial expert oversight that all current methods require and that determines the combination of signals and tasks that best modulate detectable brain activity. The main contribution presented in THEME II is the finding that the use of a detection approach, which has previously been used in other fields such as image processing (but never in BCI signal processing), in a classification context can result in performance similar to the classification-based techniques traditionally used in BCI research without necessitating the detailed system configurations by experts that are typically required. This contribution encompasses a conceptual advance as well as some algorithmic improvements. We furthermore show that this approach to signal processing can also be used as a novel way to effectively visualize brain signals in real time. These results should facilitate the translation of laboratory BCI demonstrations into clinical practice, and could also be important for clinical research and diagnosis.

**THEME III: More Intuitive Use** It has been widely assumed that detailed joystick movement parameters can be derived only from signals recorded by intracortical microelectrodes. The main contribution presented in THEME III is the finding

that, in fact, this widespread assumption is incorrect. My results demonstrate that signals recorded by electrodes on the cortical surface (ECoG) also support accurate decoding of kinematic parameters of joystick movements in humans without requiring penetration of the brain. These results suggest that ECoG could be used to design more intuitive tasks for human BCI systems, that ECoG could be a more stable and less invasive alternative to intracortical electrodes for BCI systems, and that ECoG could also prove useful in other studies of motor function. This contribution thus has direct implications for future BCI research, and is also important for basic neuroscience research on motor control.

## CHAPTER 2

### THEME I: BETTER SIGNALS

*It is a common delusion that you make things better by talking about them.* Dame Rose Macaulay (1881 - 1958).

*Change has a considerable psychological impact on the human mind. To the fearful it is threatening because it means that things may get worse. To the hopeful it is encouraging because things may get better. To the confident it is inspiring because the challenge exists to make things better.*

King Whitney Jr.

#### 2.1 Summary of Contributions and Approach

This chapter discusses THEME I of this dissertation, which is about a better BCI signal acquisition methodology. The demands and limitations of current signal acquisition techniques constitute one of the most critical impediments to translation of BCI technology demonstrations into widespread clinical practice. These limitations are mainly the clinical risks and stability issues associated with intracortical implants and the low signal fidelity and long training requirements associated with scalp-recorded electroencephalography (EEG).

The main contribution presented in this chapter is the finding that the theoretical advantages of signals recorded from the surface of the brain (called electrocorticography (ECoG)), which are smaller clinical risks than intracortical implants and higher fidelity than EEG, translate into reduced training requirements in real-time BCI experiments. While ECoG signals have been routinely recorded in humans for other purposes, they have not been used for real-time BCI experiments. The contribution of THEME I of this dissertation thus represents the successful validation of an existing sensor modality combined with modified existing BCI methodologies. The associated work is outlined in Figure 2.1. The results provide strong initial evidence that suggests that one of the principal impediments of current signal acquisition

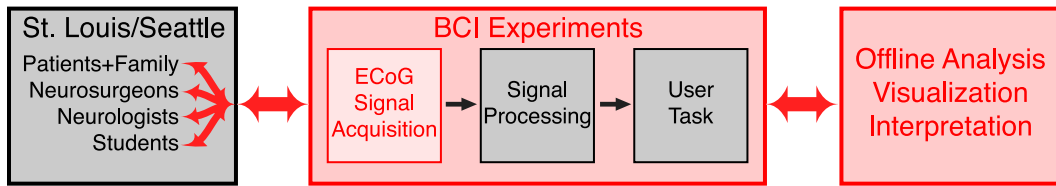


Figure 2.1: Overview of the work accomplished in THEME I. Items in red indicate work performed for this dissertation. Items in black indicate existing resources.

methodologies could be addressed using ECoG. The work accomplished in this dissertation should thus facilitate the translation of laboratory BCI demonstrations into clinical practice.

The work in this chapter depended on application of a number of methodologies from different areas of science and engineering, such as BCI research, electrical engineering, computer science, and signal processing, and was thus highly multidisciplinary. As an example, I used aspects of computer science, in particular C++ and Matlab programming, to implement the necessary interfaces between existing BCI software and existing ECoG data acquisition devices and to develop a visualization technique for signals acquired from these devices, respectively.

## 2.2 Introduction

Brain-computer interfaces (BCIs) convert brain signals into outputs that communicate a user's intent (Wolpaw et al. [2002]). Because this new communication channel does not depend on peripheral nerves and muscles, it can be used by people with severe motor disabilities. BCIs can allow patients who are totally paralyzed (or "locked in") by amyotrophic lateral sclerosis (ALS), brainstem stroke, or other neuromuscular diseases to express their wishes to the outside world.

Studies of the past two decades have shown that BCI communication is possible and that it may perform useful functions. At the same time, they have mostly remained technical demonstrations, i.e., validations of complex laboratory setups that showed that brain signals can be used to convey a user's intent. While these demonstrations have recently attracted significant attention from the scientific and popular media, the long-term success of this novel way to communicate critically

depends on achieving its goal of restoring communication and control function lost due to accidents or disease. It is thus imperative that BCI research translates the existing successful laboratory demonstrations into successful clinical applications. However, significant impediments to this translation remain. One of the principal obstacles provided the impetus for the first of the three themes in this dissertation. This obstacle is the inadequate performance and/or unsatisfactory clinical applicability of the sensor. Sensors that can support wide-spread clinical applications must provide safe recordings, long-term stability of these recordings, high signal fidelity with short time constants, and inexpensive and portable equipment.

The four sensor requirements of clinical BCI systems described above hinder laboratory demonstrations only modestly. Signal acquisition procedures that are too risky for routine human application may be tested in animals; signal acquisition methodologies that do not provide recordings that are stable over many months do not impede experiments in the laboratory, which are typically done in shorter time periods; limited signal fidelity may support adequate system performance given careful interactions of the user, the BCI system, and BCI experts; and equipment may be useful for laboratory studies even if it is stationary and expensive. In contrast, these four requirements are critical for successful clinical implementations of human BCI systems. A brain-based communication system for people who are paralyzed will not be widely adopted unless it is clinically safe over prolonged periods, can be used by users and their caregivers without substantial expert supervision, and unless it is reasonably expensive and portable. No current BCI demonstration has utilized a signal acquisition methodology that supports all four of these requirements.

The signal acquisition methodologies used to date have made use of electrical measurements (detected on the surface of the scalp using electroencephalography (EEG) or from within the brain using single-neuron recordings), magnetic measurements (using magnetoencephalography (MEG)), or metabolic measurements (using functional Magnetic Resonance Imaging (fMRI) or functional Near InfraRed (fNIR)).

Scalp-recorded EEG is convenient and safe, may support recordings that are stable over prolonged periods, and requires cheap and readily available technology

that could readily be miniaturized, but the fidelity of the signals detected using this method is modest. While these signals have been shown to support impressive demonstrations, including the control of two-dimensional movements that are similar in performance to ones achieved with electrodes implanted within the brain (Wolpaw and McFarland [2004]), their low fidelity (Freeman et al. [2003], Srinivasan et al. [1998]) and susceptibility to artifacts from sources outside the brain prescribes the use of carefully designed and expert-supervised signal processing and experiments. Furthermore, and more detrimental for clinical application, the physiological nature of the signals that can be detected on the scalp is, while not fully elucidated, most likely not associated with directional movement control in normal function (Niedermeyer [1999]). Their use thus requires a level of attention and training (Wolpaw et al. [2002]) that is prohibitive for use in severely paralyzed patients.

Recordings from individual neurons within cortex provide signals with high fidelity and short time constants and associated equipment may also become cheap and portable. Studies have demonstrated that these signals, whose sources are used for directional movement control during normal brain function, can be used to support two- or three-dimensional movement control (e.g., Taylor et al. [2002]). However, they depend on implantation of tiny electrodes within the brain whose clinical safety and long-term stability is currently uncertain (Shain et al. [2003]).

Recordings using MEG may have somewhat better signal properties than those using EEG, but they require expensive equipment and a shielded environment. Because of these demanding requirements, these signals have only sparsely been evaluated in the literature including one report coauthored by this writer (Mellinger et al. [2005], Lal et al. [2005], Kauhanen et al. [2006]).

Metabolic recordings using fMRI have high fidelity, may be safe and stable over long periods, but have low time constants (due to the slow response time of metabolic processes, and not due to technological limitations) and require expensive and non-portable equipment. Again, mainly due to these demanding requirements, these signals have only been utilized in initial BCI demonstrations (Weiskopf et al. [2003, 2004]).

Finally, recordings using the emerging fNIR technology have similar character-

	EEG	single-neuron recordings	MEG	fMRI	fNIR
<b>safe recordings</b>	✓	✗	✓	✓	✓
<b>long-term stability</b>	✓?	✗	✓	✓	✓
<b>high signal fidelity and short time constants</b>	✗	✓	✗	✗	✗
<b>cheap and portable</b>	✓	✓?	✗	✗	✓?

Figure 2.2: No currently used BCI signal acquisition method is fully compatible with the requirements of clinical BCI systems. Entries that are expected but have not been established at present are indicated with questionmarks.

istics to those using fMRI except that they may also become relatively inexpensive and portable. While the metabolic nature, and corresponding slow time constants, of these signals will always prevent rapid communication, the otherwise advantageous properties of these signals have very recently attracted significant interest (Son and Yazici [2005]). Studies are beginning to explore its application to BCIs (Coyle et al. [2004]).

In summary, all sensor methodologies that have been used to realize the plethora of BCI demonstrations up to the present have at least one serious limitation that impede their applicability to a clinically practical BCI system (see Figure 2.2). Furthermore, electrical signals can provide short time constants and can be acquired using relatively simple technologies. They will thus likely remain the best candidates for BCI communication. While the serious limitations of current methods only modestly affect the impressive laboratory demonstrations that have recently gained widespread attention in the scientific and popular media (Taylor et al. [2002], Serruya et al. [2002], Donoghue et al. [2004], Wolpaw and McFarland [2004], Hochberg et al. [2006]), they greatly impede the application of BCI technology to the communication and control needs of the paralyzed.

## 2.3 Electrocorticography (ECoG)

Electrical signal acquisition methods for BCI communication used to date have been either non-invasive (i.e., recorded on the scalp) or highly invasive (i.e., recorded from within the brain). As described in the previous section, both have serious disadvantages that severely impede clinical application. A third option, electrocorticographic activity (ECoG) recorded from the cortical surface, could be a powerful and practical alternative to these extremes. ECoG has higher spatial resolution than EEG (i.e., tenths of millimeters vs. centimeters (Freeman et al. [2003])), broader bandwidth (i.e., 0-200 Hz vs. 0-40 Hz), higher amplitude (i.e., 50-100  $\mu$ V maximum vs. 10-20  $\mu$ V), and far less vulnerability to artifacts (Freeman et al. [2003], Srinivasan et al. [1998], Taylor et al. [2002]). While ECoG also requires an invasive procedure, it does not require penetration of the cortex and is thus likely to have greater long-term stability and might also be safer than recordings within the brain (Margalit et al. [2003], Pilcher and Rusyniak [1993]). Figure 2.3 illustrates the three possible sensor locations.

ECoG signals are routinely recorded in humans in many hospitals with a neurosurgery outfit, mainly for the clinical evaluation of intractable epilepsy (Schwartz et al. [1997]) and brain cancer (Nathoo et al. [2005]) prior to surgery, but also for treatment of chronic pain. While they have also been used for research purposes (e.g., Levine et al. [1999], Freeman et al. [2003]), they have never been used for real-time BCI experiments. It has thus remained elusive whether the theoretical improvements in signal quality compared to EEG would translate into a benefit for BCI applications that would justify an invasive procedure. ECoG signals are detected using simple passive sensors (e.g., titanium electrodes) embedded in modestly flexible polymer substrates. The exposed area of these electrodes is typically about 2-3 mm with an inter-electrode distance of 5-10 mm. The electrodes are usually configured as strips (usually 4 or 6 electrodes) or grids (usually 8x8 electrodes) and are implanted directly on the surface of the brain, i.e., underneath the skull and the dura (Figure 2.3). Connection to external devices is accomplished using tethered cabling that limits the patients' mobility. Figure 2.4 illustrates an example electrode placement with associated cabling. Because the main purpose of such implants at

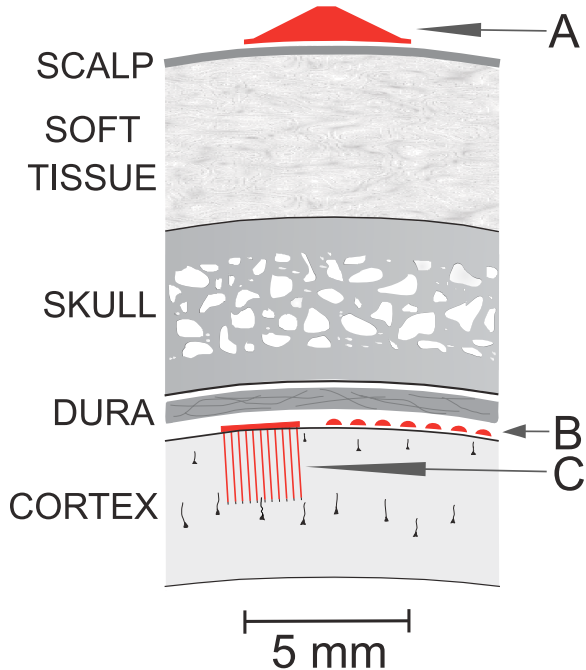


Figure 2.3: Three possible sensor locations for BCI devices. Signals from the brain are acquired by electrodes on the scalp, the cortical surface, or from within the cortex. Electrodes on the scalp (A) can be placed non-invasively, but are also far removed from the minute signals generated by neurons within the brain. Electrodes on the surface of the brain (B) are routinely used in epilepsy surgery protocols and do not require penetration of the brain, but have not previously been used for BCI communication. They can be placed close to brain areas that can convey intent. Microelectrodes that penetrate the brain (C) have to be applied in a complex surgical procedure, and they usually cannot record signals over prolonged periods. They can be brought in direct contact with relevant brain areas.

present is temporary clinical evaluation, all their characteristics (i.e., their configuration, location, and implant duration) are determined by and thus optimized for clinical rather than BCI requirements. Together with regulatory, organizational, and technical difficulties, this situation impedes systematic and controlled studies using a large number of subjects. It is the expectation that this dissertation and the studies that will follow will establish ECoG as an attractive signal acquisition methodology for BCI research. Once this has been established and appropriate approvals from the FDA have been secured, ECoG electrodes could be implanted and optimized for the purpose of BCI communication, which should eliminate the issues

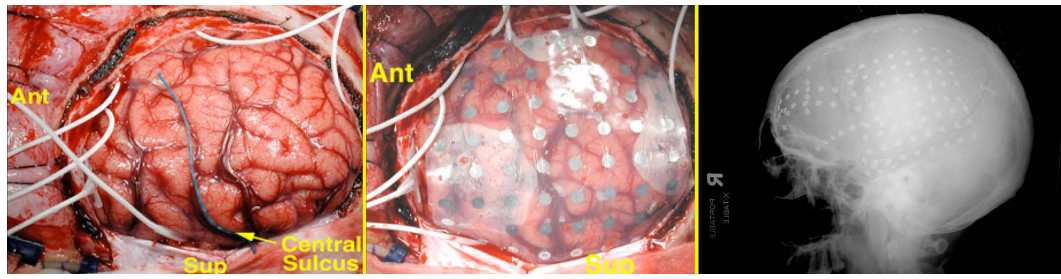


Figure 2.4: Sample ECoG electrode placement. Left: Exposed brain after a craniotomy has been performed (i.e., the skull and dura have been removed). Center: An ECoG grid with 8x8 electrodes is placed on the surface of the brain. Right: Lateral radiography shows placement of an electrode grid and several strips.

currently associated with recording these signals.

In summary, electrocorticographic signals recorded from the cortical surface are an attractive candidate for clinical BCI systems because they appear to support the four requirements detailed above. While they have been used routinely for clinical evaluations, they have not been utilized for BCI experiments. For **THEME I** of this dissertation, I set out to utilize ECoG signals, recorded in patients with epilepsy at two sites (St. Louis and Seattle), for real-time BCI experiments (see Figure 2.1). I approached this goal using three aims that are described in subsequent sections of this chapter and that are briefly summarized below. I hypothesized that the theoretical properties of ECoG signals would translate into improved BCI performance and/or reduced training requirements compared to EEG.

My first aim was to gain real-time access to ECoG signals by developing the necessary personal relationships and institutional approvals with sites that have access to ECoG signals, and by developing the necessary software to interface existing BCI software with the devices that were present at these sites. My second aim was to develop the requisite analysis and visualization techniques that could support adequate interpretation of the results. My third aim was to combine existing BCI methods with the methods and relationships developed in the previous aims, to utilize these techniques to conduct real-time BCI experiments, and to thereby validate the use of ECoG signals in the BCI context.

## 2.4 Aim 1: Real-Time Access to ECoG Signals

The first of my three aims of THEME I of this dissertation was to get real-time access to ECoG signals, which is available only at epilepsy centers. I thus started to develop relationships with individuals who had an interest in BCI research at such institutions. This was difficult because clinical personnel (in particular, neurosurgeons and neurologists) typically get rewarded only for their clinical service and not for research. In the end, I have developed relationships with two sites.

### 2.4.1 Site 1: St. Louis

The first site was Barnes-Jewish Hospital and the affiliated Medical School at Washington University in St. Louis, Missouri. Development of this collaboration encompassed two issues. The first issue was the institutional interface. I initiated collaborations with Dr. Eric Leuthardt from the Department of Neurosurgery and Dr. Dan Moran from the Department of Biomedical Engineering. Using these initial contacts, I developed further relationships, most notably with Lucy Sullivan (EEG technician), and Nick Anderson (graduate student). My collaborators and I applied for and subsequently got granted institutional approval to get access to ECoG signals.

The second issue was the technical interface. Epilepsy patients are monitored continuously and monitoring must not be interrupted during BCI experiments. In addition, any device that is to be used with patients has to be FDA approved and pass rigorous inspection by the clinical engineering department of the institution. Such a clinical environment is thus highly regulated and the use of other hardware is difficult. Consequently, utilization of existing monitoring hardware would facilitate the process. Clinical monitoring at Barnes-Jewish Hospital is accomplished using monitoring infrastructure from XLTEK, Inc. This system is based on a networked architecture in which ECoG signals are collected and digitized in each patient room and then transmitted to a central server. Dedicated monitoring stations can be used by EEG technicians or neurologists to review (in real-time or post-hoc) the patients' signals. This system did not readily provide real-time access to digitized signal samples to external hardware/software. However, my collaborators and I acquired a unit

from XLTEK (called an Analog Printer) that can convert the digital signals of any particular patient back into analog signals (i.e., essentially, a simple D/A converter unit). This unit thus made analog signals, collected from any particular patient, available for further processing in real time. To avoid aliasing, we also installed a low-pass filter (225 Hz cutoff) after this unit. This scheme thus supported the detection of signals up to the cutoff of the low-pass filter, which was sufficient given current understanding of information in ECoG signals (Pfurtscheller et al. [2003]). I then installed a computer with the existing BCI software BCI2000 developed at Wadsworth, and a 64-channel DT3003 A/D converter card from Data Translations, Inc. This A/D board supported any sampling rate up to 5 kHz per channel. To support up to 128 channels of data collection, I finally designed and implemented a BCI2000 software component that supported concurrent signal acquisition from two Data Translation devices (using DT730 patch panels with custom wiring). This software component controlled timing hardware on the A/D converter card such that it produced a clock signal. The custom wiring on the patch panels connected this clock signal to the clock input of the A/D converter circuit on each of the two A/D cards. Finally, I programmed the A/D converter circuits to utilize this external clock. The architecture of this system is illustrated in Figure 2.5 and the assembled BCI system is shown in Figure 2.6.

In summary, in St. Louis I set up collaborations and designed and implemented the necessary hardware/software to interface extended versions of existing recording and BCI software infrastructure. While the technical approach to signal acquisition (analog-to-digital conversion, transmission to a central server, transmission to the Analog Printer, digital-to-analog conversion, low-pass filtering, analog-to-digital conversion, and processing in the BCI software) was somewhat awkward, it was the most practical solution given the highly regulated environment. Furthermore, initial testing showed that system latencies were on the order of 60 ms, which was sufficient for the present purpose.

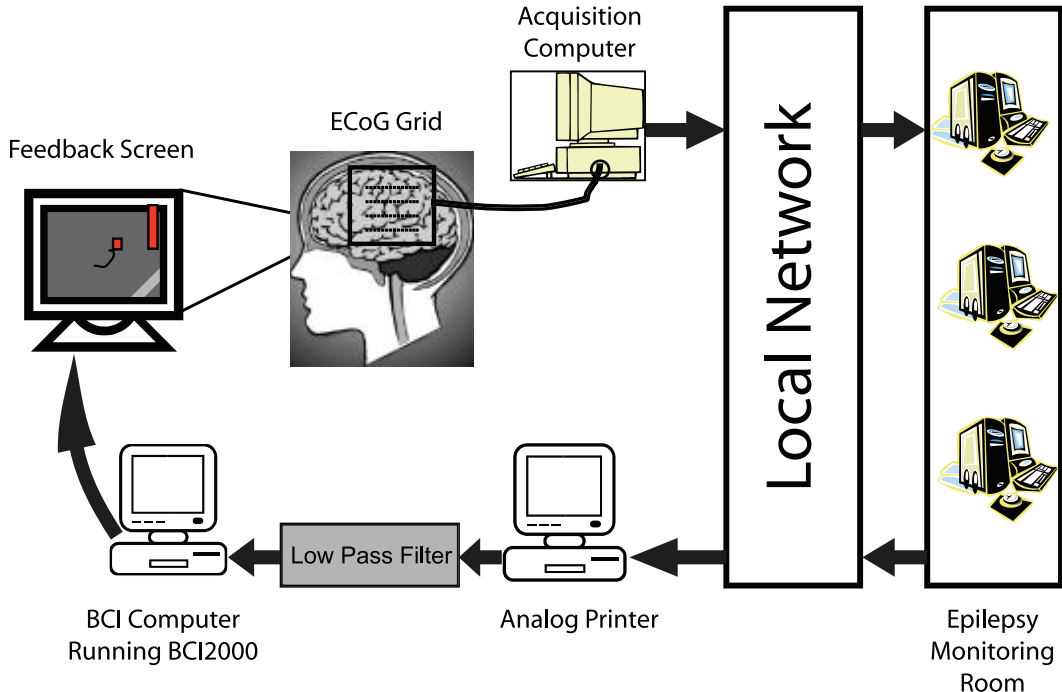


Figure 2.5: Architecture of the system in St. Louis.

#### 2.4.2 Site 2: Seattle

The second site was at Washington University School of Medicine in Seattle, Washington. At this site, I initiated collaborations with Dr. Jeff Ojemann from the Department of Neurosurgery and Kai J. Miller, a graduate student. We applied for and were subsequently granted access to ECoG signals. Our approved study protocol included the capacity to split signals that came off of the patient, so that one set of signals would be connected to the clinical monitoring system, and the other set to an FDA-approved data acquisition device. This device was a Neuroscan Synamps2 amplifier/digitizer combination that supported up to 128 channels at a fixed sampling rate of 1000 Hz and was already present at the hospital. While the Neuroscan system is a complete EEG recording solution with integrated software, it also supports real-time access to the digitized signals through a TCP/IP connection.

I then requested a test unit from Neuroscan, Inc., and used this test unit to develop software to interface the BCI2000 system with the Neuroscan EEG system. Specifically, the Neuroscan system acted as a TCP/IP server on a particular port. The component that I implemented connected to that port, requested data broadcast

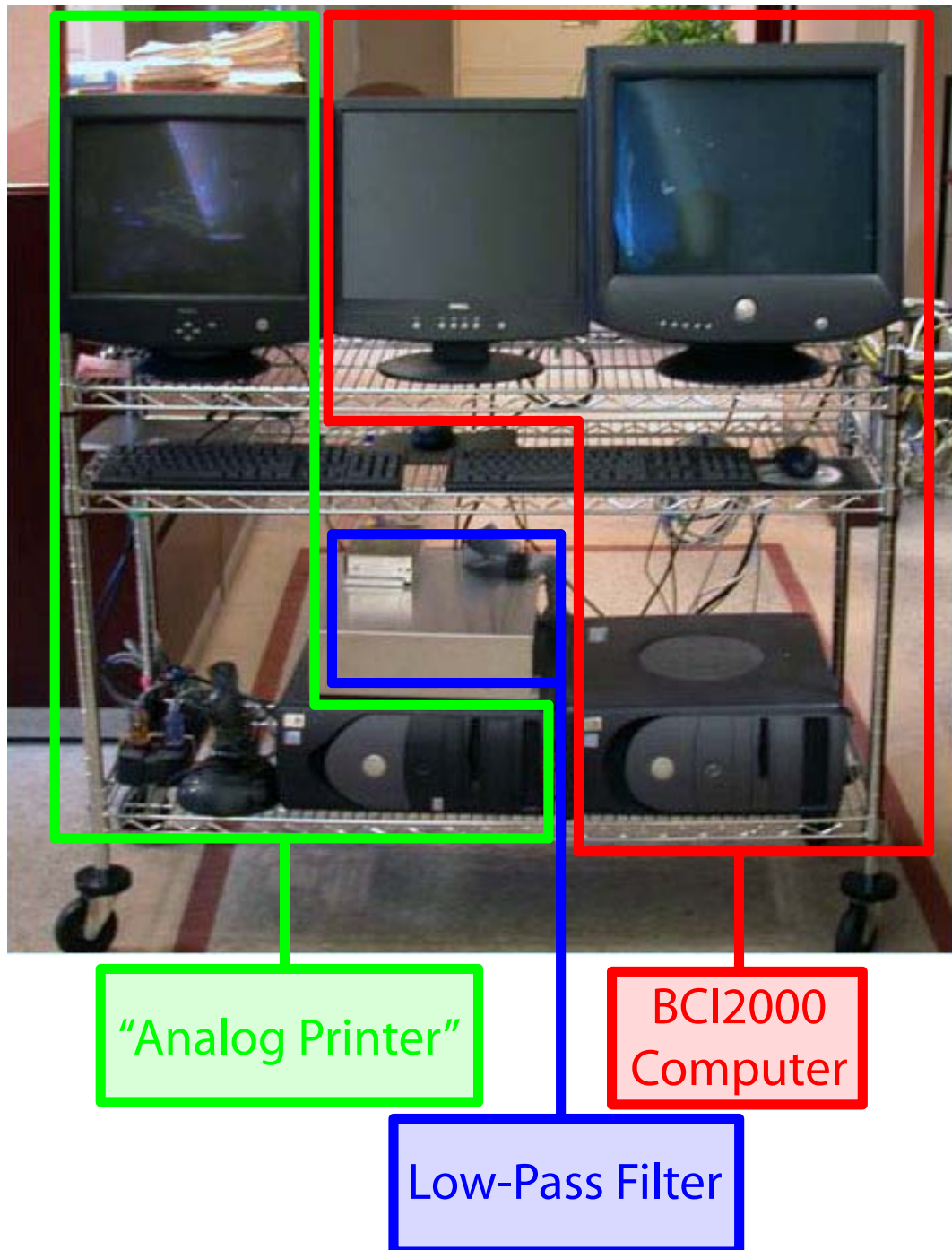


Figure 2.6: Photograph of the BCI system in St. Louis.

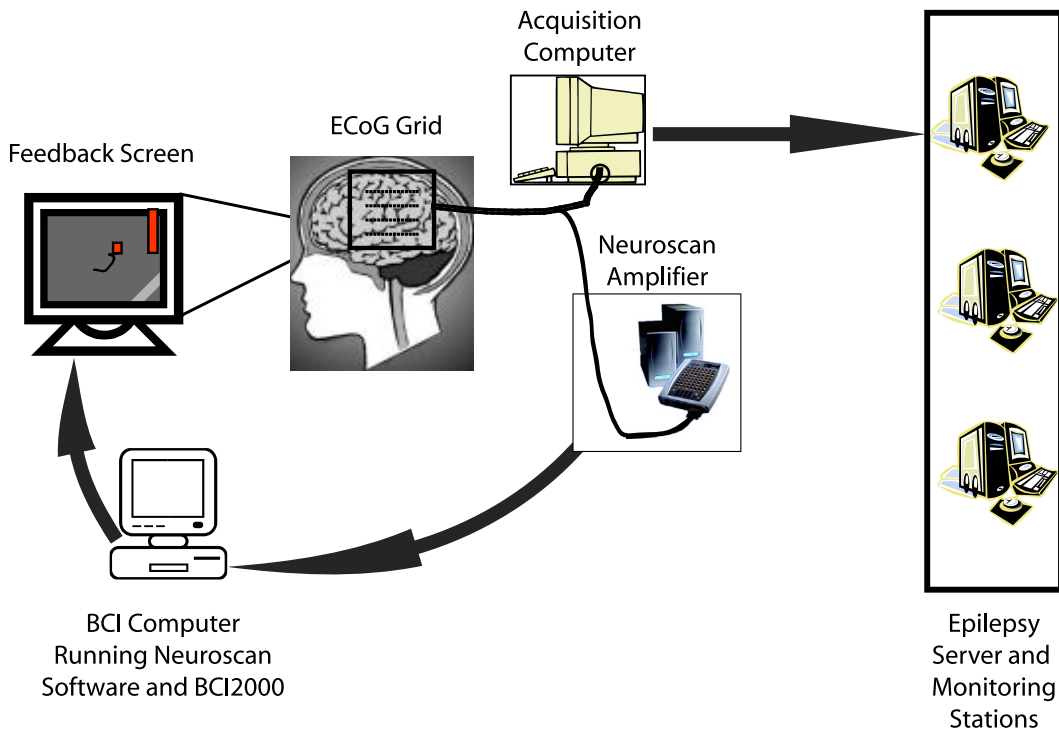


Figure 2.7: Architecture of the system in Seattle.

using a documented Neuroscan-specific application-layer protocol, and subsequently received data samples in real time that could be further processed by the BCI2000 software. The architecture of the system in Seattle is illustrated in Figure 2.7.

#### 2.4.3 Recording from Patients

The collaborations and institutional approval at the two sites in St. Louis and Seattle, and the hardware and software systems that I designed, provided the basis for real-time recordings of ECoG signals in humans. This section highlights the substantial demands and difficulties of working with a human patient population that have ECoG electrodes implanted for the purpose of clinical evaluation of their epilepsy (and not for BCI research).

The first issue relates to the human patients. They are usually people with intractable epilepsy (i.e., with epilepsy that cannot be fully controlled by drugs). The life of these individuals is often significantly affected by their condition to the extent that they may lose their jobs or drivers licenses, etc. Thus, their sole motivation when they enter the hospital is to change this situation by undergoing epilepsy

surgery. Furthermore, their schedule is determined by clinical requirements and their personal situation. For example, patients might fly in the night before surgery and have frequent visits by family and friends, or they might cancel the visit altogether on short notice. In summary, it is essential to gain the trust of the patients and to motivate them to participate in the research using engaging interactions between the clinical and research personnel, the patient, and his/her family. Despite this effort, patients may refuse (and have refused) participation for any reason (this is a critical requirement of the approved research protocol), or might simply not show up for the scheduled surgery.

The second issue relates to the clinical needs of epilepsy surgery. Surgery is a highly effective (80-90% success) treatment option for intractable epilepsy. To optimize the location and extent of the surgery, which simply resects part of the cortex, ECoG grids/strips are first implanted at a site determined by the surgeon and neurologist. Signals from the implanted electrodes are then passively monitored by experts to determine the location of the seizure focus. Furthermore, functional mapping is performed to localize motor/language cortices. To do this, electrodes are actively stimulated to provoke temporary sensations (e.g., a tingling sensation in the hand) or functional failure (e.g., loss of speech function). Location and extent of the resection is then chosen such that it best covers the seizure focus but minimally affects important motor/language areas. The grids/strips are implanted for a period that is as short as possible – typically 3-10 days. This clinical regimen impedes systematic and controlled studies. Patients are usually recovering from surgery for about three days and some are quickly explanted after that. Furthermore, patients are also affected by the functional localization procedure using electrical stimulation such that they may not be able to participate in experiments for many hours. Finally, the patients are often visited by clinical personnel, such as nurses or doctors.

In summary, the only reason why these patients are in the hospital is their medical need. Conducting experiments with a reasonable expectation of success thus depends on a personable interaction with all parties and on a full-time commitment for the duration of each patient's hospitalization, averaging about one week. Together with my collaborators in St. Louis and Seattle, I worked with a total of

14 patients. These data provided the basis for the real-time experiments and offline analyses in **THEME I**, **THEME II** and **THEME III**.

## 2.5 Aim 2: Analysis and Visualization Techniques

The second of my three aims of **THEME I** of this dissertation was to implement the two principal analysis techniques and to design and implement an effective visualization technique for ECoG signals. I used these methodologies in Aim 3 of this chapter (i.e., the validation of the ECoG recordings for BCI experiments) as well as for analyses in **THEME II** and **THEME III** of this dissertation. Subsequent sections describe only the methods that are common to all three themes of this dissertation. Methods that are specific to each theme are described in the respective chapters.

### 2.5.1 Frequency Analysis

I first implemented a routine for frequency analysis. Many studies over the past century have identified relationships between particular frequency bands of the EEG and/or ECoG and different functions. Thus, EEG and ECoG signals are often studied in the frequency domain. Studies have used a variety of techniques to convert time-domain signals into frequency-domain amplitude/power spectra. These include the Fast Fourier Transform (FFT, Brigham [1973]), wavelet transform (Rao and Bopardikar [1998]), and procedures based on autoregressive parameters (Marple [1987]). While any of these methods would be reasonably adequate, the requirements of BCI systems offer suggestions about which of these methods to select. BCIs are closed-loop systems that should provide feedback many times per second (e.g., typically, at more than 20 Hz) with a minimal group delay. The Heisenberg principle of uncertainty (e.g., Priestley [1981]) governs that it is not possible to concurrently achieve high resolution in time and frequency and hence, any of the procedures mentioned above will be subject to this limitation. However, the Maximum Entropy Method (MEM) (Marple [1987]), which is based on autoregressive modeling, has a higher temporal resolution (and thus reduced group delay) at a given frequency resolution compared to the FFT and wavelet transforms (Marple [1987]), and is thus advantageous in the context of BCI systems.

To support the offline analyses described in this dissertation, I added a Matlab interface to an existing C++ implementation of the MEM algorithm. Like other time-frequency transformations, this procedure transforms time-domain signals  $s_e(k)$  into a vector of frequency estimates  $\vec{a}_e(n)$ . ( $e$  corresponds to the electrode,  $k$  is the sample number of the time-domain signals, and  $n$  is the sample number of the frequency-domain estimate.)

### 2.5.2 Statistical Evaluation

I then implemented a method that would support statistical evaluation of results. The principal approach for EEG/ECoG analysis is to collect signals from a number of sensors under at least two conditions. Once all these data are collected, signals for each sensor are converted into the frequency domain (using, for example, the MEM procedure). This procedure then yields a set of frequency spectra for each sensor, which are then collated according to the two conditions (producing distributions  $x$  and  $y$ ), and compared. (THEME II of this dissertation suggests an alternate approach with particular benefits to BCI research.) The expectation is that this comparison reveals the signal changes that are due to the conditions.

The simplest way to perform this comparison is to calculate signal means for  $x$  ( $\bar{x} = \frac{1}{N} \sum_1^N x(n)$ ) and  $y$  ( $\bar{y} = \frac{1}{N} \sum_1^N y(n)$ ) and to then simply subtract one from the other (i.e.,  $d_{xy} = \bar{x} - \bar{y}$ ). This comparison is performed for each frequency bin and each electrode, yielding one value for  $d_{xy}$  for each combination of frequency bin and electrode. Identification of signal changes associated with the task then results in determining those frequency bins and electrodes that have a large value of  $d_{xy}$ . The problem with this simple approach is that the within- and inter-class variances between the distributions  $x$  and  $y$  can, and typically are, very different for the different frequency bins and electrodes, and that thus a given difference in mean amplitudes might be more or less significant. Consequently, simply calculating the first statistical moment, the signal mean, is suboptimal.

A better approach is to use higher-order statistics. For example, the value of  $r^2$  (Wonnacott and Wonnacott [1977], Eq. (2.1)) calculates the fraction of the total signal variance that is associated with the conditions. Its value thus accounts

for the within- and inter-class variance (which is similar to Fisher's measure of separation between two distributions (Fisher [1936])) and can range from 0 to 1.0. As an example, for an  $r^2$  value close to 1.0, the distributions  $x$  and  $y$  will have a large inter-class variance (i.e., a large difference in the distribution means) and small within-class variances. I utilized the  $r^2$  metric for evaluations throughout this dissertation.

$$r^2(x, y) = \frac{\sigma_{x,y}}{\sigma_x \sigma_y} \quad (2.1)$$

### 2.5.3 Visualization of ECoG Signals

The final topic in Aim 2 of **THEME I** of this dissertation was to design and implement an effective visualization technique for ECoG signals. The data acquisition and signal analysis methods described in the previous sections will yield results corresponding to particular aspects of BCI control or of cortical function. To facilitate interpretation, it is important to visualize these results in relation to the recording geometry (i.e., to derive topographies) and to relate results of these analyses to the anatomy or to results from other subjects. This requires the critical capacity to visualize results in relationship to the recording geometry and/or location of the cortical areas they were derived from and to the electrode location of other subjects. This visualization process would be facilitated if it could execute in an automated fashion, i.e., without requiring many manual steps, and without requiring complex computing environments.

Relating results to the recording geometry is fairly straightforward, as this is simply a two-dimensional topographical mapping problem. To create such topographies, I utilized the `topoplot` Matlab routine, which is part of the EEGLab package (Delorme and Makeig [2004]). Figure 2.8 illustrates an example of such a topographical mapping for 32 electrodes arranged in a 8x4 grid. Electrode locations are marked with black dots. For this example, electrodes were assigned arbitrary values. Colors indicate these values at each electrode location and their interpolated values in between electrodes.

Relating results to the anatomy or to results from other subjects is more challenging, because this requires 3D mapping techniques using a standardized co-

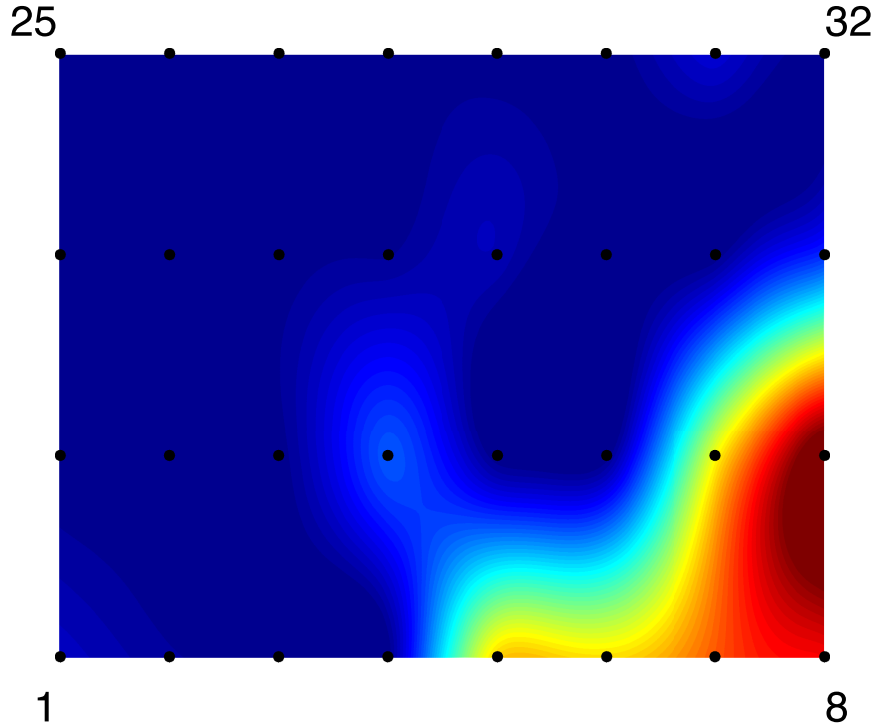


Figure 2.8: Example of 2D topographical mapping using `topoplot`.

ordinate system. Several tools have been implemented to visualize signals obtained by various medical imaging techniques (e.g., Cox and Hyde [1997], Dale et al. [1999], Darvas and Pantazis [2004], Delorme and Makeig [2004], Weber [2005]). While these tools are often powerful, they typically focus on visualization of volumes, such as those derived by functional magnetic resonance imaging (fMRI), or of signals acquired using scalp-recorded electroencephalography (EEG). In addition, some of these visualization tools are part of expensive commercial packages, or require the installation and configuration of complex environments. To facilitate the work in this dissertation, I set out to develop a practical tool that can visualize results derived from ECoG signals on a normalized template of the cortex so that results may be related to the anatomy or to those from other subjects.

This tool required three different inputs. The first input was a normalized model of the cortex (see Figure 2.9). I obtained this model (i.e., a set of triangles and vertices) in Talairach coordinates (Talairach and Tournoux [1988]) (one of the two standardized brain coordinate systems along with the MNI (Montreal Neuro-



Figure 2.9: 3D brain template. This template is in Talairach coordinates and was derived from source code provided on the AFNI SUMA website (see text).

logical Institute) system) from source code provided on the AFNI SUMA website (<http://afni.nimh.nih.gov/afni/suma>)<sup>3</sup>. The second input was the locations of the electrodes in the same (i.e., Talairach) coordinate system. I used lateral skull radiographs to identify the stereotactic coordinates of each grid electrode with custom software that realized the manual procedure described in Fox et al. [1985] and that was written by Kai Miller in work ancillary to this dissertation. The third input was the actual data to be visualized (e.g., values of  $r^2$  at different locations).

These three inputs provided sufficient information to display the ECoG data to be visualized on the standardized brain model at the locations from which they were derived (e.g., using different colors to represent data to be visualized). However, two issues complicated effective visualization and/or interpretation. First, reconstructed

---

<sup>3</sup>AFNI is a set of C programs for analyzing and visualizing data collected using functional magnetic resonance imaging (fMRI). SUMA is a program that adds surface-based visualization capabilities to the AFNI suite of programs (Cox and Hyde [1997]).

electrode locations were typically close to but not exactly on the surface of the 3D brain template. Second and more importantly, the nature of the results was such that it only provided data points at discrete points in 3D space (i.e., at the locations of the electrodes). Visualizing signal amplitudes at only these discrete points on a brain model would not effectively communicate information. (See the corresponding example for 2D visualizations in Figure 2.8.)

I thus sought to develop methods to overcome these two issues. The resulting procedure, illustrated in Figure 2.10 and Figure 2.11, first approximated each actual electrode location by projecting electrodes onto the brain model and thus resulted in more accurate visualization. Subsequently, the procedure calculated, for each data point, an activation function by convolving the data point with a point spread function so that not only discrete points but whole areas of the cortex were activated (i.e., changed their color) by a particular signal or data value. This facilitated interpretation of the results. These two steps are described in the following paragraphs.

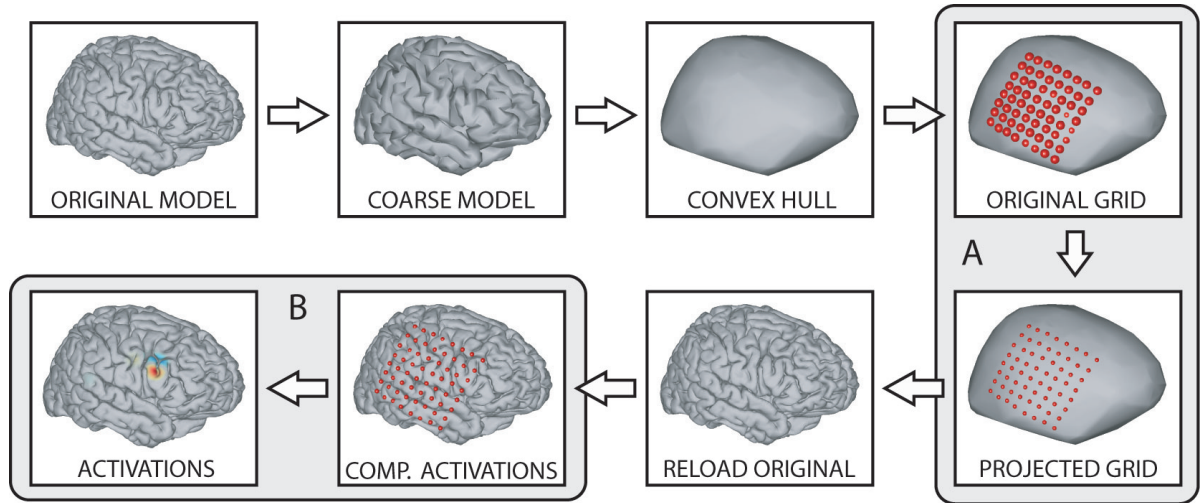


Figure 2.10: Flow chart of the visualization procedure.

**Projection of Electrode Locations** The 3D brain template and the electrode locations that are input to the procedure are both in Talairach coordinates. Thus, in theory, electrode locations should be exactly on the surface of the brain template since the real electrodes were placed directly on the surface of the brain. However,

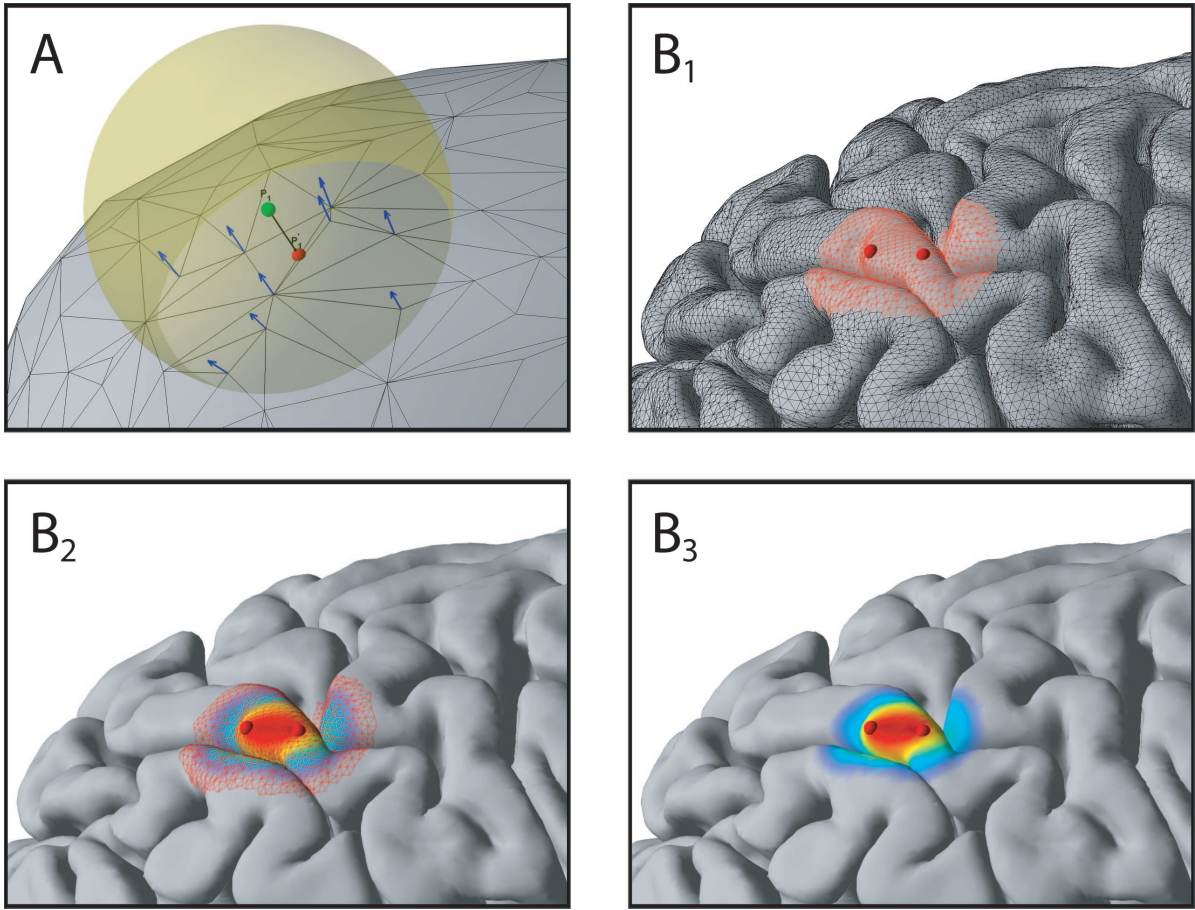


Figure 2.11: Projection and activation procedure. *A*: Electrode locations are projected onto the the brain surface using the average normal vector at all vertices within a given radius. *B*<sub>1</sub>-*B*<sub>3</sub>: Example for the computation of an activation function using two electrodes with equal data values.

small errors in the definition of the brain template and/or the electrode locations will cause the electrodes to be either below or above the cortical surface.

The first step in the visualization procedure was thus to project the electrodes onto the surface of the template brain model. To do this, I calculated the convex hull of the brain template to approximate the surface of the electrode grid that was placed on the actual brain. Because the brain template was very detailed (700k triangles, 350k vertices), computing the convex hull would be computationally expensive. I thus first calculated an approximated version of the brain template with fewer vertices before I calculated the convex hull. Both steps were computed using existing Matlab functions.

I then projected each electrode location  $P_n(x, y, z)$  onto the brain surface of the brain model BM, which consisted of 3-dimensional vertices  $V_i(x, y, z)$  ( $i = 1, 2, \dots, N$ ) that defined triangles that formed the surface. This procedure, which is formally described in Alg. 1 and illustrated in Figure 2.11-A, produced a projected location  $P'_n(x, y, z)$ .

```

input : brain surface described by the set of vertices  $V$ , set of
        triangles  $T$  and a function FindTriangles, returning the
        triangles associated with a certain vertex
        point to project  $P_n(x, y, z)$ 
output: projected point  $P'_n(x, y, z)$ 
foreach vertex  $V_i \in V : \|V_i - P_n\| < R$  do
    get vertex normal vector  $\vec{n}_i : \vec{n}_j \leftarrow \text{GetVertexNormal}(V_i)$ 
    store the vertex normal vector  $\vec{n}_i$  into a data structure  $N_{sel}$ 
    find triangles  $T_s \subset T : T_s \leftarrow \text{FindTriangles}(V_i)$ 
    store the triangles  $T_s$  into a data structure  $T_{sel}$ 
    compute average normal vector  $\vec{n} \leftarrow \text{Average}(N_{sel})$ 
foreach triangle  $T_j \in T_{sel}$  do
    for plane  $L$  defined by triangle  $T_j$  and line  $\bar{l}$  defined by the average
    normal  $\vec{n}$  and point  $P_n$ , find the intersection point
     $I \leftarrow \text{Intersection}(L, \bar{l})$ 
    if IsInsideTriangle( $I, T_j$ ) then
        store  $I$  into a data structure  $I_{sel}$ 
the projected point  $P'_n$  is the closest intersection  $I$  to the original point
 $P_n$ :  $P'_n \leftarrow \underset{I \in I_{sel}}{\operatorname{argmin}} \|I - P_n\|$ 
```

**Algorithm 1:** The algorithm that projected the electrodes onto the brain surface.

I used several external functions in this algorithm. The function **GetVertexNormal** was part of Matlab and computed vertex normal vectors. The function **Intersection** (Marschner [2003]) intersected a line with a particular triangle. The function **IsInsideTriangle** (Burkardt [2005]) determined whether this intersection produced a point that was within or outside the triangle.

**Computing Activations** The first step in the visualization procedure was the projection of all electrode locations onto the surface of the brain template. This resulted in a set of projected electrodes  $P'_n$  that were within particular triangles of

the template.

The second step in the procedure was the appropriate visualization of data values at these locations. As described earlier, the only correct way to do this is to associate the data values with their corresponding locations only (e.g., to draw a dot at each electrode location whose size corresponds to the size of the electrode and whose color corresponds to a function of the data value). This correct procedure does not facilitate comparison and interpretation.

I initially set out to interpolate data values between electrodes so as to approximate the underlying signal distribution. However, electrode locations can be irregular and thus the definition of boundary electrodes is difficult. I then resorted to a different approach, in which I performed a convolution of the data value at each electrode with a fading kernel. I chose a linear fading kernel whose value reached zero at the typical inter-electrode distance. In this case, the sum of the activations for two electrodes at any point of the cortical surface provided a linearly interpolated value between these two electrodes. If two adjacent electrodes had the same data value, brain areas on a straight line between these two electrodes would have the same color (see Figure 2.11-B). Thus, while the choice of the fading kernel was somewhat arbitrary, I felt confident that it would facilitate interpretation. Furthermore, because this procedure could be performed independently for each electrode, it would naturally support irregular electrode positions such as those from multiple subjects and would thus facilitate comparisons. Refer to Alg. 2 for the complete procedure.

## 2.6 Aim 3: Use of ECoG Signals for Real-Time BCI Control

The third and last of my three aims of **THEME I** of this dissertation was to utilize the methods and relationships developed in the previous two aims, combined with existing BCI methods, to conduct real-time BCI experiments. The principal results of this study show that humans with epilepsy can use ECoG signals to rapidly gain control over a computer cursor using imagery only. This is in marked contrast to the weeks or months typically required using EEG (Wolpaw et al. [2002]). Because training time is one of the critical issues that currently impede the translation

```

input : brain surface described by the set of vertices  $V$ 
        projected electrodes  $E_k \in E$  and assoc. data values  $a_k$ 
output: activation values  $v_i$  for each vertex  $V_i \in V$ 

function FadingKernel ( $activ, dist$ ) /* linear kernel */ 
const  $K, maxDist$ 
if  $dist > maxDist$  then
| return 0
else
| return  $activ - K * dist$ 

init:  $v_i = 0, \forall i$  /* the actual activation computation */
foreach electrode  $E_k \in E$  do
| foreach vertex  $V_i \in V : \|V_i - E_k\| < R$  do
| | add an activation value to the value at vertex  $V_i$  as a
| | contribution of electrode  $E_k$ :
| |  $v_i \leftarrow v_i + \text{FadingKernel}(a_k, \|V_i - E_k\|)$ 

```

**Algorithm 2:** Computation of the brain activations. This example makes use of a linear fading kernel.

of EEG-based laboratory demonstrations into widely used clinical applications for people who are paralyzed, the results of this study has important implications for BCI research.

### 2.6.1 Introduction

I studied four patients in St. Louis in whom ECoG electrode arrays were implanted for 3-8 days in preparation for surgery to remove an epileptic focus. (See Table 2.1 for clinical profiles.) The experimental approach was developed based on current understanding of sensorimotor rhythms and on the methodology of current EEG-based BCIs that use these rhythms (Wolpaw et al. [2003], Wolpaw et al. [2002] for review). Sensorimotor rhythms comprise mu (8-12 Hz), beta (18-26 Hz), and gamma ( $>30$  Hz) oscillations (Wolpaw et al. [1991, 2003], Pfurtscheller et al. [2000a], Kostov and Polak [2000], Levine et al. [2000]). They are thought to be produced by thalamocortical circuits and they change in amplitude in association with actual or imagined movements (Levine et al. [2000], Pfurtscheller et al. [2003], Levine et al. [1999], Huggins et al. [1999], Rohde et al. [2002], Pfurtscheller and Cooper [1975]). BCIs based on EEG oscillations have focused exclusively on mu and beta rhythms

because gamma rhythms are inconspicuous at the scalp (Pfurtscheller and Cooper [1975]). In contrast, gamma rhythms as well as mu and beta rhythms are prominent in ECoG (Levine et al. [2000], Pfurtscheller et al. [2003], Levine et al. [1999], Huggins et al. [1999], Rohde et al. [2002]). The results presented in this chapter are the first report that applied ECoG activity to online operation of a BCI system. I identified the locations and frequency bands of ECoG sensorimotor rhythms associated with specific movements or speech, or with imagery of those actions, and then determined whether people could learn to use these rhythms to control a cursor on a computer screen. (See Methods Section for additional details.)

The principal results show that people can quickly learn to use the ECoG activity associated with imagery to control a cursor. These results indicate that an ECoG-based BCI could provide control that is more precise and more quickly acquired than that provided by EEG-based BCIs, and at the same time may have signal stability advantages over BCIs that use microelectrodes implanted in cortex. Thus, BCI methods based on ECoG might prove of substantial value and thereby considerably extend and facilitate the application of BCI technology to the communication and control needs of people with severe motor disabilities.

## 2.6.2 Methods

### 2.6.2.1 Subjects and Experimental Paradigms

The subjects in this study were four patients with intractable epilepsy who underwent temporary placement of intracranial electrode arrays at Barnes-Jewish Hospital in St. Louis. They included three men (Patients A, B, and D) and one woman (Patient C). (See Table 2.1 for additional information.) All gave informed consent. The study was approved by the Human Studies Committee of Washington University Medical Center. Prior to this study, these patients had not been trained on a BCI system.

Each patient had a 48- or 64-electrode grid placed over the left fronto-parietal-temporal region including parts of sensorimotor cortex. These grids consisted of electrodes with a diameter of 2 mm and an inter-electrode distance of 1 cm (see Figure 2.12). Grid placements and duration of ECoG monitoring were based solely

Patient	Age	Sex	Cogn./Motor Capacity	Seizure Type	Seizure Focus
A	28	M	Moderately impaired	GTC	Frontal lobe
B	23	M	Normal range	CP	Left middle TL
C	35	F	Normal range	CP	Left inferior and mesial TL
D	33	M	Mildly impaired	CP+GTC	Left middle and posterior TL

Table 2.1: Clinical profiles. All patients were literate and functionally independent. During the period in which ECoG data were collected, Patient A was acutely impaired (e.g., in speech fluency, attention, and response times) by slow post-operative recovery. None of the patients had a traumatic or structural lesion that was responsible for their seizures (i.e., all had idiopathic epilepsy). Abbreviations: M, male; F, female; GTC, general tonic clonic; CP, complex partial; TL, temporal lobe.

on the requirements of the clinical evaluation, without any consideration of this study. Following placement of the subdural grid, each patient had post-operative anterior-posterior and lateral radiographs to verify its location.

### 2.6.2.2 Data Collection

Each patient sat in a hospital bed about 75 cm from a video screen. In all experiments, I recorded ECoG from 32 electrodes (i.e., the upper part of the implanted grid) using the general-purpose BCI system BCI2000 and the interface routines developed in Aim 1 (Section 2.4). All electrodes were referenced to an inactive electrode located over the temporal lobe far from the signal electrodes, amplified, bandpass filtered (0.1-220 Hz), digitized above the Nyquist rate at 500 Hz, and stored. The amount of data obtained varied from patient to patient, and depended on the patient’s physical state and willingness to continue.

### 2.6.2.3 Identification of ECoG Features to be Used for Online Cursor Control

As described in the literature, ECoG signals over certain locations can change with actual or imagined movements or speech (Crone et al. [1998b,a, 2001], Pfurtscheller et al. [2003]). Figure 2.12 shows an example of this effect that can be the basis for a BCI. Consequently, I initially determined which ECoG features (i.e., amplitudes in particular frequency bands at particular electrode locations) were cor-

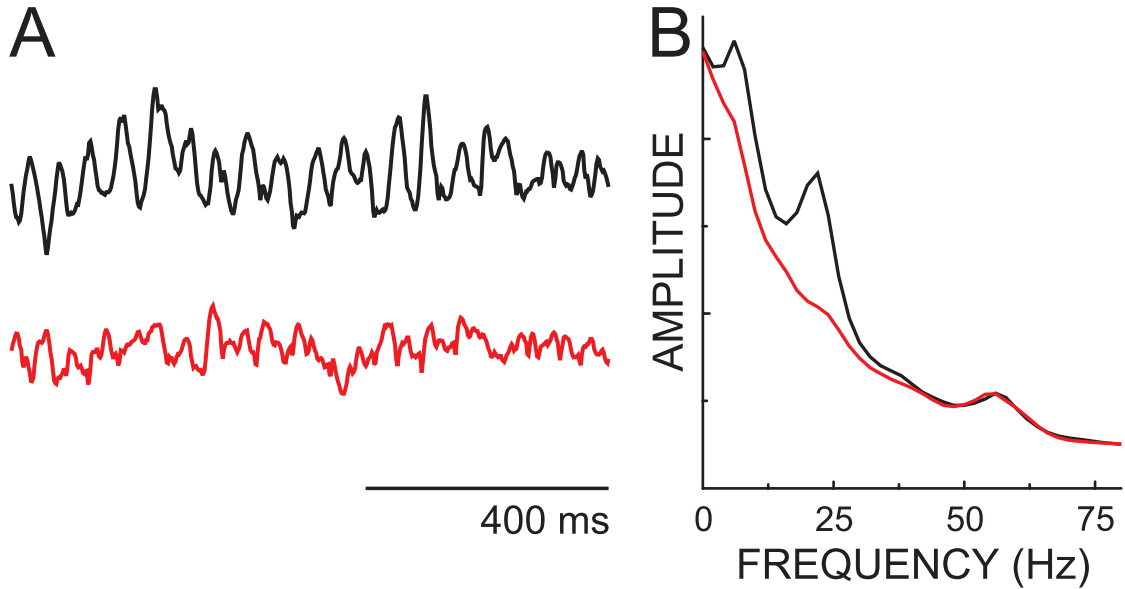


Figure 2.12: Example of ECoG signals during a task and rest. A. Raw ECoG signals from patient C during rest (black trace) and imagery of saying the word "move" (red trace). The oscillation associated with rest is evident and is suppressed during imagery. B. Spectra for the corresponding conditions. Imagery is associated with decrease in mu (8-12 Hz) and beta (18-26 Hz) frequency bands.

related with a particular movement, speech, or motor imagery task, and might thus be the basis for BCI experiments.

In each of eighteen 2-min runs, the patient was asked to perform one of six tasks (i.e., three runs for each task). The six tasks were: open and close the right or left hand, protrude the tongue, say the word "move," and imagine performing each of these three actions. In each run, the patient performed about 30 repetitions of the required task in response to a visual cue that lasted 2-3 sec (during this interval, the patient repeated the task continuously), and rested when the screen was blank for 1 sec.

I then identified, for each task, the locations and frequency bands in which amplitude was different between the task and rest. For these analyses, I converted the time-series ECoG data into the frequency domain (0 and 200 Hz in 2-Hz bins) as described in Section 2.5.1. This produced a set of frequency spectra for each location and for each task and rest. I then calculated the statistical difference for the distribution of frequency amplitudes at each location and frequency (i.e., values

of  $r^2$ , which indicated what fraction of the signal variance at that location and frequency was due to the condition of task and rest; see Section 2.5.2). In other words, this procedure identified features that could be modulated by the subject using actual or imagined tasks, and were thus candidates for the control of cursor movement in the subsequent online BCI experiments. Figure 2.13 shows an example analysis calculated for one subject and for right hand movement and rest. The top panel (A) shows the values of  $r^2$  (color coded) for each channel and frequency. Signals at particular locations and frequencies exhibit a difference between the task and rest. The middle panel (B) and bottom panel (C) show subsets of these data in (A) calculated for one electrode (B) or frequency (C). The middle panel (B) shows the average spectra (left) for right hand movement (green trace) and rest (red trace), as well as the corresponding values of  $r^2$  (right) for channel 15. The bottom panel (C) shows the topography of  $r^2$  values calculated at 20 Hz.

Using this procedure, I derived analyses for each patient and task. I then determined the features (i.e., locations and frequencies) that had the highest values of  $r^2$  and whose topographical and spectral distribution exhibited the best congruence between actual and imagined versions of the same movement. This identification procedure was most likely suboptimal, so that other tasks, locations, and frequencies might be better sources of control. This problem of identifying signal features, and a proposed solution, are discussed in **THEME II** of this dissertation.

Each task in each patient was typically associated, as expected, with decreased mu and beta rhythm amplitudes (Pfurtscheller et al. [2003]) and increased gamma rhythm amplitude at several locations over pre-frontal, pre-motor, sensorimotor, and/or speech areas (Pfurtscheller and Aranibar [1977], Pfurtscheller [1992]). The spatial and spectral foci of task-related ECoG activity, as revealed in the  $r^2$  analysis, were usually similar for action and for imagination of the same action (e.g., saying the word "move" and imagining saying the word "move") (McFarland et al. [2000]).

#### **2.6.2.4 ECoG Control of Vertical Cursor Movement Online**

I then conducted closed-loop BCI experiments in which the patient received online feedback that consisted of one-dimensional cursor movement (see Figure 2.14)

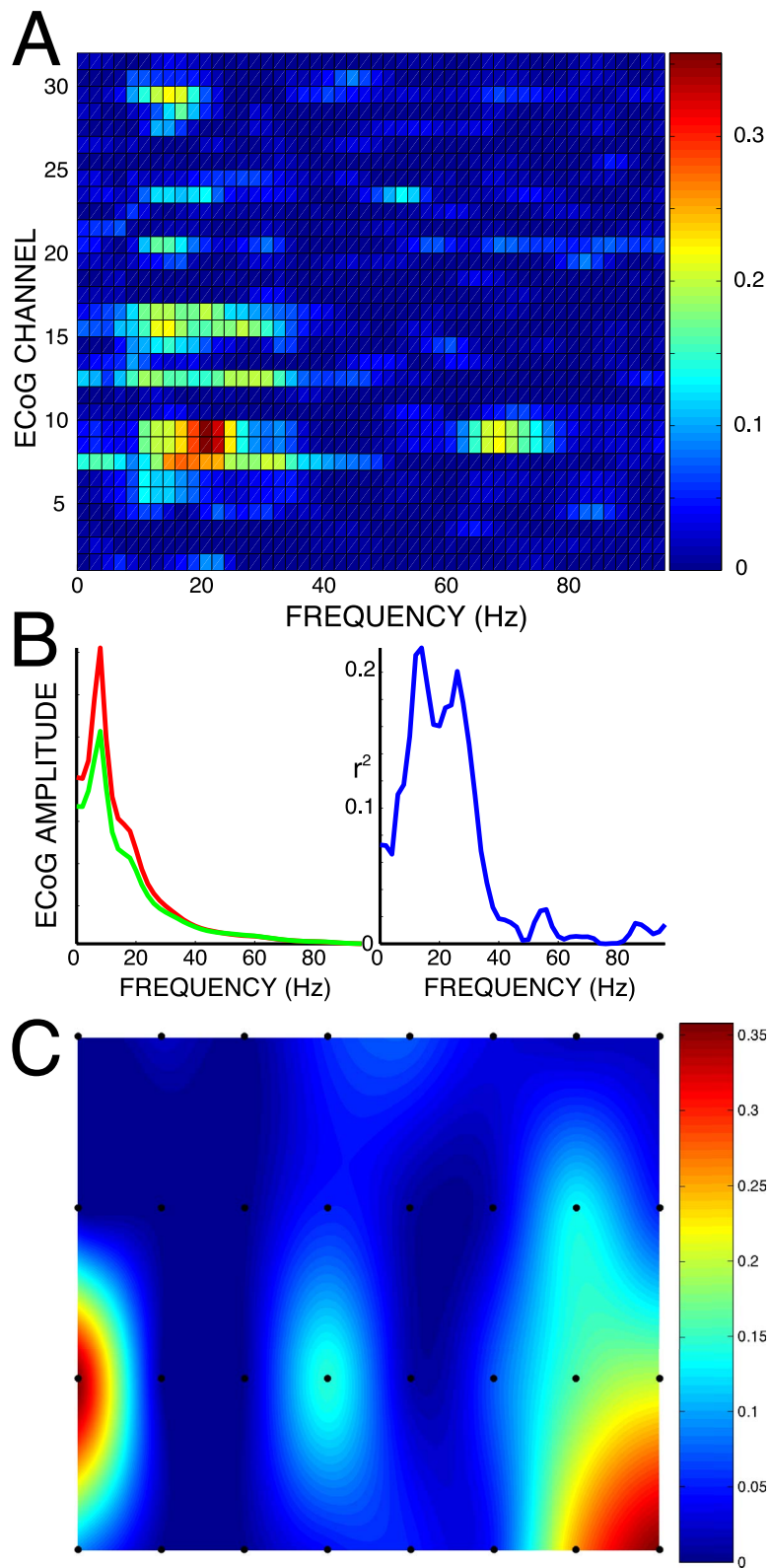


Figure 2.13: Analysis comparing right hand movement and rest. A: Values of  $r^2$  for all locations and frequencies. B: Average (left) and  $r^2$  spectra for electrode 15. C: Topographical distribution for  $r^2$  values calculated for 20 Hz.

controlled by the ECoG features that were identified as described above. In other words, the patients received one-dimensional feedback that was proportional to signal amplitude at particular channels and frequencies as follows: the cursor moved vertically every 40 ms based on a weighted, linear summation of the amplitudes in the identified frequency bands from the identified electrodes for the previous 280 ms. The weights were chosen so that the cursor moved up with task execution (e.g., imagining tongue protrusion) and down with rest. This relationship was explained to the patients prior to these experiments.

The ECoG features were integrated over time to yield the current cursor position (i.e., ECoG activity was treated as vertical velocity information (Wolpaw et al. [2003])). Data were collected from each patient for one to eight 3-min runs, each comprised of 21-37 trials. The runs were separated by 1-min breaks. Each trial began with the appearance of a target that occupied either the top or bottom half of the right edge of the screen (block randomized throughout the run). One second later, the cursor appeared in the middle of the left edge of the screen and then moved steadily across the screen over a fixed period of 2.1-6.8 sec with its vertical movement controlled continuously by the patient's ECoG features. The patient's goal was to move the cursor vertically so that it hit the appropriate (i.e., upper or lower) half of the screen when it reached the right edge. One-half sec after the cursor reached the right edge of the screen, the screen went blank, signaling the end of the trial. After a pause of one sec, the next trial started. Because there were two possible outcomes in each trial, the accuracy expected in the absence of any control was 50%.

#### **2.6.2.5 Anatomical and Functional Mapping**

Radiographs were used to identify the stereotactic coordinates of each grid electrode (Fox et al. [1985]), and cortical areas were defined using Talairach's Co-Planar Stereotaxic Atlas of the Human Brain (Talairach and Tournoux [1988]). After the experiments described above, each patient underwent stimulation mapping to identify motor and speech cortices as part of his/her clinical care. In this mapping, 1-ms 5-10 mA square current pulses were passed through paired electrodes to induce

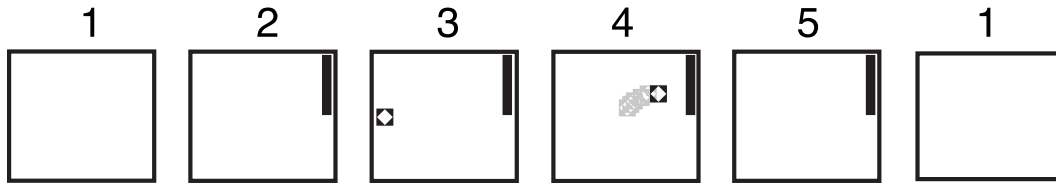


Figure 2.14: One-dimensional BCI task. First, the screen was blank. One second later, a target appeared in either on the top or bottom on the right edge of the screen. One second later, a cursor appeared on the left edge. The cursor travelled across the screen with its vertical velocity controlled by the patients' ECoG signals. The patients' task was to hit the target.

sensation and/or evoke motor responses (including speech arrest). The experimental results described above were collated with these anatomical and functional mapping data. The topographical correlations between electrical stimulation and movement or imagery were not strong enough to support clear conclusions. See Figure 2.15.

### 2.6.3 Results: ECoG Control of 1D Cursor Movements

For each patient, I selected one or two electrodes and up to four mu, beta, and/or gamma frequency bands that showed the highest correlations with one of the three actions or imagery tasks described above (i.e., the ECoG features that had the highest values of  $r^2$ ). Patients then used the amplitudes of these features to control cursor movement in an online BCI protocol in which the objective was to move the cursor up or down to a target located in the upper or lower half of the screen. For example, patient B imagined right hand movement to move the cursor up, and rested to move it down. The accuracy expected if patients lacked any ECoG control was 50%.

Patients completed one to eight 3-min runs separated by 1-min breaks. Each run comprised 33 individual trials (5.5 sec per trial). Over these short training periods (3-24 min), all four patients achieved significant control of the cursor (74%-100% final accuracy), which is in contrast to the weeks and months of training required using EEG (Wolpaw et al. [2002]). Table 2.2 summarizes all results and Figure 2.16 and Figure 2.17 show analyses for the subset of results in which patients used imagined actions to control the system. I focus on imagined actions (rather

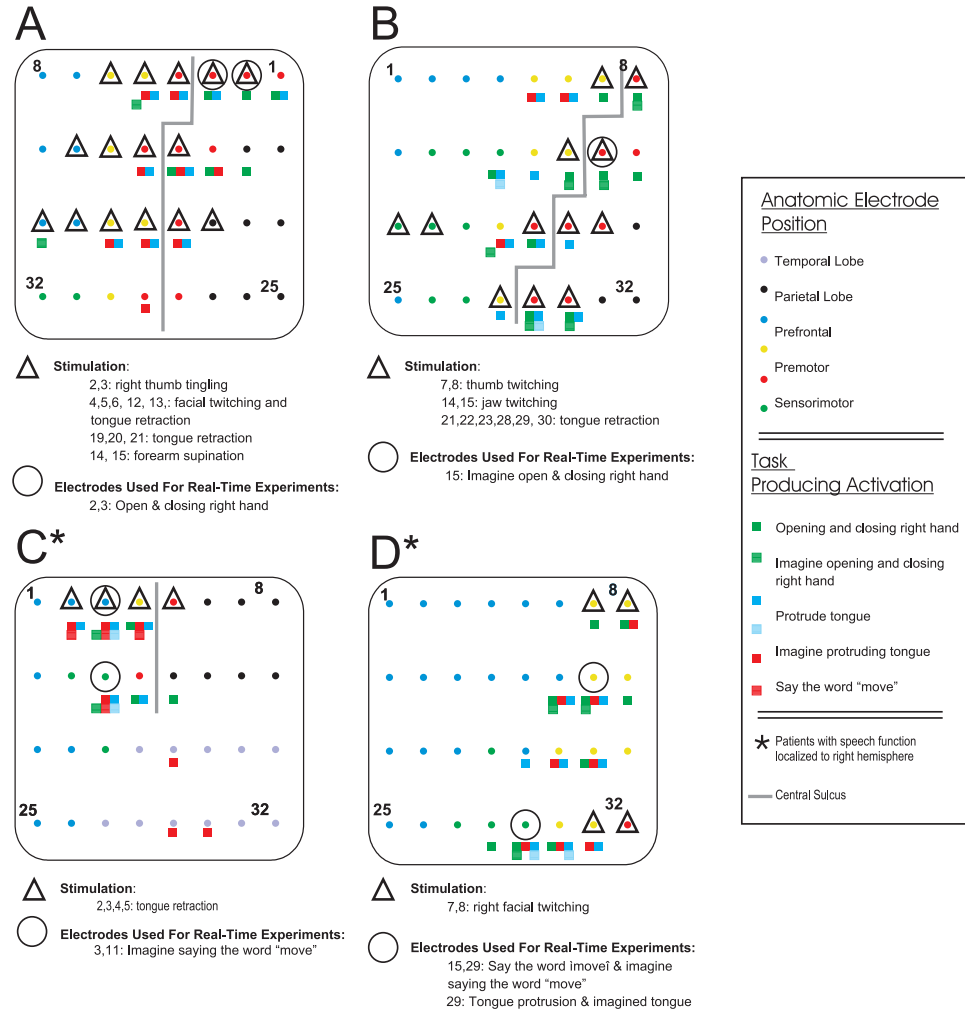


Figure 2.15: Electrode locations that showed signal differences according to the motor/imagined tasks (marked in different colors underneath each electrode), as well as using electrical stimulation (see triangles and legend). Topographical correlation is not strong enough to support clear conclusions. Figure courtesy of Dr. Eric Leuthardt.

than real actions) because they are most relevant to BCI use by people who are paralyzed. Figure 2.16 illustrates for the final runs the strong correlation between the goal (i.e., moving the cursor up or moving it down) and the ECoG activity that controlled cursor movement. Figure 2.17 shows the rapid improvements in accuracy over the brief periods of study.

Patient	Action or Imagined Action	Brodmann's Area	Frequency Band (Hz)	Amplitude Change	Final Accuracy
A	Opening and closing right hand	2	10.5-18.5	Decrease	74%
		2	48.5-54.5	Increase	
		3	30.5-34.5	Increase	
		3	48.5-50.5	Increase	
B	Imagining opening and closing right hand	3	30.5-32.5	Decrease	83%
C	Imagining saying "move"	9, 44	20.5-22.5	Decrease	97%
D	Saying "move"	6, 45	12.5-14.5	Decrease	93%
		6, 45	26.5-28.5	Decrease	
		6, 45	34.5-36.5	Decrease	
		6, 45	12.5-14.5	Decrease	97%
	Imagining saying "move"	6, 45	26.5-28.5	Decrease	
		6, 45	34.5-36.5	Decrease	
		45	12.5-14.5	Decrease	100%
	Protruding the tongue	45	12.5-14.5	Decrease	84%
	Imagining protruding the tongue	45	12.5-14.5	Decrease	

Table 2.2: Actions and imagined actions, electrode locations, and ECoG frequency bands used for ECoG control of one-dimensional cursor movement, and final accuracies of that control. Brodmann's areas were calculated using skull radiographs and a Talairach atlas.

## 2.6.4 Discussion

This study for THEME I of this dissertation demonstrates for the first time rapid learning during closed-loop real-time control of cursor movements using ECoG activity associated with motor or speech imagery (Figure 2.17). Using signal analysis and cursor control methods that were developed in BCI studies employing scalp-recorded EEG activity (Neuper et al. [2003], Wolpaw et al. [1997], Penny et al. [2000], Kübler et al. [1999]), this study found that ECoG-based control develops more quickly than EEG-based control (Wolpaw and McFarland [1994], Wolpaw et al. [2003]), and is likely to be substantially more effective in providing communication and control to people with severe motor disabilities.

Although the origin and nature of ECoG/EEG electrical oscillations are not fully understood, these results are, in general, consistent with the conventional overlapping homunculus model of cortical functional anatomy. The frequency changes elicited with various actual and imagined motor actions are consistent with previous evidence that during sensorimotor function (including speech), mu and beta rhythm amplitudes tend to decrease while gamma rhythm amplitudes tend to increase (Pfurtscheller et al. [2003], Pfurtscheller and Aranibar [1977], Crone et al.

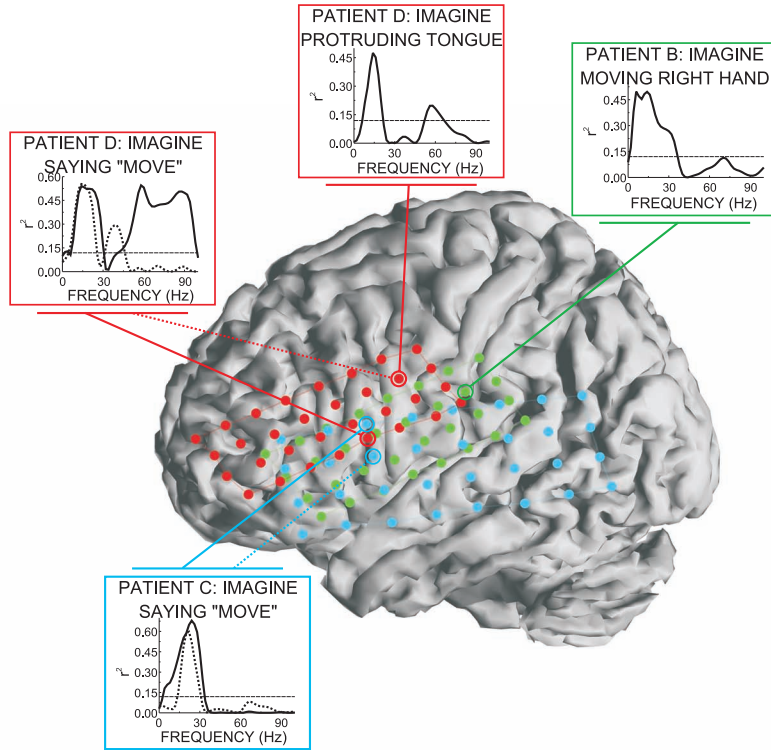


Figure 2.16: ECoG control of vertical cursor movement using imagination of specific motor or speech actions to move the cursor up and rest to move it down. The electrodes used for online control are circled and the spectral correlations of their ECoG activity with target location (i.e., top or bottom of screen) are shown. Grids for Patients B, C, and D are green, blue, and red, respectively. The particular imagery tasks used are indicated. The substantial levels of control achieved with different types of imagery are evident. (The dashed lines indicate significance at the  $p=0.01$  level.) Correlations were calculated for the final two runs of online performance. Two different locations are shown for Patients C and D: the solid and dotted  $r^2$  spectra correspond to the sites indicated by the solid and dotted line locators, respectively.

[1998b], Schalk et al. [2004], Aoki et al. [1999]).

## 2.7 Conclusions

THEME I of this dissertation was concerned with a better signal acquisition methodology for BCI research. Current non-invasive and highly invasive signal acquisition methods have significant problems that impede the translation of successful BCI demonstrations into clinical practice. These problems are mainly the significant

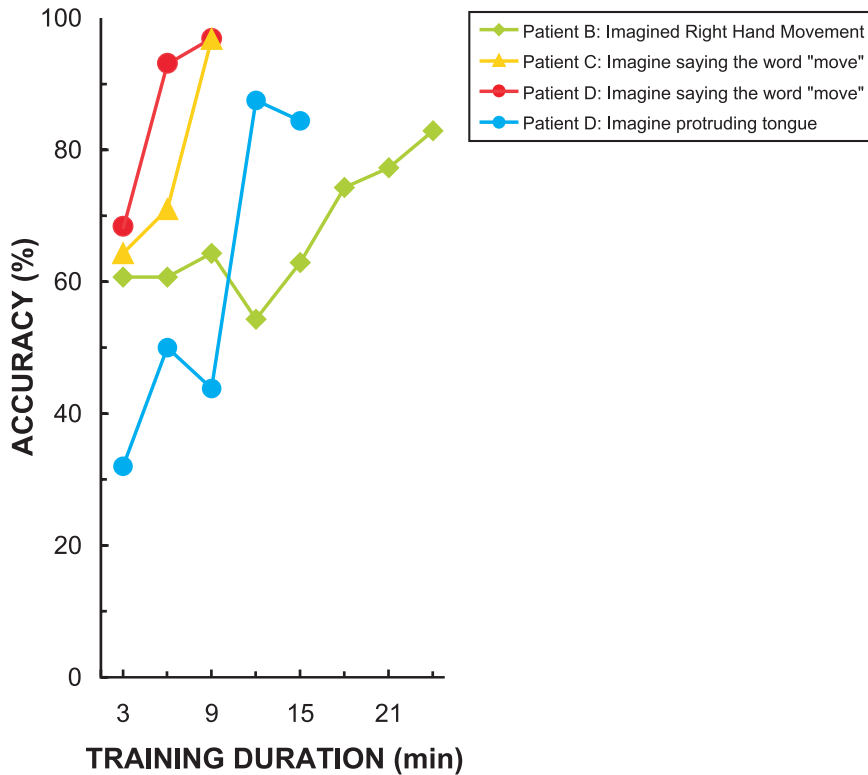


Figure 2.17: Learning curves for ECoG control of vertical cursor movement using motor imagery to move up and rest to move down (see text). Patient B (green line) imagined opening and closing the right hand, Patients C (yellow) and D (red) imagined saying the word "move," and Patient D (red) imagined protruding the tongue. In each case, the rapid acquisition of control is evident and statistically significant by  $\chi^2$  contingency test ( $p<0.05$ ,  $<0.005$ ,  $<0.005$ , and  $<0.001$ , respectively).

training requirements typically associated with EEG and the limited signal stability of intracortical recordings. Electrocorticographic (ECoG) signals are likely to be an excellent BCI modality because they have higher spatial resolution, better signal-to-noise ratio, and wider frequency range compared to EEG, and at the same time may have greater long-term stability compared to intracortical recording.

The results presented in this chapter support these expectations. The most important contribution to BCI research was the finding that the use of ECoG for on-line operation of a BCI system dramatically reduces training requirements compared to methods using EEG. In sum, further development of ECoG-based BCI methodology could greatly increase the power and practicality of BCI applications that can serve the communication and control needs of people with motor disabilities.

## 2.8 Recommendations

The results presented in this chapter demonstrate that ECoG can provide a plethora of signals that are accessible in humans and that could be utilized for BCI control. At the same time, this obvious benefit reveals two problems of traditional BCI signal processing and task methodologies.

The first problem concerns signal identification using existing signal processing techniques. As described in Section 2.6.2.3, the first step in utilizing ECoG for real-time BCI control is the identification of the features (i.e., signal amplitudes at particular locations and frequencies) that can be most effectively modulated by the subject using a particular task. Because of the higher fidelity of ECoG, the number of possible features and tasks is much higher than for EEG. This implies that the choice of features becomes more difficult, and that the subject has to execute more tasks to produce samples of these different signal features than for EEG. Moreover, ancillary analyses showed that signal features typically changed between the signal identification procedure and the real-time experiment, which is suboptimal given traditional static classification schemes. Full exploitation of the promise of ECoG signals will require addressing this problem of initial identification and subsequent tracking of signal features. **THEME II** of this dissertation proposes one solution to this problem. This methodology can be used effectively in situations in which there is not much *a priori* knowledge about signal features.

The second problem is related to the somewhat non-intuitive tasks utilized for BCI control. Using an ideal brain-computer interface, a subject with a motor disability could simply attempt a particular movement and his/her intended movement would be detected using the BCI and translated in a corresponding action of a computer cursor or robotic arm. In contrast, the subjects in the experiments presented in this chapter used somewhat non-intuitive imagery (such as imagined tongue or hand movements) to drive a computer cursor. It thus appears likely that extension of the present methodology from one-dimensional to multi-dimensional control using non-intuitive imagery will require more user training. At the same time, ECoG might also contain directional information about executed or intended movements (this information is utilized in highly invasive BCI systems in primates). This pos-

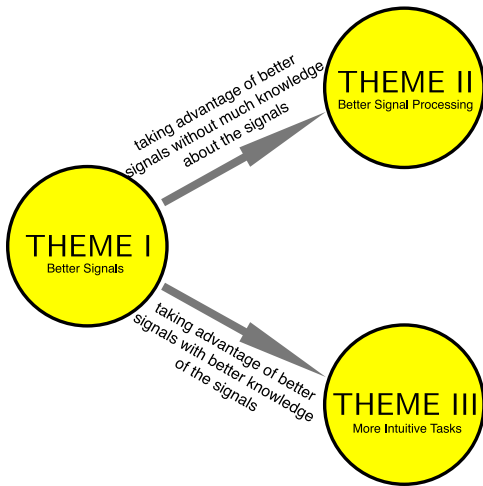


Figure 2.18: Recommendations resulting from **THEME I** of this dissertation.

sibility (which requires more specific knowledge about signal features) might more efficiently extend ECoG-based BCI control to multiple dimensions and is explored in **THEME III**.

## CHAPTER 3

### THEME II: BETTER SIGNAL PROCESSING

*It is not enough to aim; you must hit.* Italian Proverb.

#### 3.1 Summary of Contributions and Approach

This chapter discusses THEME II of this dissertation, which is about improved signal processing methodologies and implementations. At present, translation of BCI technology demonstrations into widespread clinical practice is impeded by the demands and requirements of an initial signal identification procedure that is currently required and that determines the combination of signals and tasks that best produce detectable brain activity.

The main contribution presented in this chapter is the finding that the use of a detection approach, which has previously been used in other fields such as image processing (but never in BCI signal processing), in a classification context can result in performance similar to that achieved by the classification-based techniques traditionally used in BCI research without needing the initial signal identification procedures that are typically required. This contribution encompasses a conceptual advance, algorithmic improvements, and the comprehensive validation of the corresponding method. The associated work is outlined in Figure 3.1. In addition to this contribution to BCI research, I also demonstrate that this approach to signal processing can also be used as a novel and effective way to visualize brain signals in real time. These results should thus facilitate the translation of laboratory BCI demonstrations into clinical practice, and could also be important for basic or clinical research and diagnosis.

No other BCI study has previously utilized a detection approach in a classification setting. In addition, there was no theoretical basis that could suggest the signal processing parameters that would provide optimal performance. I thus approached the validation of my novel approach using empirical evaluations that addressed mainly two questions. The first question was which signal processing procedures would provide best performance, i.e., would result in control signals that best

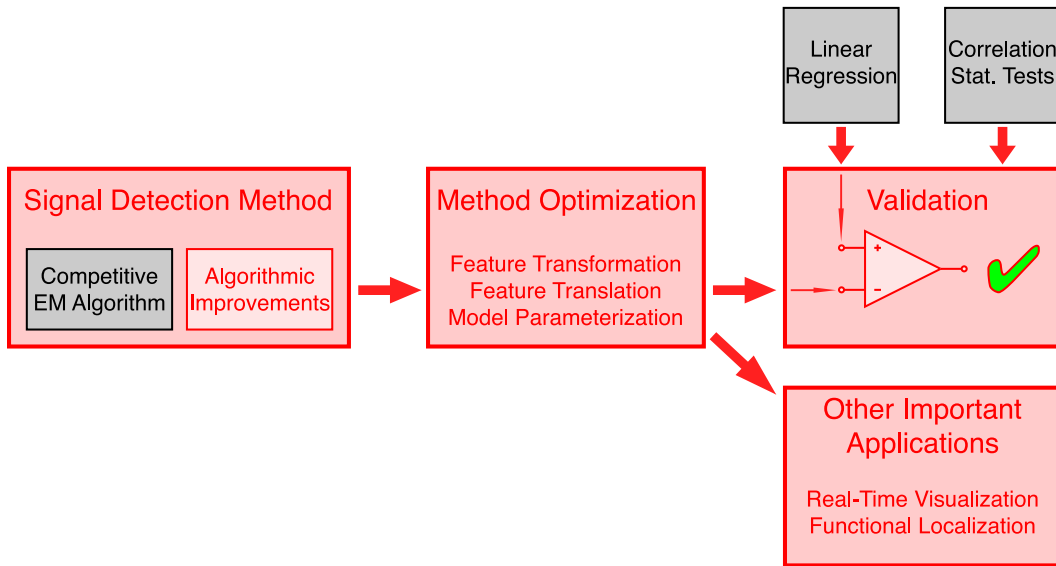


Figure 3.1: Overview of the work accomplished in THEME II. Items in red indicate work performed for this dissertation. Items in black indicate existing resources.

discriminated brain signals from different tasks. This question was thus mainly concerned with signal processing aspects of this problem. The second question was how the performance of this approach related to that of traditional (regression-based) methods.

The work in this chapter depended on application and extension of a number of methodologies from different areas of science and engineering, such as computer science, signal and image processing, and statistics, and was thus highly multidisciplinary. I used aspects of computer science, in particular C++ and Matlab programming, to implement my novel detection approach and to write software to support my analyses. I then used an array of signal and image processing methodologies to translate brain signal activity into device output signals. I finally employed statistical methods, such as regression and correlation, and parametric and non-parametric tests, to derive and to evaluate my results.

## 3.2 Introduction

Many people with severe motor disabilities need augmentative communication technology. Those who are totally paralyzed, or "locked-in," cannot use conventional augmentative technologies, all of which require some measure of muscle con-

trol. Over the past two decades, a variety of studies have evaluated the possibility that brain signals recorded from the scalp or from within the brain could provide new augmentative technology that does not require muscle control (e.g., Farwell and Donchin [1988], Wolpaw et al. [1991], Sutter [1992], McFarland et al. [1993], Pfurtscheller et al. [1993], Birbaumer et al. [1999], Kübler et al. [1999], Kennedy et al. [2000])(see Wolpaw et al. [2002] for a comprehensive review). These brain-computer interface (BCI) systems measure activity of particular brain signals and translate them into device control commands. A BCI thus creates a new communication channel that replaces the brain's normal output of nerves and muscles and the movements they produce with a new output, directly from the brain to the output device.

In contrast to typical communication systems, in BCI systems it is completely unclear which signals actually convey intent, which makes the BCI problem more conceptually and practically difficult than the information transmission problem encountered in typical communication systems. The next section expands on this issue and describes how this added difficulty currently impedes clinical application of BCI systems.

### **3.2.1 The Signal Identification Problem**

Successful creation of a new communication channel – directly from the brain to an output device – depends on two requirements. The first requirement is the use of an adequate sensor that can effectively measure the brain signal features that can communicate a user's intent. As described in Section 1.1, multiple sensors exist that can in principle detect relevant signals. However, practicality and speed considerations exclude most of these options so that almost all BCI systems to date depend on detection of electrophysiological signals using sensors within the brain or on the scalp. In humans, safety and stability issues have confined most studies to electroencephalographic (EEG) recordings from the scalp.

The second requirement is the negotiation of a mutual language (i.e., brain signal features in various domains such as time-domain or frequency-domain and detected at particular locations), so that, as in any other communication system, the user may use the symbols of this language to communicate intent, and the

computer can detect these symbols and effect this intent. This is a difficult problem for at least two reasons. It is not clear *a priori* which symbols can most effectively convey intent, and it is not clear which subset of these can also be detected by the sensor. Second, it is unclear how to most effectively instruct the user in this new language. Imagine that your task was to talk to somebody who speaks a different language that you do not understand, but you do not have a teacher to introduce you to the aspects of this different language. In other words, without guidance as to how to produce the necessary symbols, it might be impossible or impractical for a user to learn this new language. It is thus imperative to also determine how to instruct a user about the task that will produce symbols of this language.

As long as the language and its symbols are not defined, it is clearly not possible to build a detector to extract them. Unfortunately, for two reasons it is also not possible to use any arbitrary language. First, the brain might simply not be physically able to produce the symbols of this language. For example, one might define the arbitrary language as the amplitude coherence between two different frequency bands at one particular location, and its symbols could be discrete coherence amplitudes, but the brain might simply not be physically able to produce changes in amplitude coherence at the selected frequencies and locations. Second, the brain might be able to produce the symbols of this language, but might not be able to use them to convey intent. For example, one might define the arbitrary language as amplitude modulations at 10 Hz over visual areas of the brain. Many studies have shown that repetitive visual stimuli at particular frequencies (such as 10 Hz) can evoke oscillatory responses in the brain (Morgan et al. [1996]), so clearly the brain is physically able to modulate activity at 10 Hz and can thus produce different symbols of that arbitrary language. However, it might not be able to produce these symbols without the visual stimuli or might not be able to use these symbols to convey intent.

Despite these fundamental difficulties and the complete absence of any theoretical foundation that could suggest the signal acquisition methodology, location, or signal domain that are best suited for communication, experimental evidence is able to provide some basic guidance: as described in Chapter 1, many studies have

shown that actual and imagined tasks can have detectable effects on particular brain signals. These tasks, and the characteristics of the signals they modulate, could in principle be used as the basis for a BCI; Section 1.4 described the use of sensorimotor cortex rhythms for this purpose. Because these rhythms are the basis for the validations later in this chapter, their principles are briefly summarized again here.

In humans, primary sensory or motor cortical areas typically display 8-12 Hz EEG activity (i.e., the mu rhythm) when they are not engaged in motor output. The mu rhythm is typically associated with 18-26 Hz beta rhythms. While it is clear that beta rhythms are not simply harmonics of the mu rhythm, their exact relationship has not been elucidated. Because these signals can be modulated by movement but also movement imagery, they could serve as the basis for a BCI with one or more independent output channels.

In summary, a number of studies have shown that non-muscular communication and control is possible. At the same time, there is practically no theoretical basis (and thus no mathematical model) for the choice of signals for that communication. All current BCI systems are based on experimental observations that particular tasks (such as imagined hand movements) have particular effects on specific brain signals (such as the mu rhythm measured at a particular location). Nevertheless, the choice of signals and tasks is still difficult, because it is likely that it is suboptimal (so that a completely different signal and task might provide improved performance) and because it has to be optimized for each individual. In other words, even when only considering one possible physiological signal (such as the mu rhythm), the imagery task, best frequencies, and best locations have to be selected for each individual. The difficulty of choosing signals and tasks, and the reliance on experts this currently implies, could be regarded as the *signal identification problem* of BCI communication.

This critical issue, which impedes clinical application of BCI technology, provided the primary impetus for the improved signal processing methodology proposed in this chapter. Following sections further expand on this impetus. The terminology and examples in these sections are framed around mu/beta rhythm processing, but also apply to any other physiological brain signal.

### 3.2.2 Relevant Signal Processing Issues

One important reason for the difficulty of applying current BCI technology in clinical practice is that the demands and requirements of current signal processing approaches imply significant expert involvement and complex procedures. This is because current BCI signal processing techniques are similar to the feature extraction/classification approaches commonly found in communication systems (which typically demand a detailed understanding and thus a mathematical model of the transmitted signal), even though in BCI processing there is not much a-priori information about the signal used for communication.

One could thus say that current BCI signal processing approaches are unnecessarily focused on extracting the one specific brain signal that is modulated by one particular task, i.e., on the creation of a highly specific filter that works only if the user uses this very specific task. This basic approach has been implemented in numerous studies using standard signal classification techniques. All current methods thus require an initial procedure that identifies (for each user), out of all possible tasks those that best modulate any of the possible signals, and on the definition of a filter that extracts this particular brain signal. As an example of such a procedure, the subject may be asked to produce many repetitions of a number of actual and imagined tasks (e.g., moving or imagining to move both hands, both feet, left hand, right hand, etc.). Statistical analyses of the changes in the mu and beta rhythm bands then suggest the tasks, locations, and frequencies, that produce the most effective modulation in frequency amplitudes. These analyses thus suggest possible signal features to be used in subsequent BCI experiments. Paradoxically, this procedure becomes increasingly lengthy and impractical as the quality of the brain signal recordings (e.g., such as with electrocorticographic (ECoG) signals recorded from the surface of the brain), and thus the number of signals that can be detected and the number of mental tasks that might modulate these signals, increases.

Signal identification procedures become lengthy because the number of tasks that might modulate them increases, and because, with current methods, subjects have to be instructed to produce all of these tasks. They become impractical because it becomes progressively difficult to instruct a subject to consistently produce

a particular mental task (e.g., such as to imagine a particular type of movement) as the specificity of the task, and thus the specificity of the brain signals related to production of that task, increases. Furthermore, when subjects are asked to actually use the brain signals that were identified in the initial identification procedure for a different purpose, i.e., to control an output device, these brain signals (i.e., amplitudes at particular frequencies and locations) often change in response to the different task (of controlling the output device rather than producing a particular mental task, that is). It is thus possible that these different signals are not properly translated into device output signals even though the subject might exert good control over some aspects of detectable brain activity. In this scenario, which again is compounded as the feature/task space increases with better signal recording, subjects might eventually get frustrated and never properly learn the task.

In addition to these difficult initial configurations, the current approach to BCI signal processing also requires that the signal processing algorithm and BCI experts make continuous adjustments as this brain signal changes in response to plasticity in the brain and to the user's attempt to adjust mental strategies so as to optimize performance. These two requirements of all current BCI methods thus imply that the advantages of better ways to record and extract signals do not necessarily translate in corresponding performance increases, and that performance of current BCI systems crucially depends on the careful initial and continuous adjustment by BCI experts. In consequence, these demands of current methods severely impede the translation of current demonstrations of BCI technology into clinical application of practical value to people with severe disabilities. The central contribution of **THEME II** of this dissertation is a method that overcomes this significant problem. The following sections describe this method, its validation in the BCI context, and its application in other important areas.

### 3.2.3 A Novel Approach to BCI Signal Processing

The need for initial signal identification procedures and the continuous adjustments by BCI experts that are currently required could be removed if the goal of BCI signal processing was the detection of any change in a set of brain signal features (e.g., all possible mu/beta rhythm frequencies at appropriate locations), rather than

the detection of a specific change in one specific set of signal features (e.g., amplitude at 11.3 Hz at one specific location). This possibility would entirely eliminate the current requirement for determining the optimal task, location, and frequency prior to successful BCI operation. One could thus say that these problems could be overcome using a detection approach rather than a classification approach, but no previous BCI study has studied the use of a detection approach. I here propose the use of modeling techniques to characterize brain signal activity during rest, i.e., while no particular motor or imagery task is performed. This model can then be used to detect *any* change in the activity of the modeled signal. Most importantly, the creation of this model only relies on data recorded during rest and does not require data samples produced during a particular task, and thus obliterates the need for the signal identification procedures that are required by all methods that have been described in the hundreds of studies in the BCI literature to date.

The subsequent section illustrates the basics of BCI signal processing and describes which signal processing components are modified by the detection approach that is subsequently described in this chapter.

### 3.3 Overview of Traditional BCI Signal Processing

This section gives an overview of a representative example of the traditional procedures utilized in BCI signal processing. While procedures in some BCI systems might be organized somewhat differently, they are similar in the respects important to this section. Subsequent sections then describe the components of this procedure that were improved in this dissertation.

Signal processing typically consists of two major components: feature extraction and the translation algorithm<sup>4</sup> (Figure 3.2). Although this dissertation makes a contribution to the translation algorithm and not to feature extraction, common feature extraction procedures are briefly summarized in the next section to facilitate understanding.

---

<sup>4</sup>I use the term *translation algorithm* instead of *classification* throughout this dissertation, because the typically continuous nature of the device control signals produced by BCI signal processing is better expressed by the term translation algorithm rather than the discrete output that is typically implied by the term classification.

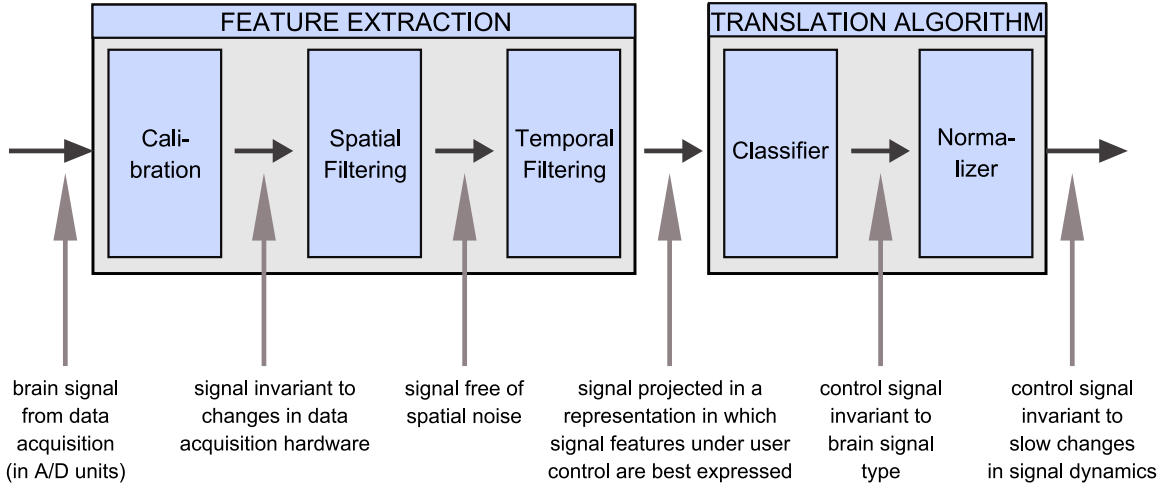


Figure 3.2: Example signal processing model. This model consists of feature extraction and translation and can describe all common BCI methods.

### 3.3.1 Feature Extraction

Feature extraction consists of a series of three procedures: calibration, spatial filtering, and temporal filtering. Each of these procedures may have different realizations. The following paragraphs describe those realizations that are relevant to mu/beta rhythm processing.

The initial step in feature extraction is signal calibration. Its purpose is to convert signals that are acquired with the data acquisition device into units of  $\mu V$  (using a scale factor  $g_h$ ), and to account for any additive signal offset  $o_h$  that might be introduced by the acquisition hardware. For a signal  $s_h(k)$  acquired at electrode  $h$  and at time  $k$ , this is accomplished using a simple linear equation with parameters  $o_h$  and  $g_h$ :

$$s'_h(k) = (s_h(k) - o_h) g_h \quad (3.1)$$

The second step in feature extraction is the application of a spatial filter that may have many possible realizations. The purpose of the spatial filter is to reduce the effect of spatial blurring. Spatial blurring occurs as an effect of the distance between the sensor and the signal sources in the brain, and because of the inhomogeneities of the tissues in between. Different approaches to spatial filtering have attempted to reduce this blurring, and thus to increase signal fidelity. The most sophisticated

approaches attempt to deblur signals using a realistic biophysical head model that is optimized for each user and whose parameters are derived from various sources such as magnetic resonance imaging (MRI) (e.g., Le and Gevins [1993]). While these approaches do increase signal quality in carefully controlled experiments, they are impractical for most experiments and for clinical application. Other approaches do not require parameterization of a complex model, but rather are simply driven by the signals that are submitted to it. For example, Independent Component Analysis (ICA) has been used to decompose brain signals into statistically independent components (Makeig et al. [1996]), which can be used to get a more effective signal representation. (This approach is called blind deconvolution in microscopy applications (e.g., Turner et al. [1997]).) Even though these approaches have less demanding requirements than the more comprehensive modeling approaches, they require non-trivial calibrations using sufficient amounts of data, and they produce output signals that do not necessarily correspond to actual physiological sources in the brain. These complex model-based and data-driven approaches are thus neither amenable nor necessarily desirable for typical BCI experimentation. At the same time, much simpler deblurring filters have been shown to be effective and yet practical (McFarland et al. [1997b]). These filters are essentially spatial high-pass filters with fixed filtering characteristics. Typical realizations include two Laplacian spatial filters and the Common Average Reference (CAR) filter.

The small and large Laplacian spatial filters are comprised of discretized approximations of the second derivative of the Gaussian distribution, and attempt to invert the process that blurred the brain signals detected on the scalp (Hjorth [1991]). The approximations are further simplified such that the weighted sum of the four nearest or next nearest electrodes is subtracted from a center electrode for the small and large Laplacian, respectively (see Eq. 3.2, Figure 3.3(a), and Figure 3.3(b)).

$$s_h''(k) = s_h'(k) - \sum_{i \in S_i} w_{h,i} s_i'(k) \quad (3.2)$$

In this equation, the weight  $w_{h,i}$  in Eq. (3.2) is a function of the distance  $d_{h,i}$

between the electrode of interest  $h$  and its neighbor  $i$ :

$$w_{h,i} = \frac{\frac{1}{d_{h,i}}}{\sum_{i \in S_i} \frac{1}{d_{h,i}}} \quad (3.3)$$

The Common Average Reference (CAR) filter, another possible spatial high-pass filter, is implemented by re-referencing the calibrated potential  $s'_h(k)$  of each electrode  $h$  at each time point  $k$  to an estimated reference that is calculated by averaging the signals from all recorded electrodes  $H$  (see Eq. 3.4 and Figure 3.3(c)). In other words, a CAR filter calculates the signal amplitude that is common to all electrodes ( $\frac{1}{H} \sum_{i=1}^H s'_i(k)$ ) and subtracts it from the signal  $s'_h(k)$  at each location. While the CAR and Large Laplacian filters have been shown to provide comparable performance (McFarland et al. [1997b]), I utilized a CAR filter for the validations later in this chapter.

$$s''_h(k) = s'_h(k) - \frac{1}{H} \sum_{i=1}^H s'_i(k) \quad (3.4)$$

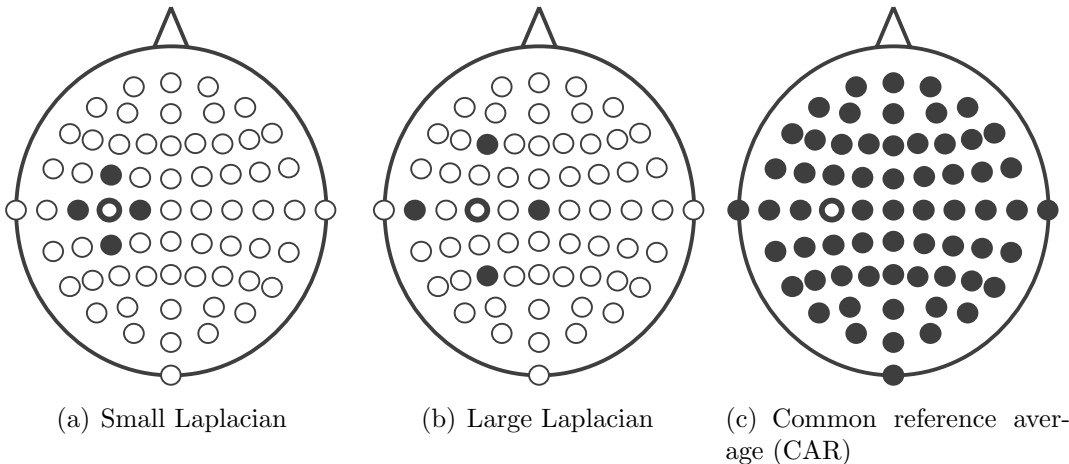


Figure 3.3: Locations (filled circles) involved in different spatial filters applied to location  $C_3$  (see Figure 3.4) (open circle). I utilized a CAR filter in my evaluations.

Whatever the realization of the spatial filter, its main purpose is to deblur the recorded signals so as to derive a more faithful representation of the sources within the brain. The example in Figure 3.5 illustrates results of this operation on signals recorded using EEG. In this example, the topographies illustrate the effect

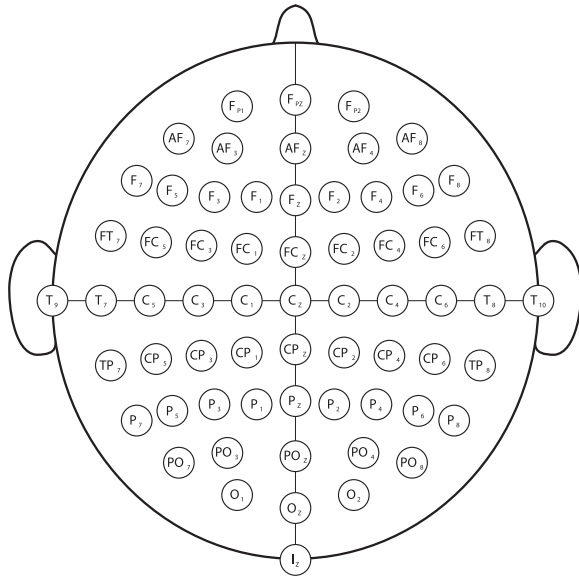


Figure 3.4: Electrode designations for a 64-channel setup of the extended 10-20 system. (Redrawn from Sharbrough et al. [1991].)

of a CAR filter on signals in space: in (A), the unfiltered signal is spatially broad, whereas in (B), the CAR-filtered signal emphasizes spatially local features. (Color indicates the cross correlation of the signal time course at each location (indicated by small dots) with the signal at the location indicated with the white star.) The signal time courses in (C) and (D) (which are recorded at the location marked with a star) illustrate the effect of a CAR filter on beta rhythms that are suppressed by right hand movement. The green bar indicates the period that a subject opened and closed her right hand. Beta rhythm oscillations (around 25 Hz) are suppressed during this period. This effect is more pronounced for the CAR-filtered signal in (D) compared to the unfiltered data in (C), and thus illustrates that the CAR filter removes some of the signal variance that is not due to the hand movement task.

The third and final step of feature extraction is the application of a temporal filter. Its purpose is to project the input signal in a representation (i.e., domain) in which the brain signals that can be modulated by the user are best expressed. As described, imagined movements have been shown to produce changes in the mu (i.e., 8-12 Hz) or beta (i.e., 18-25 Hz) frequency band. Thus, for the processing of mu/beta rhythm signals, the frequency domain is most often used, although a recent paper

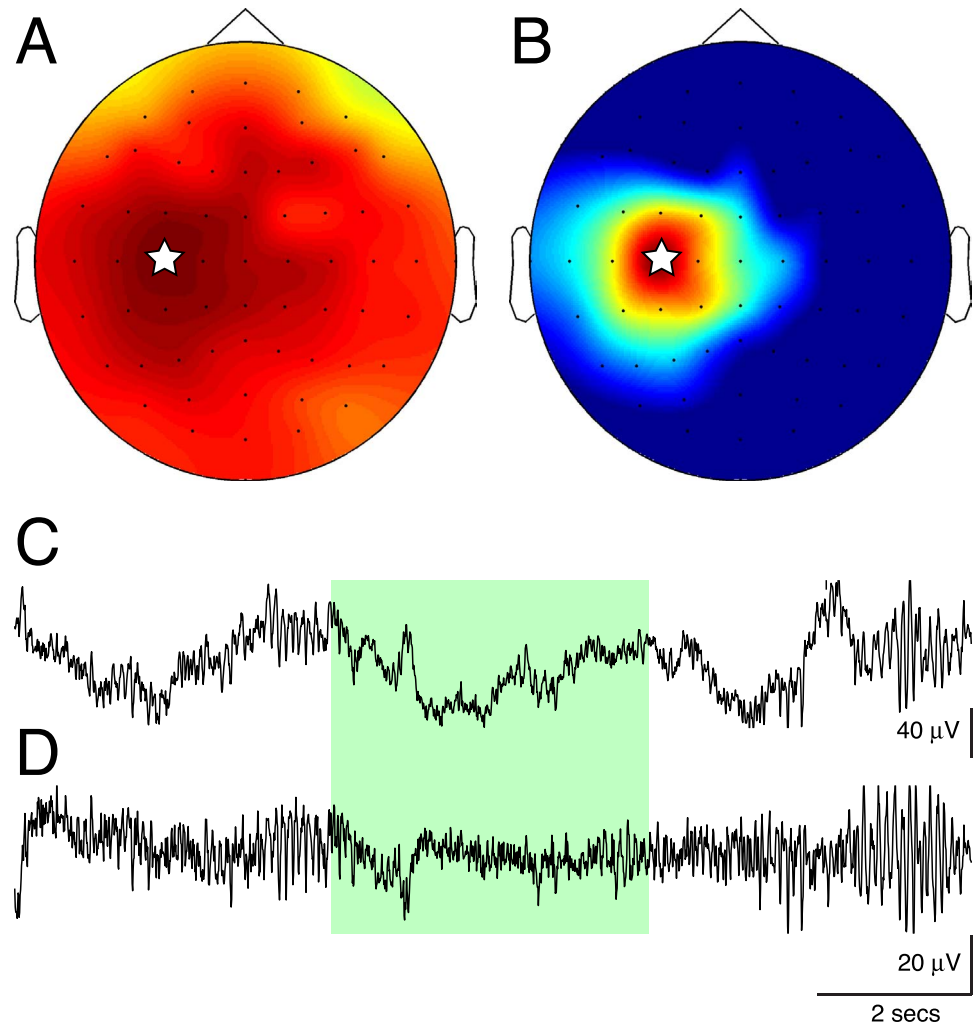


Figure 3.5: Example of application of a Common Average Reference (CAR) spatial filter. Signals are spatially more specific and better highlight beta rhythm suppression during the period indicated by the green bar when a CAR filter is applied (B and D) compared to when it is not (A and C).

co-authored by this writer suggested a matched filter in the time domain (Krusienski et al. [2006]) that better captured the non-sinusoidal components of the mu rhythm. Several methods for the transformation of time domain into the frequency domain have been proposed, such as the Fast Fourier Transform (FFT), wavelet transform, and procedures based on autoregressive parameters. The requirements of BCI systems offer suggestions about which of these methods to select. BCIs are closed-loop systems that should provide feedback many times per second (e.g., typically, at more

than 20 Hz) with a minimal group delay. The Heisenberg principle of uncertainty (e.g., Priestley [1981]) governs that it is not possible to concurrently achieve high resolution in time and frequency and hence, any of the procedures mentioned above will be subject to this limitation. However, the Maximum Entropy Method (MEM) (Marple [1987]), which is based on autoregressive modeling, has a higher temporal resolution (and thus reduced group delay) at a given frequency resolution compared to the FFT and wavelet transforms (Marple [1987]), and is thus advantageous in the context of BCI systems. (I will use the MEM method in the validations later in this chapter for this reason.) Whatever its realization, the temporal filter transforms time-domain signals  $s_e''(k)$  into frequency-domain features  $a_e(n)$ .

As an example of its function, Figure 3.6 illustrates application of the temporal filter to data collected using scalp-recorded EEG while a subject imagined hand movement or rested. I converted the CAR-filtered signals at each location into the frequency domain using the MEM algorithm and blocks of 400 ms length, and averaged the resulting spectra across blocks. This produced one average spectrum for each location and for each of the two conditions of imagined movement of the left hand and rest. (The example in Figure 3.6 illustrates spectra at location C4.) The difference in the spectrum between imagined movement (red dashed line) and rest (blue solid line) is evident and is sharply focused in frequency (around 11 and 22 Hz) and space (over location C4 of right sensorimotor cortex). (While activity at 22 Hz appears to be merely a harmonic of that at 11 Hz, evidence suggests that this relationship is more complicated (McFarland et al. [2000]).) In other words, this particular subject can use particular motor imagery to change the signal amplitude at location C4 and 11/22 Hz and could thus communicate her intent using this particular type of imagery.

To facilitate understanding of the issues in BCI signal processing, the previous sections described the first component of BCI signal processing, feature extraction, which is composed of signal calibration, spatial filtering, and temporal filtering. The purpose of feature extraction is to convert digitized brain signal samples that are recorded at various locations into features (e.g., frequency-domain spectra  $a_e(n)$ ) that express the subject's intent. The second component of BCI signal processing,

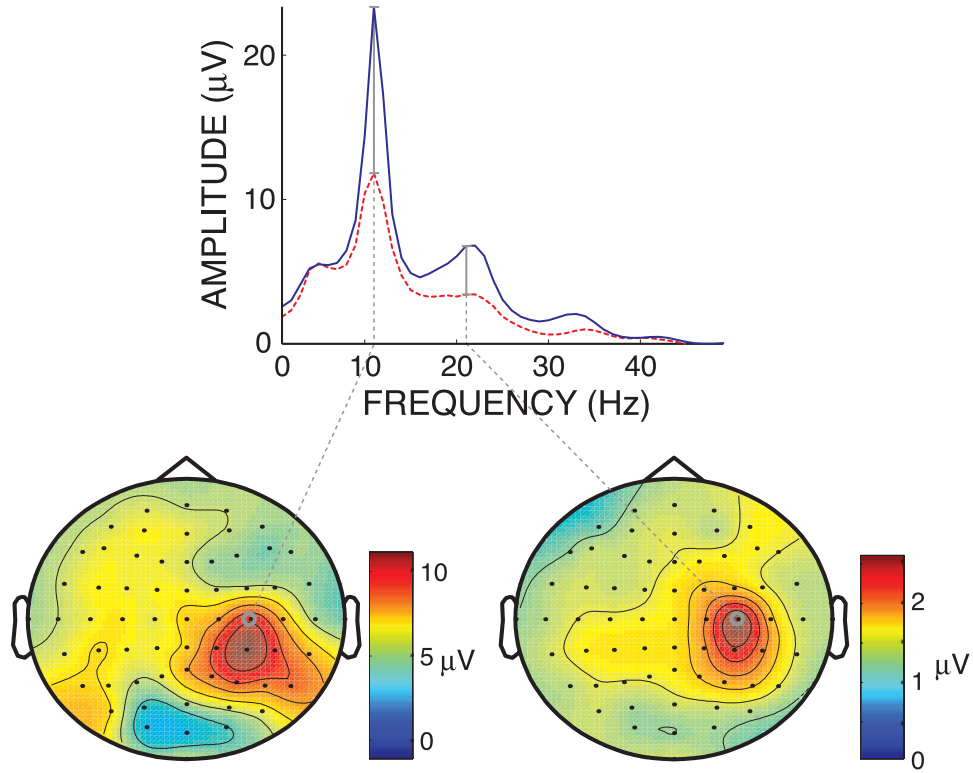


Figure 3.6: Example analyses of the temporal filter. In this example, EEG was recorded during imagined left hand movement and during rest. The spectrum for rest (blue solid line) is different from that for imagined hand movement (red dashed line). This difference is sharply focused in frequency (see spectra above) and in space (see topographies below) and could be used for BCI control.

the translation algorithm, effects this intent by translating these features into device commands. The following section describes the realizations of this function that have been described in the literature. It also describes the critical problem of these approaches that is addressed by a novel approach (the main contribution of **THEME II** of this dissertation) that is proposed, described, and validated in subsequent sections.

### 3.3.2 Translation Algorithm

The second step of BCI signal processing, the translation algorithm, is comprised mainly of a signal translation procedure that converts the set of brain signal

features  $a_e(n)$  into a set of output signals that control an output device<sup>5</sup>.

The traditional approach to BCI signal translation that is used throughout the literature realizes traditional classification/regression procedures. For example, studies have been using linear discriminant analysis (Babiloni et al. [2000]), neural networks (Pfurtscheller et al. [1997], Huan and Palaniappan [2004]), support vector machines (Müller et al. [2003], Garrett et al. [2003], Lal et al. [2004], and Gysels et al. [2005]), and linear regression (McFarland et al. [1993], McFarland et al. [1997a]). All currently used procedures are listed in a recent review article on BCI feature extraction and translation methods (McFarland et al. [2006]). This article lists 12 different methods for BCI feature translation and cites 26 corresponding articles. All these articles describe different realizations of classification/regression procedures.

All these procedures have a critical problem that impedes clinical application of BCI technology. Irrespective of its specific realization, any current procedure derives a control signal  $c(n)$  by applying a particular function to the feature vector  $\vec{a}(n)$ . Due to the variability and non-stationarity of relevant brain signals with respect to their location and features, this function necessarily has to be determined for each individual. With current methods, the parameters of that function need to be derived from data from at least two classes (e.g., rest and imagined hand movement). This requires that the best imagery task, i.e., the task that produces features that are maximally different between this and another task (such as rest), first be identified. This requires time consuming procedures under expert supervision, which become progressively lengthy and impractical as the task space increases with better signals such as electrocorticographic (ECoG) signals. As an additional problem, this approach is susceptible to non-stationarities of the signal features. Because most current BCI studies perform laboratory experiments (and thus can rely on expert supervision) and employ scalp-recorded EEG (which has low fidelity and a correspondingly small feature/task space), the actual impact of this critical problem has been modest.

To illustrate the function of this traditional approach, I produced a simple

---

<sup>5</sup>These output signals may then be further processed by a whitening procedure (e.g., a linear transformation) that produces signals with zero mean and a defined variance such that the output device does not have to account for changes in brain signal characteristics.

example. In this example, I used data derived from the previous example shown in Figure 3.6. Figure 3.7-A shows the distribution of data samples derived at C4 and 11/22 Hz (i.e., log transformed features  $a_1(n)$ ,  $a_2(n)$ , respectively). Blue dots show samples that correspond to rest and red dots show samples that correspond to imagined left hand movement. I then used linear regression to determine the coefficients of the linear function that minimized the error between the output of that function ( $c(n)$ ) and arbitrary target values for the two classes (i.e., -1, +1). Using this procedure, I derived the coefficients of the linear function that could be used to translate the features into an output signal:  $c(n) = 2560.43a_1(n) + 4581.99a_2(n)$ . The histogram of the values of  $c(n)$  calculated for the data from the rest class (blue) is different than that calculated for the data from the imagined hand class (red) (see Figure 3.7-B), which indicates that the user has some level of control over this particular signal. To quantitatively evaluate this level of user control, I determined the value of  $r^2$ , i.e., the variance in the output signal  $c(n)$  that is due to the class. I then applied the same linear function to samples from all electrodes. Figure 3.7-C illustrates that, as expected, control is sharply focused over right sensorimotor cortex.

In summary, BCI signal processing is accomplished using two components. The first component, feature extraction, extracts brain signal features that reflect the user's intent. The second component, the translation algorithm, translates these signal features into output signals that can control an output device. This translation algorithm has traditionally been realized using a variety of classification/regression approaches. While these approaches can produce output signals that can be controlled by the user and thus can be used to effectively communicate the user's intent, their definition depend on initial expert-driven signal identification procedures and their operation is susceptible to non-stationarities.

## 3.4 Feature Translation Using a Detection Approach

### 3.4.1 Overview

The novel approach that is proposed in this dissertation and that is described in the remainder of this chapter overcomes these two significant problems of all current approaches. It is based on the idea that control signals are derived by evaluating

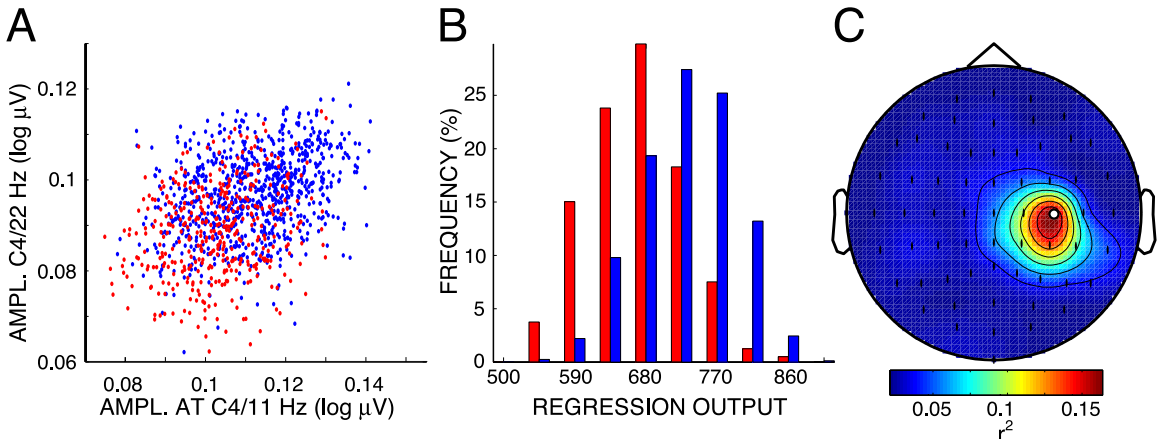


Figure 3.7: Example of a classification approach using linear regression. A: Distribution of signal features (i.e., signal amplitudes at C4 and 11/22 Hz for rest (blue dots) and imagined left hand movement (red dots)). B: Histogram of output values calculated for each of the two classes using linear regression applied to the two features. C: As expected, user control is focused over right sensorimotor cortex. See text for details.

how different a particular data sample is from a population of data samples recorded during a reference condition (e.g., rest), rather than by explicitly attempting to discriminate between two classes. In other words, all current BCI approaches to signal processing employ classification techniques, whereas the proposed method realizes a detection approach in a classification context (in general, this use of a detection approach has only been sparsely evaluated in the literature (Jordan and Jacobs [1994])). Figure 3.8 illustrates the contribution of the proposed approach in the context of BCI signal processing, and also lists the feature procedures that I used for my subsequent validations.

### 3.4.2 Gaussian Mixture Models

A number of mathematical techniques could be used to describe signal distributions for the proposed detection approach. These include parametric methods such as the use of one or more Gaussian distributions (i.e., Gaussian Mixture Models (GMMs) (Stauffer and Grimson [1999])), non-parametric methods such as k-Nearest Neighbors (kNN) (Duda et al. [2001]), or intermediate methods such as Parzen Windows (Parzen [1962]) or their extended version, Radial Basis Functions (Cacoullos

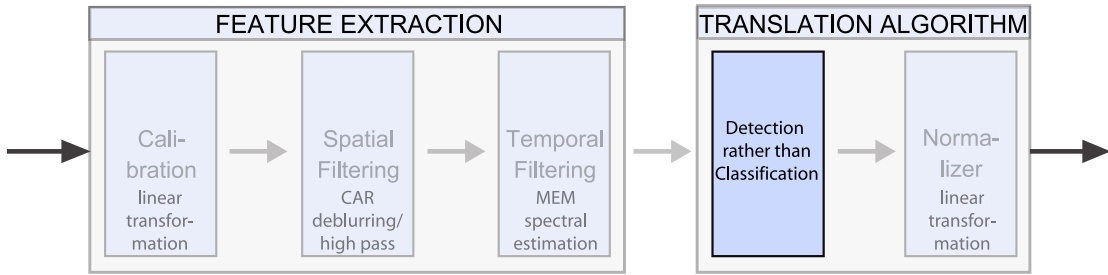


Figure 3.8: The contribution of the detection approach proposed in this dissertation mainly concerns signal translation.

[1966], Haykin [1998]). While such detection approaches have been used in other domains such as image processing (e.g., Radke et al. [2005]), they have not been used in BCIs.

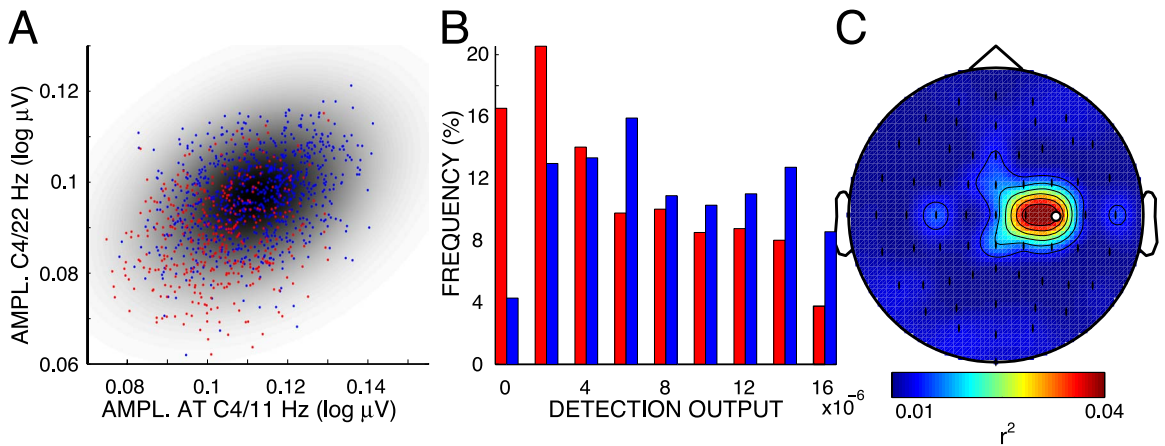


Figure 3.9: Example of signal detection. A: Distribution of signal features (i.e., signal amplitudes at C4 and 11/22 Hz for rest (blue dots) and imagined left hand movement (red dots)) and approximated probability density function (gray shades). B: Histogram of output values calculated for each of the two classes using a simple detection approach applied to the two features. C: As expected, user control is focused over right sensorimotor cortex. See text for details.

Figure 3.9 shows an example implementation of the detection approach using one Gaussian distribution and its application to the same data that were the basis for the regression example illustrated in Figure 3.7. Again, Figure 3.9-A shows the distribution of data samples derived at C4 and 11/22 Hz (log-transformed features

$a_1(n)$ ,  $a_2(n)$ , respectively). Blue dots show samples that correspond to rest and red dots show samples that correspond to imagined left hand movement. I then calculated, for the rest data only (i.e., the blue dots), the feature mean  $\vec{\mu}$  and the feature covariance matrix  $\Sigma$ . I then calculated the probability density function  $p(\vec{a})$  for all points  $\vec{a}$  in the feature space using Eq. 3.5 (see Duda et al. [2001]):

$$p(\vec{a}) = \frac{1}{2\pi\sqrt{|\Sigma|}} e^{-\frac{1}{2}(\vec{a}-\vec{\mu})^T \Sigma^{-1} (\vec{a}-\vec{\mu})} \quad (3.5)$$

Gray shades illustrate the values of  $p(\vec{a})$ . This figure illustrates that the distribution of  $p(\vec{a})$  approximates the distribution of the data samples recorded during rest and indicates qualitatively that the values of  $p(\vec{a})$  are usually higher (i.e., the shade is usually darker) for the blue dots than for the red dots. Figure 3.9-B shows a quantitative evaluation of this effect using a histogram of the values of  $p(\vec{a})$  for the two classes. This histogram demonstrates that the probability values derived from the rest class (blue) is different than that calculated for the data from the imagined hand class (red), which indicates that the user has control over the values of  $p$  using imagined hand movement. Just like in the regression example, I then quantified the level of user control by determining the values of  $r^2$ , i.e., the variance in the probability values (i.e., output control signal values) that is due to the class. I then applied the same procedure (using the same feature mean and covariance matrix) to all electrodes. Figure 3.9-C illustrates that, as expected, control is sharply focused over right sensorimotor cortex.

In summary, this simple example demonstrates that the translation of signal features into output control signals can be accomplished using a detection approach that depends only on data calculated during rest. This approach thus does not require, for the definition of the parameters of the translation algorithm, the collection of data during another task (such as imagined hand movement) and thus does not require initial signal identification procedures. (While in this example, the two frequencies were selected using such a procedure, I will show in the method validation section that the selection of frequencies is not necessary.) As an additional advantage, this approach is not vulnerable to nonstationarities in the distribution of the other class (i.e., the red dots). Figure 3.10 graphically summarizes these advantages.

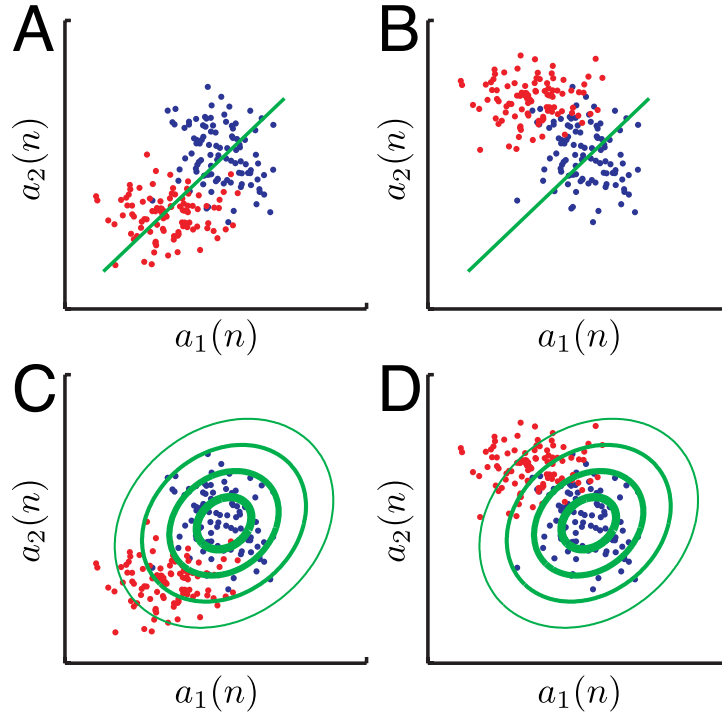
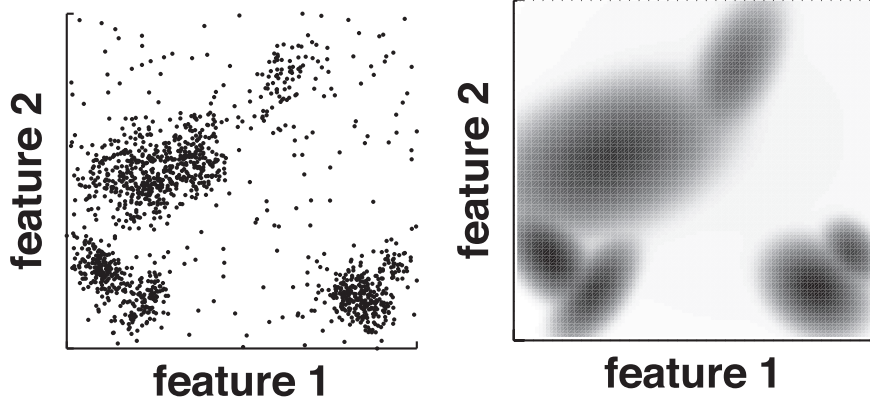


Figure 3.10: Advantages of the detection approach. A: Linear regression successfully distinguishes signal samples from class 1 (blue dots) and class 2 (red dots). Definition of the regression function depends on both classes. B: Regression cannot differentiate between class 1 and 2 in case class B is non-stationary. C: The detection function (indicated by green ellipses) is defined on class 1 (blue dots, e.g., data collected during rest) only and thus does not depend on class 2 (red dots). D: The detection function can differentiate between class 1 and 2 even if class 2 is non-stationary.

Initial evaluations and results in image processing applications (Pless [2003]) suggested the use of Gaussian distributions and indicated that multiple Gaussian distributions (i.e., Gaussian Mixture Models (GMMs), which can be viewed as generalized radial basis functions) can improve performance over the use of only one Gaussian distribution (which I used in my simple example in Figure 3.9) . I thus elected to utilize GMMs (Stauffer and Grimson [1999]) to implement my detection approach to BCI feature translation. To illustrate how a GMM can describe complex feature distributions by approximating its probability density, I generated 10 randomly shaped and oriented Gaussian distributions and added 20% uniformly distributed noise (Figure 3.11(a)). The probability density derived by a Gaussian Mix-

ture Model calculated from this distribution using 6 Gaussian distributions closely approximates the original sample distribution (Figure 3.11(b)).



(a) Data points generated by 10 Gaussian distributions.  
 (b) Approximated probability distribution.

Figure 3.11: A complex distribution of data points (a) and its probability density approximated by a mixture of six Gaussian distributions (b).

Any Gaussian distribution  $c$  can be described by its mean  $\vec{\mu}_c$  and its covariance matrix  $\Sigma_c$ . The Mahalanobis Distance (Eq. (3.6)) is a distance metric that assigns to each feature vector  $\vec{a}(n)$  calculated at a time  $n$  a distance to a cluster (i.e., Gaussian distribution defined by  $\Sigma_c, \vec{\mu}_c$ ) that is in units of estimated variance between the feature vector  $\vec{a}(n)$  and the center  $\vec{\mu}_c$  (i.e., essentially a multidimensional z score)<sup>6</sup>:

$$m(\vec{a}(n)|c) = (\vec{a}(n) - \vec{\mu}_c)^T \Sigma_c^{-1} (\vec{a}(n) - \vec{\mu}_c) \quad (3.6)$$

Using this distance metric, the conditional probability  $p(\vec{a}(n)|c)$  can be defined (Eq. (3.7), see Duda et al. [2001]):

$$p(\vec{a}(n)|c) = \frac{1}{(2\pi)^{\frac{D}{2}} |\Sigma_c|^{\frac{1}{2}}} e^{-\frac{m(\vec{a}(n)|c)}{2}} \quad (3.7)$$

The conditional probability is weighted by the prior probability  $\omega_c$  (which is calculated as the proportion of data points assigned to each Gaussian distribution):

$$p_c(\vec{a}(n)) = \omega_c p(\vec{a}(n)|c) \quad (3.8)$$

---

<sup>6</sup>I here calculate the feature vectors and GMM parameters for a particular electrode  $h$  and should thus denote these variables with a corresponding index  $h$ . I dropped this index for the sake of clarity.

With this, the probability density function is defined as:

$$p(\vec{a}(n)) = \sum_{c=1}^C p_c(\vec{a}(n)) \quad (3.9)$$

The weighted probability can be log-transformed to determine the negative log likelihood:

$$\begin{aligned} LL(\vec{a}(n)|c) &= -\log [p_c(\vec{a}(n))] \\ &= -\log(\omega_c) + \frac{D}{2} \log(2\pi) + \frac{1}{2} \log(|\Sigma_c|) + \frac{m(\vec{a}(n)|c)}{2} \end{aligned} \quad (3.10)$$

To determine a global measure of model fit (which I will use later for my algorithmic improvements), one could sum up the log likelihoods of all points for the best cluster (i.e., maximized likelihood), which is given below in equation form:

$$L = \sum_{n=1}^N LL(\vec{a}(n)|c_{best}) \quad (3.11)$$

where  $c_{best}$  was derived as

$$c_{best} = \operatorname{argmax}_{c_i} p_{c_i}(\vec{a}(n)) \quad (3.12)$$

The number of free parameters for each of  $C$  clusters is the sum of parameters in the covariance matrix  $\Sigma_c$ , the cluster mean  $\vec{\mu}_c$ , and its weight  $\omega_c$  (Eq. (3.13)). Thus, the total number of parameters in the signal model,  $N_p$ , can be determined as follows:

$$\begin{aligned} N_p &= (N_{pcovariance} + N_{pcenter} + N_{pweight}) C \\ &= \left[ \frac{D(D+1)}{2} + D + 1 \right] C \end{aligned} \quad (3.13)$$

In this equation,  $D$  is the number of dimensions in the feature vector.

### 3.4.3 Parameterization of Gaussian Mixture Models

Gaussian Mixture Models (GMMs) can be used to approximate signal distributions and could thus form the basis for the BCI detection approach proposed in this chapter by modeling the probability density function of the data recorded during

rest. However, four sets of variables have to be determined to define a GMM ( $C$ , the number of Gaussian distributions (i.e., clusters); and for each cluster  $c$ ,  $\vec{\mu}_c, \Sigma_c, \omega_c$ , the feature mean, covariance matrix, and prior probability, respectively).

To determine those  $\vec{\mu}_c, \Sigma_c, \omega_c$  that produce an effective approximation of the original sample distribution given the number of clusters  $C$ , various algorithms have been proposed. One of the most well known of these algorithms is the Expectation Maximization (EM) algorithm (Dempster et al. [1977]). Each iteration of the EM algorithm consists of two steps: an Estimation (E) step and a Maximization (M) step. The M step maximizes a likelihood function that is redefined in each iteration by the E step. The Competitive EM (CEM) algorithm (Celeux and Govaert [1992], Biernacki et al. [2003]) improves on the EM algorithm mainly in regards to speed of convergence (and thus execution speed). It does this by assigning, in a C step, each sample to the most likely cluster, whereas the EM algorithms requires accumulation of fractional statistics. Because speed of execution was an important criterion for my application, I chose the CEM algorithm over the EM algorithm.

Each of these two algorithms has three relevant issues. First, it requires definition of the number of Gaussian clusters  $C$ , which is typically done manually. This is not acceptable because my goal was to reduce the expert oversight that current methods require. Second, it is not robust, i.e., it can produce covariance matrices that are singular. This creates numerical problems with the necessary inversion of these matrices in Eq. 3.6. Third, EM and CEM algorithms do not include the capacity to update the model to account for non-stationarities in the data distribution. Because even the resting state that is to be modeled might be non-stationary, automatic updating may be necessary.

### 3.4.4 Algorithmic Improvements

The algorithmic improvements described in the subsequent sections address these three problems by providing automatic model selection, robustness, and model adaptation.

### 3.4.4.1 Automatic Model Selection

The first improvement was automated model selection. In any Gaussian Mixture Model (GMM), the number of clusters  $C$  has to be selected, and typically, this is done manually. For my application, which aimed to decrease expert intervention, I was interested in automating this manual procedure.

This is not a straightforward problem, because the approximation of the GMM model to the source distribution improves with the number of mixtures. In the end, the source distribution would be best described by a model with as many Gaussian mixtures as data points. This is not resource efficient and might also not provide optimal discrimination when used in a classification setting. I thus considered to penalize the performance of the model with the complexity of the model. In the literature, such terms are generally referred to as information criteria and typically are in the form of Eq. (3.14).

$$\text{information criterion} = \text{measure of fit} + \text{complexity penalty} \quad (3.14)$$

A number of these information criteria have been described in the literature, e.g., the Akaike Information Criteria (AIC) (Akaike [1973]), Vapnik's Structural Risk Minimization (SRM) (Vapnik and Chervonenkis [1974]), Schwarz's Bayesian Information Criteria (BIC) (Schwarz [1978]), Rissanen's Minimum Description Length (MDL) and Shortest Data Description (SSD) (Rissanen [1978]) and Bozdogan's Corrected Akaike Information Criterion (CAICF) and Consistent Akaike Information Criterion (Bozdogan [1974]) (see Torr [1997] for a comprehensive review).

Because there was no theoretical basis with which I could select one of these criteria over the other, I arbitrarily picked two with somewhat opposite goals, i.e., Bayesian Information Criteria and Akaike Information Criteria. They are described in more detail below.

The Bayesian Information Criteria (BIC) promises to select the model that the data was generated from (Schwarz [1978]). The complexity penalty is chosen conservatively, accounting for the number of samples  $N$  and the number of free parameters  $N_p$ . The BIC in (3.15) tends to select the best structure instead of the

best predictor.

$$\begin{aligned} K_{BIC} &= -2 \cdot \text{maximized likelihood} + \text{bayesian compl. penalty} \\ K_{BIC} &= -2 \cdot L + 2N_p \log N \end{aligned} \quad (3.15)$$

The Akaike Information Criteria (AIC) promises to select the model that will have the best likelihood for future data (Akaike [1973]), and is thus not influenced by the number of observations  $N$  (Eq. (3.16)). AIC does not produce an asymptotically consistent estimate of the order of the model and tends to overfit.

$$\begin{aligned} K_{AIC} &= -2 \cdot \text{maximized likelihood} + \text{akaike compl. penalty} \\ K_{AIC} &= -2 \cdot L + 2N_p \end{aligned} \quad (3.16)$$

Because there was no evidence that indicated which of these two criteria might provide better performance, I chose to introduce another parameter that defined a linear combination of AIC and BIC. Eq. (3.17) defines the information criterion  $K$  as a linear combination of AIC and BIC with the linear constant  $k$ . For  $0 \leq k \leq 1$ , the information criterion  $K$  selected on the continuum between AIC and BIC. In other words,  $k$  modulated the impact of the number of samples  $N$  on the information criteria.

$$K = (1 - k)K_{AIC} + kK_{BIC}, \quad 0 \leq k \leq 1 \quad (3.17)$$

In summary, I implemented automatic model selection (i.e., automated determination of the number of clusters  $C$ ) by optimizing the information criterion described above as a function of  $C$ . I did this by starting using a predefined number of clusters (i.e., number of seed clusters) and by then testing whether decrease or increase of the number of clusters would improve the information criterion as described below. An example for the iteration through my procedure, and the resulting clustering results, are illustrated in Figure 3.12.

**Selection Criteria for Model Order Decrease** At predefined times, my algorithm tested whether deletion of the cluster  $d$  with the lowest contribution to the model improved the information criterion of the whole model.

I did this by calculating the improvement in information criteria  $\Delta K$  (as defined in Eq. (3.20)) that was associated with a reduction of the model order (i.e.,

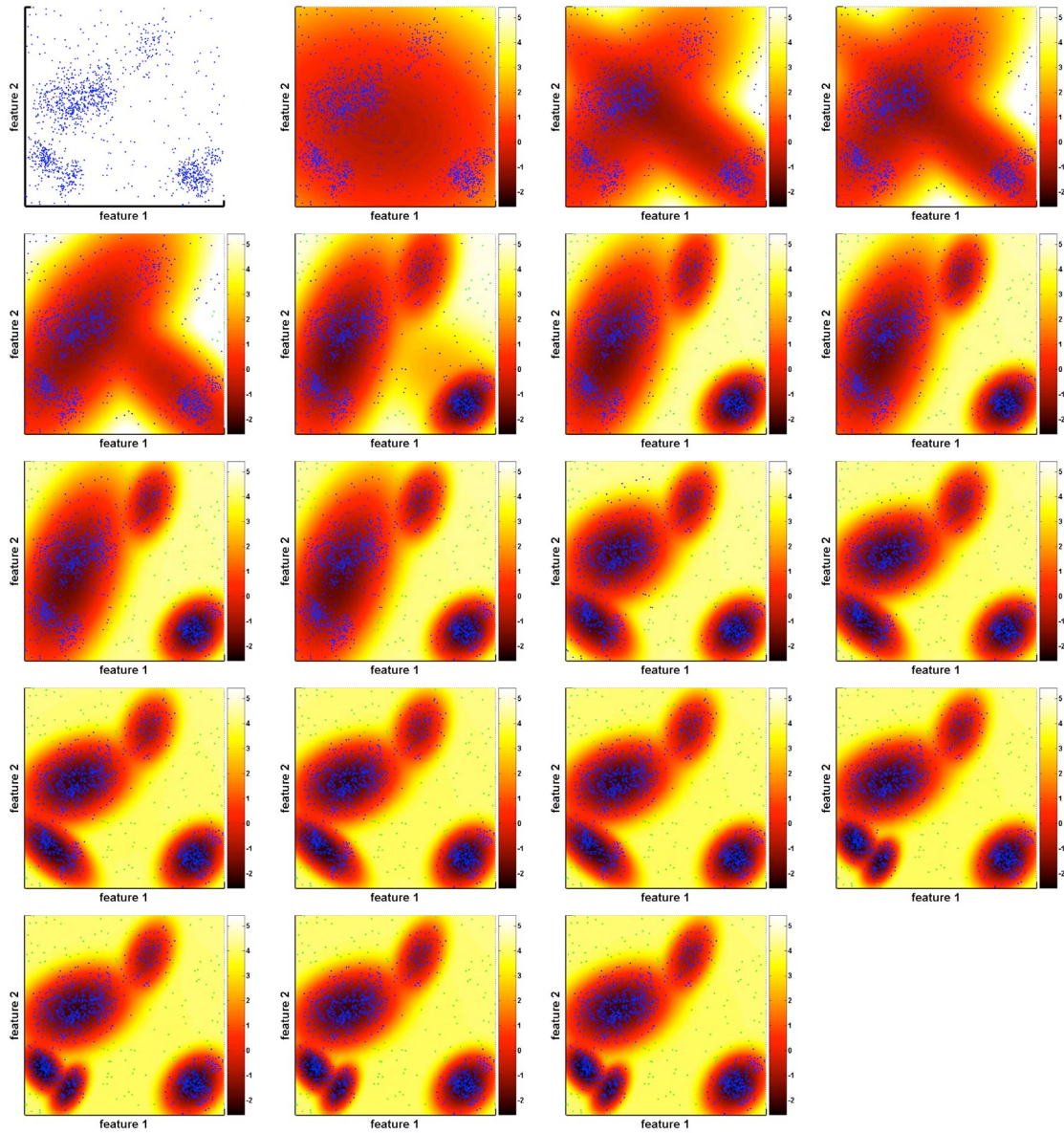


Figure 3.12: Automated model selection. This figure illustrates the iterative steps in the improved CEM algorithm (from left to right and top to bottom). The original data distribution is shown in the first image. The second image illustrates the initialization of the algorithm with one cluster. Subsequent images illustrate optimization and splitting of clusters until the final approximation is obtained.

number of Gaussian mixtures) from  $C$  to  $C - 1$ .

The contribution of each cluster  $i$  to the model is defined in Eq. (3.18) as the

difference in the total negative log likelihood as the data points are assigned from the best cluster  $i$  to the second best cluster  $j$ . The cluster  $d$  (Eq. (3.19) with the minimal contribution  $LL_d$  to the model was selected as a candidate to be deleted.

If  $\Delta K > LL_d$ , the cluster  $d$  was deleted.

$$\Delta LL_i = \sum_{n' \in N_i} LL(\vec{a}(n')|c_j) - LL(\vec{a}(n')|c_i) \quad (3.18)$$

where  $N_i$  was the set of all samples that were assigned to the cluster  $i$ .

$$\Delta LL_d = \min [\Delta LL_i], \quad i = 1 \dots C \quad (3.19)$$

$$\Delta K = K(C) - K(C-1) \quad (3.20)$$

**Selection Criteria for Model Order Increase** The algorithm also tested whether splitting one cluster  $i$  into two clusters improved the information criterion of data points assigned to cluster  $i$  and also the information criterion of the whole model (i.e., all data points).

I did this by iterating through all clusters  $i$  and, for each cluster, splitting it into two clusters. I then optimized the model parameters for the data points associated with cluster  $i$  as described in the next section, and I did this both for one cluster  $i$  (i.e., unsplit case) and for the two (i.e., split) clusters derived from cluster  $i$ . If the model restricted to this subset of all datapoints improved ( $K_{i_{\text{split}}} < K_{i_{\text{unsplit}}}$ ), the cluster  $i$  remained split. In this case, I then tested whether the split model also improved the information criterion on all datapoints. I did this by again optimizing the model parameters for all datapoints (now using  $C+1$  clusters). If the information criterion for the whole model improved ( $K_{C+1} < K_C$ ), I kept the model with  $C+1$  clusters. Otherwise, I reverted back to the original model using  $C$  clusters.

#### 3.4.4.2 Robustness

The second improvement was guaranteed robust output. As described, the CEM algorithm does not guarantee that clusters may not have singular covariance matrices, which can lead to numerical problems. I addressed this problem by eval-

uating the matrix determinant at predefined iterations of the algorithm and by deleting the corresponding cluster  $c$  if the determinant was smaller than a constant  $k$ .

### 3.4.4.3 Model Adaptation

The third improvement was to propose a scheme that could to account for instationarities in the modeled data distribution. To prevent adaptation to spurious outliers, I only updated clusters of the model if the negative log likelihood (calculated between the data point and this cluster) was smaller than a pre-defined constant. I thus updated the cluster weights (i.e., prior probabilities)  $\omega_c$ , cluster means  $\vec{\mu}_c$ , and covariance matrices  $\Sigma_c$ , for each cluster  $c$  (of a total number  $N_c$  of adapted clusters) that passed this criterion.

I updated the cluster weights using a simple infinite impulse response (IIR) filter:

$$\omega_c(N+1) = (1 - \eta)\omega_c(N) + \eta\lambda_c \quad (3.21)$$

In this equation,  $\eta$  was the update rate (i.e., a small constant  $<< 1$ ) and  $\lambda_c$  was the update target value that was calculated as follows:

$$\lambda_c = \begin{cases} 1/N_c, & \text{if adapted} \\ 0, & \text{else} \end{cases} \quad (3.22)$$

Because I updated  $N_c$  clusters, the sum of all  $\lambda_c$  was always 1:

$$\sum_{c=1}^C \lambda_c = 1 \quad (3.23)$$

Without updating, the sum of all prior probabilities was 1 by definition:

$$\sum_{c=1}^C \omega_c(N) = 1 \quad (3.24)$$

By substituting Eq. 3.23 and Eq. 3.24 into Eq. 3.21, I show in Eq. 3.25 that

this also holds after applying my updating scheme:

$$\begin{aligned}
 \sum_{c=1}^C \omega_c(N+1) &= \sum_{c=1}^C [(1-\eta)\omega_c(N) + \eta\lambda_c] \\
 &= \sum_{c=1}^C \omega_c(N) - \eta \sum_{c=1}^C \omega_c(N) + \eta \sum_{c=1}^C \lambda_c \\
 &= 1 - \eta + \eta \\
 &= 1
 \end{aligned} \tag{3.25}$$

I then updated the mean of each cluster,  $\vec{\mu}_c$ , to its new value,  $\vec{\mu}'_c$ , by moving it towards a new data sample:

$$\vec{\mu}'_c = (1-\alpha)\vec{\mu}_c + \alpha\vec{a}(n) \tag{3.26}$$

In this equation, the cluster-specific learning rate  $\alpha_c$  depended on the weight  $\omega_c$  of the cluster  $c$  (i.e.,  $\alpha_c = \eta\omega_c$ ) so that clusters with a lower prior probability were updated slower than those with a higher prior probability.

Finally, I also updated, in Eq. 3.28, the cluster covariances  $\Sigma_c$  using the updated mean  $\vec{\mu}'_c$  and the formula for the covariance in Eq. (3.27).

$$\Sigma_{c_i,j} = \frac{1}{N} \sum_{n=1}^N (a_i(n) - \mu_{c_i})(a_j(n) - \mu_{c_j}) \tag{3.27}$$

$$\Sigma'_{c_i,j} = (1-\alpha)\Sigma_{c_i,j} + \alpha [a_i(n) - \mu'_{c_i}] [a_j(n) - \mu'_{c_j}] \tag{3.28}$$

### 3.4.5 Using Signal Detection for BCI Signal Translation

The previous sections described techniques (i.e., existing algorithms with improvements proposed in this dissertation) that can model the probability density distribution of brain signal features recorded during rest. The use of these techniques constructs a Gaussian Mixture Model with  $C$  clusters (where the value of  $C$  is automatically determined) and cluster (i.e., feature) means  $\vec{\mu}_c$ , covariance matrices  $\Sigma_c$ , and prior probabilities  $\omega_c$ . This model of resting activity may be used to convert brain signal features into output control signal features (and may thus act as an alternative to conventional classification/regression approaches) as described below.

A model of brain activity during rest is first established. Subsequently, for

each signal sample, the posterior probability  $p(\vec{a}(n))$  and its negative log likelihood  $LL(\vec{a}(n))$  can be calculated, which provide a measure of the probability that this sample was produced by the resting data distribution:

$$p(\vec{a}(n)) = \sum_{c=1}^C \omega_c p(\vec{a}(n)|c) \quad (3.29)$$

$$LL(\vec{a}(n)) = -\log(p(\vec{a}(n))) \quad (3.30)$$

The negative log likelihood  $LL$  can thus be expected to be small for samples that are similar to the data distribution (i.e., other samples during rest), and large for samples that are dissimilar (i.e., rest during a task such as imagined hand movement) and thus produces an output signal that may be controlled by the user. In essence, my procedure translated an input feature vector into a control signal that could be used for device control, which is similar in purpose to traditional classification/regression methods. The critical difference to the traditional approaches is that the proposed approach only requires data samples from one class (e.g., rest), and not from multiple classes (e.g., signals associated with a variety of different actual or imagined movements), and thus does not require initial signal identification procedures that impede clinical application of BCI technology.

## 3.5 Method Validation

### 3.5.1 Summary

The previous section described the general principles and implementation details of a novel approach to BCI feature translation. This detection approach does not require an initial definition of a classification/regression function, and thus does not require the lengthy initial signal identification procedures (and corresponding expert involvement) that are currently required.

I validated this detection approach by conducting a study in which I applied it offline to data gathered from online BCI experiments. In these experiments, subjects used motor imagery to modulate signals in the mu/beta rhythm band over select locations to move a cursor vertically towards one of four targets on a computer screen. The goal of the present study was to determine whether signal translation using a detection approach (i.e., the calculation of  $LL(\vec{a}(n))$ ) given a feature vector

$\vec{a}(n)$ ) could provide similar performance (i.e., discrimination for signals associated with the different targets) to those achieved using a widely used conventional method (i.e., linear regression). (While the choice of the feature extraction methods was somewhat arbitrary, I utilized Common Average Reference spatial filtering and the MEM-based spectral estimation techniques.)

This study is described in the subsequent section. Its results indicate that the proposed detection approach provides similar performance to a successful conventional approach without requiring initial signal identification and corresponding expert oversight that are currently required. These results thus suggest that the use of a signal detection approach should facilitate the application of BCI technologies in clinical environments.

### 3.5.2 Methods

#### 3.5.2.1 Dataset

To validate my novel signal translation method, I used a BCI dataset that was made available at the 2001 and 2003 NIPS data competition (Blankertz [2003], Blankertz et al. [2004], Blanchard and Blankertz [2004]). These data were collected from three experienced BCI users and were comprised of 64 channels of EEG digitized at 160 Hz. These data were the basis for the offline analyses in the present study. The following paragraphs briefly describe how they were collected.

Initial signal identification procedures suggested the imagined tasks, locations, and frequencies, that most effectively modulated mu or beta rhythm amplitude (i.e., frequencies between 8-12 Hz or 18-24 Hz, respectively). The subjects subsequently used the signals suggested by this procedure to control vertical cursor movement toward the vertical position of a target located at one of four evenly spaced positions at the right edge of a video screen.

#### 3.5.2.2 The Present Analyses

I analyzed this dataset offline using the detection approach proposed in the previous section. In these analyses, I constructed a model for data associated with the top or bottom target (i.e., data from one of the four classes). I then calculated the negative log-likelihood for each data sample  $LL(\vec{a}(n))$  associated with bottom

and top targets, which indicated the probability that this sample was produced by the resting distribution described by the model. In consequence, I expected that the output of this procedure would produce small numbers for the data samples from the class that was used to train the model and large numbers for data samples from the other class.

Subsequent analyses describe the features that were input to these analyses and the performance metric that I used to evaluate the results.

### 3.5.2.3 Feature Extraction and Selection

In the online BCI experiments that produced the data for my evaluation, the imagined tasks, ideal location, and ideal frequencies were determined using an initial signal identification procedure and manual selection by an expert.

In the end, I was interested in defining a procedure that would not require signal identification procedure or expert oversight. Because for EEG, only a few locations are candidates for mu/beta rhythm BCI control, the feature selection task mainly concerns the selection of appropriate frequencies. My offline analyses thus focused on the location that was used for online feedback and on amplitudes from all relevant frequencies. I derived these features using Common Average Reference spatial filtering and MEM-based spectral estimation as described in Section 3.3.1. This procedure is briefly summarized below.

I first converted signals at each location into units of  $\mu V$ . I then applied a common average reference spatial deblurring filter, from which I then extracted spectral estimates. To do this, I first partitioned signals  $s_h$  of each channel  $h$  into windows of a constant number of samples  $L_w = 64$  that corresponded to 400 ms ( $f_s=160$  Hz). Let us denote these windows as  $s'_h(k')$  where  $k' = 0, 1, \dots, L_w - 1$ . After spatial filtering, I passed each  $s'_h$  (i.e., the whole window) to the MEM spectral estimator (model order was 16), which produced a continuous estimation of spectral amplitudes  $\hat{S}_h$  that I discretized in frequency. I did this by creating frequency bins that were defined using lower and upper frequency boundaries  $f_{i,l}$  and  $f_{i,u}$ :

$$\begin{aligned} f_{i,l} &= f_e + (i - 1)f_b \\ f_{i,u} &= f_e + if_b \end{aligned} \tag{3.31}$$

$f_b=2$  Hz was the width of the bins and  $f_e = 10$  Hz was the lowest frequency that I calculated. Unless otherwise noted, I used  $J = 10$  frequency bins  $i$  (i.e., features  $a_i$  representing the 10-30 Hz frequency range important for mu/beta rhythm processing) that were calculated as defined in Eq. 3.32:

$$a_i = \frac{1}{f_{i,u} - f_{i,l}} \int_{f=f_{i,l}}^{f_{i,u}} \hat{S}_h df \quad (3.32)$$

Feature transformation was another issue. While there was no theoretical basis that could suggest the feature transformation that would provide the best performance, experimental evidence in the literature indicated that non-linear transformations to frequency features may be useful (Garrett et al. [2003]). I was thus interested in the impact of such transforms (i.e., *log* and *sqrt* transformation (Eq. (3.33) and (3.34))) on the performance of my new method. (The evaluation was only performed on spectral estimation features, which by definition are positive.)

$$\vec{a}'_{log} = log(\vec{a}) = [log(a_1), \dots, log(a_J)] \quad (3.33)$$

$$\vec{a}'_{sqrt} = \sqrt{\vec{a}} = [\sqrt{(a_1)}, \dots, \sqrt{(a_J)}] \quad (3.34)$$

### 3.5.2.4 Performance Metric

My primary interest in my evaluations was how well the output of my proposed feature translation method would discriminate between the source distribution and a target distribution, and not how well my model accounted for the original data distribution. I thus wanted to utilize a measure of discrimination.

Because the posterior probabilities for each class were known, *Bayes Decision Theory* could be used to calculate the error (e.g., Duda et al. [2001]). Thus, for the two posterior probability distributions corresponding to the two classes, I selected the threshold  $k$  that minimized the error rate  $E$ :

$$E = \int_k^{\infty} P(\omega_1|x) + \int_{-\infty}^k P(\omega_2|x) \quad (3.35)$$

This minimum error rate, calculated between the source and target distribution, was used as a performance metric for the subsequent evaluations.

### 3.5.3 Results

To validate the use of my proposed detection approach to feature translation in the BCI context and to compare the results of its use to those achieved using a traditional technique, I set out to answer three questions. The first question was which effect various parameters had on offline BCI classification performance. The second question was whether results achieved using my novel approach were comparable to those achieved using a conventional method (i.e., linear regression) that relied on signal identification procedures. The third question was whether signals produced by my proposed method had characteristics that would make them amenable to real-time experiments. The following three sections address these three questions.

#### 3.5.3.1 Effect of Parameters on Classification Performance

The first question was how the detection approach should be configured and used so that it maximized performance in the BCI context. The following paragraphs discuss empirical evaluations that address which feature transformation, processing method (i.e., diagonal or full covariance matrices), model selection methodology, number of seed clusters, and training time provided optimal performance. These evaluations were organized such that they suggested practical recommendations for the use of these parameters.

**Effect of Feature Transformation** Data can be pre-processed using a variety of transformations. In my analyses, untransformed frequency features collected during rest typically were not normally distributed, and square root and log transforms tended to produce distributions that were more similar to Gaussian distributions. Thus, it might seem to be natural to choose such transformations if signals were modeled with Gaussian distributions, as they are with GMMs. However, there were two reasons why I felt an evaluation of this issue was warranted. First, a good model fit on a background signal does not necessarily mean that discrimination performance will also be maximized, and second, I incorporated automatic model selection in my algorithm, which further complicated interpretations.

To determine which feature transformation (i.e., no transformation, square

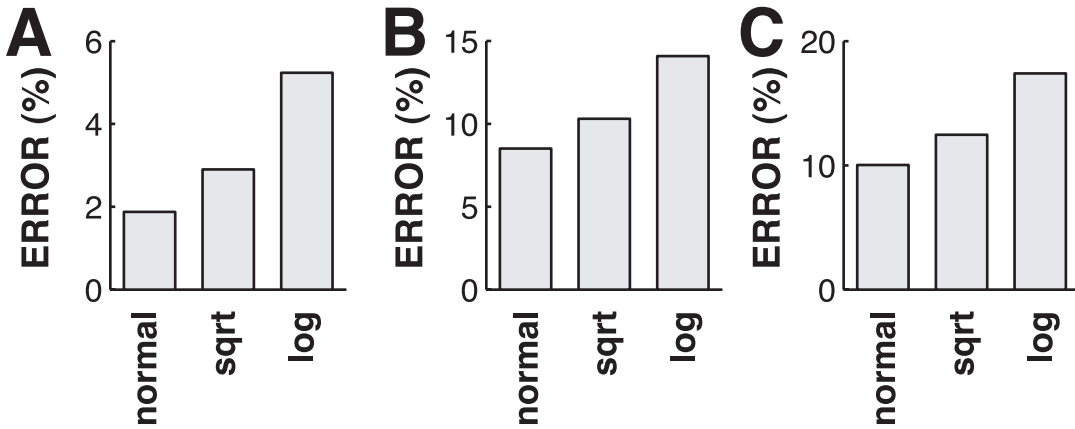


Figure 3.13: Effect on performance of feature transformation prior to submission to my algorithm. In all three subjects, normal (i.e., no transformation) outperformed square root and log transform. The difference between no transformation and log transformation was statistically significant in all three subjects. See text for details.

root or log transformation) provided best performance, I evaluated the average classification error rates for each subject using each of the three transformations using 20-fold cross validation. For each evaluation, I evaluated all combinations of the following variations: AIC/BIC from 0 to 1 in steps of 0.2, 2 to 20 seed Gaussians (i.e., the initial number of Gaussians that was then further optimized by my automatic model selection procedure), and full and diagonal covariance matrices. Thus, for each subject, transformation, and cross validation fold, I evaluated 228 combinations of these parameters and averaged their results for each cross validation fold. The results of this evaluation are shown in Figure 3.13. They indicate the surprising result that at least for the three subjects in this study, the use of non-transformed features clearly outperformed the use of the log transform ( $p < 0.001$ ,  $p < 0.01$ ,  $p < 0.01$ , Mann-Whitney Rank Sum Test). In consequence, I used untransformed features for the subsequent evaluations.

**Effect of Using Diagonal/Full Covariance Matrices** In my algorithm, I included the capacity to model the feature variances using three methods, i.e., full covariance matrices, covariance matrices that were diagonalized after estimation of the full covariance matrices (i.e., diagonal), and estimation of only the diagonal elements in the covariance matrices (i.e., estimated diagonal). Again, it might seem

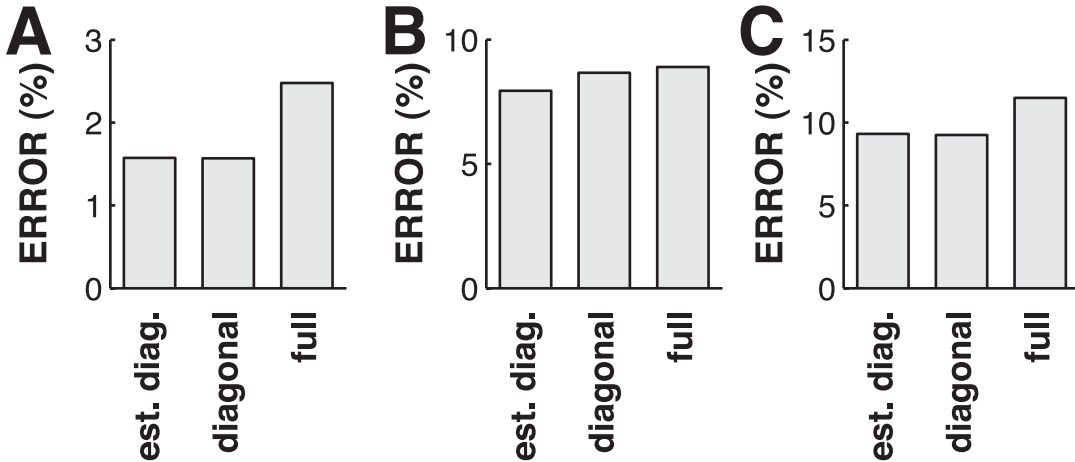


Figure 3.14: Effect on performance of using full, diagonal, and estimated diagonal covariance matrices. The small differences in performance were not statistically significant at the 0.05 level.

obvious to use full covariance matrices, but a method might provide a more accurate description of the background signal but still deliver inferior results when used for discrimination. To determine whether full or diagonal covariance matrices provided better results, I evaluated the average classification error rates for each subject using full, diagonal, and estimated diagonal covariance matrices using 20-fold cross validation and no feature transformation. For each evaluation, I evaluated all combinations of the following variations: AIC/BIC from 0 to 1 in steps of 0.2, and 2 to 20 seed Gaussians. Thus, for each subject, full, diagonal, and estimated diagonal covariance matrix evaluation and cross validation fold, I evaluated 114 combinations of these parameters and averaged their results. The results of this evaluation are shown in Figure 3.14. Although for all three subjects diagonal and estimated diagonal covariance matrices provide slightly better results on average compared to full covariance matrices, the results of these three different methods were not statistically different at the 0.05 level (Mann-Whitney Rank Sum Test). I used diagonal covariance matrices for all subsequent evaluations.

**Effect of Different Model Selection Methodologies** To determine which model selection methodology (i.e., model selection using AIC or BIC penalty scores) produced better results, I evaluated the average classification error rates for each

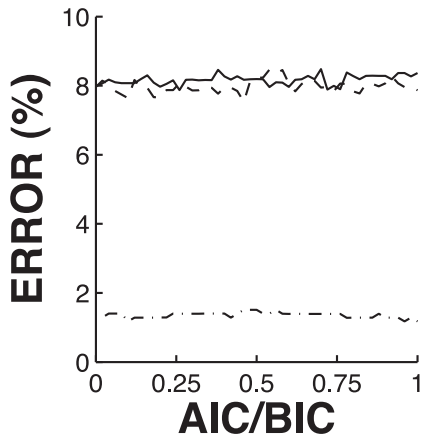


Figure 3.15: Performance achieved using different combinations of the AIC and BIC penalty score for each subject. Dash-dotted, dashed and solid lines correspond to subjects A, B, and C, respectively. The results indicate that performance does not depend on the type of penalty score.

subject using 20-fold cross validation, no feature transformation, and diagonal covariance matrices. For each evaluation, I varied AIC/BIC from 0 to 1 in steps of 0.02, and I used 6 seed Gaussians. Thus, for each subject and cross validation fold, I calculated and averaged 51 results. The results of this evaluation are shown in Figure 3.15. They indicate that performance does not depend on which combination of these penalty scores is used.

**Effect of The Number of Seed Clusters** The number of seed clusters determined the initial number of Gaussians in the GMM that was subsequently optimized using my automatic model selection procedure. To determine the effect on performance of the number of seed clusters and of my automatic model selection procedure on performance, I evaluated the average classification error rates for each subject using 20-fold cross validation, no feature transformation, and diagonal covariance matrices. For each evaluation, I varied the number of seed clusters from 2 to 20, and I used an arbitrary AIC/BIC combination of 0.6. The results of this evaluation are shown in Figure 3.16. These results show that performance does not depend on the number of seed clusters and that automatic model selection was not necessary for these data. This is surprising in particular because analyses indicated that (in particular the not transformed) features were not very Gaussian and thus had to

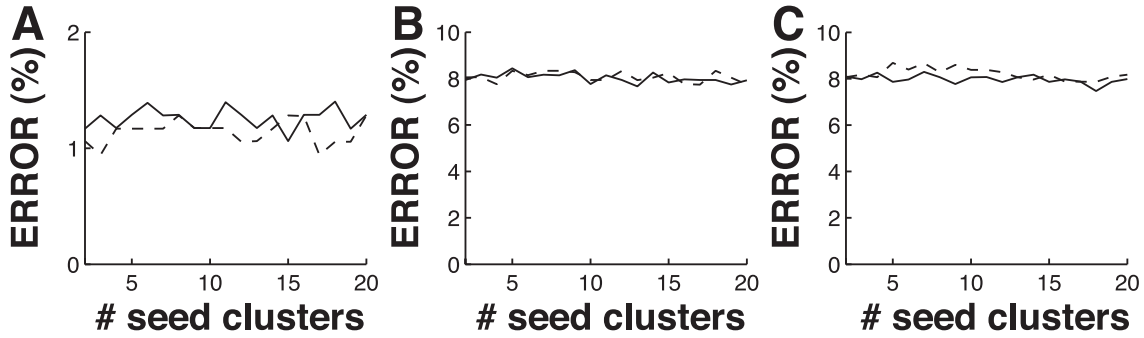


Figure 3.16: Performance achieved using different numbers of seed clusters for each subject. Solid and dashed lines represent results using and not using the model selection feature, respectively. These results reveal that performance does not depend on the number of seed clusters and that thus automatic model selection is not necessary for these data.

be modeled by an appropriate number of Gaussian distributions. This is empirical evidence that supports the notion that better background modeling does not necessarily imply increased performance in classification applications.

**Effect of Training Time and Number of Features** An important question was how much training time is required to provide consistent results. Intuitively, more features should require longer training time. To evaluate the effect of training time on performance, I evaluated the average classification error rates for each subject using 20-fold cross validation, no feature transformation, and diagonal covariance matrices. For each evaluation, I used 1, 2, and 4 Hz frequency bins (i.e., resulting in 20, 10, and 5 features, respectively) and I varied the amount of training time from 2:08 to 9:45 minutes (corresponding to 15 to 65 percent of the available training time in 10 percent increments, respectively). The results of this evaluation are shown in Figure 3.17. They do not indicate a clear effect of training time, but suggest that, depending on the dataset, the number of features can have a substantial effect.

### 3.5.3.2 Comparing Signal Detection to Linear Regression

The second question was how my novel approach compared in performance to a conventional method (that relies on initial signal identification procedures). To answer this question, I calculated average classification error rates using linear

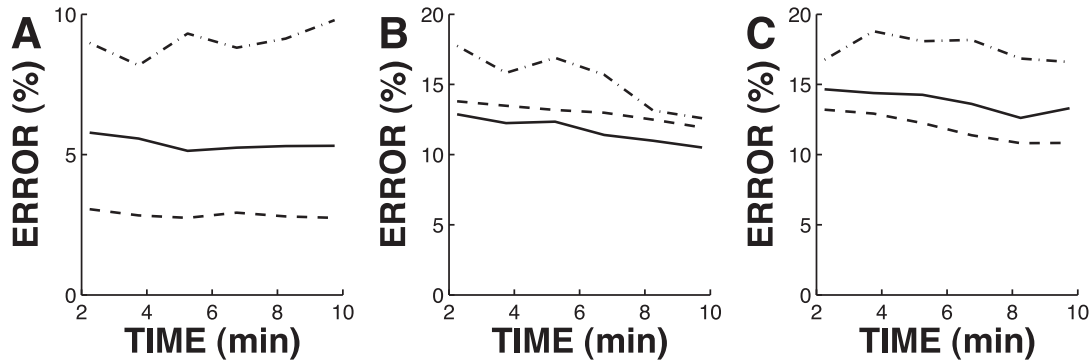


Figure 3.17: Effect of training time and the number of features on performance. Dash-dotted, solid and dashed lines correspond to results achieved using 20, 10, and 5 features, respectively. The results do not indicate a clear effect of training time, but do indicate that depending on the dataset, the number of features can have a substantial effect.

regression applied to the same features used in the previous evaluations (i.e., 2 Hz bins from 10 to 30 Hz) using 20-fold cross validation. The results of this evaluation are shown in Figure 3.18. These results show that my proposed approach produced results that are within the range of those achieved using linear regression. Further statistical analyses (Mann-Whitney Rank Sum Test) indicated that the results produced by these two methods were not different at the 0.05 level.

These important results suggest that current BCI approaches to feature translation could be replaced by the proposed method, which does not require the initial signal identification procedures that impede clinical application, without a loss in BCI performance.

### 3.5.3.3 Characteristics of BCI Control Signals

The third and final question was whether control signals produced by the detection approach have characteristics that would make them amenable to real-time BCI experiments. Real-time BCI experiments demand two requirements. First, signal processing can only consist of causal procedures (i.e., procedures that use past data) and should provide rapid feedback. Because my procedure can be applied to the same features as conventional methods in a causal fashion, and because the generation of control signals (i.e., the calculation of posterior probabilities) is computationally simple, my method can easily meet this first requirement. The second

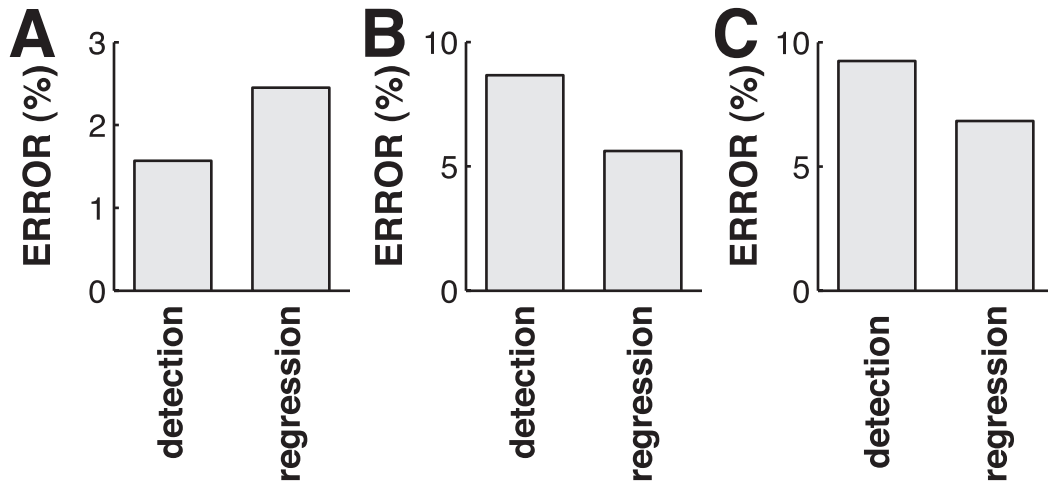


Figure 3.18: Performance comparison of results achieved using my detection approach to results achieved using linear regression. The results show that the results using my novel method are within the range of those that can be achieved using linear regression. Statistical analyses did not reveal a significant difference between these two methods at the 0.05 level.

requirement is that a subject can produce the whole range of possible control signal values equally easily and that inevitable noise be normally distributed around the desired control signal value. Because the present data set was recorded from a 4-target task in which the targets were evenly spaced long the y axis of the screen, and thus the subjects produced a graded modulation of the mu/beta rhythm, I was able to evaluate the output of my proposed algorithm according to this second requirement.

I calculated average control signal values (i.e., one value for each trial) using no feature transformation, diagonal covariance matrices, AIC/BIC of 0.6, and the number of seed Gaussians (chosen between 8 and 20) that delivered the best results; as before, I used 20-fold cross validation. This procedure produced four distributions of control signal values, i.e., one distribution for each of the four targets. I then evaluated the histogram of these distributions for untransformed control signal values and for log-transformed control signal values. The results are shown in Figure 3.19 and Figure 3.20 and summarized in Table 3.1. These results illustrate that the distribution of log-transformed control signal values have means that are evenly spaced along the value axis, that the standard deviations of distributions are

roughly similar for all targets, and that those characteristics compare favorably to characteristics achieved using linear regression. These results indicate that control signals produced by my detection approach have characteristics that make them amenable to real-time feedback. Together with the results in Section 3.5.3.2, these results further suggest that when used in real-time experiments, signal detection should perform comparably to linear regression.

In summary, signal detection removes the need for the lengthy and difficult signal identification procedures that are currently required, which constituted a major impediment to translation of the current generation of mainly laboratory BCI demonstrations into clinical practice, while still delivering results that are comparable to a major current method.

### 3.6 Discussion and Interpretation

This study showed how signal detection, a novel approach to BCI feature translation, could be used to overcome one of the significant impediments to the translation of laboratory BCI demonstrations into clinical applications. This is accomplished mainly because signal detection has two favorable characteristics: First, it reduces the BCI configuration problem from a problem of identifying both the location and the frequency of the signal that the subject can modulate to the problem of merely choosing an appropriate location. Because with EEG typically only very few locations are used for BCI control (e.g.,  $C_3$ ,  $C_4$ ), very little, if any, configuration is now necessary to initially configure a system for a user. Second, the signal detection approach is invariant to which features in the model are modulated by the user. Because in this study I tested models that used all frequency bands in one particular location, my method could provide adequate user feedback even if the frequency that is modulated by the user is initially unknown or changes.

In addition to discussing its advantageous theoretical properties, I also demonstrated that offline results achieved using signal detection favorably compare to results using linear regression. In summary, I showed that signal detection produces results that are similar to ones using linear regression techniques calculated on the same features, but that those results do not depend on initial signal identification

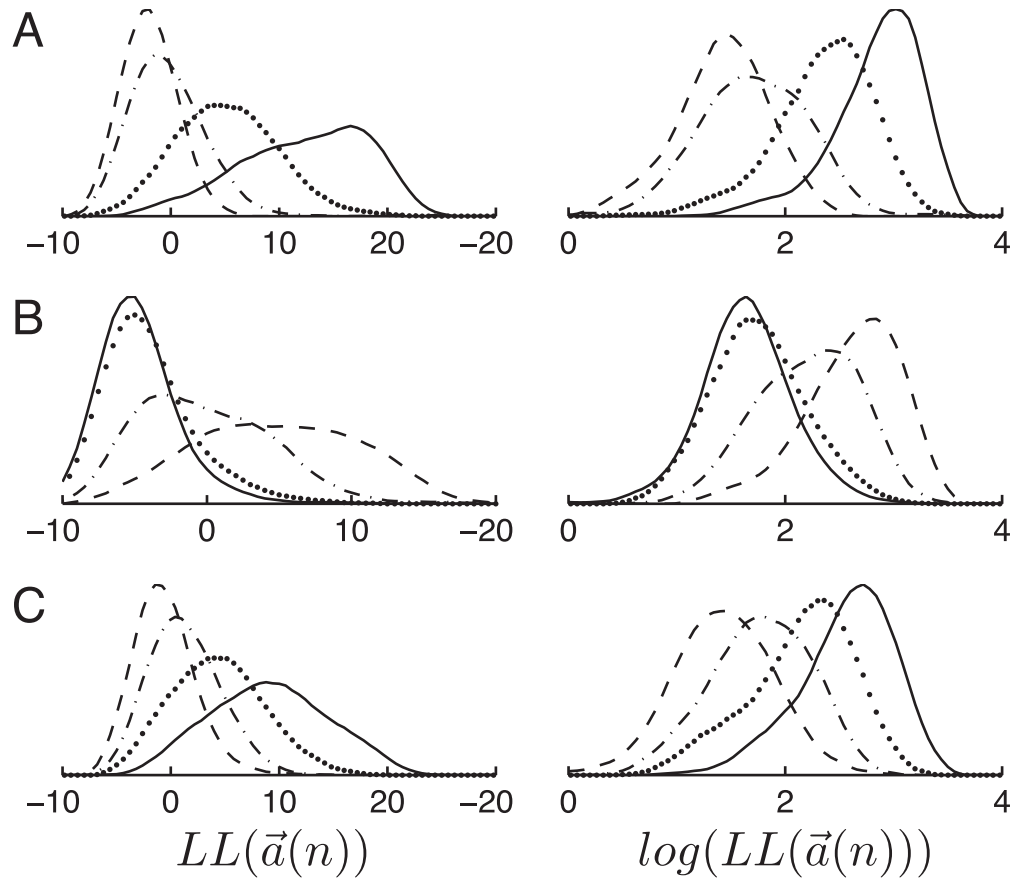


Figure 3.19: Histogram of trial averages of control signal values and their log transform for each of the four target locations. The results indicate that the log transformed control signal values are more evenly spaced and have standard deviations that are more similar than the ones for the untransformed control signals.

and system configuration procedures. In consequence, when using signal detection, BCI experiments could be conducted without those procedures and configurations, and could thus take better advantage of the more comprehensive signal features provided by recording techniques that can detect signals with higher fidelity (such as the ECoG signals used in other chapters of this dissertation).

The fundamental limitation of the present technique is that it reduces the BCI problem from a classification problem to a detection problem. Because signal detection cannot distinguish between modulation of different features within one model (e.g., one brain location), it can produce only one control signal per such

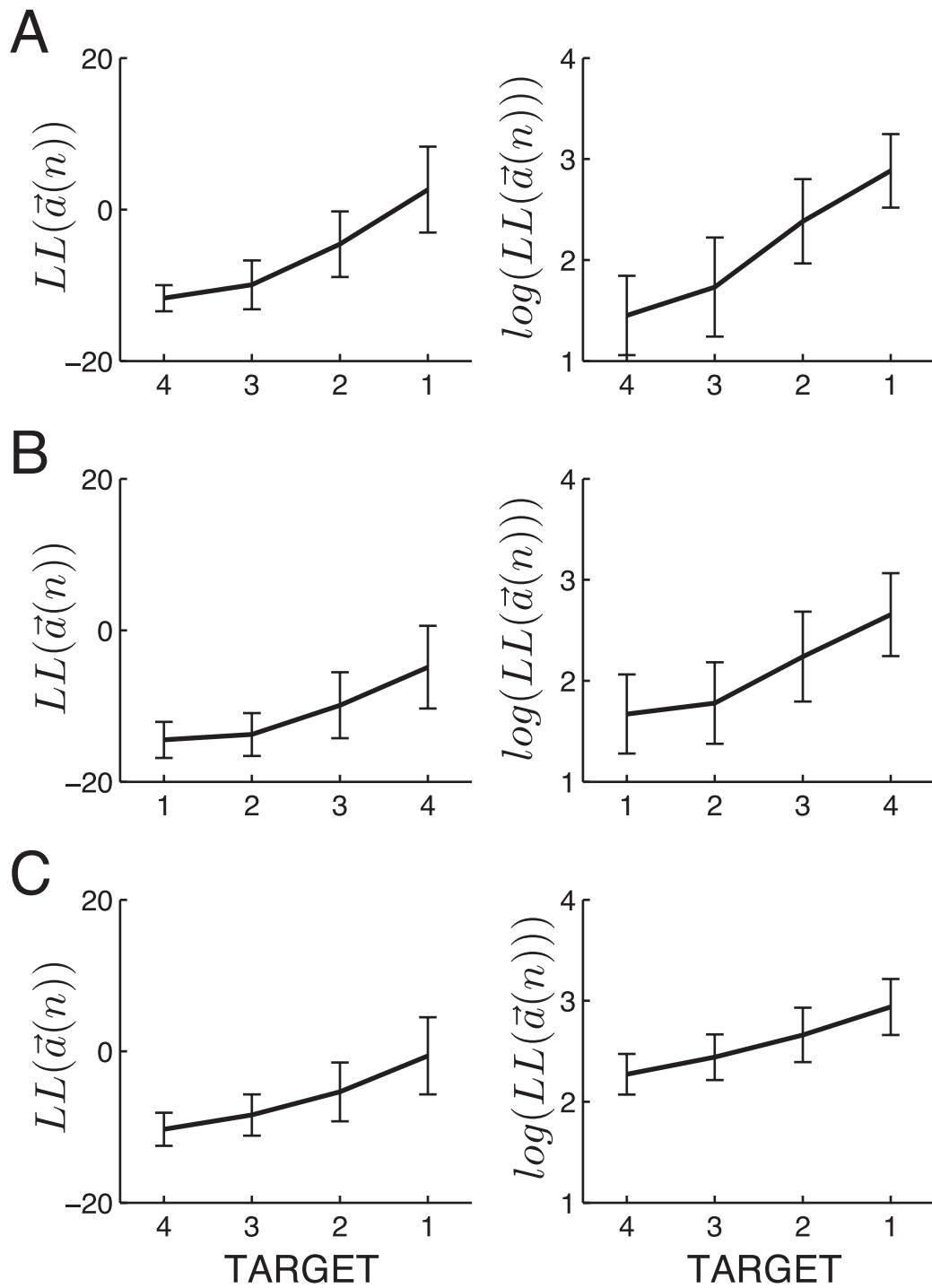


Figure 3.20: Plots of averages and their standard deviation of control signal values and their log transform for each of the four target locations. The results indicate that the log transformed control signal values are more evenly spaced and have standard deviations that are more similar across the four targets than the ones for the untransformed control signals.

subject A	$LL(\vec{d}(n))$				$\log(LL(\vec{d}(n)))$				linear regression			
	$\mu$	$\sigma$	$\beta_2$	$\gamma_1$	$\mu$	$\sigma$	$\beta_2$	$\gamma_1$	$\mu$	$\sigma$	$\beta_2$	$\gamma_1$
<b>target 1</b>	2.63	5.67	2.37	-0.46	2.88	0.36	4.45	-1.26	-1.00	0.70	2.35	0.19
<b>target 2</b>	-4.57	4.33	2.90	0.30	2.38	0.42	3.89	-0.84	-0.28	0.44	3.44	-0.48
<b>target 3</b>	-9.95	3.23	12.67	2.03	1.73	0.49	3.75	-0.28	0.32	0.40	5.26	0.26
<b>target 4</b>	-11.70	1.72	3.16	0.62	1.45	0.39	2.94	-0.39	0.58	0.29	2.93	0.14
$r(\mu)$	0.97				0.98				0.99			
$p(\mu)$	0.03				0.02				0.01			
subject B	$\mu$	$\sigma$	$\beta_2$	$\gamma_1$	$\mu$	$\sigma$	$\beta_2$	$\gamma_1$	$\mu$	$\sigma$	$\beta_2$	$\gamma_1$
<b>target 1</b>	-14.47	2.38	8.48	1.74	1.67	0.39	4.56	-0.15	-0.26	0.23	5.94	-0.91
<b>target 2</b>	-13.76	2.82	5.34	1.40	1.78	0.40	2.86	0.26	-0.12	0.25	3.28	0.34
<b>target 3</b>	-9.90	4.37	3.14	0.62	2.24	0.45	2.48	-0.29	0.34	0.38	3.16	-0.03
<b>target 4</b>	-4.87	5.46	2.22	0.02	2.65	0.41	3.34	-0.83	0.82	0.54	2.62	0.06
$r(\mu)$	0.96				0.97				0.98			
$p(\mu)$	0.04				0.03				0.02			
subject C	$\mu$	$\sigma$	$\beta_2$	$\gamma_1$	$\mu$	$\sigma$	$\beta_2$	$\gamma_1$	$\mu$	$\sigma$	$\beta_2$	$\gamma_1$
<b>target 1</b>	-0.61	5.10	2.30	0.05	2.60	0.41	3.46	-0.83	-0.72	0.50	2.88	-0.07
<b>target 2</b>	-5.37	3.89	2.63	0.30	2.18	0.45	2.78	-0.63	-0.25	0.36	2.74	-0.32
<b>target 3</b>	-8.42	2.72	2.96	0.63	1.80	0.43	2.51	-0.26	0.02	0.31	2.89	-0.23
<b>target 4</b>	-10.30	2.18	7.26	1.55	1.46	0.44	3.36	-0.06	0.28	0.23	4.04	0.07
$r(\mu)$	0.98				1.00				0.99			
$p(\mu)$	0.02				0.00				0.01			

Table 3.1: Statistic moments of the control signals derived using signal detection (untransformed and log-transformed values) and using linear regression. These results illustrate that log-transformed control signal values have characteristics that favorably compare to results achieved using linear regression. Together with the results in Section 3.5.3.2, these results indicate that signal detection should produce online results that are comparable to results achieved using linear regression.

model. The number of possible control signals is thus limited to the number of models that can be constructed and not to the total number of brain signal features that can be modulated by the user. One could say that signal detection constitutes a trade-off between specificity and practicality.

Signal and background modeling has been used extensively in other domains such as in image processing (see Friedman and Russell [1997], Stauffer and Grimson [1999], Toyama et al. [1999], Harville et al. [2001], Pless [2003], Kuo et al. [2003], Liyuan et al. [2004] and Lee [2005]). For reasons that are not entirely clear, with very few exceptions (e.g., Harris et al. [2000], Costa and Cabral [2000] and Pernkopf and Bouchaffra [2005]), this approach has been practically absent from biosignal

processing. At the same time, there are many applications within biosignal processing that could benefit from signal detection. For example, detection of P300 evoked potentials of the EEG (see Farwell and Donchin [1988]) is typically achieved using standard classification techniques. These techniques work very well with the stable responses typically found in healthy individuals, but often fail if responses vary in time or in space as often encountered with patients. Signal detection could be applied to this problem by rendering detection performance invariant to time and space. Artifact detection (see Anderer et al. [1999], Schloegl et al. [1999] and Goncharova et al. [2003]) is another potentially attractive application. Furthermore, automated detection of epileptic seizures is also typically performed using hand-crafted or machine-learned classification criteria. This approach thus has problems if the signature of the seizure changes, which is typically the case across and even within subjects.

All these examples demonstrate that typically, there is little *a priori* knowledge about the nature of particular signal changes in the brain. This implies that traditional classification-based methods have to be applied after the fact, which forgoes a number of attractive applications within but also outside of BCI research that could benefit from real-time (i.e., prospective) analysis of brain signal changes. The following section expands on this possibility and demonstrates that the method presented in this chapter has important applications in other areas.

## 3.7 Other Important Applications of Signal Detection

### 3.7.1 Introduction

The previous sections demonstrated that signal detection can improve BCI signal processing because it depends on fewer a-priori assumptions than signal classification. This attribute of signal detection has important implications for more general areas of biosignal processing, in particular when combined with the favorable characteristics of ECoG signals demonstrated in **THEME I**.

For example, in neuroscientific investigations or clinical evaluations of brain function, the complex nature of brain signals implies (just like in BCI research) that they first have to be translated before they can be readily interpreted. This translation is typically accomplished using statistical approaches that, again, by

definition have to be applied after all data are collected. Because these statistical relationships typically do not generalize to other datasets, this current procedure inherently prohibits real-time signal analysis with the requisite fidelity and thus excludes prospective study of many important problems. For example, it has been demonstrated that movements and language produce spatially localized changes in various features derived from the electrocorticogram (ECoG) (Crone et al. [1998b,a, 2001]) and thus, in theory, function could be located passively by analyzing these changes. This capacity could be a valuable clinical tool that could augment or even replace current methods to locate function such as electrical stimulation. However, these changes often manifest themselves in signal features that are different from individual to individual, which limits analyses to post-hoc evaluations. This problem is similar to the signal identification problem in BCI research in that traditional approaches apply procedures that inherently require significant knowledge about a signal to a situation that has limited *a-priori* such knowledge. This is unfortunate since real-time visualization of brain function that can be readily interpreted by a non-expert or an algorithm would be a new tool, essentially a new imaging method, that would open up many new avenues for the study of brain function.

As an additional problem, current methods usually require averaging in cue-based studies. Such studies test whether a particular experimental condition (such as a task or a stimulus) will elicit a particular signal. For example, if it is hypothesized that opening and closing eyes will produce detectable brain signal changes, this hypothesis can be tested by collecting brain signals under these two experimental conditions. Once all data from these two conditions are collected, statistical comparisons can reveal the specific changes associated with the experimental condition. This serious limitation prohibits interactive and exploratory studies.

In summary, current approaches to study brain function are typically limited to retrospective evaluation and cue-based experiments. A method that can visualize brain signal changes (which might be expressed in a number of brain signal features) prospectively and in real time without averaging would be a boon to many applications in applied research and clinical diagnosis.

I here demonstrate that the signal detection approach presented in the previous

sections, here called SIGFRIED (SIGnal modeling For Real-time Identification and Event Detection), can be used to prospectively analyze brain signal changes in real time. Using data collected for **THEME I** of dissertation, I also show that when paired with electrocorticography (which produces signals with high signal-to-noise ratio and spatial resolution), SIGFRIED can produce results that can be readily interpreted by an untrained observer without averaging, thus removing the need for cue-based experimental paradigms. I demonstrate this capacity by using SIGFRIED to visualize and localize in real-time the changes that occur to electrocorticographic (ECoG) activity during motor and language function.

Localization of motor or language function is often performed prior to excision of mass lesions adjacent to eloquent cortex or with surgery for intractable epilepsy. Functional mapping (i.e., mapping of motor or language function) is typically performed using subdural electrodes and electrical stimulation, which is time consuming, disrupts normal brain function, may be false localizing, and can induce seizures. Recent results suggest that passive mapping using electrocorticography can produce results that can correspond to electrical stimulation and thus may be an attractive alternative to present techniques (e.g., Sinai et al. [2005]), but all current methods to derive this mapping have to be done in retrospect using cue-based experiments, which do not make them amenable to rapid clinical testing.

### **3.7.2 Methods**

#### **3.7.2.1 Subjects**

In preparation for the BCI experiments conducted for this dissertation (that are described in **THEME I**), I recorded data from several patients at Barnes-Jewish hospital with intractable epilepsy who underwent temporary placement of intracranial electrode arrays to localize seizure foci prior to surgical resection. The study was approved by the Human Studies Committee of Washington University Medical Center.

#### **3.7.2.2 Data Collection**

Each patient sat in a hospital bed about 75 cm from a video screen. In all experiments, I used the recording methodology developed in **THEME I**. All electrodes

were referenced to an inactive electrode, amplified, bandpass filtered (0.1-220 Hz), digitized at 500 Hz, and stored. In several patients, I collected data while the subject was resting, i.e., not actively engaged in any motor or motor imagery task. I then collected data from several 2-min runs, during which the patient was asked to perform different motor or language tasks in response to visual cues. In offline analyses, every 200 ms the time-series ECoG data from the past 400 ms were re-referenced using a common average reference (see Section 3.3.1) and converted into the frequency domain using an autoregressive model of order 25 (see Section 3.3.2). The frequency domain amplitudes for traditional mu/beta or gamma bands were input to the modeling approach described in Section 3.4.2 (which I will here refer to as SIGFRIED). Just like with the BCI data, I then calculated negative log-likelihood values for these data. In summary, I produced one output signal per signal channel (i.e., the negative log-likelihood) that indicated the statistical difference between the feature vector calculated at that time to the distribution of feature vectors recorded during the rest period.

In the following sections, I illustrate three example applications of SIGFRIED to ECoG activity recorded during a variety of tasks. These three examples demonstrate that SIGFRIED can be used to determine useful information from changes in brain signals without detailed a-priori information about the nature of the change and illustrate that the methodologies developed in this dissertation may have important applications in other areas.

### 3.7.3 Results

#### 3.7.3.1 Example 1: Real-Time Visualization

The first example demonstrates that SIGFRIED can be used to visualize brain signal changes in real time (i.e., in a prospective fashion). To do this, I recorded two datasets using ECoG. In the first dataset, the subject was simply resting. In the second dataset, which was recorded on a different day than the first dataset<sup>7</sup>, the subject moved his hand or shoulder, or simply rested, in response to visual cues.

I first created one model of the signal distribution for the resting dataset

---

<sup>7</sup>This important detail demonstrates that the model of resting brain signal activity generalizes to data recorded from a different day.

for each location using 7 features (i.e., traditional gamma-band frequencies (which produce signals that are highly specific but less sensitive than mu/beta frequencies) for 10 Hz bins between 40 and 100 Hz). I then derived the negative log-likelihood of the signals for each sample in the second dataset and each location.

Figure 3.21 illustrates the results of this analysis. Panel A illustrates the running averages of the output calculated using SIGFRIED (i.e., the negative log-likelihood) for the three conditions of rest, shoulder, and hand movement. (The three average brain figures were created with identical analysis and display settings.) The different locations that are active for shoulder and hand but not for rest are evident. Active locations are rapidly defined and remain stable over longer periods. Panel B illustrates that responses to hand and shoulder movement can also be readily identified without averaging, which would support rapid clinical localization of brain function associated with these two motor tasks. The black and red trace show SIGFRIED time courses for two electrodes responding to hand and shoulder movements, respectively. Shaded bars indicate times of cue presentation.

### 3.7.3.2 Example 2: Localization of Face Motor/Language Function

The second example demonstrates that SIGFRIED can be used to localize face motor and language function passively, i.e., without using the active procedure (i.e., electrical stimulation of different brain areas) that is typically employed. To do this, I recorded four datasets using ECoG. In the first dataset, the subject was simply resting. In three additional datasets, which were recorded on a different day than the first dataset, the subject protruded the tongue, repeatedly said the word "move," or generated in a verb in response to a noun, in response to visual cues.

I first created one model of the signal distribution for the resting dataset for each location using 7 features (i.e., traditional mu/beta-band frequencies (which are less specific, but more sensitive than gamma frequencies (Crone et al. [1998b,a])) for 5 Hz bins between 5 and 35 Hz). I then derived the negative log-likelihood of the signals for each sample in the other three datasets and each location. Averages for the log-likelihood values for each electrode and condition identified the locations with significant changes during these conditions. I then collated the results of this passive mapping procedure with the anatomical and functional mapping data, which

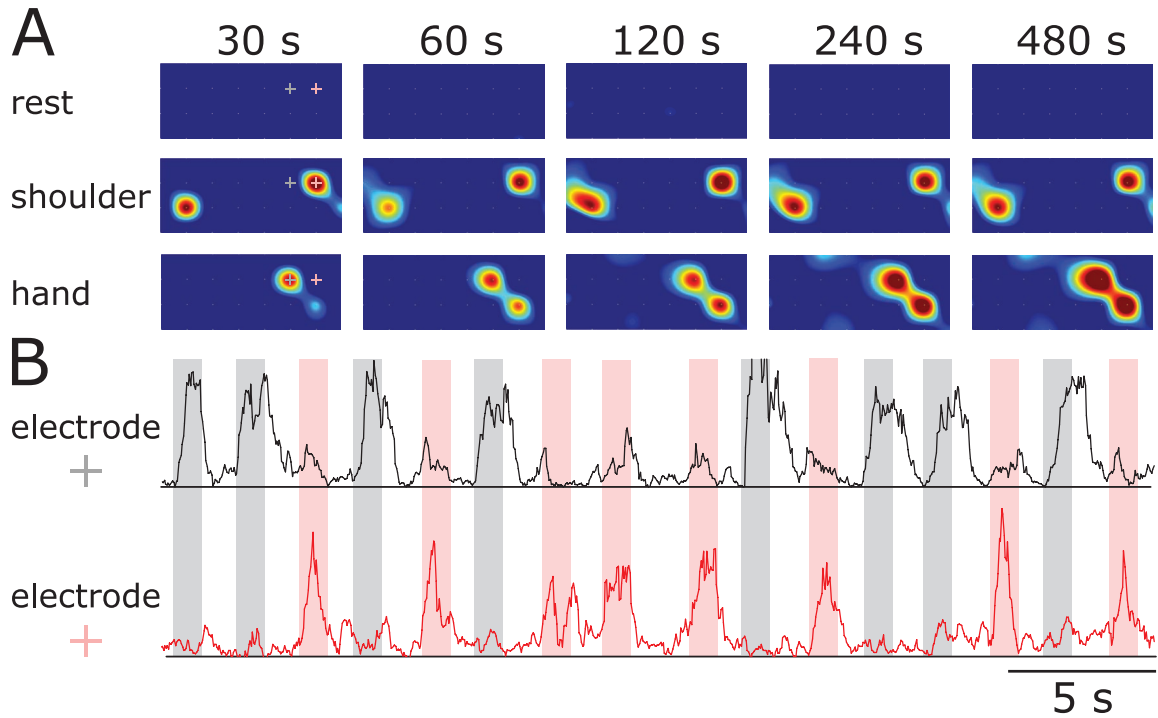


Figure 3.21: Real-time visualization of brain function. A: SIGFRIED quickly identifies the locations of the signal changes associated with shoulder and hand movement. This localization remains stable over longer periods. B: The signal time course of specific locations detects shoulder and hand movements (during the red and gray periods, respectively) without averaging. See text for details.

were derived using the electrical stimulation procedure typically employed.

Figure 3.22 illustrates the results of this analysis. Panel A shows activations calculated using SIGFRIED. (The three brain topographies were created with identical analysis and display settings.) Symbols indicate locations identified using electrical stimulation. The congruence of the results using SIGFRIED to the results using electrical stimulation is evident. Panel B shows the SIGFRIED time course for the electrode that was responsive to the verb generation task. Arrows indicate times of cue presentation. Activations in Broca's area can be readily identified in the time course. These results indicate that, with further verification, these techniques could provide a new clinical tool that could eliminate the need for the traditional mapping techniques using electrical stimulation.

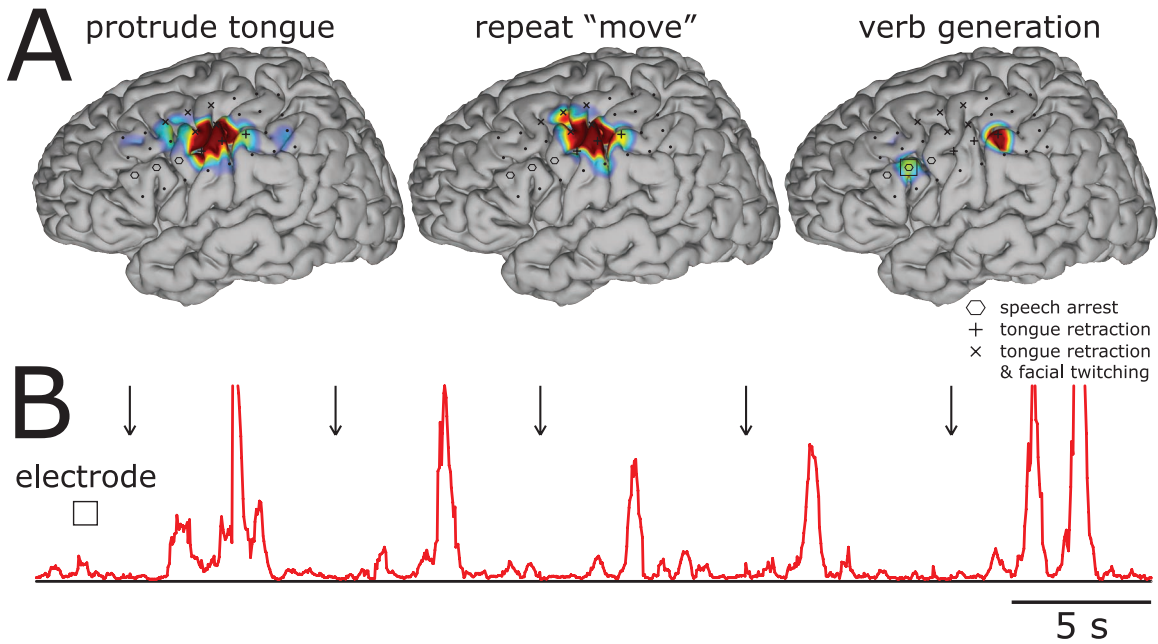


Figure 3.22: Language and face motor mapping without electrical stimulation. A: SIGFRIED identifies the areas that are responsive to the different tasks. There is substantial congruence to the results achieved using electrical stimulation (indicated by the symbols). B: SIGFRIED time course of one electrode shows, without averaging, the activation of one location over Broca's area with the verb generation task.

### 3.7.3.3 Example 3: Localization of Motor Function

The third example expands on the use of SIGFRIED to passively localize motor function. To do this, I recorded two datasets using ECoG. In the first dataset, the subject was simply resting. In the second dataset, which was recorded on a different day than the first dataset, the subject executed repetitive movements of different body parts in response to visual cues.

To localize motor function, I first created one model of the signal distribution for the resting dataset for each location using several features (i.e., traditional mu/beta-band frequencies for 5 Hz bins between 5 and 30 Hz, or traditional gamma-band frequencies for 5 Hz bins between 40 and 100 Hz). I then derived the negative log-likelihood of the signals for each sample in the second dataset and each location. Averages for the log-likelihood values for each electrode and condition identified the locations with significant changes during these conditions. I then collated the results

of this passive mapping procedure with the anatomical and functional mapping data, which were derived using the electrical stimulation procedure typically employed.

Figure 3.23 illustrates the results separately for the mu/beta and gamma band analysis. In the brain model on top, black dots indicate the recorded electrodes, and the black square shows the area that is shown in more detail below. The activation patterns below highlight the brain areas that responded to the different tasks and were identified using SIGFRIED. (The activation patterns were created with identical analysis and display settings.) Stars indicate locations identified using electrical stimulation. As expected, the use of mu/beta frequencies produces is more sensitive, but less specific, than the use of gamma frequencies. These results indicate that these techniques might provide a new clinical tool that could eliminate the need for the traditional mapping techniques using electrical stimulation.

### 3.8 Conclusions

This chapter discussed **THEME II** of this dissertation, which first proposed the use of a detection approach for BCI signal translation. The main contribution presented in this chapter is the finding that the use of this approach can result in performance similar to that achieved by the classification-based techniques traditionally used in BCI research without necessitating the initial signal identification procedures that are typically required. These procedures define the location and particular brain signal features that best express the subjects' intent, and have been necessary with traditional methods due to the substantial variability across subjects in these parameters. Because these tedious procedures, and the necessary expert oversight they imply, present one of the principal impediments to clinical use of BCI devices, the results presented in this chapter should facilitate the translation of laboratory BCI demonstrations into clinical practice. In addition to this contribution to BCI research, I also demonstrated that this methodology can be used as a novel and effective way to visualize brain signals in real time. The methodologies presented here could thus contribute to basic or clinical research and diagnosis.

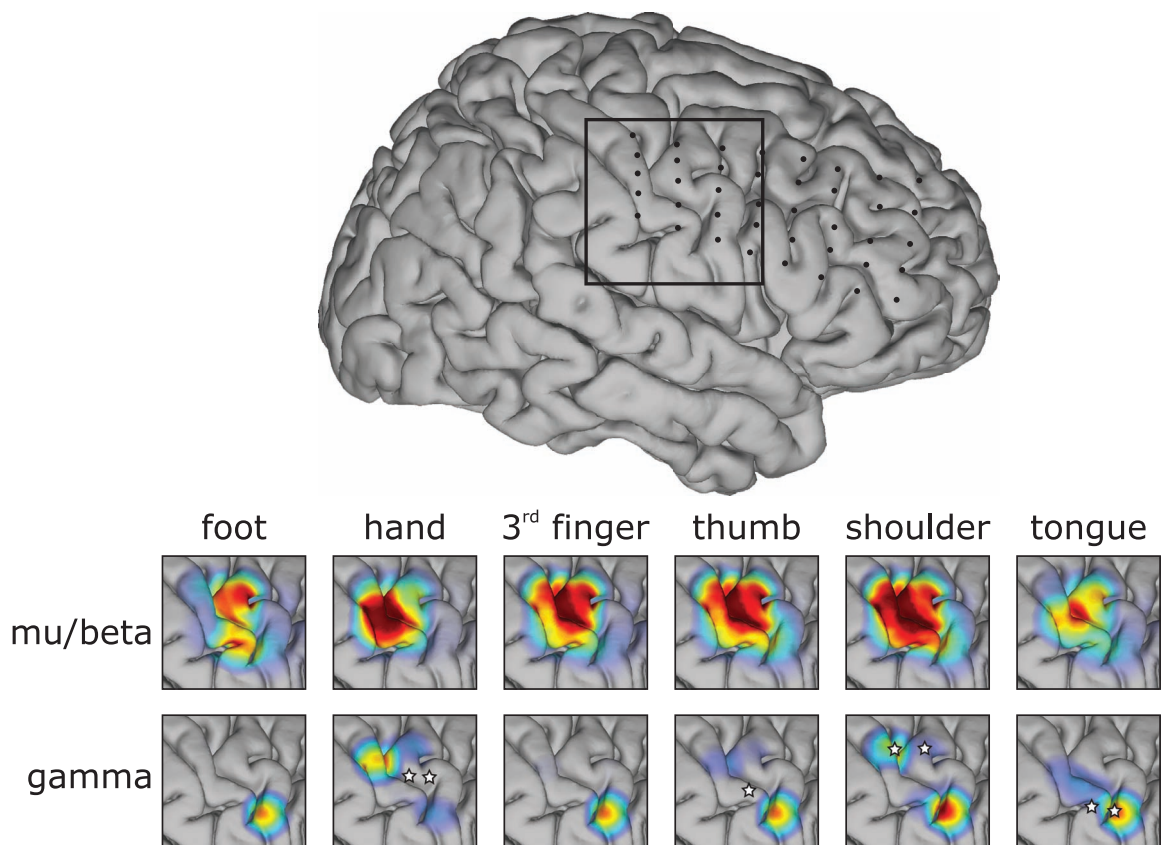


Figure 3.23: Motor mapping without electrical stimulation. Activation patterns derived using SIGFRIED and mu/beta frequencies are more sensitive, but less specific, than those using gamma frequencies. The congruence of the results using SIGFRIED and gamma frequencies to the results derived using electrical stimulation (indicated by the stars) is evident.

## CHAPTER 4

### THEME III: MORE INTUITIVE TASKS

*A man paints with his brains and not with his hands.* Michelangelo Buonarroti (1475 - 1564).

#### 4.1 Summary of Contributions and Approach

This chapter discusses THEME III of this dissertation, which is about designing more intuitive tasks for BCI devices. Current non-invasive BCI systems in humans make use of arbitrary tasks (such as imagined limb movement) in the context of movement control, which is not intuitive, may limit the degrees of freedom of the BCI system, and may also result in extended training. Current invasive BCI systems in non-human primates use more intuitive tasks. Corresponding experiments start by decoding detailed movement parameters (such as position or direction) from brain signals recorded during actual arm movement, and subsequently use decoded kinematic parameters related to these movements for device control. *It has been widely assumed that such detailed movement parameters can be derived only from signals recorded by intracortical microelectrodes. The main contribution presented in this chapter is the finding that, in fact, this widespread assumption is incorrect.*

The results presented in subsequent sections demonstrate for the first time that signals recorded by electrodes on the cortical surface (ECoG) also support accurate decoding of kinematic parameters of joystick movements in humans without requiring penetration of the brain. These results suggest that ECoG could be used to design more intuitive tasks for human BCI systems, that ECoG could be a more stable and less invasive alternative to intracortical electrodes for BCI systems, and that ECoG could also prove useful in other studies of motor function. This contribution thus has direct implications for BCI research, and is also important for basic neuroscience research on motor control.

Decoding movement parameters from ECoG signals has not been demonstrated previously. In addition, there was no theoretical basis and little experimental evidence that could suggest which signals (i.e., signal features in different domains

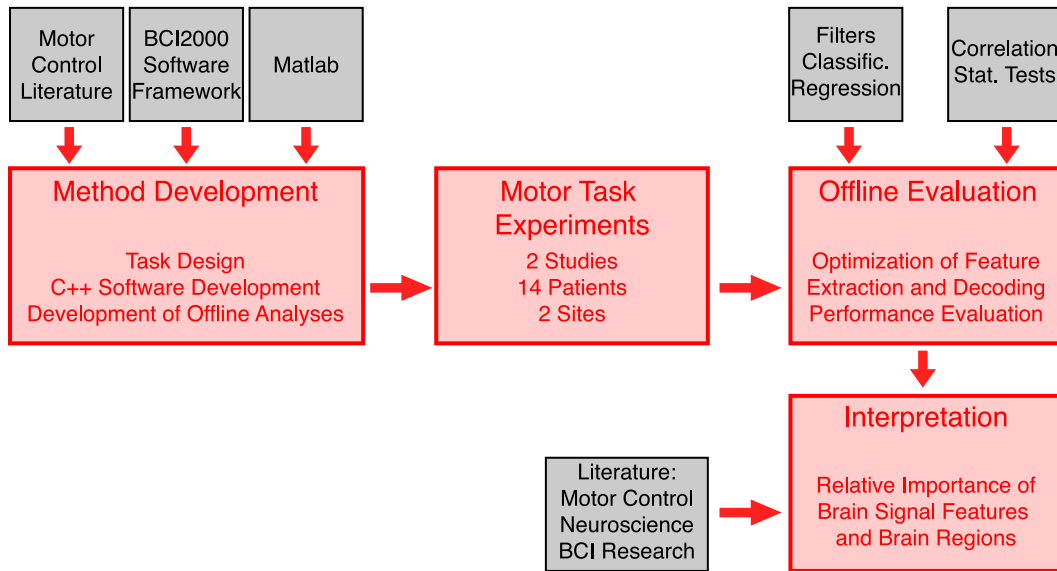


Figure 4.1: Overview of the work accomplished in THEME III. Items in red indicate work performed for this dissertation. Items in black indicate existing resources.

recorded at different locations) or decoding mechanisms might work best to decode movement parameters.

I thus tackled this problem using an experimental approach with subsequent empirical evaluations. I first designed motor tasks that were similar to those that have been used previously in research with non-human primates and implanted microelectrodes. I then designed empirical evaluations that addressed mainly two questions. The first question was which feature extraction and decoding methodologies would provide best performance, i.e., could best restore various kinematic parameters related to the movements in the motor tasks, and was thus mainly concerned with signal processing aspects of this problem. The second question was how the results, i.e., the quality of the decoding, the particular signal features that were implicated, and the characteristics of these features, related to the current body of understanding in neuroscience. The associated work is outlined in Figure 4.1.

The work in this chapter depended on application and extension of a number of methodologies from different areas of science and engineering, such as neuroscience, computer science, signal processing, and statistics, and is thus highly multidisciplinary. I utilized understanding of neuroscience to design the experimental

approach and to put the results in context to the established body of understanding. I used aspects of computer science, in particular C++ and Matlab programming, to write the software that supported the online experimental tasks, and to write the analysis routines for offline evaluations of these tasks, respectively. I also used an array of signal processing methodologies, in particular feature extraction, processing, and classification, to extract from brain signals that were recorded at many locations certain kinematic parameters of hand movements. I finally employed statistical methods, such as regression and correlation, and parametric and non-parametric tests, to derive and to evaluate the results of the study.

## 4.2 Introduction

Brain-computer interfaces (BCIs) convert brain signals into outputs that communicate a user's intent (Wolpaw et al. [2002]). Because this new communication channel does not depend on peripheral nerves and muscles, it can be used by people with severe motor disabilities. BCIs can allow patients who are severely paralyzed by amyotrophic lateral sclerosis (ALS), spinal cord injury, brainstem stroke, or other severely disabling neuromuscular conditions to express their wishes to the outside world. However, applications of BCI technology to the needs of people with severe disabilities are impeded by the limitations and requirements of the currently used non-invasive and invasive methods.

Non-invasive BCIs use electroencephalographic activity (EEG) recorded from the scalp (Wolpaw et al. [2002]). While these systems have been shown to support accurate non-muscular control, including 2D movement with a speed and accuracy comparable to those reported for invasive studies in monkeys (Wolpaw and McFarland [2004]), clinical applications using this approach have largely remained elusive due to several factors. Because they are detected far away from their sources within the brain, signals captured using EEG have low spatial resolution (Freeman et al. [2003]) and can thus detect only the concerted activity of large brain areas. Moreover, they are susceptible to artifacts such as electromyographic (EMG) signals. Perhaps most detrimental to practical clinical use, BCI systems using non-invasive methods often require extensive user training over weeks or months.

In contrast, invasive BCIs use single-neuron activity recorded within the brain (Georgopoulos et al. [1986], Taylor et al. [2002], Serruya et al. [2002], Lebedev et al. [2005]). Signals recorded within cortex have high spatial resolution, can be used to extract control signals with many degrees of freedom, and might support BCI systems that require less training than EEG-based systems. However, clinical implementations of these successful technical demonstrations (Donoghue et al. [2004], Hochberg et al. [2006]) are impeded mainly by the short- and long-term risks of surgical implantation of the electrodes and by the substantial problems in achieving and maintaining stable long-term recordings (Shain et al. [2003]). These issues are crucial obstacles that currently prohibit widespread clinical use in humans.

In the current absence of techniques to extract high-fidelity signals from EEG and of methods to record activity from many individual neurons safely and over long periods, an intermediate BCI methodology, using electrocorticographic activity (ECoG) recorded from the cortical surface, could be a powerful and practical alternative. ECoG has higher spatial resolution than EEG (i.e., tenths of millimeters vs. centimeters), broader bandwidth (i.e., 0-200 Hz vs. 0-40 Hz), higher amplitude (i.e., 50-100  $\mu$ V maximum vs. 10-20  $\mu$ V), and far less vulnerability to artifacts such as EMG (Freeman et al. [2003]). At the same time, because ECoG is recorded by subdural (or even epidural) electrode arrays and thus does not require electrodes that penetrate into cortex, it is likely to have greater long-term stability (Loeb et al. [1977], Bullara et al. [1979], Yuen et al. [1987], Pilcher and Rusyniak [1993], Margalit et al. [2003]) and to produce less tissue damage.

In **THEME I** of this dissertation, I showed that ECoG signals produced by motor imagery can provide one-dimensional BCI control with little training (Chapter 2), but it is not clear whether control could easily be extended to multiple dimensions with these methods (i.e., signal modulations associated with imagery of arbitrary motor tasks). It is possible that using more intuitive tasks (such as imagery of joystick movements) might further cut down on training requirements and could more easily be extended to multi-dimensional movements. However, most studies using intracortical local field potentials (LFPs) (i.e., signals derived within cortex but somewhat comparable to ECoG) have been in monkeys (Mehring et al. [2003],

Andersen et al. [2004], Rickert et al. [2005]). Limited relevant information is available in humans (Toro et al. [1994], Leuthardt et al. [2004], Georgopoulos et al. [2005]). In this dissertation, I conducted two studies (described in Sections 4.3 and 4.4) that address two aspects of the question whether joystick movements can also be decoded in humans without requiring penetration of the brain. Because the spatial resolution achieved using intracortical microelectrodes is about two orders of magnitude higher than that achieved using ECoG, it was completely unclear whether this would be possible at all, and, if it was possible, which brain signal features might carry relevant information.

In the first study, I asked whether movement direction for a discrete set of movements could be decoded from ECoG signals. In this study that is described in Section 4.3, I show for the first time that gamma rhythms that are prominent in ECoG, but not in scalp EEG, are correlated with the direction of discrete joystick movements in two dimensions when averaging signals over the movement period. These promising results encouraged systematic and comprehensive further investigations using real-time predictions and using a continuous movement task.

In the second study, I thus determined if it was possible to faithfully decode in real time two-dimensional movement parameters (i.e., position and velocity) from ECoG signals recorded from humans during a tracking task. In this study, I determined the effect on prediction performance of various sets of features, filtering, and classification techniques.

The principal results of these studies show that ECoG signals can be used to accurately decode two-dimensional joystick kinematics in humans, and that these results are within the range of the results that have previously been achieved only using intracortical microelectrode recordings in monkeys. Furthermore, they also describe a new brain signal component, which I labeled the local motor potential (LMP), that holds substantial information about movement direction. The LMP can also exhibit the same kind of cosine tuning (i.e., signal amplitude that is a cosine function of movement direction) previously detected only with intracortical microelectrodes in monkeys (Georgopoulos and Massey [1988], Salinas and Abbott [1994], Turner et al. [1995], Kettner et al. [1996], Amirikian and Georgopoulos [2000],

Baraduc and Guigon [2002], Todorov [2002], Rickert et al. [2005], Shoham et al. [2005], Nozaki et al. [2005]). These results provide strong evidence that ECoG could be used to provide accurate multidimensional BCI control with little training, and furthermore indicate that ECoG is a potentially powerful tool for the study of brain function.

### 4.3 Decoding Discrete 2D Joystick Movements

In the first study, I determined whether the average movement direction for a discrete set of movements can be decoded from ECoG signals. I first recorded ECoG signals while patients moved a joystick from the center of the screen towards one of four non-moving targets that were located on the periphery of the screen. I then compared the ECoG signals for the different directions of movement. These results show that ECoG signals are different for the different directions, and thereby encode information about movement direction. The following sections discuss data acquisition, analysis, and the results of this initial study.

#### 4.3.1 Data Collection and Analysis

I first collected data for these experiments. To do this, my collaborators in St. Louis and I recorded ECoG signals (from 32 locations) from four patients at Jewish Barnes Hospital. The patients had intractable epilepsy and underwent temporary placement of intracranial electrode arrays to localize seizure foci prior to surgical resection. These patients also participated in the BCI experiments in **THEME I**. See the corresponding Chapter (Section 2.6.2) for more details on patients and data collection. The following paragraph briefly summarizes the experimental paradigm.

In several 3-min runs (about 50 trials each), each of the four patients used a joystick (with the hand contralateral to the implanted electrode array) to move a cursor in two dimensions from the center of the screen to a target at one of four possible locations (i.e., a "center-out" joystick task; Figure 4.2) spaced around the periphery of the screen. (One patient completed an additional 13 joystick runs with eight target locations.) The sequence of this task was composed of three periods: rest, movement preparation, and movement. During the first period (rest) the screen was blank for one second. During the second period (movement preparation) a

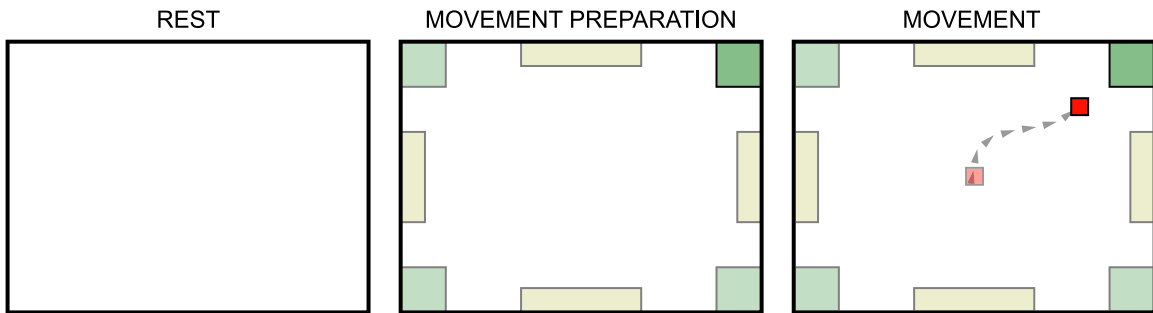


Figure 4.2: Design of the 2D center-out task. First, the screen was blank. Then, a target appeared in one of four or eight locations on the periphery of the screen. Finally, a cursor appeared whose velocity was controlled by the patient's joystick movements. The patient's task was to move the cursor into the target.

rectangular target appeared in one of four or eight possible locations on the periphery of the screen. 400 ms later, a cursor appeared in the center of the screen. In this final period (movement) the patients' task was to use a joystick to move the cursor into the target. The patients typically moved the cursor in a straight trajectory into the target within 1-1.5 seconds.

I then extracted ECoG signal features associated with each of the task periods. To do this, I utilized the autoregressive spectral estimation technique described in Section 3.3.1. I applied this technique to the ECoG signals from each electrode in 300ms blocks, and calculated frequency estimates between 0 and 200 Hz in 1 Hz bins. I then averaged all spectra within each task period (e.g., within one movement towards a target) to yield one average spectrum for each electrode location and each task period within each trial (e.g., 150 spectra (3 runs times 50 trials each) associated with each of the 32 ECoG locations and each of the three task periods).

To determine the effect of movement on the ECoG signal features, I analyzed these average spectra in two ways. First, I determined whether the features were different for joystick movement (in any direction) and for rest. To do this, I calculated, for each spectral bin and each location, the value of  $r^2$ , i.e., the fraction of the signal variance at that electrode and frequency that was accounted for by the task (of moving the joystick in any direction and rest). While limb movements can be differentiated from rest also using scalp-recorded EEG, this first analysis was intended to validate the recording and decoding technique. In fact, all four patients

showed at one or more electrodes significant spectral changes (i.e.,  $r^2 > 0.1$ ) between these conditions. This confirmed that limb movements can also be detected in these recordings, and thereby validated the experimental setup.

In the second analysis, I also compared the spectra for different directions of movement (e.g., right vs. left). No previous study in humans (using EEG or ECoG) has demonstrated effects on brain signals that were different for different movement directions. In Patients B and D, I found mu (i.e., 8-12 Hz), beta (i.e., 18-25 Hz), and/or gamma ( $> 30$  Hz) frequency bands at specific electrodes that were strongly correlated with movement direction. (Patient A had great difficulty executing the joystick task due to acute (i.e., post-operative) and chronic cognitive impairment. In Patient C, the electrode grid was placed very low (see Figure 2.16) so that it barely touched the lateral edge of the hand area.)

#### 4.3.2 Results

Figure 4.3A-C summarizes the principal results of this initial study. It illustrates with data from Patient D the directionally-specific effect on specific ECoG locations both immediately before movement (i.e., the movement preparation period) and during movement.

The upper panels (Figure 4.3-A) illustrate that ECoG carries information about movement direction (which has not been demonstrated in humans before.) (At -400 msec the target appeared, and at 0 msec the cursor appeared and began to move controlled by the joystick.) Left and center panels: Average time-frequency plots for left and right movements, respectively, for frequencies between 0-200 Hz and calculated between two adjacent electrodes. Right panel: The absolute value of the difference between left and right time courses. These results indicate that movement direction is reflected in ECoG across a wide frequency range, including frequencies far above those that can be detected using scalp-recorded EEG (i.e., greater than about 40 Hz). In general, amplitudes at frequencies below and above 50 Hz change in opposite directions. Figure 4.3-B displays the correlation (expressed in  $r^2$ ) between the signal shown in A and movement direction (left vs. right) calculated for the movement period.

Figure 4.3-C demonstrates that ECoG also carries information about move-

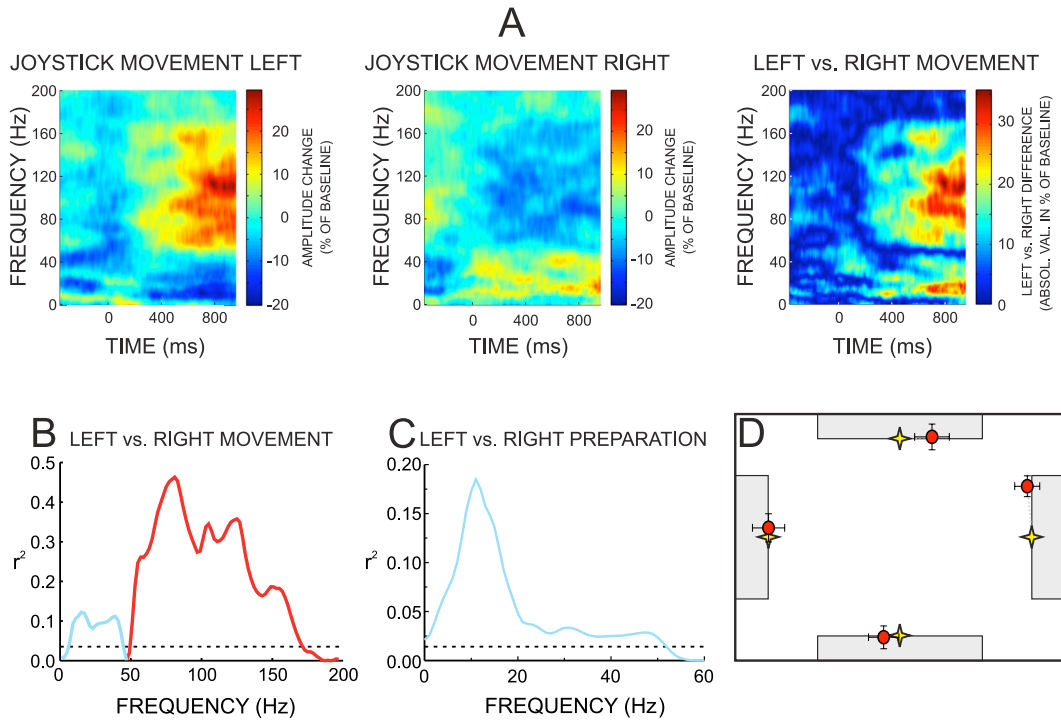


Figure 4.3: ECoG correlations with joystick movement direction before (panels A and C) and during movement (panels A and B) for Patient D. The directionally specific signal change during, but also prior to, movement is evident. Panel D: Average predicted final cursor positions (red circle) are close to the actual average final cursor positions (yellow star) (see text).

ment direction prior to the actual movement. In other words, these results demonstrate that it is possible to use ECoG signals to infer movement direction prior to the actual movement. It shows, for one particular electrode location, the correlation of this signal during the movement preparation period with movement direction. Mu rhythm activity (i.e., changes around 12 Hz) predicts movement direction. (In B and C, the blue and red traces indicate negative correlation and positive correlation, respectively, with the amplitude of left movement minus right movement; and dashed lines indicate the value of  $r^2$  that is significant at the 0.01 level.)

In further offline analyses of the joystick data from Patients B and D, I quantified the fidelity of the decoding afforded by the ECoG signals, i.e., the degree to which the actual movement directions could be decoded from the features extracted from the ECoG. To do this, I manually selected the ECoG features (i.e., amplitudes

in specific frequency bands at specific electrodes) as those that had the highest correlations with movement direction (i.e., the highest level of  $r^2$ ). These ECoG features were then submitted to a neural network with no hidden layer and two linear output neurons (i.e., achieving a procedure similar to linear regression)<sup>8</sup>. Specifically, I used, for each trial, average frequency amplitudes (averaged during the movement period) in 10-Hz bands (see Table 4.1 for details) at 3 or 4 electrode locations as the input features to the neural network that attempted to decode (using a backpropagation learning procedure (Haykin [1998])) the vertical and horizontal directions of joystick movement. One output neuron decoded average horizontal direction and the other one vertical direction.

Figure 4.3-D shows that the average predicted final cursor positions (i.e., red circles) (derived by adding the predicted direction to the starting point of the cursor (the center)) was close to the actual final cursor positions (yellow stars). (Error bars indicate the standard error of the mean.) This congruence is quantified in Table 4.1, which shows that the predictions were highly correlated with the actual movement directions and generally showed substantial generalization to other data sets. Columns (A), (B), and (C) show the high correlations between actual horizontal and vertical movements and the neural network predictions of these movements. (In the case of 8 targets, these calculations were done for the subset of 4 targets that were the same as the targets in the 4-target task.) In A, the network was trained on the whole data set and applied to the same data set. In B, the network was trained on the first half of the data and applied to the second half. In C, the network was trained on the even trials and applied to the odd trials. The network predictions obtained from one data set generally show substantial generalization to another data set. (The last column shows the values of  $r^2$  that are significant at the 0.01 level.)

These initial joystick results demonstrate for the first time that ECoG activity over select locations is correlated with movement direction. When combined with the known effect that real and imagined motor actions typically display similar brain signal changes (McFarland et al. [2000]), the exciting results of this initial evaluation suggest that people could use ECoG activity recorded from a few properly selected

---

<sup>8</sup>When I used a hidden layer, which allows the neural network to describe non-linear functions, decoding performance deteriorated when I tested the network on unseen parts of the datasets.

Subject	Trials (#)	Frequ. (Hz)	Loc. (#)	A		B		C		Sig. Level (p<0.01)
				$r^2(x)$	$r^2(y)$	$r^2(x)$	$r^2(y)$	$r^2(x)$	$r^2(y)$	
B (4 targets)	326	40-110	3	0.47	0.45	0.02	0.14	0.13	0.11	0.05
D (4 targets)	556	40-100	4	0.61	0.57	0.45	0.45	0.54	0.49	0.03
D (8 targets)	924	70-160	4	0.65	0.26	0.50	0.06	0.59	0.10	0.035

Table 4.1: Prediction of the direction of joystick movement from ECoG activity. Columns (A), (B), and (C) show the high correlations between actual and predicted horizontal and vertical movements when the neural network was trained and tested on all data (A), trained on the first half and applied to the second half (B), or trained on the even trials and tested on the odd trials (C). The network predictions obtained from one data set generally show substantial generalization to another data set.

sites for rapid and accurate multi-dimensional control of cursor movement. These encouraging results prompted further systematic evaluations, which are described in Section 4.4. The following section discusses and interprets the results of the present initial study.

#### 4.3.3 Discussion and Interpretation

In this initial study, offline analysis of ECoG data recorded during a 2D center-out joystick task showed substantial directional information (Fig. 4.3). Since Fetz and Finocchio's 1971 study showed that a motor cortical neuron can be used to control movement in a single dimension, researchers have strived to expand this to multiple dimensions (Fetz et al. [1971]). In 1986, Georgopoulos and colleagues identified an accurate representation of three-dimensional arm movements in motor cortex, and proposed an effective decoding algorithm for predicting arm movements from a population of motor cortical neurons (Georgopoulos et al. [1986]). Due to technological limitations preventing real-time recording and analysis of data from many individual cortical neurons simultaneously, it was not until 2002 that Schwartz and colleagues became the first to obtain three-dimensional closed-loop, real-time control of a cursor in a monkey (Taylor et al. [2002]). In 1994, Wolpaw and McFarland demonstrated significant two-dimensional control with scalp-recorded EEG signals in human subjects (Wolpaw and McFarland [1994]), and in recent work they achieved EEG-based two-dimensional control comparable to that reported in monkey single-neuron studies (Wolpaw and McFarland [2004]). This EEG-based control

relies on substantial training to establish two independent control signals (i.e., for vertical and horizontal movements, respectively) that are not evident prior to training. The two-dimensional joystick task used in the present study was similar to a wide variety of planar hand movements typically coordinated by the brain, and analysis revealed directionally specific ECoG activity at frequencies well above those usually discernible in scalp-recorded EEG. In combination with the known effect that brain signal changes associated with motor imagery and with actual movement are similar to each other, the present results suggest that ECoG activity comparable to that normally associated with behaviors such as joystick control could support more natural BCI operation that requires less training and achieves superior control.

The results also suggest the reason that directionally-specific effects have not previously been described for scalp-recorded EEG. As Figure 4.3 illustrates, the ECoG frequencies that best reflected movement direction were in the high gamma range (i.e., 40-180 Hz), well above the frequency range (up to 40-50 Hz) readily discernible in the scalp-recorded EEG. ECoG's superior frequency range is attributable to two factors. First, the capacitance of cell membranes of the overlying tissue combined with their intrinsic electrical resistance constitutes a low-pass (RC) filter that largely eliminates higher frequencies from the EEG (Pfurtscheller and Cooper [1975]). Second, higher frequencies tend to be produced by smaller cortical assemblies (Pfurtscheller [1999b]). Thus, they are more prominent at electrodes that are closer to cortex than EEG electrodes and thereby achieve higher spatial resolution (Freeman et al. [2003], Srinivasan et al. [1998]).

ECoG directional representation is likely to be further improved by using a grid with closer electrode spacing. The 1-cm inter-electrode distance in the grids used here is significantly larger than the suggested optimum ECoG spatial sampling resolution of 1.25 mm (Freeman et al. [2003]). Indeed, I often observed correlations limited to one or two recording sites. Thus, recording with higher spatial resolution might substantially improve ECoG-based BCI operation and facilitate control of multi-dimensional movements.

In conclusion, the present results are exciting initial evidence that directional information can be decoded from ECoG signals, and might thereby be used to

support BCI systems that require less training than current EEG-based methods. At the same time, the present study only utilized movements towards a discrete set of targets and predictions were made only for trial averages. The subsequent section describes the systematic and comprehensive follow-up study that evaluates whether real-time continuous movements can also be decoded using ECoG.

## **4.4 Decoding Real-Time Continuous 2D Joystick Movements**

The previous section demonstrated that, using frequencies that are inconspicuous on the scalp, ECoG can be used to provide directionally-specific information about average movement direction of discrete movements. Use of such signals might support BCI systems with several discrete choices.

The study presented in the following sections builds on these initial results. In this study, I evaluated the possibility that ECoG might also be used to decode, in a real-time and continuous fashion, information about two-dimensional hand movements. This possibility could support BCI systems that might allow for intuitive mouse-like control. Subsequent sections first present the methods related to the utilized experiments (in particular data acquisition and result presentation), and the signal processing methodologies that I used to study this question. I then demonstrate which signal processing approaches most effectively support the decoding of movement-related information from ECoG signals, and I finally study the results of corresponding decodings to elucidate their relationship to the established body of understanding.

### **4.4.1 Methods: Data Acquisition and Result Presentation**

#### **4.4.1.1 Subjects**

The subjects in this study were ten patients with intractable epilepsy who underwent temporary placement of subdural electrode arrays to localize seizure foci prior to surgical resection. My collaborators in Seattle and I collected data for five of these subjects at the University of Washington School of Medicine. My collaborators in St. Louis and I collected data for the other five subjects at Jewish Barnes Hospital in St. Louis. Each study was approved by the Institutional Review Board of the

respective institution. Each patient had a 48- or 64-electrode grid placed over the fronto-parietal-temporal region including parts of sensorimotor cortex. In addition, patients often had additional electrode grids or strips over other areas. The grids and strips consisted of flat electrodes with an exposed diameter of 3 mm and an inter-electrode distance of 1 cm, and were implanted for about one week. Grid placements and duration of ECoG monitoring were based solely on the requirements of the clinical evaluation, without any consideration of this study. As described in Section 2, these issues illustrate the difficulties of working with a patient population in an acute setting, and impede detailed statistical and performance comparisons across the patient population. Following placement of the subdural electrodes, each patient had postoperative anterior-posterior and lateral radiographs to verify their location. Grid location is shown for patients A-E (Seattle patients) in Figure 4.4. I could not confidently reconstruct electrode location for patients M-Q (St. Louis patients) and thus do not show them for these patients.

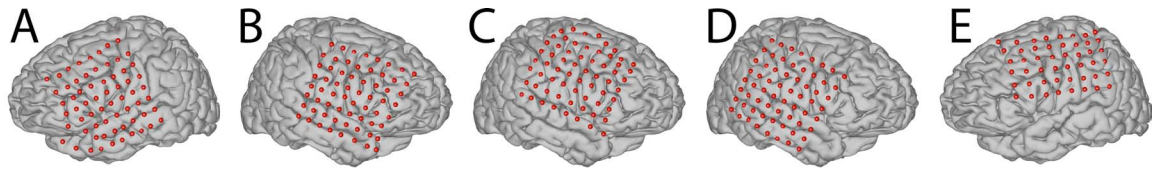


Figure 4.4: Electrode locations in the five Seattle patients.

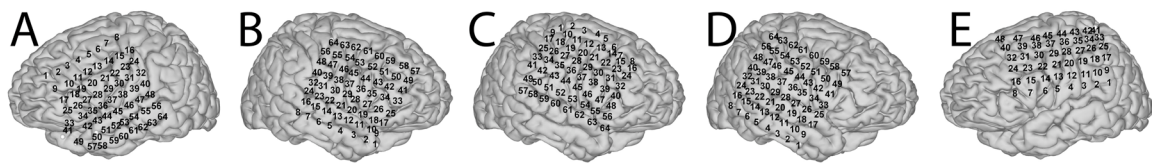
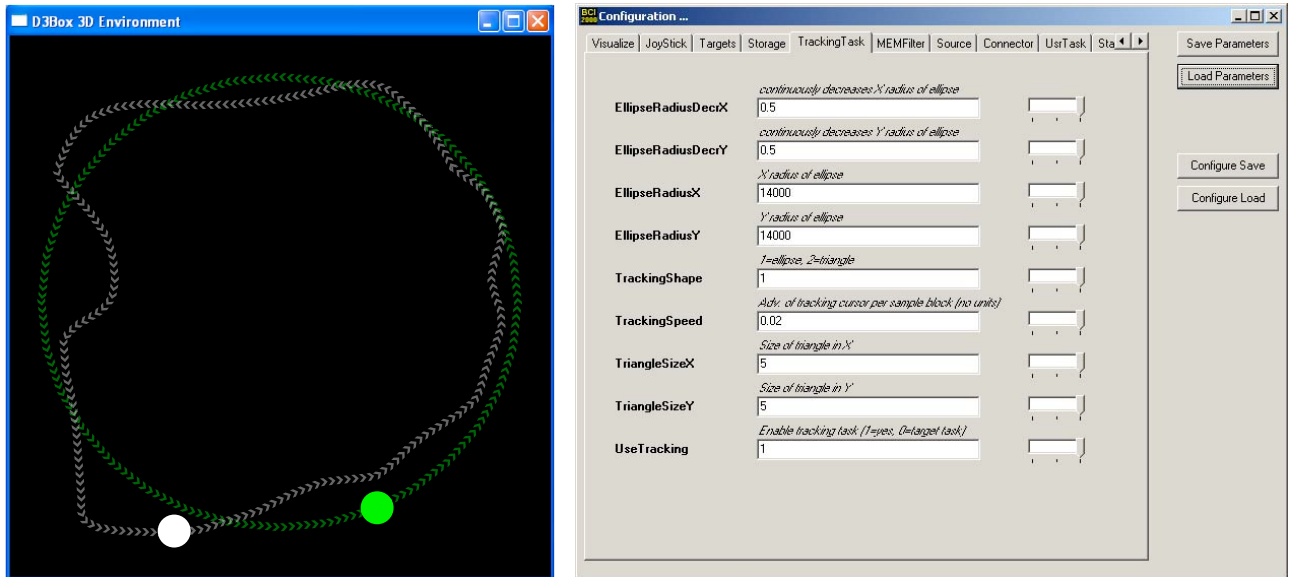


Figure 4.5: Electrode numbering in the five Seattle patients.

#### 4.4.1.2 Experimental Paradigm

Using C++ programming, I designed software that could realize tracking tasks similar to those described in the literature that studied motor control in primates. This software (see Figure 4.6(b)) could be parameterized using a number of different variables that affected particular characteristics of the task (such as the speed of the target, the radius of the circle, etc.).



(a) Illustration of the tracking task. The patients' task was to use a joystick or a mouse to control movement of a white cursor so as to track a green target that moved counter-clockwise in a circle on a computer screen.

(b) Parameters of the tracking task implementation

Figure 4.6: The tracking task and its parameters.

In these experiments, each patient used a joystick or a mouse (with the hand contralateral to the implanted electrode array) to move a white cursor in two dimensions to track a green cursor (i.e., the target) (see Figure 4.6(a)). In the joystick task, joystick position was mapped to cursor velocity and the joystick produced significant force feedback to the patient so that this task approached the isometric force tasks used in (Kalaska and Hyde [1985], Taira et al. [1996], Sergio et al. [2005]). In the mouse task, hand kinematics and cursor kinematics were mapped directly (i.e., velocity to velocity). For the joystick task, patients were asked to use shoulder and proximal arm movements (Seattle) or wrist movements (St. Louis). They were also asked to maintain a constant posture, but neither body, head, or hand were restrained in any way. The performance of each patient (i.e., how accurate he/she tracked the target) depended on his/her condition. The target moved counterclockwise in a circle that was positioned in the center of the screen. The diameter of the circle was approximately 85% of the screen's height. One full revolution of the target took approximately 6.5 seconds for all subjects.

#### 4.4.1.3 Data Collection

During study, each patient was in a semi-recumbent position in a hospital bed about 1 m from a video screen. In all experiments, I recorded and subsequently visualized ECoG signals using the data acquisition and 3D cortical mapping techniques developed in **THEME I** (Section 2). In short, I recorded signals from the electrode grid using the existing BCI2000 software system connected to Neuroscan Synamps2 or XLTEK systems (Seattle and St. Louis, respectively), which were available in the hospitals. In Seattle, simultaneous clinical monitoring was achieved using a connector that split the cables coming from the patient into one set that was connected to the clinical monitoring system and another set that was connected to the BCI2000/Neuroscan system. In St. Louis, BCI2000 acquired data directly from the clinical XLTEK system. Thus, at no time was clinical care or clinical data collection compromised. All electrodes were referenced to an inactive electrode. The signals were amplified, bandpass filtered (0.15-200 Hz or 0.3-200 Hz in different datasets) and digitized at 600 or 1000 Hz (St. Louis and Seattle, respectively)<sup>9</sup>. The signal samples  $\vec{s}(k)$  and the coordinates of the patients' cursor and target, which I will refer to as  $t_x(k)$ ,  $t_y(k)$ ,  $t_{rx}(k)$ ,  $t_{ry}(k)$ , respectively, were stored in a data file. The amount of data obtained varied from patient to patient, and depended on the patient's physical state and availability.

My collaborators and I collected 40 datasets from the ten patients (see Table 4.2). Patients used a joystick in 17 datasets (J), a mouse in 16 datasets (M), and simply tracked the target with their eyes (i.e., without hand movements ("watch" datasets, W)) in 7 datasets. Datasets were collected in runs of 2-3 min duration that were grouped together if they were recorded in close proximity in time (sometimes data were recorded on multiple days). The duration of the datasets ranged from 62-3033 sec. Each dataset was visually inspected and bad channels (such as those corresponding to electrodes that had broken connections) were removed prior to analysis, which left 48-64 channels for subsequent analyses.

---

<sup>9</sup>The 600 Hz sampling rate used with the initial experiments in St. Louis was well above the Nyquist rate given the 200 Hz lowpass cutoff. The 1000 Hz sampling rate in the experiments in Seattle, which were started later, were used because the Neuroscan system is confined to a 1000 Hz sampling rate.

Location	Subject	Modality	Group	Total time(s)	Runs
Seattle	A	J	1	436	1-4
	A	M	1	321	1-2
	B	J	1	248	1-4
	B	M	1	372	1-6
	B	J	2	430	1-6
	B	M	2	306	1-4
	C	J	1	134	1-2
	C	M	1	62	1
	D	J	1	260	1-4
	D	M	1	321	1-5
	E	J	1	611	1-4
St. Louis	M	J	1	550	1-3
	M	M	1	585	1-3
	M	W	1	570	1-3
	M	J	2	540	1-3
	M	M	2	560	1-3
	M	W	2	540	1-3
	M	J	3	540	1-3
	M	M	3	593	1-3
	M	W	3	540	1-3
	N	J	1	3033	1-7
	N	M	1	1717	1-6
	N	W	1	2000	1-5
	O	J	1	920	1-6
	O	M	1	700	1-6
	O	J	2	650	1-2
	O	M	2	708	1-3
	O	J	3	300	1
	O	M	3	240	1-2
	O	J	4	300	1
	O	M	4	400	1-2
	P	J	1	300	1
	P	M	1	303	1
	P	W	1	300	1
	P	J	2	300	1
	P	M	2	300	1
	P	W	2	300	1
	Q	J	1	1260	1-7
	Q	M	1	1090	1-6
	Q	W	1	900	1-5

Table 4.2: Datasets collected from the 10 patients in Seattle and St. Louis.

#### 4.4.1.4 3D Cortical Mapping

The lateral skull radiographs were used to identify the stereotactic coordinates of each grid electrode with custom software that realized the manual procedure described in Fox et al. [1985]. Cortical areas were defined using Talairach's Co-Planar Stereotaxic Atlas of the Human Brain (Talairach and Tournoux [1988]) and a Talairach transformation (<http://ric.uthscsa.edu/projects/talairachdaemon.html>). I obtained a 3D cortical brain model from source code provided on the AFNI SUMA website (<http://afni.nimh.nih.gov/afni/suma>). Finally, I projected each patient's electrode locations on this 3D brain model and generated activation maps using the Matlab program developed in **THEME I** (Section 2).

### 4.4.2 Methods: Signal Processing

#### 4.4.2.1 The Decoding Problem

The main impetus of the present study was to determine whether it is possible to infer (i.e., decode) from signals recorded on the surface of the brain particular kinematic parameters of hand movements in real time. Because this has not been done before, it was completely unclear which kinematic parameters (e.g., position, velocity, speed, movement angle, etc.) could be decoded from which input (i.e., joystick, mouse, or watch data sets from Seattle or St. Louis), and which decoding strategy might be best.

In essence, this situation constitutes an optimization problem that could be attacked with traditional optimization techniques such as genetic algorithms (Goldberg [1989]) or particle swarm techniques (Kennedy and Eberhart [1995]). However, these techniques are typically highly computationally complex and their output (i.e., the final configuration of the optimized decoding procedure) typically does not lend itself to human interpretation. Both of these issues are problems in the light of the context of the present study because in the end, these techniques should be amenable to rapid online processing (in BCI experiments) and their configuration should facilitate understanding of the biological relevance of the chosen components of that configuration. In addition, studies in non-human primates, which have also attempted to decode kinematic parameters of hand movement from brain signals (usually neural firing rates recorded within the brain), have also utilized relatively

simple decoding techniques (Kim et al. [2006]). Thus, I decided to investigate the efficacy of several common techniques in isolation.

In summary, I approached the decoding problem using a series of questions that were related to the input (which datasets), output (which kinematic parameters), and to the decoding method (which signal pre-processing, feature extraction, feature processing, feature selection, and decoding methodologies) that translated the inputs into the outputs. In other words, I generated a procedure, which is illustrated in Figure 4.7, that translated different inputs into different outputs using different processing methods. I used the correlation coefficient  $r$ , calculated between an actual and decoded kinematic parameter, as a performance metric to decide which components of this procedure were superior to others.

The following sections describe all six components of this procedure. Subsequent sections then evaluate the effect on performance of those components that are highlighted in red in Figure 4.7.

#### 4.4.2.2 Signal Pre-Processing

The first component of the decoding procedure was signal pre-processing, which consisted of signal interpolation and a spatial filter that are described below. (See Appendix A for a description of the notation used in subsequent sections.)

**Signal Interpolation** Data collected in St. Louis were collected using one sample-and-hold element on the A/D converter board (i.e., the hardware multiplexed signals from different channels in time). Spatial filtering operations (such as those described in the next paragraph) will produce residual noise if signal samples are sampled at different times (McFarland et al. [1997b]). In consequence, I applied a linear interpolation that attempted to restore signal sample values at one particular time point: for every channel  $h \in \{1, 2, \dots, H\}$ , the new signal value  $s_h(k)'$  at channel  $h$

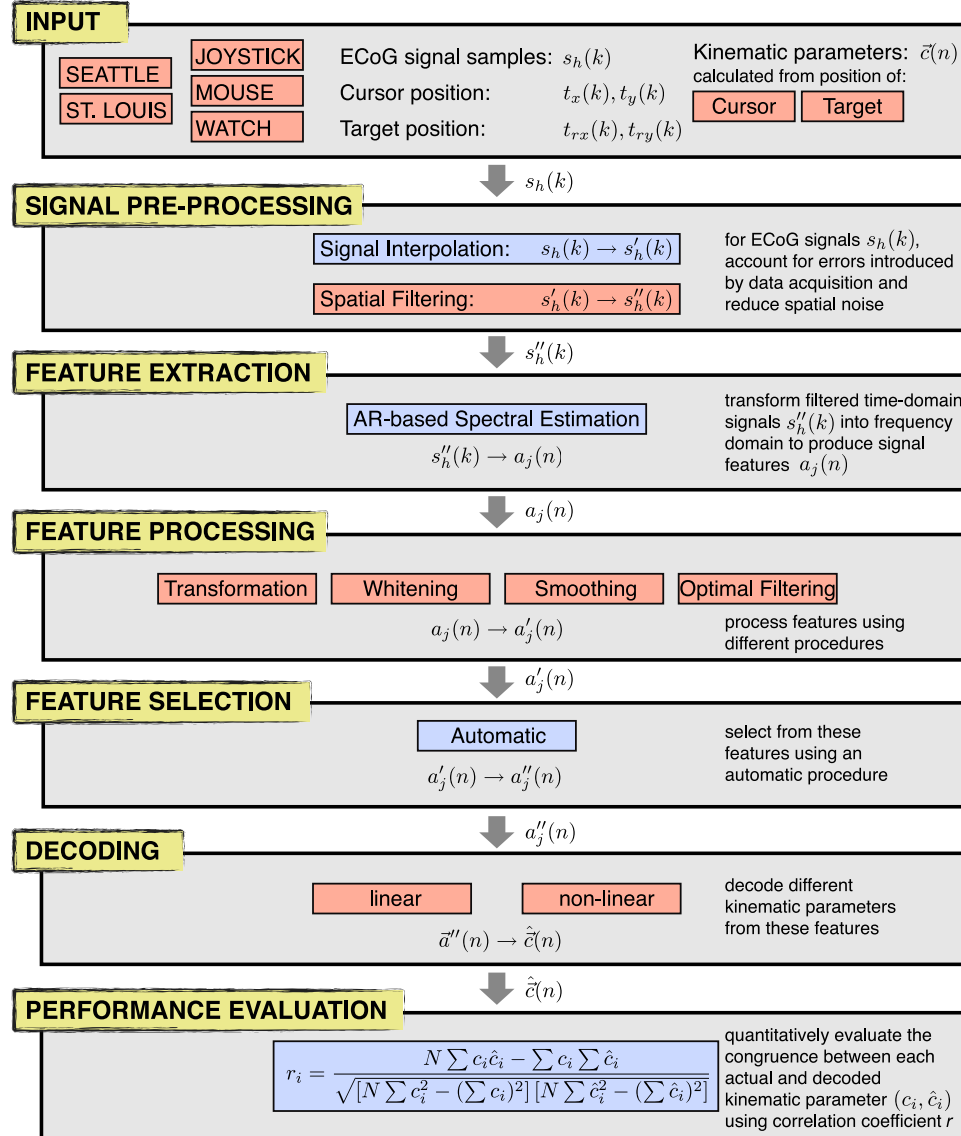


Figure 4.7: Overview of the decoding procedure. See text for details.

and time  $k$  was determined as

$$s'_h(k) = c_h s_h(k-1) + (1 - c_h) s_h(k)$$

$$c_h = \frac{h-1}{H}$$

Data collected in Seattle were collected using one sample-and-hold element for each channel. Consequently, each channel was sampled at the same time and thus I

did not interpolate the Seattle data ( $s'_h(k) = s_h(k)$ ).

**Spatial Filtering** As described in Section 3.3.1, spatial deblurring procedures (such as spatial high-pass filters) can improve the fidelity of brain signals. I thus evaluated the effect of a common procedure, the common average reference (CAR) filter, that was defined as follows:

$$s''_h = s'_h - \frac{1}{H} \sum_{q=1}^H s'_q$$

$H$  was the total number of channels,  $h$  was the channel index, and  $s'_h$  was the interpolated signal sample at a particular time.

#### 4.4.2.3 Feature Extraction

The second component of the decoding procedure consisted of feature extraction. Because no study had attempted to decode movement parameters from ECoG signals, I could not base the choice of features on an established body of understanding, with the exception that EEG and ECoG signals are typically studied in the frequency domain and that particular frequency bands (such as those in the mu/beta/gamma range have been shown to display changes with other tasks). In consequence, I used different frequency-domain features for subsequent evaluations.

The feature extraction algorithm used here was the same autoregressive spectral estimator described in Sections 2.5.1 and 3.3.1. As in this previous section, the raw signal, i.e., signal  $\vec{s}''$  in the time domain, was converted into an output, i.e., signal  $\vec{a}$  in the frequency domain. Specifically, I first partitioned signals  $s''_h$  of each channel  $h$  into windows of constant time  $L_w = f_s/3$  samples ( $\hat{=} 333$  ms), overlapping by  $L_o = L_w/2$  samples ( $\hat{=} 166$  ms), unless otherwise noted, thereby producing  $N$  windows. I write these windows as  $s''_h(k', n)$  where  $k' = 0, 1, \dots, L_w - 1$  and  $n$  was the window index. I passed each  $s''_h(n)$  (i.e., the whole window) to the spectral estimator, which produced spectral estimates  $\left[ \hat{S}_{f_1}^h(n), \hat{S}_{f_2}^h(n), \dots, \hat{S}_{f_Z}^h(n) \right]^T$  for frequencies  $f_1 = 0, f_2 = 1, \dots, f_Z = 200$  Hz (i.e., in 1 Hz intervals).

It was not clear which of these frequency amplitudes would best reflect movement parameters. Based on my initial study described in this dissertation (see

Section 4.3, which suggested that high Gamma frequencies up to 180 Hz might hold movement-related information) and the sparse evidence available in the literature that investigated movement encoding in different frequency bands (e.g., Rickert et al. [2005]), I manually defined  $B = 7$  frequency bins: 8-12 Hz, 18-24 Hz, 35-42 Hz, 42-70 Hz, 70-100 Hz, 100-140 Hz, and 140-190 Hz.

Using these frequency bins, I then averaged all 1 Hz spectral estimates within each bin to obtain brain signal features for channel  $h$  and window  $n$  denoted  $\vec{a}_h(n)$ . In addition, I extended the feature vector  $\vec{a}_h(n)$  by a novel brain signal feature that I called Local Motor Potential (LMP) after I identified brain signal channels whose time course appeared to correlate with kinematic parameters. Because these observations indicated that the signal time course, rather than modulation of a particular frequency band, was correlated with the signal, I decided to calculate the LMP feature using a simple running average in the time domain: the LMP was calculated simply as the mean value of the signal over the window  $n$  and was added to the feature vector  $\vec{a}_h(n)$ :  $\vec{a}'_h(n) = \left[ \frac{1}{L_w} \sum_{k'=0}^{L_w-1} s''_h(k', n), \quad \vec{a}_h(n) \right]$ . I derived the complete feature vector  $\vec{a}(n)$  (i.e., 8 features) as the concatenation of the feature vectors  $\vec{a}'_h(n)$  for all channels  $H$ .

#### 4.4.2.4 Feature Processing

The third component of the decoding procedure was feature processing. The purpose of feature processing was to improve decoding performance. To do this, I evaluated use of four commonly used procedures, i.e., feature transformation, feature whitening, feature smoothing, and optimal filtering. These four procedures are listed below and are evaluated in subsequent sections.

**Feature Transformation** Analyses showed that the distribution of the extracted frequency estimates was typically not Gaussian, but rather in many cases appeared to resemble the  $\chi$ -square distribution. Consequently, it was possible that feature transformation might provide superior prediction performance. Because the application of the simple functions *sqrt* and *log* led to feature distributions that closer resembled Gaussians, I included the two transformations in my evaluations. To evaluate the opposite effect, I also included the square transformation.

**Feature Whitening** I hypothesized that feature amplitudes could be subject to slow changes that were the effect of other sources (e.g., amplifier drift or non-stationarities in the brain). To remove these slow trends, and to render signals stationary with respect to their mean, I partitioned, in particular analyses, the feature time course  $a_j(n)$  into windows of length  $T_1 d$  where  $T_1$  was the length of one period of the circular tracking movement and  $d \in \mathbb{N}$  (typically  $d = 3$ ). Within each window ( $w = 0, 1, \dots$ ), I subtracted the mean feature value in this window from each feature value:

$$a'_j(n) = a_j(n) - \frac{1}{T_1 d} \sum_{n'=wT_1d+1}^{n'=wT_1d+T_1d} a_j(n')$$

In other analyses, I also normalized  $a_j(n)$  by its standard deviation calculated for each window  $w$ .

**Feature Smoothing** I also evaluated the effect of feature smoothing. To do this, I smoothed the feature time course by averaging subsequent  $Q$  feature values  $a_j(n - Q + 1), a_j(n - Q + 2) \dots a_j(n)$  to form the average  $a'_j(n)$ . This was a specific realization of a finite impulse response (FIR) filter that can be written as

$$a'_j(n) = \sum_{z=0}^{Q-1} h_j(z) a_j(n - z) \quad (4.1)$$

where all coefficients had the same value (i.e.,  $h_j(z) = \frac{1}{Q}$ ).

**Optimal Filtering** It was possible that a FIR filter with optimized coefficients  $h_j(z)$  might provide improved performance. In particular analyses, and for each kinematic parameter  $c_i(n)$ , I thus filtered each feature  $a_j(n)$  using a FIR filter (Eq. 4.2), whose coefficients  $h_{ij}^*(z)$  were optimal in the sense that they minimized the mean square error between the processed feature and the kinematic parameter.

$$a'_j(n) = \sum_{z=0}^{Q-1} h_{ij}^*(z) a_j(n - z) \quad (4.2)$$

To obtain the filter coefficients  $h_{ij}$ , I first constructed a vector  $\vec{a}_j(n)$  of  $Q$

subsequent feature values  $a_j(n)$ :

$$\vec{a}_j(n) = [a_j(n), a_j(n-1), \dots, a_j(n-Q+1), 1] \quad (4.3)$$

I then determined the coefficient vector  $\vec{h}_{ij} = [h_{ij}(0), h_{ij}(1), \dots, h_{ij}(Q)]^T$  using

$$\vec{h}_{ij}^*(z) = \underset{\vec{h}_{ij}}{\operatorname{argmin}} E(\|c_i(n) - \vec{a}_j(n) \cdot \vec{h}_{ij}\|^2) \quad (4.4)$$

In Eq. 4.3,  $h_{ij}(Q)$  contained the bias of the regression, which I discarded before applying Eq. 4.2.

#### 4.4.2.5 Feature Selection

The fourth component of the decoding procedure was feature selection. The present procedure produced a large number of features (i.e., up to 64 channels times 8 feature per channel = 512). Ancillary testing showed that generalization performance of the decoding procedure was poor with this large number of features. I thus reduced the feature space using the Correlation-based Feature Selection (CFS) algorithm (Hall [2000]), a commonly used procedure (e.g., Liu and Yu [2005]). CFS evaluates and ranks feature subsets rather than individual features, and is thus based on a heuristic for evaluating the merit of a subset of features. This heuristic takes into account the utility of individual features in predicting the class label along with the level of inter-correlation among them. The heuristic is based on the hypothesis that good feature subsets contain features that are highly correlated with the class and are uncorrelated with each other. Formally, it is:

$$Merits_S = \frac{\overline{kr_{ca}}}{\sqrt{k + k(k-1)\overline{kr_{aa}}}}$$

where  $Merits_S$  is the heuristic merit of a feature subset  $S$  containing  $k$  features,  $\overline{kr_{ca}}$  the average feature-class correlation, and  $\overline{kr_{aa}}$  the average cross-correlation between features.

#### 4.4.2.6 Decoding

The fifth component of the procedure, decoding, implemented the main element of this study, i.e., to infer from brain signals (i.e., a set of feature vectors  $\vec{a}'$  in

a particular data set) various kinematic parameters  $c_i$  (which are described below in Section 4.4.2.7). While a recent study has not found significant differences in decoding performance for different linear and non-linear methods (Kim et al. [2006]), this study has been investigating single neuron activity in monkeys (and thus, different features of brain signals). I thus felt it was justified to evaluate two commonly used methodologies. To do this, after applying a particular set of the feature pre-processing methods and the feature selection methods, I used either a parametric or a non-parametric technique to decode each kinematic parameter. The parametric technique was realized using a linear model in which the coefficients were obtained using statistical linear regression. The non-parametric technique was realized using a kNN statistical model based on distance-weighted similarity (similar to a Parzen window (Parzen [1962])). These techniques are detailed in subsequent paragraphs.

**Parametric Technique** When I used the parametric technique, the kinematic parameter  $\hat{c}_i$  was decoded from the feature vector  $\vec{a}''$  using linear regression. To incorporate the bias of the linear regression, I extended the vectors  $\vec{a}''$  and  $\vec{m}_i$

$$\vec{a}_{ext} = \begin{pmatrix} \vec{a}'' \\ 1 \end{pmatrix} \vec{m}_{i_{ext}} = \begin{pmatrix} \vec{m}_i & m_{J_R+1} \end{pmatrix} \quad (4.5)$$

and decoded the target kinematic parameter as

$$\hat{c}_i = \vec{m}_{i_{ext}}^* \cdot \vec{a}_{ext}'' \quad (4.6)$$

The coefficients  $\vec{m}_{i_{ext}}^*$  were computed as

$$\vec{m}_{i_{ext}}^* = \underset{\vec{m}_{i_{ext}}}{\operatorname{argmin}} E(\|c_i(n) - \vec{m}_{i_{ext}} \cdot \vec{a}_{ext}''(n)\|^2) \quad (4.7)$$

that is, by regressing the features  $\vec{a}_{ext}''$  to the kinematic parameter  $c_i$ . (The last element of  $\vec{m}_{i_{ext}}$  represented the bias of the regression.) Eq. 4.6 can also be rewritten so as to decode the entire kinematic parameter vector  $\vec{c}$ :

$$\vec{c} = \mathbb{M}^* \cdot \vec{a}'' \quad (4.8)$$

**Non-Parametric Technique** When I used the non-parametric technique, the kinematic parameter  $\hat{c}_i$  was decoded from the feature vector  $\vec{a}''$  by maximizing the expected value of the kinematic parameter vector  $\vec{c}(n)$  given a feature vector  $\vec{a}''$ :

$$\hat{\vec{c}}(n) = \operatorname{argmax} E(\vec{c} | \vec{a}''(n)) = \int \vec{c} \frac{p(\vec{c} | \vec{a}''(n))}{p(\vec{a}''(n))} d\vec{c}$$

This can be carried out numerically similar to the approach in Averbeck et al. [2005]:

$$\hat{\vec{c}}(n) = \frac{\sum_{b=n_1}^{n_2} \vec{c}(b) f(\|\vec{a}''(b) - \vec{a}''(n)\|)}{\sum_{b=n_1}^{n_2} f(\|\vec{a}''(b) - \vec{a}''(n)\|)} \quad (4.9)$$

The function  $f(x)$  represents the influence of distance. For these evaluations, I used  $f(x) = \frac{1}{x}$ . All samples in the training set (i.e.,  $[n_1, n_2]$ ) were used for the computation of (4.9).

#### 4.4.2.7 Definition of Kinematic Parameters

In addition to the choice of input (i.e., the choice of datasets) and the choice of decoding methodology, the choice of output (i.e., kinematic parameters to be decoded) that was to be decoded from these datasets was another concern. I first extracted the position of the subject's cursor ( $c_x(n)$  and  $c_y(n)$ ) from the corresponding values stored in the BCI2000 data file (i.e.,  $t_x(k)$  and  $t_y(k)$ ) using the equation

$$\begin{aligned} c_x(n) &= t_x((n-1)L_o + D) \\ c_y(n) &= t_y((n-1)L_o + D) \end{aligned}$$

In this equation,  $L_o$  was the window overlap mentioned in Section 4.4.2.3 and  $D$  was a constant that determined the temporal offset between the kinematic parameter and the signal window.  $D$  should equal  $L_o$  for a causal prediction in an online system.

In a similar fashion, I defined the position of the target that was tracked by the subject:

$$\begin{aligned} c_{trx}(n) &= t_{rx}((n-1)L_o + D) \\ c_{try}(n) &= t_{ry}((n-1)L_o + D) \end{aligned}$$

This defined the position of the subjects' cursor and target. However, it was possible that other kinematic parameters could also be inferred from brain signals. While there was no theoretical basis for determining which of the plethora of possible kinematic parameters could be decoded, previous studies in non-human primates typically decoded position and velocity. Clearly, these parameters should be included in the evaluations. In addition, I also defined several additional kinematic parameters that were relevant to movement of the cursor and target. These ten parameters are listed below:

$c_1 = c_x$	(horizontal cursor position)
$c_2 = c_y$	(vertical cursor position)
$c_3 = c_\phi = \text{atan}2(c_x, c_y)$	(angular cursor position)
$c_4 = c_{dx} = \frac{dc_x(n)}{dn}$	(horizontal cursor velocity)
$c_5 = c_{dy} = \frac{dc_y(n)}{dn}$	(vertical cursor velocity)
$c_6 = c_{d\phi} = \frac{dc_\phi}{d\phi}$	(angular cursor velocity)
$c_7 = c_{ex} = c_{trx} - c_x$	(horiz. dist. between cursor and target)
$c_8 = c_{ey} = c_{try} - c_y$	(vert. dist. between cursor and target)
$c_9 = c_{e\phi} = \text{atan}2(c_{trx}, c_{try}) - \text{atan}2(c_x, c_y)$	(difference in angular position between cursor and target)
$c_{10} = c_{edst} = \  [c_{trx}, c_{try}] - [c_x, c_y] \ $	(eucl. dist. between cursor and target)

#### 4.4.2.8 Evaluation

The sixth and final component of the decoding procedure evaluated the performance of each studied configuration of processing and decoding technique using 5-fold cross-validation, i.e., each data set was divided in 5 parts, the linear/kNN models were determined from 4/5th of the data set (training set) and tested on the remaining 1/5th (test set). This procedure was then repeated five times – each time,

a different 1/5th of the data set was used as the test set. Results were averaged across the five cross-validation folds. (The automatic feature selection procedure was always applied to the training set only.)

I evaluated the performance of each of the models by cross-correlating the predicted kinematic parameters with their actual values. This procedure yielded, for each data set, cross-validation fold, and each of the movement parameters, a correlation coefficient  $r$  at a level of significance  $p$  (i.e., p-value). I finally used a variety of appropriate statistical tests<sup>10</sup> to evaluate the differences between these different techniques.

#### 4.4.3 Results: Decoding Procedure

The previous sections described the six components, and their different implementations, of the decoding procedure used in this study. The following sections describe the results of various evaluations that evaluated the effect on decoding performance of the various inputs (i.e., datasets), outputs (i.e., kinematic parameters), and decoding methodologies, which thereby pursued the main question of this study, which was whether it is possible to decode kinematic parameters related to hand movement. These evaluations were purely empirical because there was no theoretical basis for choosing one method over the other.

Each evaluation determined the effect on decoding performance of the particular aspects of the decoding procedure that are highlighted in red in Figure 4.7. I did this by utilizing a default decoding procedure and then varying the one aspect in question. This default procedure was to use a Common Average Reference (CAR) spatial filter, no feature pre-processing (i.e., feature transformation, whitening, temporal smoothing or optimal filtering), and to use the linear decoding technique.

##### 4.4.3.1 Selection of Datasets and Kinematic Parameters

The initial evaluation was concerned with the question which inputs (i.e., datasets) could be used to decode which outputs (i.e., kinematic parameters). I

---

<sup>10</sup>When the observed values were normally distributed, I utilized a t-test (a parametric method). When the values were not normally distributed, I used a Wilcoxon Rank Sum test (a non-parametric method). When I compared the effects of multiple variables, I used an Analysis of Variance (ANOVA). I also used the Kruskal-Wallis test, which is a nonparametric version of the classical one-way ANOVA and an extension of the Wilcoxon Rank Sum test to more than two groups.

did this because the literature did not suggest which of the kinematic parameters could potentially be extracted from the ECoG signals and because it was not clear which of the data sets collected under which condition (Seattle/St. Louis, joystick/mouse/watch) would allow for adequate prediction. Consequently, I initially determined those kinematic parameters and datasets that allowed for adequate predictions, and then used only those for all subsequent evaluations.

I first selected the kinematic parameters. To do this, I decoded all kinematic parameters for each dataset and cross-validation fold using the linear model. This resulted, for each cross-validation fold of each dataset and each kinematic parameter, in a correlation coefficient  $r$  and an associated level of confidence  $p$  (i.e., p-value). The results for the kinematic parameters  $c_x, c_y, c_{dx}, c_{dy}$  (i.e., the position and velocity of the cursor) appeared to be better than those for the rest of the kinematic parameters. To statistically assess the difference between these two groups, I collected the correlation coefficients for all available datasets (joystick, mouse, watch) and compared them between the two groups (i.e., those for the position and velocity ( $N = 80$  values) and the rest ( $N = 120$  values))). A Wilcoxon Rank Sum test suggested that the difference in the median values between the two groups was statistically significant ( $p < 0.001$ ). In other words, decoding performance for position and velocity of the cursor (i.e., those kinematic parameters typically studied in the literature in non-human primates) was better than that for other parameters. I thus used only these kinematic parameters for all subsequent testing.

I then selected the datasets that I would use for more detailed examination. To do this, I averaged the  $p$  values for the four chosen kinematic parameters (the position and velocity of the cursor) across all cross-validation folds. (I used  $p$ -values for this evaluation rather than the correlation coefficients  $r$  to account for the different lengths of the datasets.) I then selected all datasets whose average  $p$  values were smaller than 0.01, i.e., all datasets for which the decoding performance was significant at the 0.01 level. These five data sets (out of the total of 40) comprised four joystick data sets from four of the five Seattle subjects, and one mouse data set from one of the Seattle subjects. In other words, almost all Seattle joystick data sets (four of five), but no St. Louis dataset, allowed for adequate prediction and were

selected for further analyses. Please see the Discussion and Interpretation Section (4.4.6) for further information.

After determining which input (i.e., datasets) and output (i.e., kinematic parameters) allowed adequate decoding, I set out to evaluate the effect on decoding performance of the various signal pre-processing, feature processing, feature selection, and decoding procedures indicated in red in Figure 4.7. These evaluations are described in the next sections.

#### 4.4.3.2 Spatial Filtering

The first evaluation of the decoding procedure was concerned with the effect of spatial filtering (see Section 4.4.2.2) on performance<sup>11</sup>. The results are shown in Figure 4.8. A t-test, calculated between the results for the CAR-filtered signals and for the unfiltered signals, shows that the apparent advantage of the CAR filter was not statistically significant ( $p = 0.103$ ). However, because the application of a CAR filter also suppresses signals that could be induced by external sources (i.e., artifacts), application of a CAR filter is still recommended.

These results demonstrate that unlike for EEG, for which CAR filtering does improve performance (McFarland et al. [1997b]), CAR filtering does not significantly improve performance for ECoG signals recorded using the joystick movement paradigm used here. These results may indicate that the decreased spatial blurring inherent in ECoG signals (that is due to the close proximity to the sources in the brain) also decreases the demand for spatial filtering.

#### 4.4.3.3 Feature Transformation

The second evaluation of the decoding procedure was concerned with the effect of feature transformation (see Section 4.4.2.4) on performance. Figure 4.9 shows the results, which indicate that feature transformation does not have a significant impact on decoding performance. Statistical evaluations confirm these conclusions: a t-test between no transformation and log, sqrt, and square produced  $p=0.345$ ,  $p=0.357$ ,  $p=0.428$ , respectively; an ANOVA rejected an influence of feature transformation ( $p=0.964$ ).

---

<sup>11</sup>This evaluation utilized the default decoding configuration and a temporal smoothing of length 9.

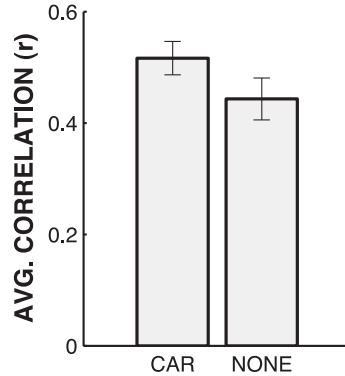


Figure 4.8: Effect of spatial filtering on performance. Application of a common average reference (CAR) filter provides improved performance, but this improvement was not statistically significant (see text).

These results demonstrate that global application of one particular feature transformation does not improve performance and thus indicate that feature transformation is either not necessary (because the combination of the large number of features in the decoding stage might, according to the *Central Limit Theorem* (Tijms [2004]), approximate a Gaussian distribution), or would have to be optimized for each feature.

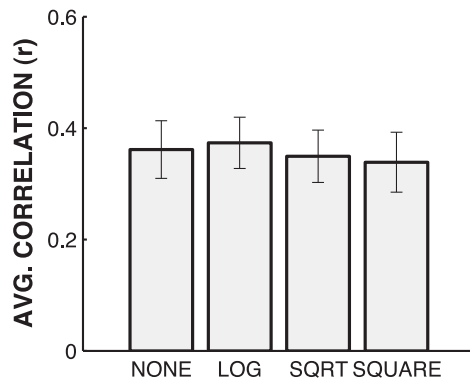


Figure 4.9: Feature transformation does not have a significant influence on decoding performance.

#### 4.4.3.4 Feature Smoothing

The third evaluation of the decoding procedure was concerned with the effect of feature smoothing (see Section 4.4.2.4) on performance. The results are shown in Figure 4.10 and indicate an obvious effect of averaging length on performance. This

is confirmed by an ANOVA ( $p = 0.017$ ). As a compromise between filter length and performance, I chose to use filtering over the past 9 samples (60 degrees of the circular movement) for subsequent analyses.

The present feature smoothing might be expected to initially, with short filter lengths, reduce the noise-related variance in the features and thus improve performance. With increasing filter length and thus an increased group delay (the present filter was applied in a causal fashion), one may expect substantial performance degradation. However, the filtering procedure was applied to the features, and not to the output of the decoding, which is similar to simply predicting future kinematic parameters. With the slow cursor speed utilized in the present experiments, future kinematic parameters can be expected to be predicted reasonably well even with a linear model. In summary, the present filtering approach might be efficacious only with slow movement speeds such as those used here.

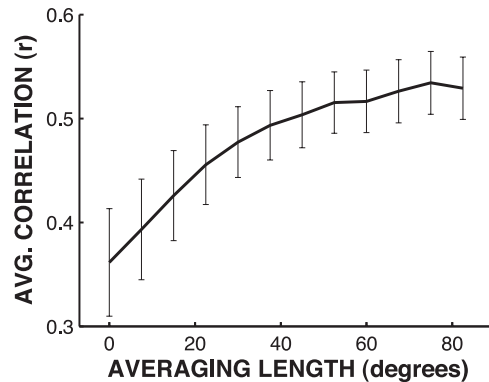


Figure 4.10: Effect of feature smoothing. Causal FIR averaging filter of lengths 1 to 12 (corresponding to 0 to 80 degrees of the circular movement).

#### 4.4.3.5 Optimal Filtering

The fourth evaluation of the decoding procedure was concerned with the effect of optimal filtering (see Section 4.4.2.4) on performance. The results are shown in Figure 4.11 and demonstrate that optimal filtering reduces performance.

This effect goes in parallel with increased filter lengths and thus an increased number of filter coefficients. This is in contrast to the results achieved using the simple averaging filter described above, which used constant coefficients. The present

results thus indicate that the coefficients of the optimal filter cannot be reliably estimated from the training data set and/or do not generalize to the test data set.

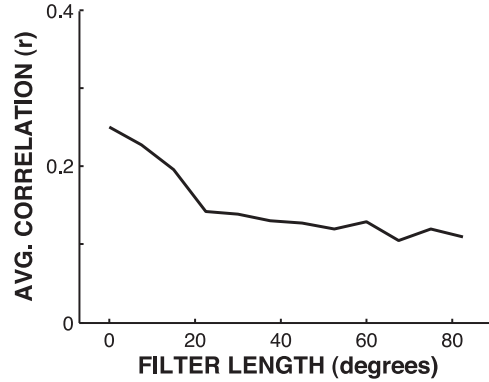


Figure 4.11: Optimal filtering of lengths 1 to 12 (corresponding to 0 to 80 degrees of the circular movement).

#### 4.4.3.6 Feature Whitening

The fifth evaluation of the decoding procedure was concerned with the effect of feature whitening (see Section 4.4.2.4) on performance. To do this, I used either no feature whitening, whitening according to one or three periods of the circular movement (P1 or P3, respectively), and whitening by the mean or standard deviation (S0 or S1, respectively). The results are shown in Figure 4.12. A Kruskal-Wallis ANOVA revealed a significant influence of whitening procedure on performance ( $p = 0.013$ ) such that some procedures produced results that were inferior to no whitening procedure.

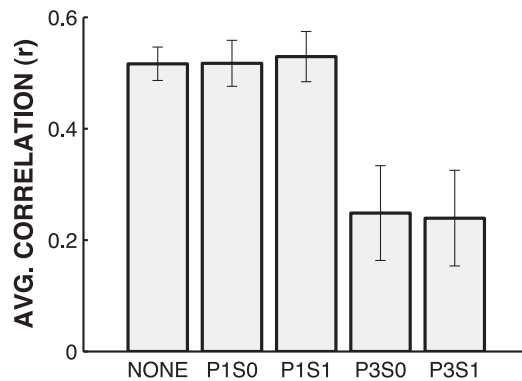


Figure 4.12: Influence of feature whitening on performance. See text for details on column labels.

#### 4.4.3.7 Parametric/Nonparametric Methods

The sixth and last evaluation of the decoding procedure was concerned with the effect of the linear/non-linear decoding methods (see Section 4.4.2.6) on performance. The results are shown in Figure 4.13. A t-test revealed that there was no significant difference between the results for the linear model and the non-parametric kNN method ( $p = 0.561$ ).

This suggests one of two possibilities. First, the decoding problem may be well served by a linear approach. This could be because the mapping from features to kinematic parameters is linear, or because certain features could be non-linear functions of other features (in which case a non-linear mapping could be described even using only a linear mapping technique). As a second and alternative explanation, the theoretical advantage of the non-linear approach (to be able to approximate more complex functions, that is) might be compensated by a smaller level of generalization (from the training data set to the test data set, that is). In either case, the present results are in line with a recent study that decoded hand movements in non-human primates using intracortical microelectrodes (Kim et al. [2006]). This study evaluated 9 different linear and non-linear decoding techniques and concluded that all techniques provided comparable performance.

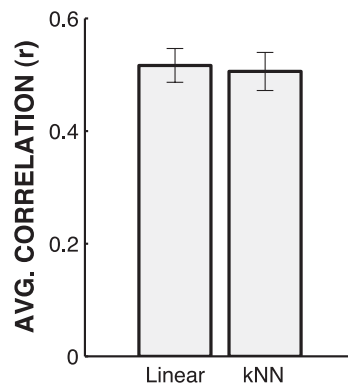


Figure 4.13: Comparison of linear and kNN methods.

#### 4.4.3.8 Conclusions: Decoding Procedure

The six evaluations described above indicate that almost all Seattle joystick datasets allowed for adequate decoding of joystick position and velocity. This con-

firms the main hypothesis of this study, which was that it is possible to decode particular kinematic parameters from ECoG signals in humans. These evaluations also indicate that a simple decoding procedure that utilizes a linear model and smoothed features derived using a commonly used frequency estimation technique (Figure 4.14), can provide optimum performance.

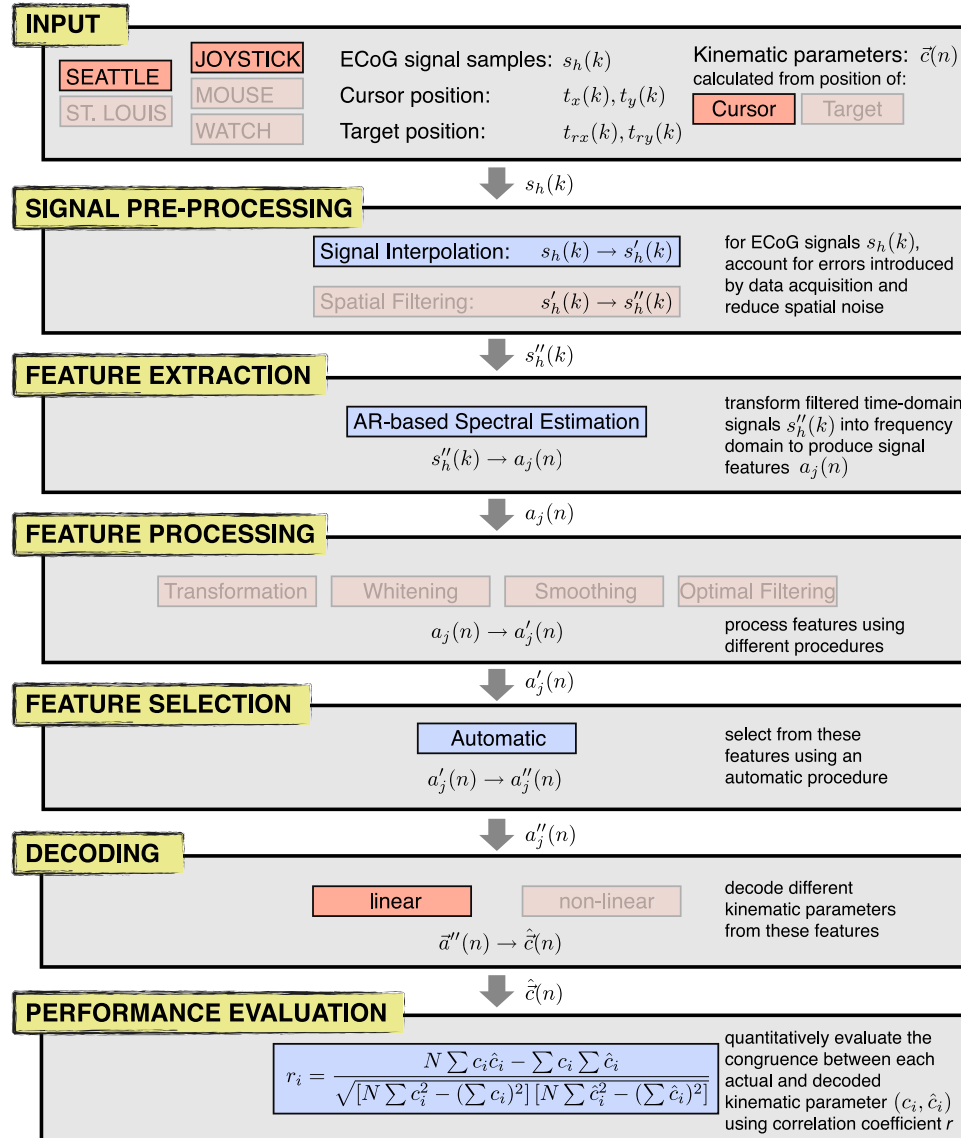


Figure 4.14: Overview of the final decoding procedure.

I will use this simple decoding procedure later in this chapter (Section 4.4.4) to address neuroscientific questions. Prior to these analyses, I conducted four ancillary tests to evaluate additional aspects of the decoding that are described below.

#### 4.4.3.9 Additional Evaluations

**Number of Cross Validation Folds** The first ancillary evaluation was concerned with the number of cross-validation folds. I typically used five cross-validation folds to evaluate the results. I expected that the number of cross-validation folds would influence the results because with more folds, more data were used for training and less for testing. At the same time, I was interested in the extent of that impact because it would speak to the robustness of the decodings if results for fewer folds were similar to those of more folds. This impact of the number of cross-validation folds on performance is shown in Figure 4.15.

These results demonstrate that performance that can be achieved with 10 fold cross-validation was not significantly different ( $p > 0.05$ ) from those achieved for 5 fold cross-validation. This is an indication that the decoding performance is robust even if the decodings are applied to more test data.

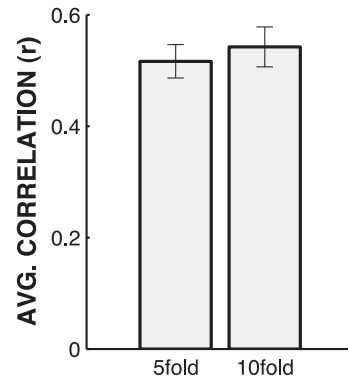


Figure 4.15: Effect of the number of cross-validation folds.

**Temporal Offset** The second ancillary evaluation was concerned with the temporal offset of the features to the decoded kinematic parameters. It was possible that the use of features from different temporal offsets might have an effect on decoding performance (such that, for example, relevant brain signal activity might precede or follow the actual joystick movement). To evaluate this possibility, I modified the value of the offset  $D$  (see Section 4.4.2.7). If  $D$  was zero, the brain activity used for decoding preceded the kinematic parameter (i.e., causal decoding). I also used two non-causal offsets. First, I used  $D = \frac{\textit{blocksize}}{2}$  (HALF), i.e., I used both future and

past feature values for decoding. I finally used  $D = \text{blocksize}$  (AFTER), i.e., I used future feature values only. The results are shown in Figure 4.16. They demonstrate that there was no significant effect of temporal offset on performance. Again, in the light of the results presented later in this chapter, which will show that the LMP (which changed with the movement parameters and thus slowly compared to the offsets used here) held the most information, these results are not surprising.

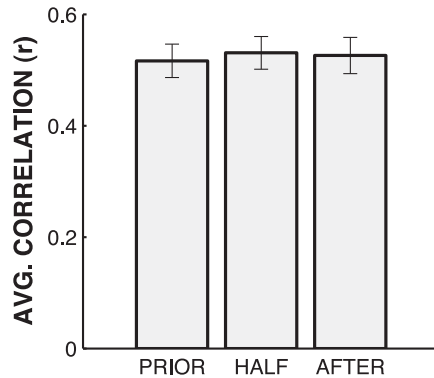


Figure 4.16: Effect of feature offset on performance. PRIOR: causal offset, using past feature values. AFTER: non-causal offset, using future feature values only. HALF: non-causal offset, using both future and past feature values.

**Smoothing: Pre-processing versus Post-processing** The third ancillary evaluation was concerned with further details of the smoothing procedure. When I applied temporal smoothing, this procedure was applied to the frequency features prior to feature selection and decoding. I was interested in the relationship between this default procedure and two other procedures that filtered signals after the decoding stage in a non-causal and causal fashion.

The results are shown in Figure 4.17. They demonstrate that filtering features prior to decoding is desirable over filtering kinematic parameters after decoding when causal filtering is desired. When features were filtered causally prior to decoding (such as the application of the smoothing filter used in Section 4.4.3.4), the decoder essentially predicted future values (because only past signal values were used for decoding) and thus compensated for the added group delay caused by the smoothing. When features were filtered causally after decoding, the decoder could not account

for the increased group delay caused by increasing filter lengths. The effective phase difference between the decoded and actual kinematic parameters thus increased with the length of the filter, leading to deteriorating performance (dotted line).

In summary, the causal smoothing procedure I had used throughout this work was the most desirable among these three methods in the context of real-time decoding of movement parameters.

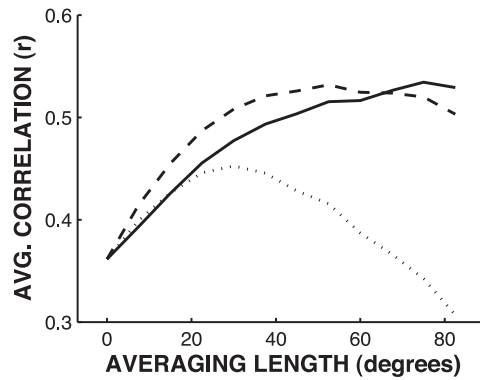


Figure 4.17: Effect of smoothing pre/postprocessing. Temporal smoothing filters of lengths 1 to 12 (corresponding to degrees 0 to 80) applied either on the features or on the decoded kinematic parameters. Solid line: Smoothing of features prior to classification (same procedure as used in Figure 4.10). Dashed line: Smoothing decoded movement predictions using a non-causal filtering procedure. Dotted line: Smoothing decoded movement predictions using a causal filtering procedure.

**Data Shuffling** The fourth and last ancillary evaluation was concerned with a verification to validate my results. I wanted to ensure that the significant correlation between the decoded and actual kinematic parameters were not due to a mistake in the algorithms. To evaluate this possibility, I randomly shuffled the datasets and evaluated the results. When I did this, the average correlation coefficient, calculated between the actual and decoded kinematic parameters, dropped to practically zero (see Figure 4.18). This confirms that the decoding results were due to properties of the brain signals and not due to a mistake in the decoding procedures.

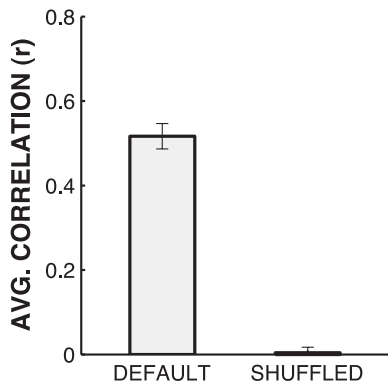


Figure 4.18: Effect of data randomization. DEFAULT: Results using non-shuffled data. SHUFFLED: Results achieved using shuffled data.

#### 4.4.4 Results: Neuroscience

The previous sections suggested which features and decoding methodologies optimized decoding performance. They demonstrated that 2D position and velocity of hand movements can be decoded from ECoG signals, and answered mainly signal processing questions. Subsequent sections describe a number of further analyses that allowed to answer neuroscientific questions.

##### 4.4.4.1 Relative Importance of Different Features

I was interested in determining the relative importance of the features on decoding performance. As described in the previous sections, I chose the features based on the results of the first study in **THEME III** (Section 4.3), which demonstrated that high gamma frequencies up to 180 Hz can hold information related to movement direction. I also included features from other gamma bands, traditional mu/beta bands, and the LMP (which was first described and used in this dissertation).

I calculated an index of relative importance for each feature by first normalizing each of the eight features by their standard deviation prior to decoding so as to render the impact of each feature independent of its amplitude. I then accumulated, for each of the eight frequencies, the absolute value of the weights that were determined by the linear regression for the features that were selected by the CFS feature selection procedure. I then summed the results across the five cross validation folds.

The following four figures (4.19, 4.20, 4.21, 4.22) show the results of these analyses for each of the five datasets and each of the four kinematic parameters

(horizontal/vertical position and velocity). In these four figures, bars indicate the relative importance of each feature, and the length of error bars indicate the sum of negative weights. These error bars thus gave an indication about the stability of the weights for each feature across the cross validations: if the weight was always positive or negative, the length of the error bar would thus be either zero or as long as the relative importance bar for that feature. If the length of the error bar was somewhere in between, this indicated that this particular feature had positive and negative weights for the different folds of the cross validation.

The clinical nature of ECoG recordings (that prescribes a limited number of subjects whose electrodes are implanted in different locations) does not permit detailed analyses and interpretations of these results. At the same time, the results can support the general statement that they demonstrate that the LMP provided much information about all kinematic parameters in all datasets, whereas high gamma frequencies contributed substantially in only a few. Traditional mu/beta frequencies, which could potentially also be detected on the scalp, typically did not contribute much information. This is surprising information in two ways. First, while the LMP held substantial information about movement direction, it has not been described previously in the literature. Second, the initial study that evaluated joystick movements in this dissertation (see Section 4.3) concluded that high gamma frequencies, and not very low frequencies, were most useful for decoding movement direction. This difference can be reconciled because the data in the initial study were high-pass filtered prior to analysis, which removed the influence of the LMP component. See the discussion in Section 4.4.6 for more details.

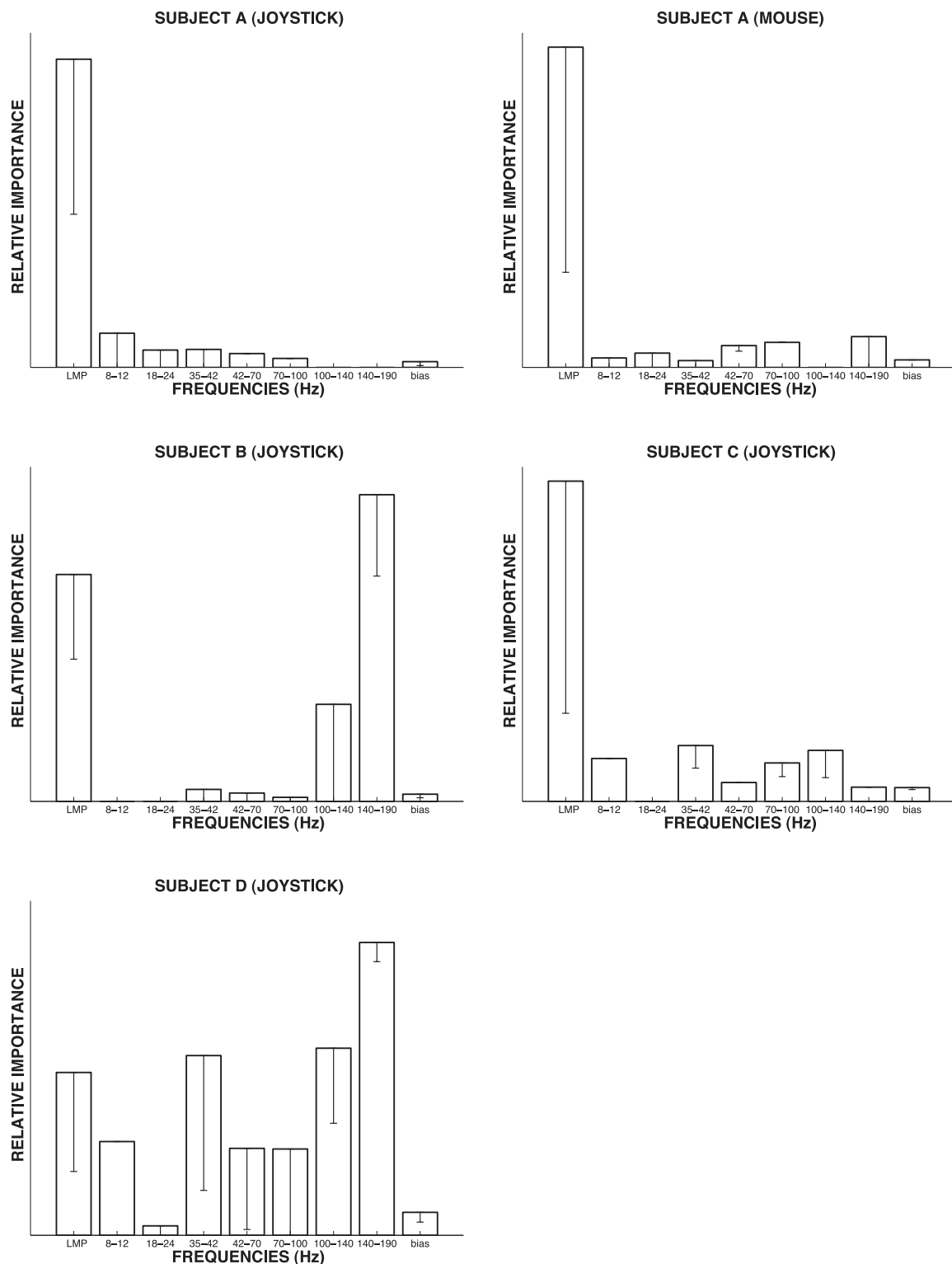


Figure 4.19: Relative importance of different features for predicting horizontal cursor position.

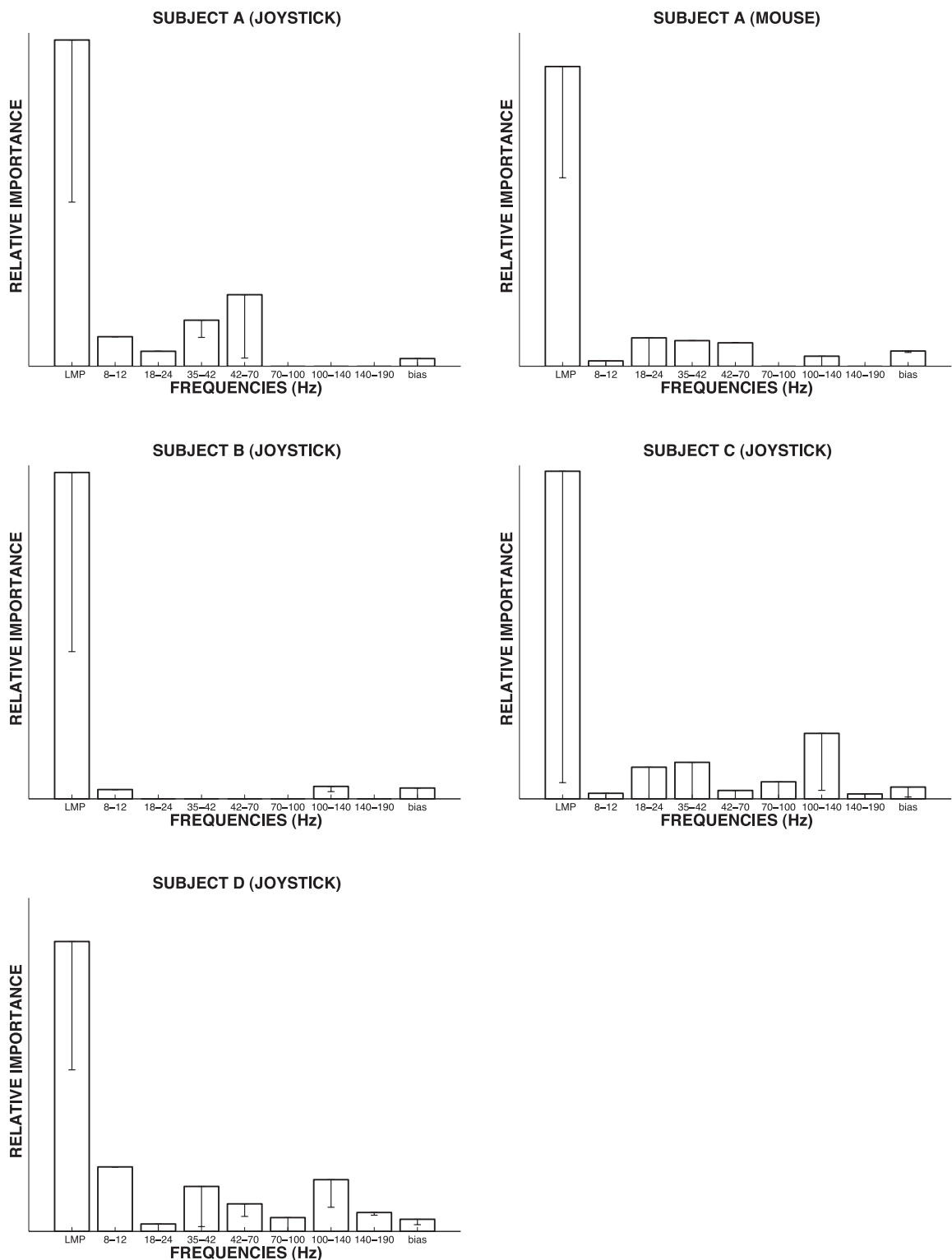


Figure 4.20: Relative importance of different features for predicting vertical cursor position.

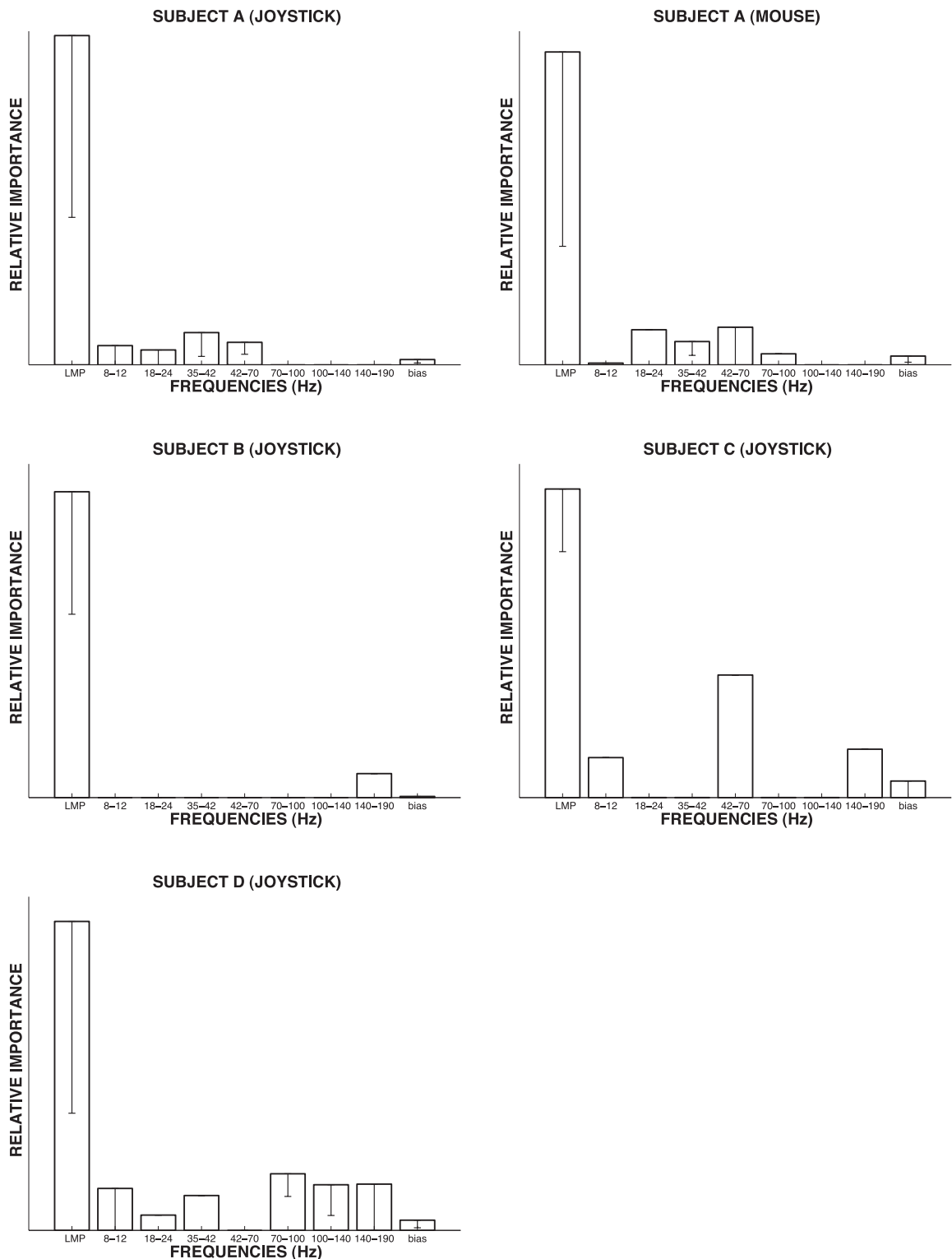


Figure 4.21: Relative importance of different features for predicting horizontal cursor velocity.

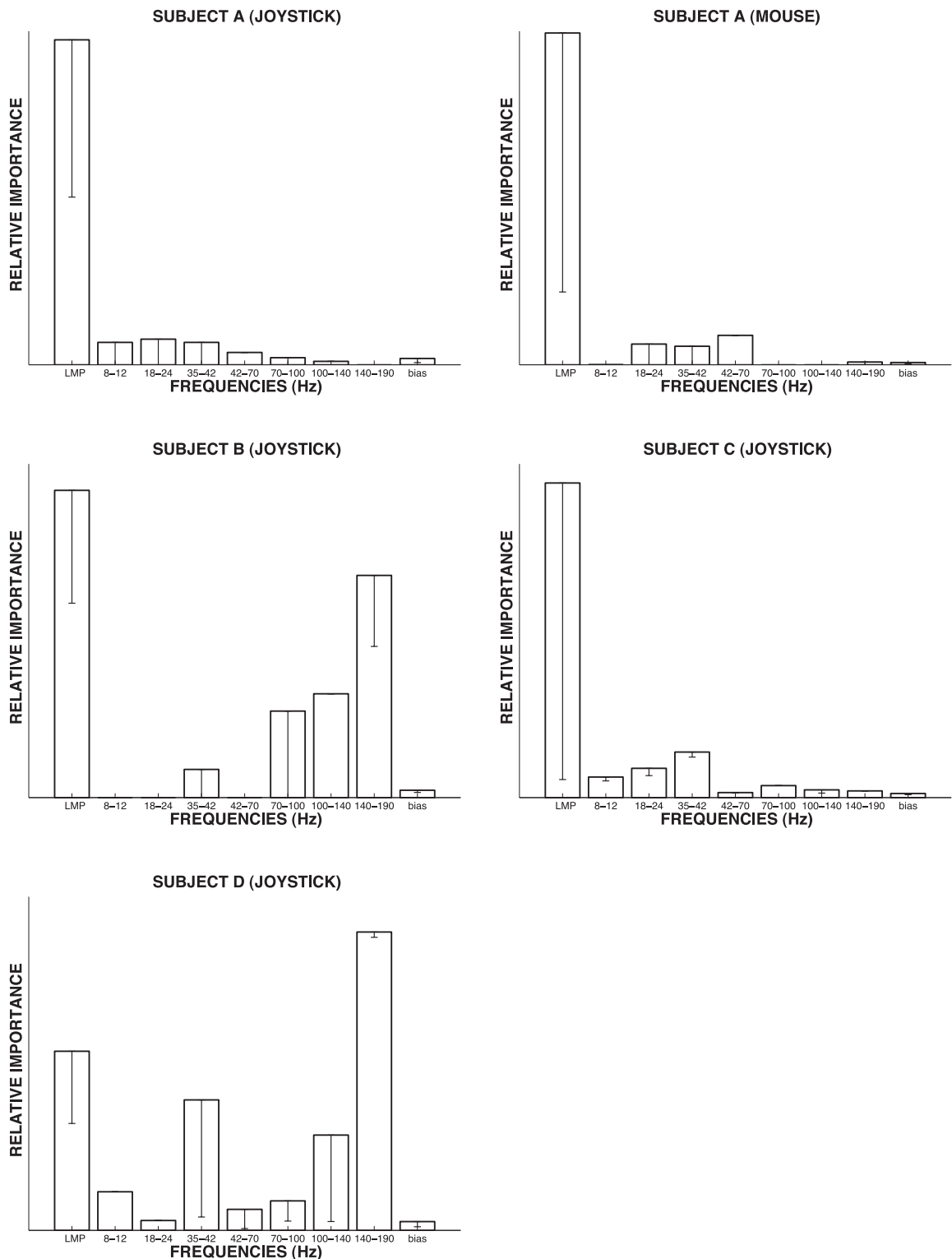


Figure 4.22: Relative importance of different features for predicting vertical cursor velocity.

#### 4.4.4.2 Significance of the LMP Component

The results of the previous section strongly suggested a marked influence of the LMP feature on detection performance. This was an exciting finding, because the LMP had not been described previously in the literature. To confirm this possibility, I studied decoding performance using three sets of features. The first set was comprised of the eight standard features. The second set was comprised of seven features (i.e., all eight features except the LMP). The third set was comprised of only the LMP.

The results are shown in Figure 4.23. When excluding the LMP, average correlation with the kinematic parameters dropped from 0.52 to 0.16. When I used only the LMP, the results remained practically identical.

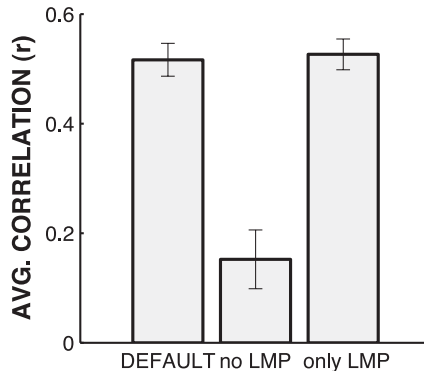


Figure 4.23: Significance of the LMP component. DEFAULT: the default feature bins listed in Section 4.4.2.3. No LMP: the LMP component was not used. Only LMP: I used only the LMP component.

#### 4.4.4.3 Topography of Locations Implicated in the Decoding

I also examined the topography of locations that were important for the decodings. This provided an additional opportunity to derive evidence of the physiological relevance of the LMP. Thus, for locations selected by the CFS feature-selection procedure, I calculated regression weights for the LMP component only and mapped these weights on a 3D model of the cortex. The results are shown in Figure 4.24. Activations in this figure were calculated by averaging the absolute values of the regression weights across all cross validation folds for the indicated kinematic parameter and dataset. Colors represent the weights associated with the LMP feature

at the respective locations, and thus indicate the relative importance of these sites in predicting kinematic parameters. (Red colors indicate positive weights and blue colors indicate negative weights.)

Just like with the analysis of the relative importance of the different frequency bands, the clinical nature of ECoG recordings (only a limited number of subjects whose electrodes were implanted in different locations) does not permit comprehensive interpretations. At the same time, these results indicate that hand and proximal arm areas of motor cortex were often implicated, but that other locations were involved for which the anatomical relevance was not clear. These results thus suggests that the brain offers an array of opportunities to infer position and velocity of hand movements. This view is shared by recent behavioural and computational studies that suggest that access to internal predictive models of arm and object dynamics is widespread in cortex, and that several systems, including those responsible for oculomotor and skeletomotor control, perceptual processing, postural control and mental imagery, can be used to derive predictions of the motion of the arm (see Davidson and Wolpert [2005] for a review).

#### **4.4.4.4 Decoding Cursor and Target Kinematics**

The underlying hypothesis for this work was that kinematic parameters of the cursor can be decoded from brain signals. Consequently, decoding performance for the cursor should be superior to decoding performance for the target. To validate this assumption, I compared decoding performance for cursor and target (see Figure 4.25). While the decoding performance for the target was also substantial (which is not surprising given that there was correlation between the movement of the cursor and the target), performance was significantly higher for the cursor ( $t$ -test,  $p < 0.05$ ). This reinforced my hypothesis and thus the notion that the parameters decoded from the brain were in fact related to the actual hand movement.

#### **4.4.4.5 Decoded Movement Trajectories**

To graphically illustrate the performance of the decoding, I here show, for the best cross validation fold of each data set and for horizontal and vertical position of the cursor, actual and decoded trajectories. These trajectories are shown in

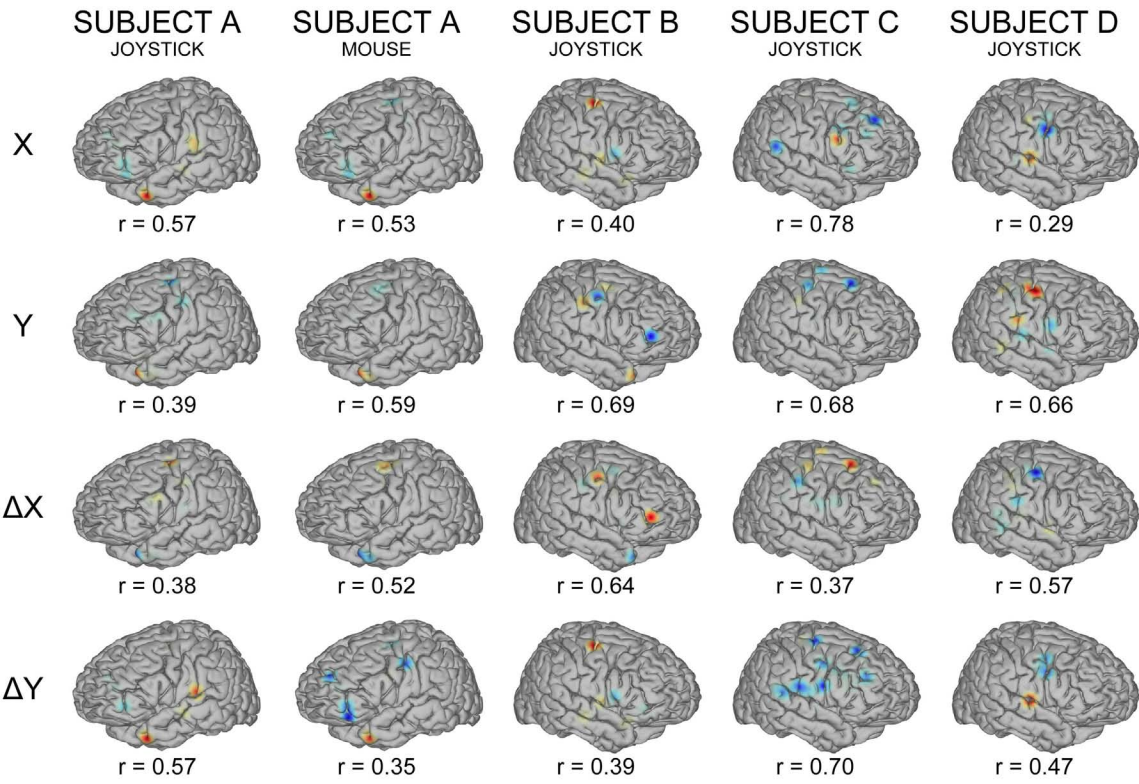


Figure 4.24: Electrode locations holding information in the LMP about movement parameters. See text for details.

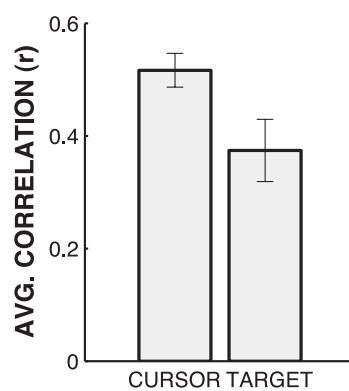


Figure 4.25: Decoding kinematics of the user's cursor and target. The results demonstrate that decoding performance for the user's cursor is better than that for the target.

figures 4.26, 4.27, 4.28, 4.29, and 4.30. The sole purpose of these figures is to qualitatively illustrate the generally close concurrence between actual and decoded cursor position. These results are quantitatively tabulated and discussed in the Summary Section 4.4.5.

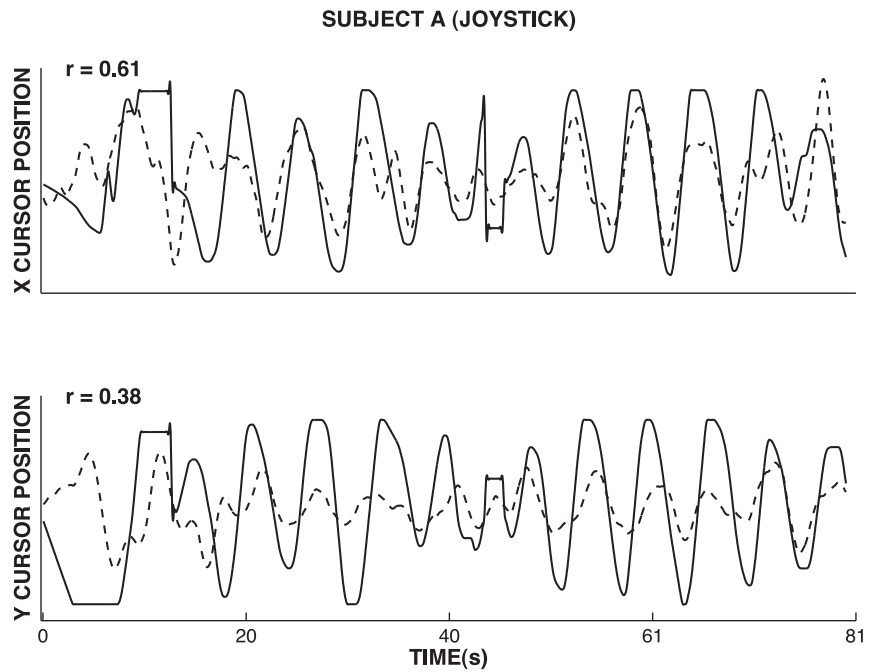


Figure 4.26: Actual and decoded trajectories for subject A (joystick). The traces show actual (solid) and decoded (dashed) cursor position.

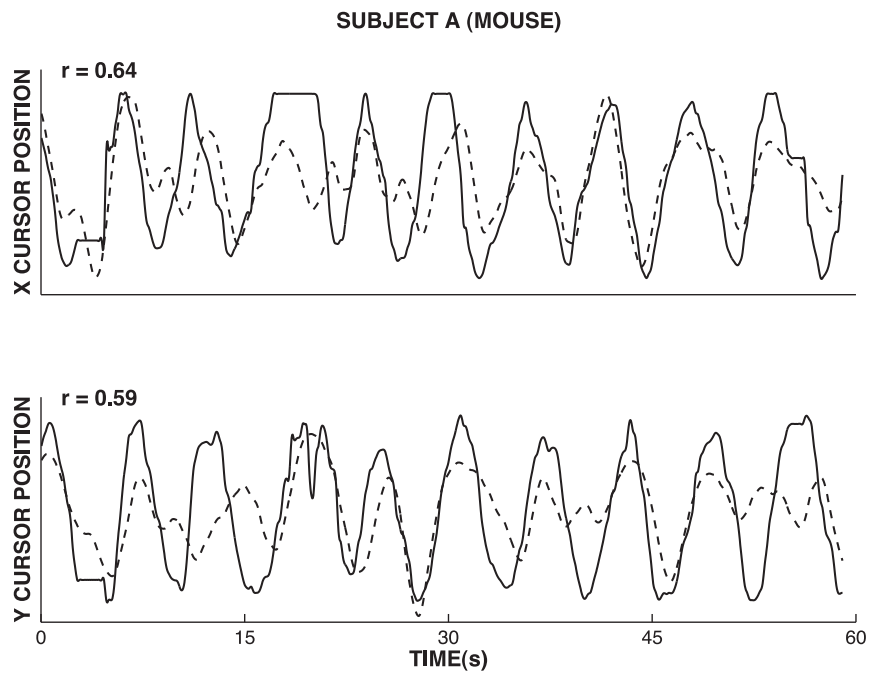


Figure 4.27: Actual and decoded trajectories for subject A (mouse). The traces show actual (solid) and decoded (dashed) cursor position.

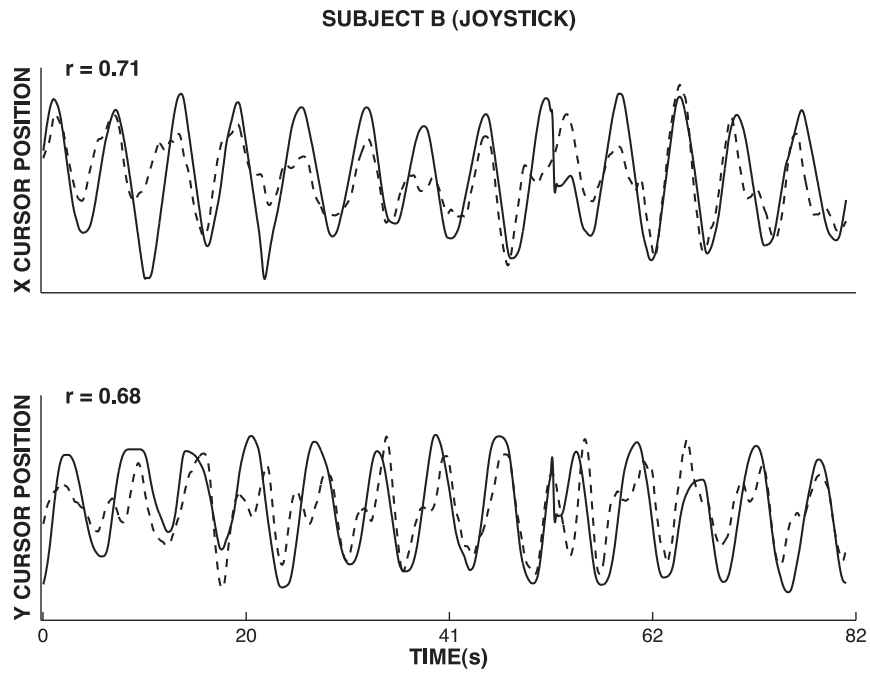


Figure 4.28: Actual and decoded trajectories for subject B. The traces show actual (solid) and decoded (dashed) cursor position.

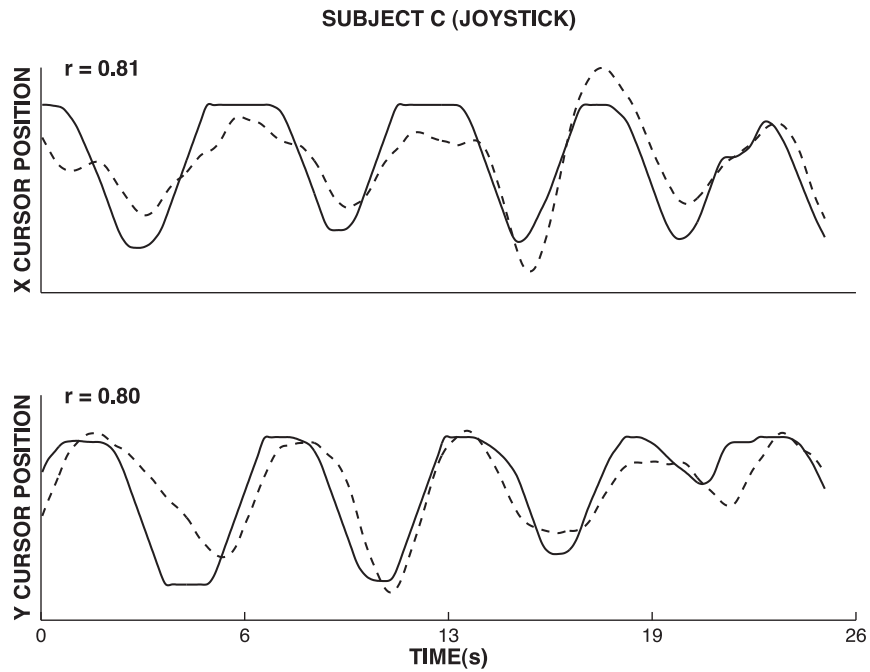


Figure 4.29: Actual and decoded trajectories for subject C. The traces show actual (solid) and decoded (dashed) cursor position.

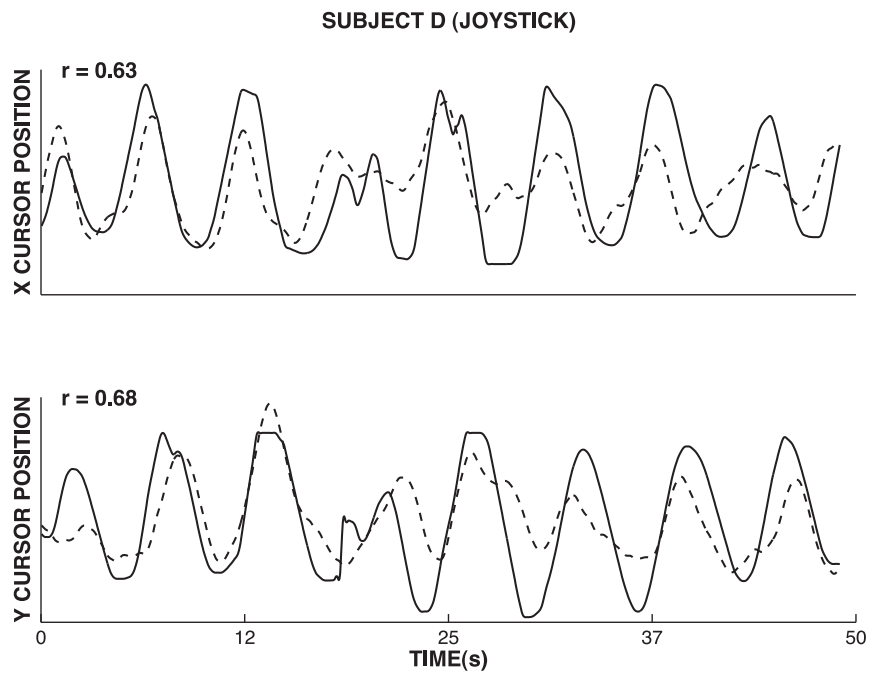


Figure 4.30: Actual and decoded trajectories for subject D. The traces show actual (solid) and decoded (dashed) cursor position.

#### 4.4.4.6 Directional Tuning

Many previous studies using intracortical microelectrodes in monkeys demonstrated that neuronal firing rates can be *cosine tuned*, i.e., their firing rate was a function of movement direction (e.g., Georgopoulos and Massey [1988], Salinas and Abbott [1994], Turner et al. [1995], Kettner et al. [1996], Amirikian and Georgopoulos [2000], Baraduc and Guigon [2002], Todorov [2002], Rickert et al. [2005], Shoham et al. [2005], Nozaki et al. [2005]). While the present investigations were based on ECoG features derived from superposition of many thousands of neurons and thus on signals quite different to those utilized in previous research, it was still possible that they exhibited similar characteristics. Once again, I was most interested in this relationship for the LMP component.

I thus calculated, for the best cross validation fold for each dataset, average LMP amplitude as a function of movement direction. I did this by binning movement direction in 20 equidistant angular bins, and by calculating average LMP amplitude and its standard error. Each bins comprised 7-24 values. If an electrode had been excluded from analysis, I replaced all bin values with zero.

Figures 4.31, 4.32, 4.33, 4.34, and 4.35 illustrate that often, LMP amplitude was a function of movement direction. In addition, these figures show that for some electrodes, LMP amplitude was a cosine function of movement direction. This finding was exciting in particular since no previous study has demonstrated movement-related cosine tuning with signals other than neuronal firing rates recorded using implanted microelectrodes.

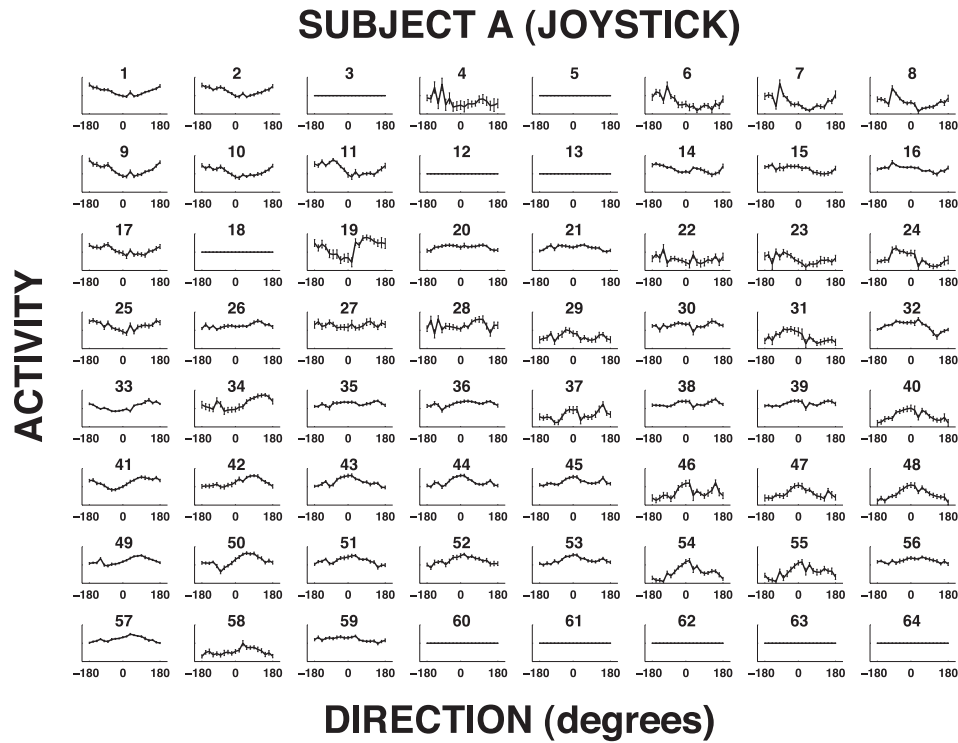


Figure 4.31: Directional tuning results for subject A.

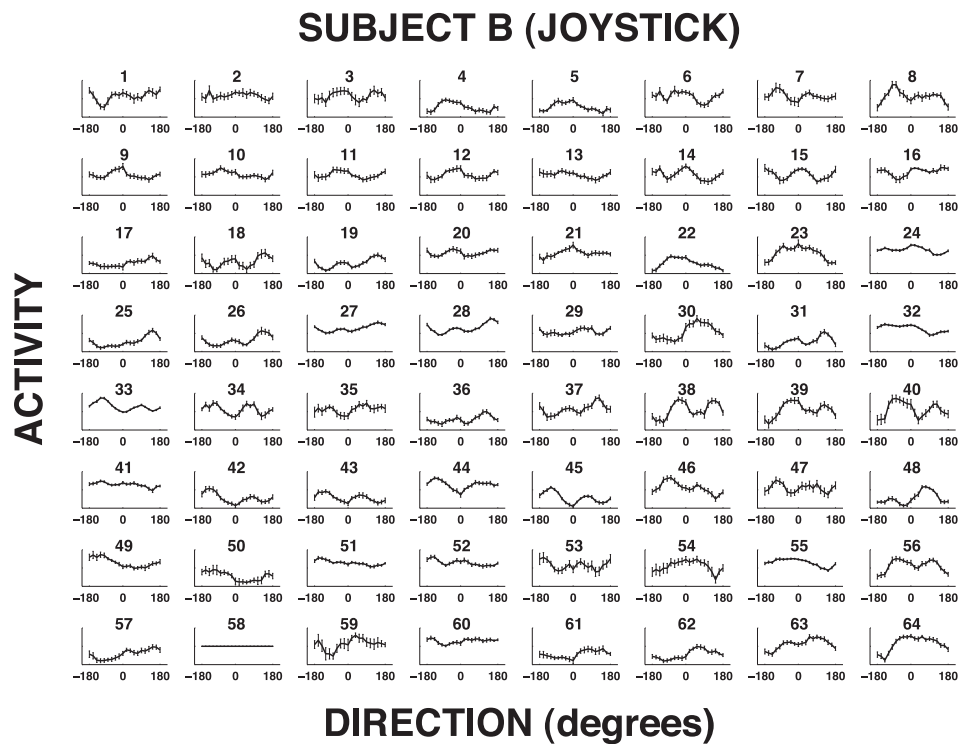


Figure 4.32: Directional tuning results for subject B.

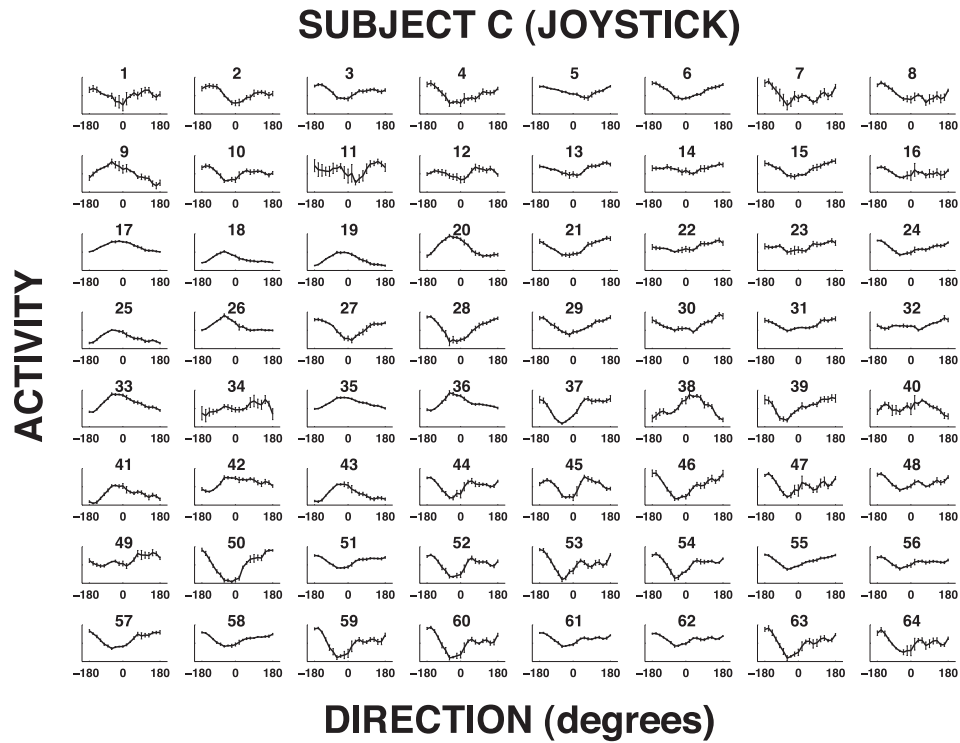


Figure 4.33: Directional tuning results for subject C.

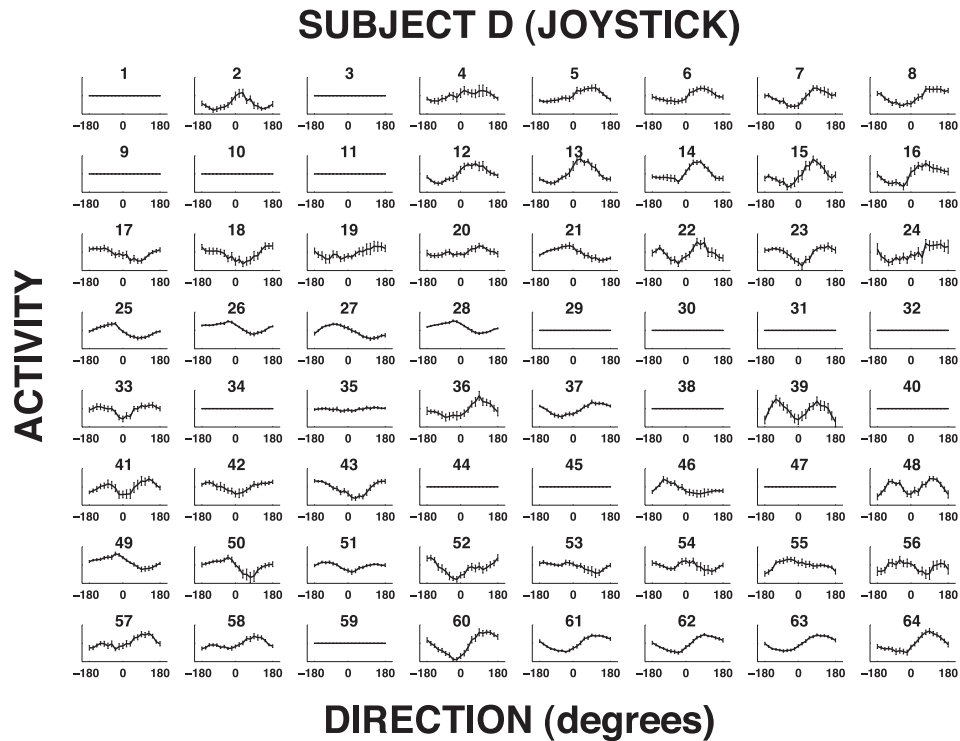


Figure 4.34: Directional tuning results for subject D.

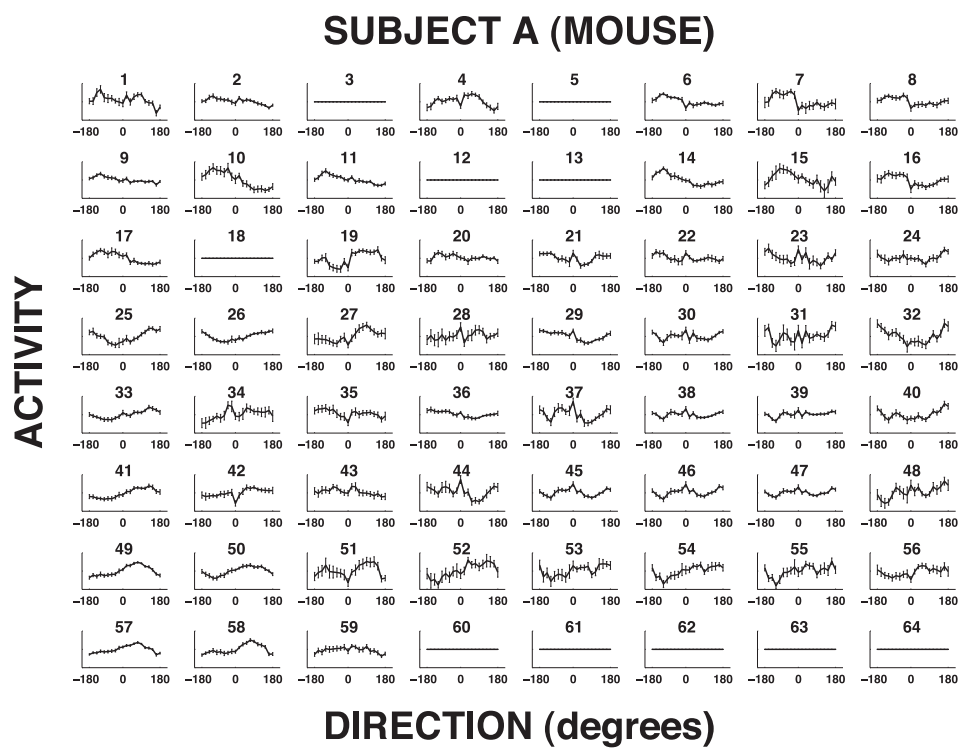


Figure 4.35: Directional tuning results for subject A (mouse dataset).

#### 4.4.4.7 Tracking vs. Decoding Performance

Because in this task the target moved in a circle (i.e., a predictable shape with substantial interrelations between kinematic parameters), it was possible that the quality of the decoding (i.e., how well I decoded kinematic parameters from the brain signals) was mainly determined by the quality of the tracking (i.e., how well the patients tracked the target that moved in a circle).

The final question was thus whether there was a correlation between tracking performance and decoding performance. I defined tracking performance as the cross-correlation between the kinematic parameters of the cursor and those of the target, and decoding performance as the cross-correlation between actual and decoded kinematic parameters. Figure 4.36 shows these variables, calculated for each cross-validation fold and all joystick data sets (including the one joystick data set that did not support consistent decoding and that had been excluded from previous analyses).

These analyses demonstrate that there was no significant correlation between tracking performance and decoding performance, and that thus decoding performance was determined mainly by brain signal features that were related to movement kinematics rather than by signal features that were merely in sync with the frequency of the movement task.

#### 4.4.5 Summary of Results

The previous sections described a comprehensive study that attempted to faithfully decode kinematic parameters from ECoG signals collected during a tracking task. This comprehensive study encompassed the evaluation of a range of signal processing parameters and the analysis of a number of neuroscientific questions. The following sections succinctly summarize this comprehensive study.

##### 4.4.5.1 Accurate Decoding of Movement Parameters

Five literate and functionally independent patients (see Table 4.3)<sup>12</sup> were asked to use a joystick or a mouse to move a cursor on a computer screen in order to track a target that moved counter-clockwise in a circle on a computer screen. The patients'

---

<sup>12</sup>These patients were selected from all 10 patients by the procedure described in Section 4.4.3.1.

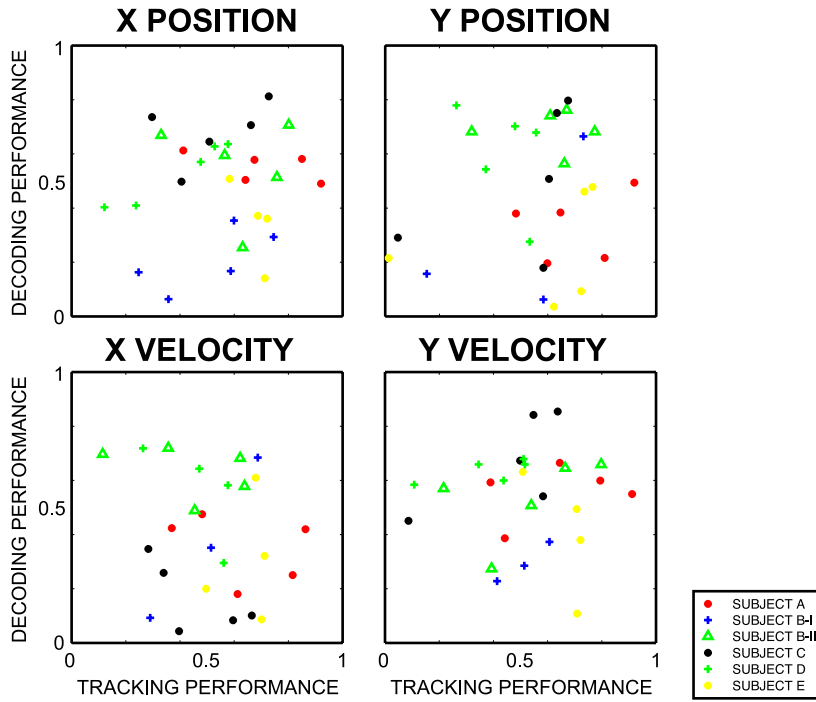


Figure 4.36: Tracking performance vs. decoding performance. See text for interpretation.

Patient	Age	Sex	Hand	Cognitive Capacity	Grid Location	Seizure Focus
A	23	M	R	Normal (IQ 88)	left frontal temporal	left temporal
B	24	F	R	Normal (IQ 97)	right frontal temporal	right orbitofrontal and temporal
C	38	M	R	Borderline (IQ 70)	right frontal	right frontal
D	48	M	R	Normal (IQ 82; right sup quadrant deficit)	right temporal	right temporal occipital focus
E	18	F	R	Normal (IQ 86)	left frontal	left frontal

Table 4.3: Clinical patient profiles.

tracking performance (i.e., how well they tracked the moving cursor) depended on their current condition and ranged from modest to very good.

I used ECoG signals in eight different frequency bands to decode four movement parameters of the cursor: horizontal and vertical position, and horizontal and vertical movement velocity. The lowest band was calculated as a running average of the signal over the past 333 ms and was called the local motor potential (LMP). To briefly summarize the technique that I used to decode movement parameters, I calculated, for each electrode, the amplitude in eight frequency bands. This procedure yielded up to 512 features (8 frequencies \* 64 electrodes). I then used the Correlation-based Feature Selector (CFS) to select the features that best predicted

each movement parameter. To determine the relationship between these features and each movement parameter, I performed a linear regression and used this model to predict those movement parameters on a different part of the dataset. All elements of this methodology were designed such that decoding of the movement parameters, and thus decoding of the cursor's position and velocity of movement, could have been achieved in real-time in online experiments. In other words, I could have used some data to establish the relationship between ECoG activity and cursor position and/or velocity, and then, in real-time, controlled the movement of the cursor using brain signals rather than joystick movements. As in previous studies in monkeys, one may expect that the actual joystick movements would eventually subside, resulting in an intuitive brain-computer interface that supported two-dimensional movements.

Table 4.4 shows the principal results of this study. These results demonstrate that it is possible to infer accurate information about joystick/mouse movement parameters in real time using ECoG signals in humans. Similar results were achieved in previous studies only using intracortical implants in non-human primates (see Table 4.5 for a comparison of the present results to these previous results). The present results further indicate that accurate decoding of joystick/mouse movement parameters can be achieved in human patients with epilepsy (whose cognitive and motor performance is often impaired by their condition) and in uncontrolled environments (i.e., during a busy hospitalization).

#### **4.4.5.2 The Local Motor Potential (LMP)**

The features used in this study represented a range of frequencies (8-12 Hz, 18-24 Hz, 35-42 Hz, 42-70 Hz, 70-100 Hz, 100-140 Hz, 140-190 Hz). These frequencies were in the mu, beta, and gamma frequency bands and were similar to those used by Rickert et al. [2005] with intracortical microelectrodes. In addition, I included the low-frequency LMP component (i.e., the signals' running average of the past 333 ms) after visual inspection identified specific channels in which ECoG voltage level seemed to correlate with movement parameters.

To study the relative importance of these different frequencies, I first normalized the features with respect to their standard deviations. This allowed the weights that were derived by the linear regression and associated with particular

Subj.	Task	X	Y	$\Delta X$	$\Delta Y$	Avg. $r$	Subj.	Task	X	Y	$\Delta X$	$\Delta Y$	Avg. $r$
A	J	0.61	0.49	0.48	0.66	0.56	A	J	0.55	0.33	0.35	0.56	0.45
B	J	0.71	0.76	0.72	0.66	0.71	B	J	0.55	0.69	0.63	0.53	0.60
C	J	0.81	0.80	0.35	0.85	0.70	C	J	0.68	0.51	0.17	0.67	0.51
D	J	0.64	0.78	0.72	0.68	0.71	D	J	0.53	0.60	0.52	0.64	0.57
A	M	0.64	0.62	0.62	0.47	0.59	A	M	0.50	0.58	0.51	0.24	0.46

Table 4.4: Decoding of movement parameters. Correlation coefficients ( $r$ ) between the actual and predicted movement parameters (horizontal position of the cursor (X), vertical position (Y), horizontal direction of the cursor ( $\Delta X$ ), and vertical direction ( $\Delta Y$ )) and the average across movement parameters (Avg.  $r$ ) when the patient used a joystick (J) or a mouse (M). Left: Correlation coefficients were calculated, for each parameter and dataset, for the best of the five folds of the cross-validation. Right: Average correlations between the actual and predicted movement parameters averaged across all five cross validation folds. These results demonstrate that faithful reconstruction of movement parameters is possible using ECoG signals in humans.

Study and Source	Position $r$	Velocity $r$
Schwartz and Moran, 1999, p. 2713	–	0.77
Carmena et al., 2003, Fig. 1F & 3C	0.33-0.63	0.27-0.73
Paninski et al., 2004, Table 1	0.47	–
Lebedev et al., 2005, Table 2	–	0.56
Averbeck et al., 2005, est. from Fig. 8A,B	–	0.74
Present study, 2006, Table 4.4	0.55	0.48

Table 4.5: Comparison to other studies. I compared the results of the present study to published results using two-dimensional tasks and microelectrode recording in monkeys. (I only selected reports that described methods that could have been achieved in real time.) To do this, I calculated average correlation coefficients for published position and velocity values (Position  $r$  and Velocity  $r$ , respectively) across all subjects. The correlation of the actual to the predicted trajectories, and thus the fidelity of the decoding, reported in the present study is within the range of those achieved using implanted microelectrodes in monkeys.

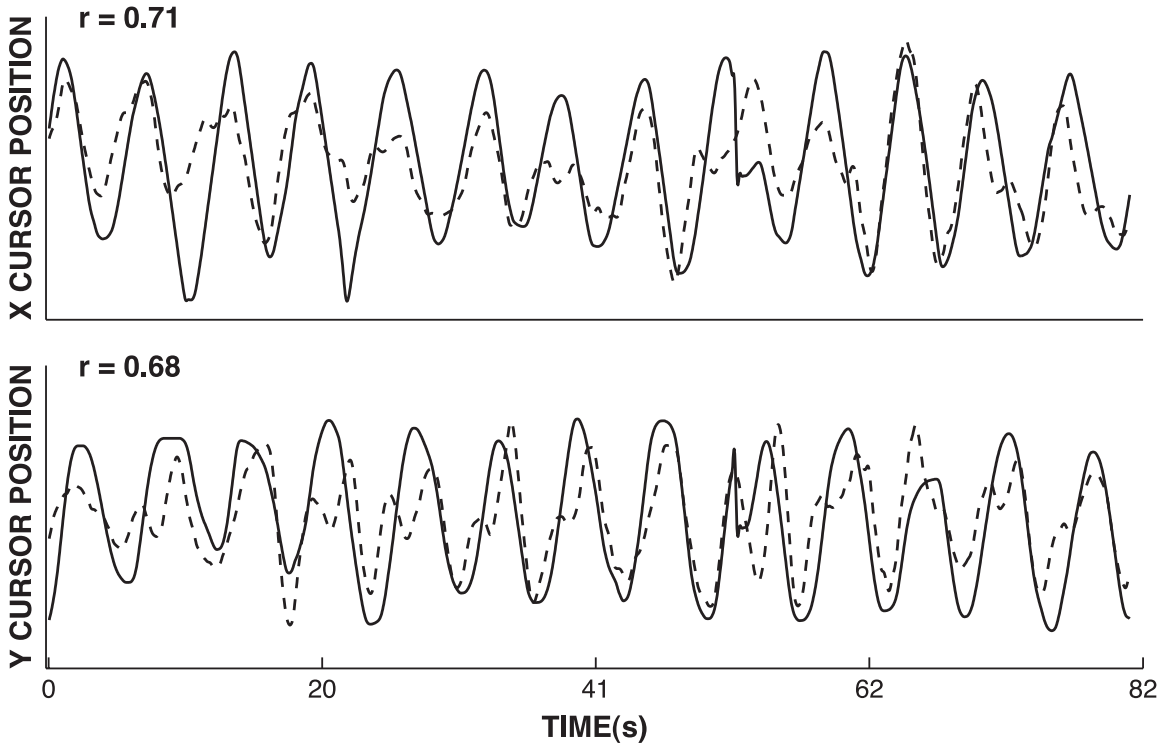


Figure 4.37: Example of actual and predicted movement trajectories. This figure shows actual (solid) and predicted (dashed) X and Y cursor position for one of the five cross validation folds for the joystick data set of patient B. The close concurrence between actual and predicted cursor position is evident. Because the calculation of prediction parameters only involves the training, but not the test data set, similar results can be expected in online experiments.

features and channels to be used as a measure of the importance of these features in predicting a certain movement parameter. For each dataset, for each of the four movement parameters, and for each of the features selected by the CFS feature selection method, I then summed the absolute value of the associated weights across all signal channels.

The results of this procedure indicated that mu/beta frequencies generally added very little information and gamma frequencies held substantial information for only some of the datasets/movement parameters (see Figure 4.38). Surprisingly, the LMP component carried substantial information about all movement parameters in all datasets. In fact, when I excluded the LMP component from the analyses, the averaged correlation coefficient (averaging the reported values for position and

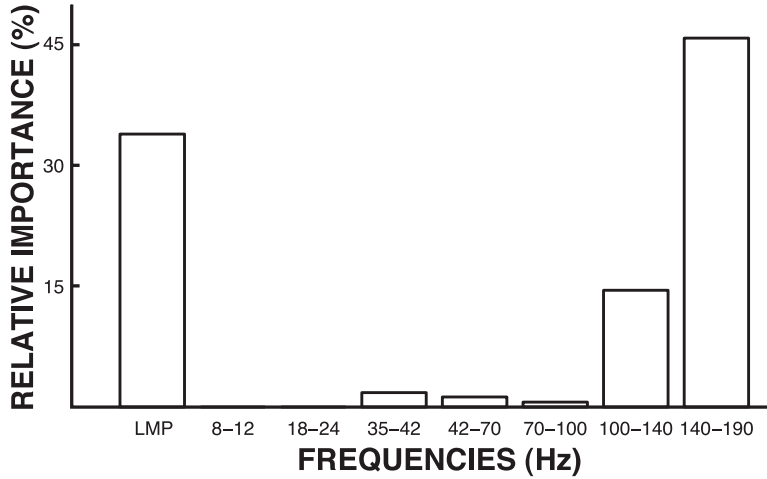


Figure 4.38: Example of the relative importance of different frequency bands. This example was calculated for the joystick dataset of patient B and for the horizontal position of the cursor. I did this by first normalizing the eight features by their standard deviation prior to classification so as to render the impact of each feature independent of their amplitude. I then accumulated, for each of the eight frequencies, the absolute value of the weights that were determined by the linear regression for the features that were selected by the CFS procedure. These results indicate that in this example, the LMP component and high gamma frequencies held the most information about the horizontal position of the cursor. While the LMP component contributed much information about the four kinematic parameters in all datasets, high gamma frequencies provided substantial information in only a few.

velocity in Table 4.5) dropped from 0.52 to 0.16. When I only used the LMP component, the results remained practically identical, which indicates that almost all the information obtained from the full analysis was captured by the LMP component.

#### 4.4.5.3 Anatomical Relevance of Sites Involved in Predictions

I also examined the anatomical relevance of electrode locations involved in the predictions. This provided an additional opportunity to derive evidence of the physiological relevance of the LMP. Thus, for locations selected by the CFS feature-selection procedure, I calculated regression weights for the LMP component only and mapped these weights on a 3D model of the cortex. The analyses revealed that locations over motor cortex (Brodmann's area 4) were typically involved (see Figure 4.39 for an example). Other predictive areas included premotor areas (area 6/44

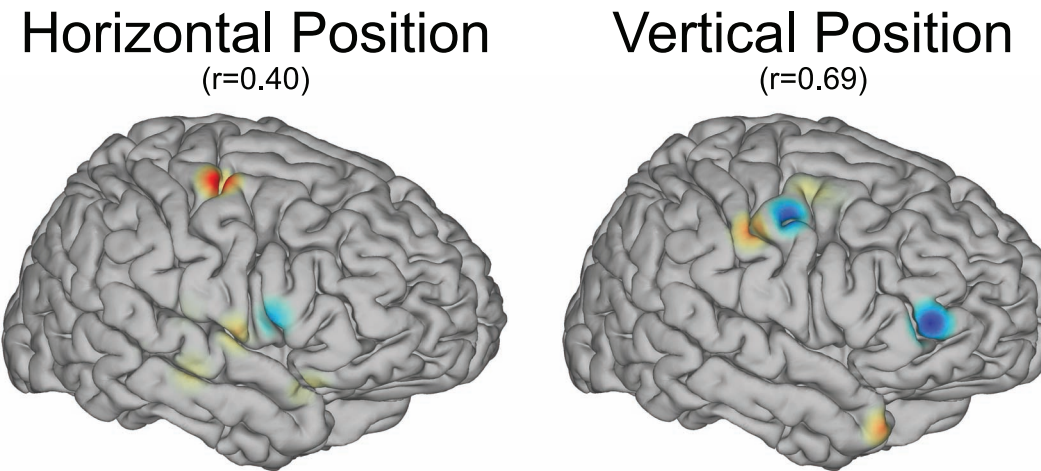


Figure 4.39: Electrode locations holding information about movement parameters.

This example was calculated by averaging the absolute values of the regression weights across all cross validation folds for the cursor position for patient B using a joystick. Colors represent the weights associated with the LMP feature at the respective locations, and thus indicate the relative importance of these sites in predicting cursor position (red colors indicate positive weights and blue colors indicate negative weights). The activations over hand and proximal arm areas of motor cortex are evident. In addition, other locations are involved for which the anatomical relevance is not clear (such as the activation over inferior frontal gyrus, etc.).

– well inferior to the classic frontal eye fields) and widely distributed areas such as middle and superior temporal gyrus, anterior inferior frontal lobe, and temporal pole that do not have obvious motor planning components. I can draw three conclusions from these analyses. First, LMPs correlated with movement are evident over widespread areas of cortex, not only over classical sensorimotor areas. This is in line with the recent findings (Davidson and Wolpert [2005]). Second, eye movements almost certainly do not play a substantial role in movement prediction in this paradigm (see further evidence on this aspect in the Discussion (Section 4.4.6)). Finally, the spatial specificity and the eminent anatomical relevance of the LMP component provide further indication that this new brain signal feature is not an artifact but rather reflects physiological events related to movement control.

#### 4.4.5.4 Directional Tuning

The LMP component contained substantial information for all datasets and movement parameters. I hypothesized that its origin might be the synaptic activity responsible for the movement-related modulation of firing rates of neurons immediately underneath the electrode. The LMP could thus be a spatially integrated (i.e., population) version of local field potentials (LFPs) that have been described using microelectrodes (Mehring et al. [2003]), and could exhibit similar characteristics. To investigate this possibility, I calculated LMP amplitude as a function of movement direction (i.e., the angle of the movement measured in -180 to +180 degrees). I found that over a number of brain regions, LMP amplitude was a function of movement direction, and over some, was a cosine function of movement direction. These *cosine tuning curves*, which had previously been reported in monkeys using implanted microelectrodes, were typically isolated groups and involved one or a few adjacent locations. Figure 4.40 shows examples of such tuning curves recorded from the hand area of motor cortex in three patients.

#### 4.4.6 Discussion and Interpretation

This study showed for the first time that ECoG signals can be used to accurately predict two-dimensional joystick trajectories in humans, and that these results were comparable in accuracy to those achieved in monkeys using implanted microelectrodes to record neuronal activity. Furthermore, a newly characterized brain signal, the local motor potential (LMP), held substantial information about movement parameters. The LMP component can exhibit the same kind of cosine tuning that has been previously described for neuronal firing rates and local field potentials (LFPs) recorded using intracortical microelectrodes. These results demonstrated that ECoG provides much more information than scalp-recorded EEG and does so without needing to penetrate the cortex. This study further implied that ECoG has characteristics that make it attractive not only for BCI research, but also for basic neuroscience investigations of brain function.

The impressive decoding of joystick achieved in this study depended in large part on the LMP component. Because no previous report has, to my knowledge, described the relationship of this new brain signal feature to movement parameters,

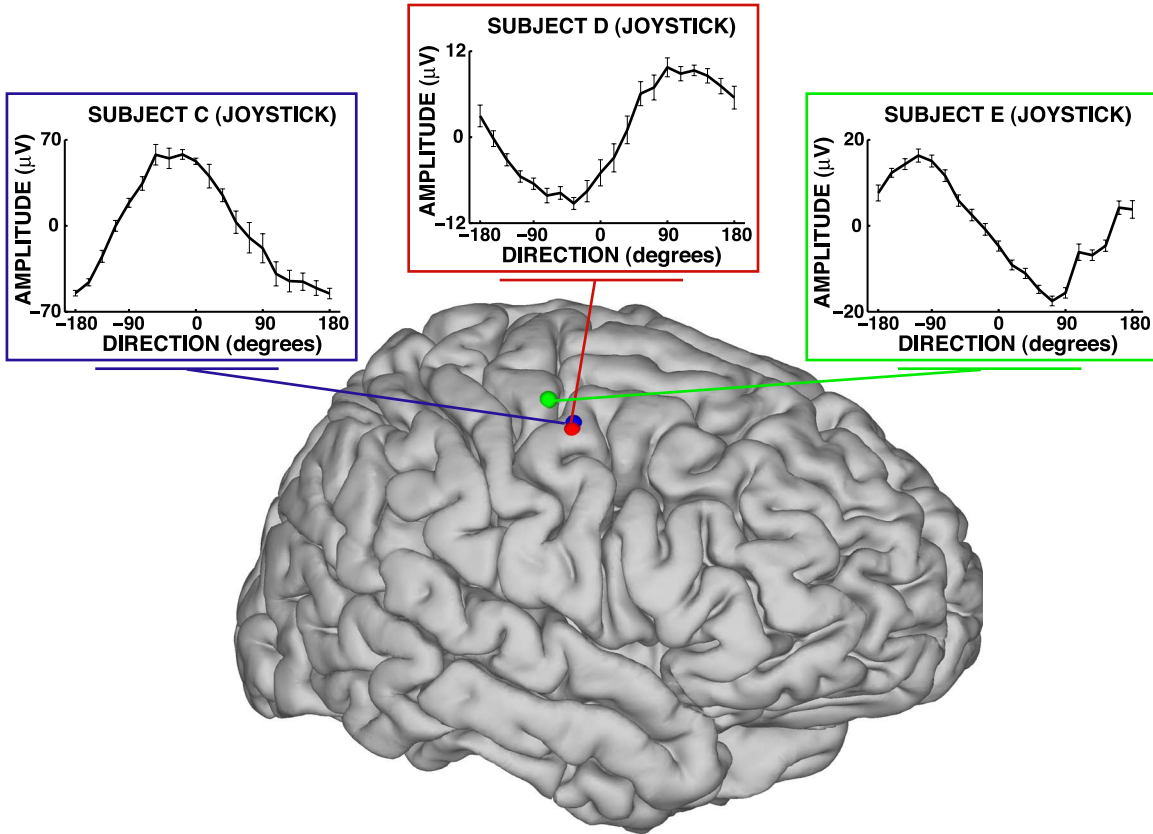


Figure 4.40: LMP Tuning Curves. Amplitude modulations of the LMP component over hand area of motor cortex as a cosine function of movement direction in three patients. (Subject E's grid was on the left hemisphere. I projected the shown electrode onto the right hemisphere.) The similarity of these ECoG results to the many published results achieved using implanted microelectrodes is compelling.

I was concerned that it might merely be an artifact generated by movements of the wires coming from the patient. The present evidence indicates that this is not the case. First, the initial step in feature extraction was the application of a common average reference filter. This filter, which provided improved performance, removed signals with low spatial frequencies such as those that could be expected from external induction of an artifact. Second, my analyses showed that the LMP was often spatially specific, located over anatomically relevant areas, and can exhibit cosine tuning similar to that described for neuronal firing rates and local field potentials (LFPs) recorded by intracortical microelectrodes.

It is surprising that the LMP has apparently not been previously described.

It is possible that it is too spatially specific to be detected on the scalp. Moreover, in the present paradigm movement speed and direction changed rather slowly (i.e., one full circle in 6.5 seconds=0.15 Hz), whereas previous studies in monkeys often utilized higher speeds (i.e., around 1-2 Hz). In the latter cases, associated LMP components could have been masked by other ECoG activity. Finally, it is possible that in previous studies the LMP component was filtered out at the amplification or post-processing stage. Indeed, when I re-analyzed data from the first study described in this chapter (Section 4.3) without high-pass filtering of the signals, I found that LMP amplitude in one particular location was modulated by the direction of joystick movement, and LMP amplitude in one immediately adjacent location was modulated by hand opening/closing and rest (see Figure 4.41). These results indicate that the LMP can be present in other subjects, other datasets, and for other tasks. They also show that at least in this particular subject, LMP activity and activity at 18 Hz (i.e., in the beta frequency band) were topographically similar, which corroborates the hypothesis that the LMP has a physiological origin related to hand movements.

Another concern was that the results depended in part on cortical activity related to eye movements rather than to joystick movements. While it is possible to rule out the influence of eye movements by monitoring them with an eye tracker, the clinical environment of the patients made this impractical. Nevertheless, other evidence strongly suggests that a marked influence of eye movements was unlikely. First, the anatomical mapping provided little evidence for eye-movement influence. Areas that are implicated in eye movements, such as frontal eye fields, typically did not hold movement-related information. Second, Schwartz et al. [2004] have shown that in a tracking task, eyes typically saccade rather than smoothly pursuing the cursor or target, and that eye movements would therefore provide only limited information on the cursor's movement parameters.

As described in the Methods section, four out of six joystick datasets were significant at the  $p=0.01$  level and were subsequently selected for the study. In contrast, only one of the five mouse datasets was selected. While the visual feedback was the same for the two tasks, the required motor output to arm was much different. For the mouse task, the position of the mouse was mapped directly to the position

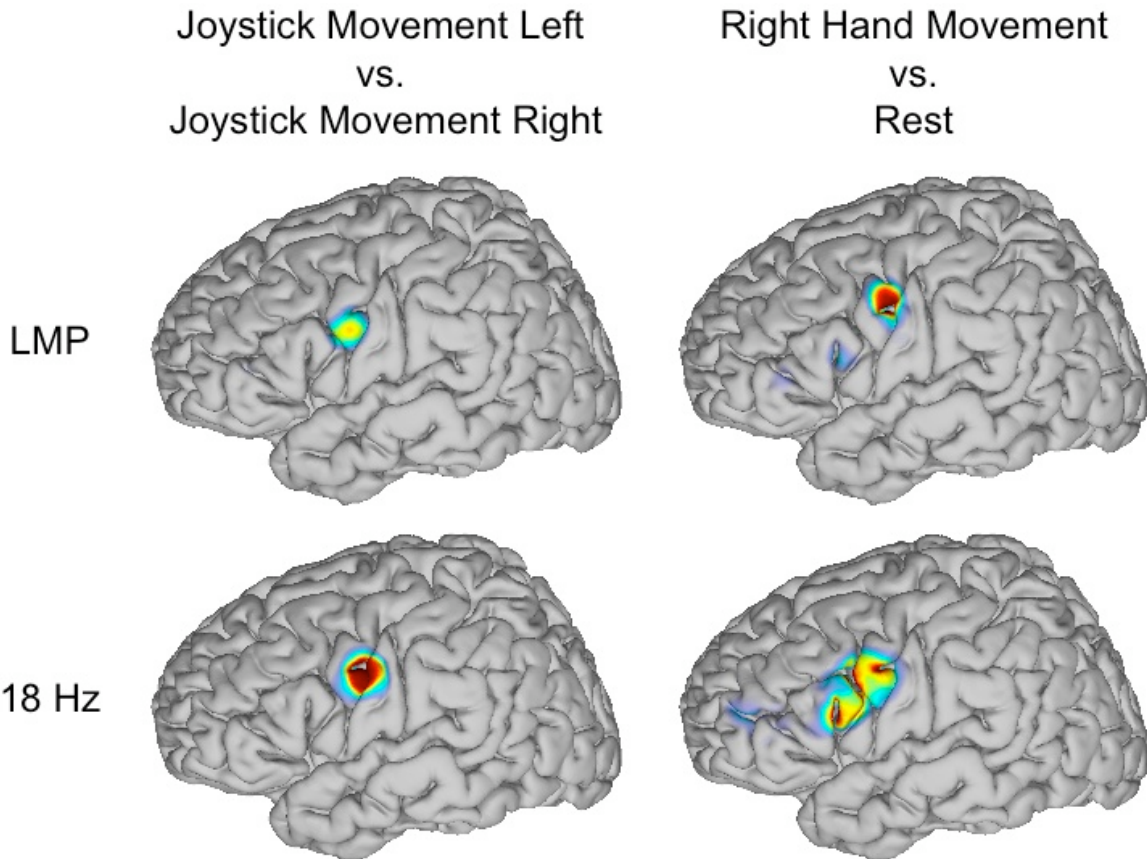


Figure 4.41: LMP in other subjects and tasks. This figure demonstrates that the LMP can also be present in other subjects and for other tasks. It was calculated for Subject E from the previous study (Section 4.3). The four images show maps of the statistical difference (calculated as  $r^2$ ) between two conditions (i.e., joystick movement left and right, and hand movement and rest).

of the cursor on the screen and for any given static cursor position within the workspace, the arm musculature only had to account for gravitational forces on the arm. Given the relatively low speed of the tracking task, the inertial forces/torques due to centripetal and coriolis accelerations would be minimal, leaving gravity as the dominant kinetic parameter affecting muscle recruitment throughout the mouse movement. Furthermore, from a kinematics view, the fact that directional tuning in motor cortical neurons is modulated by speed in a gain-field fashion (Moran and Schwartz [1999a]), one would expect a very small change in the underlying motor cortical activity due to velocity encoding during the mouse task. Therefore, the only movement parameter that was significantly modulated throughout the mouse task

was hand position, which has been previously shown to have a significant yet limited effect on motor cortical activity levels. In contrast, in the joystick task, the position of the force-feedback joystick was mapped to the velocity of the cursor. In order to accurately move the cursor in a circle, the patients had to continually rotate the joystick in the outer regions of its range of motion. The joystick provided a large force-feedback to the patient's hand that always tried to push the joystick back to the center of the workspace (i.e., zero velocity). As such, the patient was continually modulating arm muscle activity to keep the joystick away from its central position. Given that bias forces applied to the hand have been previously shown to have a significant effect on motor cortical activity, it was expected that the joystick task would modulate both premotor and primary motor cortical activity much more than the mouse task.

Three additional factors help explain why almost all of the Seattle joystick data, but only one of the other 35 datasets, allowed for adequate decoding. First, the ECoG data described in this study were gathered in the patients' rooms in a busy hospital setting and amid their complex and continually changing circumstances (e.g., recent surgery and anesthesia, recent seizures, a variety of pharmacological agents). As a result, the level and consistency of the attention and effort that patients were able to devote to joystick or mouse control varied markedly from session to session. Second, no St. Louis data set was included. This suggested the possibility that the setup in St. Louis might prohibit adequate predictions. In fact, I determined after completion of the study that in addition to analog filtering, a digital high-pass filter (cut-off 2 Hz) was applied by the clinical clinical XLTEK. This filter removed the LMP low-frequency component that I found was critical for the successful decoding in the Seattle datasets. Third and finally, no watch dataset was included. This supports the hypothesis that actual movements, rather than simply eye movements, are necessary for accurate predictions.

Together with results from previous studies in monkeys, the present results suggest that BCI use could be made more intuitive, i.e., subjects could use movement-related imagery rather than imagined limb movements to perform a movement task. Thus, training time might be reduced using ECoG and a joystick task. However,

aside from empirical observations it is not clear what factors govern the need for BCI training time. It is possible that the physiological nature of the brain signal is important. In a typical mu- or beta-rhythm EEG-based BCI, brain signals associated with imagined limb movements are first identified. These signals, i.e., modulations in the mu or beta rhythm frequency bands (i.e., 8-12 Hz or 18-25 Hz, respectively), are then used alone or in combination to provide one- or two-dimensional control. While the origin of these scalp-recorded rhythms remains unclear (da Silva [1991]), they are not believed to be strongly correlated with movement direction. Thus, their use for directional movement control might require considerable plasticity and thus user training. In contrast, BCI systems using implanted microelectrodes may require less user training. These systems typically record single-unit action potentials from neurons in motor cortex. Neurons are then identified whose firing rate is associated with movement parameters (such as direction) of hand movements (Georgopoulos and Massey [1988], Schwartz and Moran [1999], Moran and Schwartz [1999a,b, 2000], Wessberg et al. [2000], Schwartz et al. [2001], Reina et al. [2001], Rokni et al. [2003], Paninski et al. [2004], Merchant et al. [2004], Schwartz et al. [2004], Averbeck et al. [2005]). Firing rates of those neurons are then combined to produce multidimensional control signals. When monkeys are provided feedback based on brain signals rather than actual joystick movements, they initially continue to move the joystick but quickly learn to produce the same signals, and thus similar control over the BCI system, without the actual physical movements (Taylor et al. [2002]). While BCIs based on EEG and neuronal firing rates both require new behaviors that will necessitate cortical plasticity and thus training, it is likely that the transformation of brain signals that typically encode movement direction into directional non-muscular commands demands less cortical reorganization and thus less user training than when using phenomena that typically do not encode direction, such as scalp-recorded mu and beta rhythms. Thus, the results of the present study suggest that the perceived training-time advantage of implanted microelectrode recordings could also be achieved using ECoG, and thus strongly support the hypothesis underlying **THEME III** of this dissertation.

For clinical applications of BCI technology, chronic implants of ECoG elec-

trodes would be required. The literature suggests that subdural/epidural electrodes exhibit good long-term stability (Loeb et al. [1977], Bullara et al. [1979], Yuen et al. [1987], Pilcher and Rusyniak [1993], Margalit et al. [2003]). In addition, there are several theoretical reasons why ECoG electrodes will probably not be affected by the substantial stability problems associated with implanted microelectrodes. The area covered by ECoG electrodes is much larger (and thus their impedance much lower) compared to microelectrodes. Moreover, since ECoG electrodes do not penetrate cortex, the short- and long-term reactive responses of the brain typical with microelectrodes should be substantially reduced. Even if scar tissue were to form underneath the electrodes, the electrodes' low impedance should allow for sustained recordings. Other important issues could also be potentially addressed. Whereas human ECoG studies to date have relied on electrode grids implanted in preparation for epilepsy surgery and thus often do not contain locations important for BCI studies, grids implanted to create a BCI communication device would be ideally located to cover target locations. Their size and design could be optimized to eliminate the need for a craniotomy. Furthermore, ECoG recordings require a dramatically lower bandwidth (i.e., 500-Hz sampling, and much less if only the LMP is extracted) compared to single-neuron recordings using microelectrodes (i.e., 10-50 kHz). These lower technical needs translate to substantially decreased processing and power requirements. Lower power requirements correspond to less heat dissipation and to longer battery life. In the end, these technical advantages will thus facilitate the design of electrode/telemitter systems that could be chronically implanted and would not require any percutaneous connection. This would greatly reduce the long-term risk of infection.

The present study does not specify exactly which kinematic parameters are actually encoded in the ECoG signals. Future studies could use different movement patterns, directions, and speeds to determine how the results in humans using ECoG relate to the body of understanding that has been established for signals recorded from intracortical microelectrodes.

## 4.5 Conclusions

The main impetus of THEME III of this dissertation was to pursue more intuitive human BCI systems by using approaches similar to those that have previously been described only for microelectrode recordings in animals. These approaches start by decoding detailed movement parameters (such as position or velocity) from brain signals recorded during actual arm movement, and subsequently using decoded kinematic parameters related to these movements for device control. It has been widely assumed that such detailed movement parameters can be derived only from signals recorded by intracortical microelectrodes.

The primary contribution of this chapter of this dissertation is that I showed that this widespread assumption is incorrect; that, in fact, signals recorded by electrodes on the cortical surface (ECoG) in humans also support accurate decoding of kinematic parameters of joystick movements without requiring penetration of the brain. These results thus strongly suggest that ECoG could be used to design more intuitive tasks for human BCI systems, and thus are likely to remove one of the critical barriers that currently impede translation of human laboratory BCI demonstrations into clinical practice.

## CHAPTER 5 INTEGRATION

In the three themes of this dissertation, I demonstrated that a new sensor methodology, signal processing technique, and user task can facilitate the move of current BCI laboratory demonstrations towards clinically applicable communication devices. This chapter will show three examples of how the methodologies developed in these themes can be combined with each other or with other techniques to provide potential additional benefits.

### 5.1 Use of Signal Detection With Other Brain Signals

In THEME II of this dissertation, I showed that the use of a detection approach in BCI signal processing has advantages over traditional techniques when applied to amplitude modulation of mu/beta or gamma oscillations in EEG or ECoG signals. However, this novel technique also lends itself to other types of brain signals utilized in BCI research, such as the P300 potential.

Infrequent stimuli typically evoke a positive response in the EEG over parietal cortex about 300 ms after stimulus presentation (see Walter et al. [1964], Sutton et al. [1965], Donchin and Smith [1970]). This response (called the P300 potential) has been used as the basis for a BCI system (see Farwell and Donchin [1988], Bayliss [2001], Allison [2003], Schalk et al. [2004], Sellers and Donchin [2006]). In these systems, the user is presented with a 6 x 6 matrix of characters (see Figure 5.1). The rows and columns in this matrix flash successively and randomly at a rapid rate (e.g., around eight flashes per second). The user can select a character by focusing attention on it and counting how many times it flashes. The row or column that contains this character evokes a P300 response, whereas the others do not (see Figure 5.2). After averaging a number of responses, and applying one of traditional classification routines, the computer can determine the character's row and column, and thus the desired character. Compared to BCIs using mu/beta rhythm processing, BCIs using P300 have the advantage that they do not require any training because they simply depend on the user's ability to pay attention to a particular character.

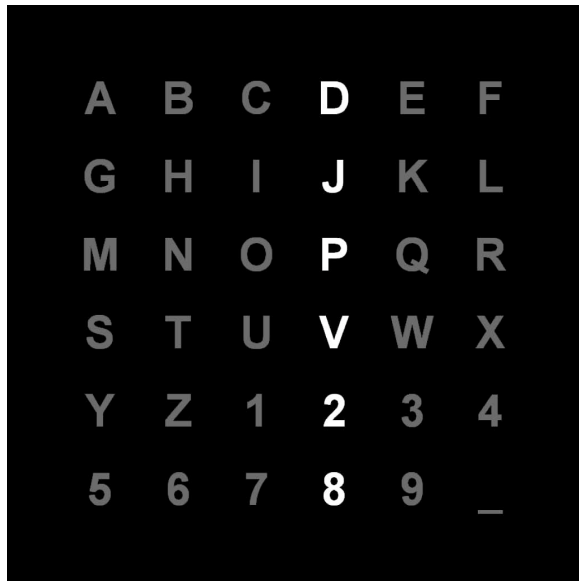


Figure 5.1: A P300-based spelling application (as in Farwell and Donchin [1988] and Donchin et al. [2000]). Rows and columns of the matrix flash in a block-randomized fashion. The BCI user focuses attention on a particular character. Flashing of the row or column that contain that character produces a response that is different from that to the other rows or columns. This difference can be used by the BCI system to predict the character the user wants.

At the same time, they also have disadvantages, because they rely on a structured and tiring environment (the flashing rows/columns), are most effective only when combined with visual feedback, and, even for visual feedback, the independence of gaze movement from system performance has not yet been established. Thus, it remains to be determined whether these systems are merely brain-based eye gaze systems (and could thus not be used by people who are totally paralyzed) or derive their function mainly from the subject's ability to focus attention on a particular character.

Just like the processing for mu/beta rhythms, P300 detection is typically accomplished using traditional classification techniques (such as linear discriminant analysis) that discriminate between signals that contain the P300 response and ones that do not. This also requires a signal identification procedure that can be used to parameterize a discriminant function. In healthy individuals, this discriminant function, once established, can generalize to other datasets from the same individ-

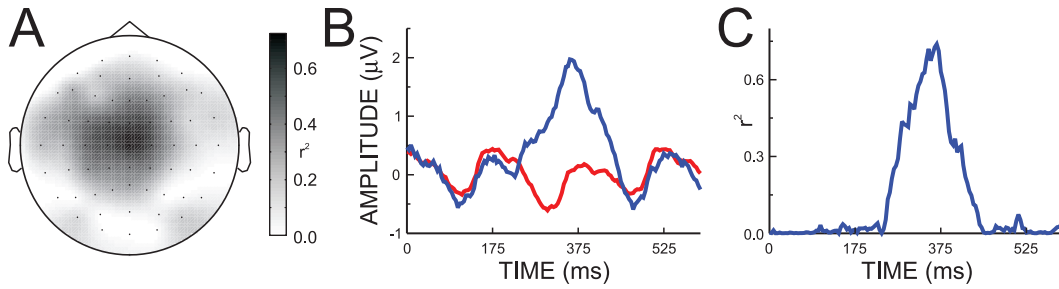


Figure 5.2: The use of P300 potentials in the EEG for spelling. A: Topographical distribution of the P300 potential at 340 ms after stimuli, measured as  $r^2$  (calculated from averages of 15 stimuli) for stimuli including versus not including the desired character. B: The time courses at the vertex of the voltages for stimuli including (blue line) or not including (red line) the desired character. C: Corresponding  $r^2$  time course that indicates the statistical difference between the two desired and undesired stimuli. Stimulus rate was 5.7 Hz (i.e., one every 175 ms).

ual. Thus, for healthy individuals, the use of discriminant functions is adequate. However, in patient populations, the P300 response can be more variable, so that discriminant functions may not generalize well to other datasets. Consequently, the use of the signal detection approach described for **THEME II** of this dissertation may also have advantages when applied to the detection of P300 responses. For example, a model of baseline activity could be established for the responses to those rows and columns that do not contain the correct character, such as the red line in Figure 5.2-B. Signal detection could then derive the probability that indicates how different any particular response is from the baseline model. This probability should thus be small for a response to the desired row/column (such as the blue line in Figure 5.2-B) and large for a response to all other rows/columns, and could thus be used to discriminate between the two types of responses.

## 5.2 P300-Based BCIs Using ECoG

In **THEME I** of this dissertation, I showed that the increased signal fidelity of electrocorticographic (ECoG) signals recorded from the surface of the brain has advantages when used with BCIs based on mu/beta rhythms. It is possible that P300-based BCIs can also benefit from the qualities of ECoG.

Simple P300-based BCIs using EEG derive their classification function by

merely picking the best feature (i.e., signal amplitude at the best location (such as the center of the vertex in Figure 5.2-A) and latency (around 350 ms in Figure 5.2-C). Using this simple approach, accurate prediction of the desired character (i.e., close to 100% correct) may require averages of approximately 15 responses for each row and column.

More comprehensive approaches derive their classification function by optimizing signal filtering using adaptive downsampling and by using automated feature selection together with linear discriminant analysis. These more sophisticated approaches can reduce the number of averages that are necessary to approximately 4 responses for each row and column for the same datasets that require 15 averages with the simple approach. At a stimulus presentation rate of 175 ms, and 4 averages per 12 stimuli (6 rows and 6 columns), a P300-based BCI can allow users to make accurate letter selections every 8.4 seconds. Despite such impressive demonstrations, such systems often still cannot compete with existing (i.e., muscle-based) augmentative communication aids such as systems based on eye gaze (e.g., Gerhardt and Sabolcik [1996]). Thus, in order to be competitive with conventional augmentative devices, the performance of BCIs based on P300 potentials should be improved.

One possible avenue for such improvements could be the use of ECoG signals for P300-based BCI communication. This possibility is encouraged by my preliminary results that show that the P300 potential can also be detected in ECoG signals (see Figure 5.3). Moreover, the use of ECoG and P300 potentials could also be combined with the detection approach developed in **THEME II** of this dissertation as described in the previous section. This could produce a P300-based system with higher speeds compared to current P300-based BCIs using EEG, while also providing additional system robustness in patient populations.

### **5.3 Decoding Hand Movements Using Signal Detection**

In **THEME III** of this dissertation, I showed that it is possible to decode kinematic parameters of hand movements using ECoG signals and linear models. This method was effective and produced results that were within the range of those that previously had been achieved only using microelectrodes implanted within the cor-

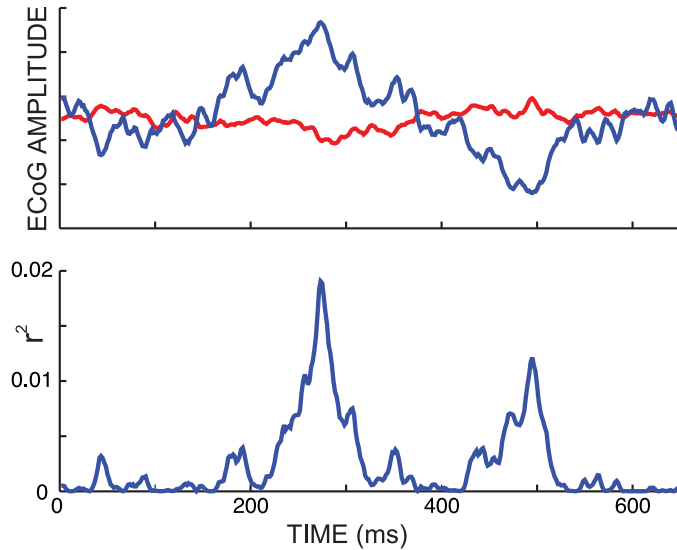


Figure 5.3: P300 potentials can also be detected in the electrocorticogram. Top: The time courses at a particular ECoG electrode of the voltages for stimuli including (blue line) or not including (red line) the desired character. Bottom: Corresponding  $r^2$  time course that indicates the statistical difference between the two desired and undesired stimuli. Just like the EEG example in Figure 5.2, this ECoG example shows that the brain produces different brain responses for desired vs. undesired stimuli.

tex. However, this methodology assumes that the regression function that translates features into kinematic parameters of hand movements remains stationary within and across datasets. In this dissertation, I tested this underlying hypothesis in part (i.e., across datasets) by applying cross-validation (i.e., training on parts of the data and testing on the rest). Thus, the results that I presented clearly generalize across data sets.

At the same time, it is possible that there is non-stationarity within each dataset and that thus this decoding problem might be better served by the detection approach presented in **THEME II** of this dissertation. For example, it would be possible to generate one Gaussian model for each of horizontal and vertical movement utilizing all possible features. This methodology might prove more robust and/or might yield higher performance compared to the results achieved using linear regression.

## CHAPTER 6

# CONCLUSIONS AND RECOMMENDATIONS

### 6.1 Conclusions

Studies over the past few decades have shown that brain-computer interfaces (BCIs) can allow people who are paralyzed to communicate again by creating a new communication channel directly from the brain to an output device. These studies have demonstrated in the laboratory that non-muscular communication and control is no longer merely speculation, and that direct communication from the brain to the external world is possible and might serve useful functions. While some of these technical demonstrations have been impressive, clinical applications of BCI technology have remained scarce for primarily three reasons. These are the limitations of current sensor technologies, the requirements implied by traditional signal processing approaches, and the non-intuitive tasks that have been used for BCI communication. In this dissertation, I set out to address these problems and to thereby work towards a BCI system that can leave the confines of laboratory research to address the actual communication and control needs of the severely paralyzed. To do this, I focused my work on three themes that corresponded to the problems listed above.

In **THEME I** of this dissertation, I was concerned with a better signal acquisition methodology for BCI research. The results presented in Chapter 2 support the expectation that signals recorded from the surface of the brain (ECoG) have higher fidelity than those recorded on the scalp (EEG). Furthermore, and as a critical contribution to BCI research, I demonstrated the first use of ECoG for online operation of a BCI system, which indicated dramatically reduced training requirements compared to methods using EEG.

In **THEME II** of this dissertation, I proposed the first use of a detection approach for BCI signal processing. The main contribution presented in Chapter 3 is the finding that the use of this approach can result in performance similar to that achieved by the classification-based techniques traditionally used in BCI research without necessitating the tedious expert-supervised signal identification procedures

that are typically required. In addition to this contribution to BCI research, I also demonstrated that this methodology can be used as a novel and effective way to visualize brain signals in real time, and could thus also be important for basic or clinical research and diagnosis.

In **THEME III** of this dissertation, I pursued more intuitive human BCI systems by using approaches similar to those that have previously been described only for microelectrode recordings in non-human primates. These approaches decode detailed movement parameters from hand movements, which makes the use of BCI systems intuitive. It has been widely assumed that these approaches require signals recorded by intracortical microelectrodes. The main contribution presented in Chapter 4 is that I show that this widespread assumption is incorrect; that, in fact, ECoG signals recorded in humans also support accurate decoding of kinematic parameters of joystick movements without requiring penetration of the brain.

In summary, the three themes of this dissertation address the chief problems that currently impede translation of laboratory BCI demonstrations into clinical practice. By showing that ECoG signals are superior in performance to EEG and less invasive than electrodes that penetrate the brain, by demonstrating that alternative approaches to BCI signal processing can reduce the amount of necessary expert oversight, and by illustrating that human BCI systems can be made more intuitive, the work in this dissertation provides a critical contribution to BCI research towards its ultimate purpose – the clinically practical restoration of communication and control function for severely disabled individuals.

## 6.2 Recommendations

The results presented in this dissertation encourage further work in several areas. These are the use of the detection approach described in **THEME II** for real-time experiments, further study and subsequent online experiments of ECoG signals relating to hand movements, and approval of ECoG for the purpose of BCI applications. These areas are described in the following sections.

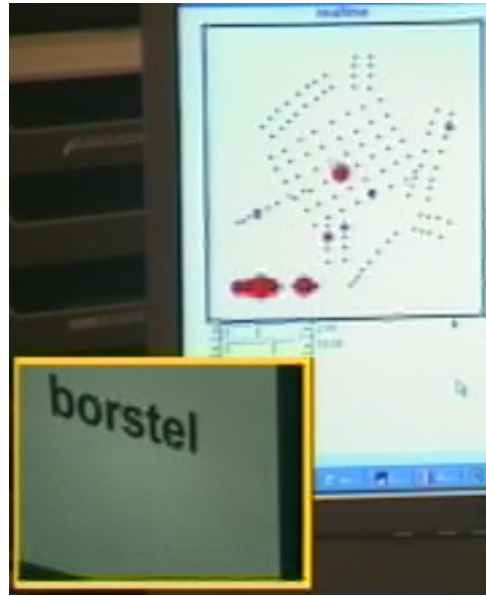


Figure 6.1: Initial test that demonstrates that SIGFRIED can be used in real time. In this test, data from 128 channels of ECoG were collected (i.e., from one grid and several electrode strips). SIGFRIED used data recorded during rest to define a model of baseline activity. The amplitude of changes from this baseline is indicated by the radius of red circles (insert on upper right). Activity at various sites change in response to a particular language task (insert on bottom left). Figure courtesy of Dr. Erik Aarnoutse and Dr. Nick Ramsey, Utrecht, The Netherlands.

### 6.2.1 Real-Time Experiments Using Signal Detection

THEME II of this dissertation described the use of a detection approach for BCI signal processing. Its application has several advantages compared to traditionally used classification-based approaches. While I have shown the benefits of this approach to BCI research and to applications in other areas, I have only demonstrated these benefits in offline analyses. The next logical step is to take advantage of the favorable properties of the detection approach, whose implementation I labeled SIGFRIED, in real-time experiments. Figure 6.1 shows a screenshot of a first test that demonstrated that SIGFRIED can successfully decode and visualize brain activity from 128 channels in real time. It is my expectation that this methodology will lead to an established methodology for the real-time visualization of complex brain signals.

### 6.2.2 Decoding of Hand Movements: Further Studies

In Chapter 4, I described that kinematic parameters relating to joystick movements can be faithfully decoded from ECoG signals in humans. At the same time, in this initial study patients tracked a target that moved in a circle, which confounds several movement parameters. For example, horizontal cursor position and vertical cursor velocity are correlated. Consequently, this initial study does not specify exactly which kinematic parameters are actually encoded in the ECoG signals. Future studies could use different movement patterns, directions, and speeds to determine how the results in humans using ECoG relate to the body of understanding that has been established for signals recorded from intracortical microelectrodes, and to determine which of the resulting ECoG features might be best for the actual BCI experiments.

Once it has been established which specific kinematic parameters are encoded in ECoG signals, to which degree each of the corresponding ECoG features support accurate real-time decoding, and which brain locations can provide optimum detection of these features, real-time experiments should be conducted. These experiments will be preceded by an initial offline evaluation that, similar to that used in Chapter 4, will determine the mapping between ECoG signals and kinematic parameters. This mapping can subsequently be used in real-time experiments to provide feedback to the patient that is initially driven by actual hand movements. Based on monkey studies (Taylor et al. [2002]), I expect that arm movements will eventually subside so that humans should be able to control a computer cursor in two dimensions by thought alone using an intuitive task.

### 6.2.3 ECoG for BCI Purposes: Recommendations

The results in this dissertation depended significantly on ECoG signals (i.e., the real-time BCI experiments described in Chapter 2, some of the demonstrations of the usefulness of the detection approach described in Chapter 3, and the real-time decoding of joystick movements described in Chapter 4). While the results in these chapters are strong evidence that ECoG is an ideal sensor platform for BCI research, further progress requires systematic study and optimization of several parameters such as the optimum electrode size, spacing, and location. Furthermore,

while theoretical considerations and evidence in the literature suggest robust long-term stability of ECoG recordings, no study to date has specifically addressed this issue. It is impossible to conduct these systematic studies, which are required to realize the promise of ECoG signals for BCI applications, using the epilepsy patient population utilized for the studies in this dissertation. As described in Chapter 2, all sensor parameters (i.e., their number, size, spacing, location, and implant duration) are currently undefined by the epilepsy surgery protocol, and thus cannot be optimized for a different purpose.

Further progress thus requires that the parameters of ECoG sensors be optimized, followed by the use of ECoG-based BCI systems for the purpose of communication in people with disabilities, which will require FDA approval. In consequence, sensor optimization will most practically be accomplished in non-human primates. The results presented in this dissertation and the studies that will follow should provide ample evidence to support FDA approval of implantation of ECoG electrodes for the BCI purpose. This process will be further facilitated by the development of telemitter systems that can remove the need for chronic percutaneous wire placement, which poses unnecessary risks of infection.

Compared to signals acquired with microelectrodes implanted within cortex, signals acquired using ECoG lend themselves particularly well to wireless transmission. This is because the signal features that are important for BCI communication (such as those used for the BCI experiments in Chapter 2 or for the decoding of hand movements in Chapter 4) are decoded from ECoG signals using analysis of particular frequency bands up to 200 Hz. This is in marked contrast to the features derived from signals acquired using microelectrodes within cortex. The most common features of these signals are the firing rates of action potentials of individual neurons. Just like with ECoG-based BCIs that use different signal features, subjects can be trained to modulate these firing rates to control a BCI system. However, the duration of each individual action potential is very short (i.e., on the order of one ms), and data thus have to be sampled at many times this rate (usually between 20 and 50 kHz) so that action potentials can be effectively detected and discriminated (often, multiple action potentials are detected on each sensor). In summary,

while the feature extracted from individual neurons within the brain and from ECoG are estimated at comparable rates (e.g., 20-50 Hz), the extraction of features from neuronal firing rates requires much higher sampling rates compared to ECoG-based signal features.

The low bandwidth of the carrier of relevant features in ECoG signals is a chief advantage compared to features based on action potential detection and discrimination. This is because the sampling rate can be 100-1000 times lower for ECoG signals than for neuronal action potentials, which implies that processing and power requirements are dramatically reduced. This would facilitate development of telemitter-based ECoG BCI systems. As an alternative use of this benefit, one could keep the processing and power requirements the same as those of current action potential-based systems, but scale the number of signals acquired from the brain by the same factor (100-1000). Furthermore, theoretical considerations (Freeman et al. [2003]), as well as the results presented in this dissertation, support the notion that recordings on the surface of the brain have much higher spatial resolution than those currently used (i.e., 0.5-1 cm inter-electrode spacing). Together with the technical possibility to sample more locations, the notion that signals from more locations actually provide independent information (which is not the case for EEG due to the substantial blurring that occurs on the scalp) has substantial implications.

All current non-invasive sensor modalities are constrained either by the number of possible signals that can practically be acquired, or by the temporal resolution that can be achieved. For example, while EEG sensors on the scalp could be placed in high densities, the signals recorded with these sensors have low spatial resolution. Restoration of the sources within the brain (i.e., reconstruction of signals with high spatial resolution) from these sensors is mathematically difficult and successful only in highly controlled situations, which makes this approach impractical for widespread application. Signals based on action potentials recorded within the brain have high spatial resolution but also high processing requirements. This puts a practical limit on the number of sensors that can be processed. Other techniques, such as functional magnetic resonance imaging (fMRI) can yield a large number of independent signals, but their temporal resolution is only on the order of a few seconds. In consequence,

no current methodology can practically derive a large number of signals from the brain at high temporal resolution (see Figure 6.2). The use of ECoG (indicated in this figure by the star) might overcome this problem such that one could acquire potentially thousands of independent signals at a high temporal resolution.

It is likely that this possibility would introduce a new quality to the study of brain function. Furthermore, it is likely that BCI performance would also benefit. For example, the decoding of joystick movements described in Chapter 4 was based on sensors with 1-cm spacing. Even at this low spatial resolution (compared to that which could be achieved with ECoG), the fidelity of the decoding was within the range of those results that have been achieved using microelectrodes implanted within the cortex. Furthermore, my results show that signals from widespread areas of the cortex held information about joystick movements, indicating that recording from large brain areas is beneficial. Together with the notion that the spatial resolution of ECoG is much higher than the 1 cm that was used, this suggests the possibility that scaling the number of sensors by two orders of magnitude would also equally scale the amount of information that could be decoded from the brain. In summary, this technical possibility suggests the possibility for dramatic improvements in BCI performance, and in turn, for a much larger number of individuals that could benefit from BCI technology. This technical possibility, and the powerful implications derived from it, are further elucidated in the next and final section of this dissertation.

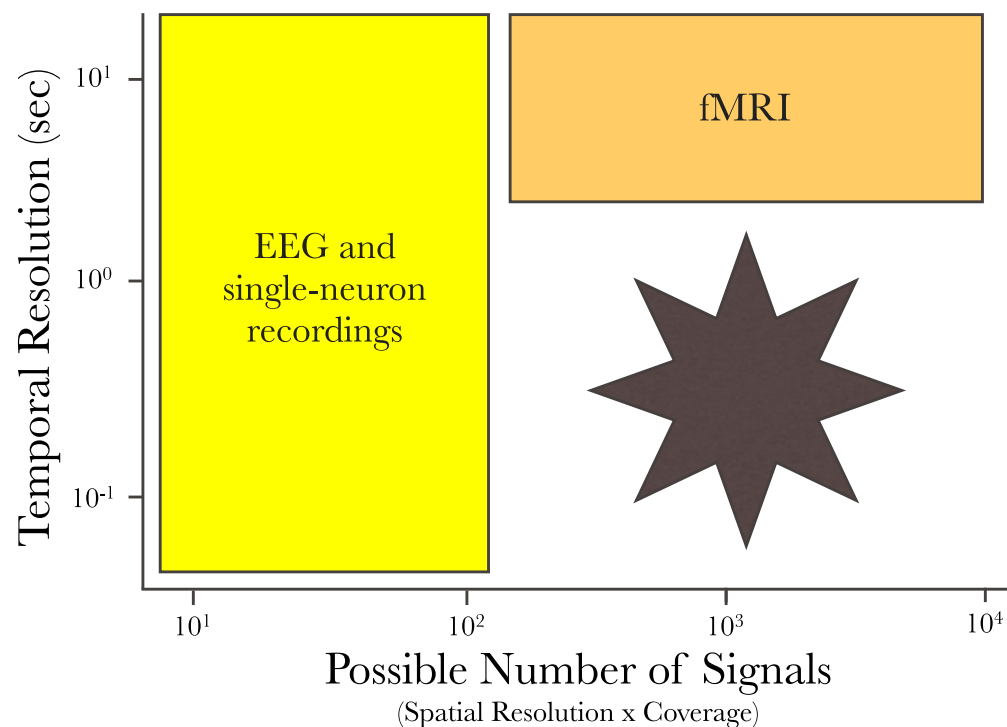


Figure 6.2: Potential role of ECoG in BCI and neuroscience research. Current non-invasive sensor modalities are constrained either by the number of possible signals that can practically be acquired, or by the temporal resolution that can be achieved. The use of ECoG (indicated by the star) might overcome this problem such that it could acquire signals from potentially thousands of sensors at a high temporal resolution.

## 6.3 Potential Impact of Brain-Computer Interface Technologies

*We can only see a short distance ahead, but we can see plenty there that's needs to be done.* Alan Turing (1912 - 1954), final sentence in "Computing Machinery and Intelligence."

*It would appear that we have reached the limits of what it is possible to achieve with computer technology, although one should be careful with such statements, as they tend to sound pretty silly in 5 years.* John von Neumann (ca. 1949).

### 6.3.1 Introduction

#### 6.3.1.1 The Communication Problem

In their seminal articles *Man-Computer Symbiosis* (Licklider [1960]) and *Augmenting Human Intellect* (Engelbart [1962]), J.C.R. Licklider and Doug Engelbart highlighted the potential of a symbiotic relationship between humans and computers. Realizing that people spend most of their time on what essentially are clerical or mechanical tasks (i.e., the fundamental information processing bottleneck at that time), they envisioned a future in which humans dynamically interact with computers such that the human devises the mechanical task to be performed; and the computer executes that task and presents the human with the results.

This vision capitalizes on the fundamental differences between the brain and the computer. The brain uses billions of cells in a massively parallel organization. Each cell represents a computing element that operates at very low speeds. In contrast, a computer is comprised of billions of transistors that are mainly organized for sequential processing. Each transistor represents a computing element that operates at speeds millions of times faster than a computing element in the brain. One could thus say that the brain has a wealth of computational breadth (i.e., using parallel processing it can convert many inputs into many outputs) but little computational depth (i.e., it cannot process a long sequence of commands of a given algorithm). In contrast, a computer typically executes only a few algorithms at a time (i.e., it has little computational breadth), but can execute any particular algorithm at extremely high speed (i.e., large computational depth). While it is not clear theoretically which

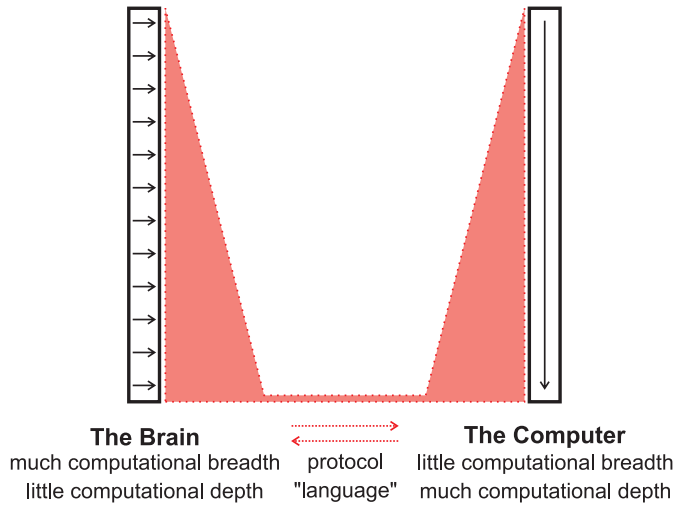


Figure 6.3: The systems problem. The brain can process information from many different sources (much computational breadth) in parallel, but is fairly slow in processing any particular algorithm (little computational depth). In contrast, the computer typically only processes information from few sources (little computational breadth), but is extremely fast executing any particular algorithm (much computational depth). In addition, the communication speed (i.e., the speed at which information that changes the behavior of humans or computers is communicated) between the brain and the external world is rather slow. There is thus a tremendous opportunity for exploiting the mutual advantages of the brain and the computer, and for increasing the communication speed between the brain and the computer.

class of problems the brain can actually attack (Bringsjord and Arkoudas [2004]), it is clear that each of the respective approaches to computation of the brain and the computer naturally lends itself to different problems. This duality, and potential trade-off, between computational breadth and computational depth constitute perhaps not the theoretical, but certainly the practical difference between the brain and the computer. This difference constitutes a mismatch between these two systems, which in the end hinders effective interactions. In absence of the ability to modify brain function to make it more similar to computers and of methods to make computers operate like human brains, this difference can still be useful.

Forty-five years after Licklider and Engelbart articulated their visions, most of the impediments to a fruitful relationship with the machine that they described (i.e., largely technical or economical hurdles) have vanished. In the age of Internet

search engines, vast digital libraries, and large-scale mathematical simulations, we routinely work with computers in a highly interactive fashion – we devise the task, and the computer executes it and presents us with the results. Donald Norman calls this *People propose ... and Technology conforms* (Norman [1993]). We have overcome this *information processing bottleneck*, that is, computers now perform many of humans' clerical tasks, revealing yet another source of inefficiency, i.e., a *communication bottleneck*: While the brain is fantastic at distilling input and concepts into plans and the computer's ability to execute these plans continues to improve, we are confronted with the increasing difficulty of communicating these plans with the low speed supported by our nervous system.<sup>13</sup>

Based mainly on classic methods developed by Shannon (Shannon [1951]) and Fitts (Fitts [1954]), numerous studies have evaluated the communication rates between humans and humans (Reed and Durlach [1998], for review) and between humans and computers (MacKenzie [1992], for review). These studies indicate that the external information transfer rates supported by the nervous system (i.e., the rates between humans and humans, or humans and computers) are very low and for communication methods (e.g., reading, speaking, Morse code, eye tracker, mouse or joystick movements) range from around 1 bit per second to not more than 50 bits per second (see Figure 6.4). In addition, many people with certain motor disabilities (such as Amyotrophic Lateral Sclerosis, Muscular Dystrophy, Cerebral Palsy, or certain types of stroke) are confined to communication rates that can be even lower. In contrast, computers can not only communicate, but also store and process information at a rate exceeding 1 terabits per second (Hewlett Packard, Inc. [2005]). In other words, even discounting the two orders of magnitude improvement in computing technology that is predicted by Moore's law for the next decade, there already is a 12 orders of magnitude difference between the external communication capacity of the nervous system and the external and internal communication and processing capacity of the computer. Moreover, while our motor system is highly adept at controlling movement of our limbs, those limbs have been optimized to

---

<sup>13</sup>This idea is similar to the *Theory of Constraints* (e.g., Goldratt and Cox [2004]) that postulates that, for example in a manufacturing plant, total system output is limited by the slowest operation in the process.

address the challenges experienced by our ancestors, but not necessarily to address the complex challenges of today.

When interacting with computers, the context-independent nature of this communication further impedes communication. Our brain has at its disposal highly complex semantic relationships that put the input to the brain into context. When we communicate a plan to a computer, we need to use syntactic commands void of any semantics, even though the more semantic contexts have been agreed upon by a particular sender and a particular receiver, the more economical the act of communication can become (Sapir [1931]).

The low communication rate between the brain and the computer, the constraints of our motor system, and the communication's highly syntactic and thus context-independent nature, constitute the most fundamental inefficiency as well as the biggest potential for dramatic improvements in human efficiency on tasks that are constrained by this low speed and the physical limits of our bodily movements. For example, a jet pilot might have to execute a number of syntactic commands in sequence (e.g., turn left and then accelerate), when it would be more efficient to communicate a semantic command that combines these sequential commands in one rich parallel instruction. Human-Computer Interaction, an area within Computer Science, has been aware of these issues and has engaged in many efforts (such as context-aware software or the Semantic Web) that attempt to address them. Because the capacity to represent and relate information constitutes the primary advantage of the brain over the computer (and we thus cannot easily reproduce these capacities in a computer), and because these efforts cannot address the low communication rate of our sensory and motor system, all current corresponding efforts are thus restricted to alleviate merely the symptoms of this fundamental communication problem.

This chapter lays out a proposed solution to this problem that I expect to be realized in the coming decades. It describes how direct communication between the brain and the computer can overcome the low rate, context independence, and physical constraints imposed to communication using our regular motor and sensory communication channels. While this possibility has been contemplated in science fiction for some time (e.g., Thomas [1977], Gibson [1995], Anno [1995], Clarke [1997],

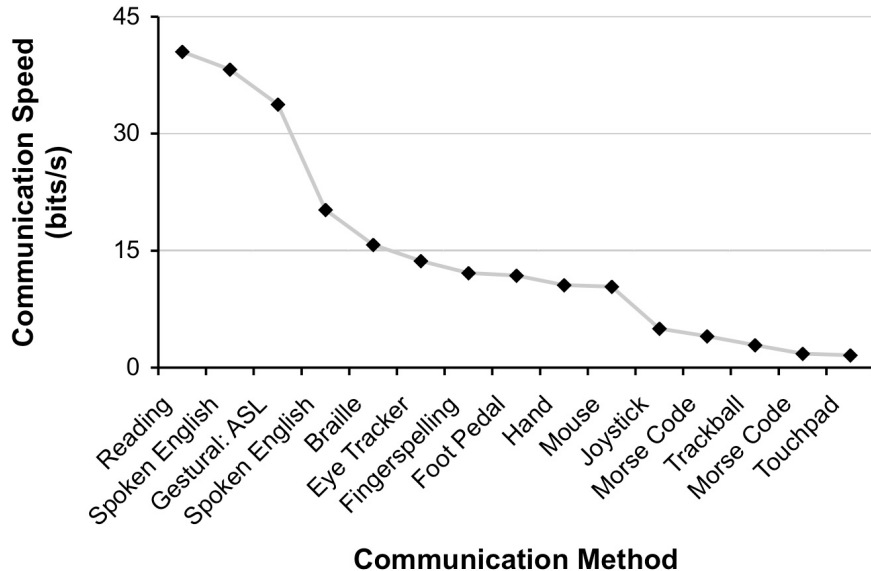


Figure 6.4: Comparison of communication rates between humans and the external world (sources: Reed and Durlach [1998], MacKenzie [1992]).

Kurzweil [2000], Morgan [2003], Asher [2003], David [2004]), many studies over the past two decades have already demonstrated that non-muscular communication is possible and can, despite its early stage of development, already serve useful functions (Wolpaw et al. [2002]). This chapter is thus *not* science fiction. It is about improvements to existing technology that will lead to a close and highly interactive relationship between the brain and the computer. It is also about the major implications that these developments will have on rehabilitation and human productivity.

### 6.3.1.2 Feasibility

As bold as the assertion of direct brain-computer communication may sound, its implementation, and all the powerful implications derived from it, merely rests on two assumptions. First, direct interaction with the brain requires understanding of the *language* of the communication. Second, it also requires a physical interface that can communicate the symbols of this language with the requisite clarity to and from the brain so that they can be understood the same way as if those symbols originated from within the brain.

**Assumption 1: Understanding the Language** Many studies over the past decades have demonstrated that it is feasible to understand the language of the

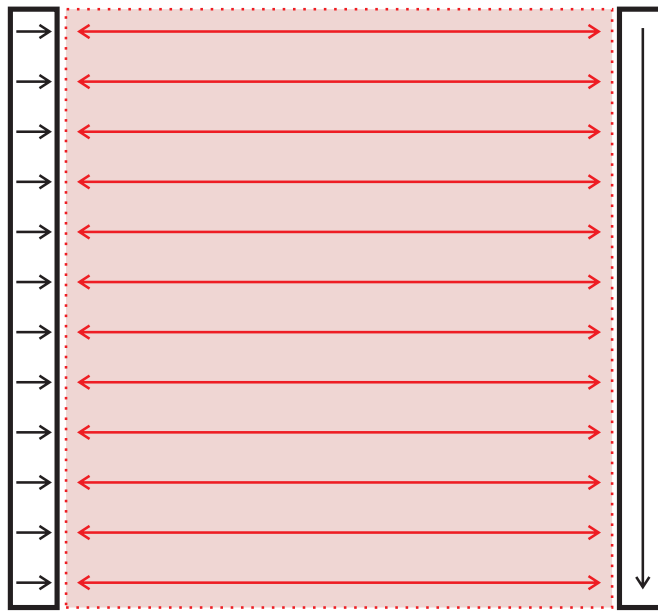
brain, i.e., the symbols that the brain uses to encode particular pieces of information. With these studies, it has become increasingly clear that mental faculties can be decomposed into a multitude of information-processing systems (which Minsky called *agencies* (Minsky [1988, 2006])) and that brain activity in these systems can be analyzed or modified to detect and change function in the associated mental faculties. For example, studies have shown that it is possible to stimulate motor or sensory areas to induce particular motor function or sensory perception (i.e., to communicate from the computer to the brain), and that it is also possible to analyze brain signals to decode motor function and sensory perception (i.e., to communicate from the brain to the computer). These studies have encompassed essentially all primary motor and sensory areas and have even extended into highly personal feelings such as sympathy and empathy (e.g., Decety and Chaminade [2003] and Jackson et al. [2005], respectively). Furthermore, it is becoming increasingly evident that the brain signals that accompany *imagined* movements, sensations, and feelings are, while smaller, similar in characteristics to signals that accompany *actual* movements, sensations, and feelings (Kosslyn [1988]). This opens the possibility that one could not only decipher and produce brain images corresponding to actual, but also imagined, experiences.

Based solely on the language of the brain and its individual symbols, it thus clearly appears feasible to interact with the brain on the basis of the mental faculties realized by these areas, even with the sensing and decoding technologies in use today. In other words, this suggests that it should be possible to decode, or produce, a clear and complete image of the actually experienced or imagined visual, auditory, movement, language, olfactory, tactile, or taste sensations encoded by the symbols communicated within the brain. Because our plans can also be described in terms of such features (Bracewell et al. [1996], Mazzoni et al. [1996], Snyder et al. [1997], Cohen and Andersen [2002], Shenoy et al. [2003]), it should be possible to replace or augment the inadequate communication of an intent from the brain to the computer by an interpretation of these images, and to replace or augment the communication of these results back to the brain. (For the purpose of this section, *intent* corresponds to the state of the brain areas that activate brain areas actually

producing a particular behavior.) One should not be distracted by the dramatic problems that we face understanding how brain functions encode semantic relationships and use them to produce the intent that is represented by these images. For the purpose of removing the current communication bottleneck in many tasks, it is sufficient to understand the brain's intent and not necessary to understand the ways in which the brain produces this intent. In fact, it is this very capacity of the brain that constitutes the basis for the tremendous gains derived from closer and more efficient relationship between the brain and the computer.

Direct communication with the brain will eventually be limited by the difficulty of establishing the language of communication. If the communication was to use the language that the brain uses for its internal communication, the symbols of this language could be determined using what may be called a calibration procedure. This procedure would utilize an understanding of the mental faculties to be decoded (i.e., a reference such as motor movements such as those discussed in **THEME III** in Section 4). This calibration procedure can thus only be performed if there is a reference (which is regarded in philosophy as the *reference problem* (Quine [1964])) and thus will be impossible for mental faculties whose function is not understood. If the communication were to use a new mutual language, this would by definition require mutual adaptation of the brain and the computer. The more complex the syntax and taxonomy of the new language, the longer this training process will become. Consequently, practical considerations will eventually limit this time and thus the complexity of the language.

**Assumption 2: An Adequate Interface** An efficient physical interface between the brain and the computer can be realized by measuring and influencing the electrical or chemical properties of the brain cells in contact with the interface. Studies indicate that these properties have different functions in the nervous system. Electrical activity in the brain (i.e., action potentials that are produced by the cell body and communicated from the cell's axon to other adjacent neurons) is mainly responsible for communication and information processing. Chemical properties typically communicate the results of past information processing so as to produce changes in



**The Brain and The Computer**  
 much computational breadth  
 much computational depth

Figure 6.5: The communication problem solved. Close interaction between the brain and the computer through direct communication can break the fundamental communication bottleneck.

the brain that optimize future processing. For example, increased neurotransmitter production triggered by increased electrical activity may start chemical signal cascades that eventually modify gene function that modify future cell behavior. These two communication methods have been studied in detail and – in some areas – are well understood. Decoupling the language problem from the interface problem reduces the latter to the task of designing a physical structure with well-defined physical and chemical properties. In consequence, the construction of a physical interface that can interact with requisite speed, safety, and sensitivity with the brain using electrical as well as chemical means is, while a complex issue that will require considerable attention, ultimately an engineering problem with clearly defined mechanical, electrical, and chemical specifications that can be expected to be solved.

### 6.3.2 Expected Development

The previous sections described the *communication bottleneck* as the fundamental impediment to exploiting the mutual advantages of the brain and the computer, and illustrated the two requirements that have to be met in order to break this bottleneck (see Figure 6.5), an adequate language and interface. Subsequent sections will discuss the expected development and the profound implications of the expected possibilities of this brain-computer interfacing technology that will allow humans to communicate, work, and think, radically different from how we do now.

#### 6.3.2.1 Towards the Limit

To further elucidate the limits and the further development of this novel way to communicate, we may first review what is possible today and then ask how we might increase the modest capacities of current brain-computer interfacing technologies. Current devices have been demonstrated in many studies to support simple non-muscular communication. These capacities can be used by people with or without disabilities to communicate their wishes to their environment. At the same time, the rate of this communication is rather low, i.e., typically not more than 25 bits/min.

To examine how this current modest performance could be improved, is illustrative to consult some mathematics: In *Mathematical Theory of Communication* (Shannon and Weaver [1964]), Claude Shannon showed that any noisy communication channel has a channel capacity measured in bits per second. Consider a communication channel of bandwidth  $B$  Hz and a signal-to-noise ratio  $\frac{S}{N}$ . The channel capacity  $C$  in bits per second is then defined as  $C = B \log_2(1 + \frac{S}{N})$ . Because the properties of any communication channel, including the electrical, chemical, or metabolic ones that are relevant to brain-computer communication, can be expressed in this form, this formula can be used to calculate the capacity of any communication channel between the brain and the computer. In lay terms, the total information rate thus depends on the clarity of the transmitted information (i.e., the sensing/stimulation resolution in a particular domain (e.g., spatial, temporal, frequency, chemical, etc.) and on the amount of noise incurred at the sensor/stimulator or during transmission) and on the number of such communication channels.

Hence, I postulate that the communication rate between the brain and the

computer will increase with the number of mental faculties that can be interacted with and with the clarity of that interaction. This concept strongly suggests that, as technologies improve to interact with more areas of the brain with higher fidelity, the communication rate between the brain and the computer will also increase. At the same time, it is not clear which factors will eventually limit this rate improvement. The brain contains about 100 billion neurons (e.g., of Scientific American [1999], Wade [1998], Katz and Chang [2005]) and the theoretical upper bound for the information rate was estimated at 300 bits per second per neuron (Eliasmith [2000] and originally in Rieke et al. [1999]). It was actually measured, in a number of different brain systems, at about 80 bits per second per neuron (Borst and Theunissen [1999]). The measurements suggest a high upper bound for the information rate for interaction with the whole brain. Whatever the true limit, there is no reason to believe that using direct communication with the brain, we should not be able to achieve the 50 bits per second that humans can currently achieve using conventional methods.<sup>14</sup>

### 6.3.2.2 Expected Performance and Price Development

The radical promise of these novel communication capacities will remain elusive if they remain a theoretical possibility rather than a practical reality, and practical reality is determined by at least two important factors: performance and price.

Many historic examples in technical history, including ones in sensor and communication technologies, have exhibited radical and sustained improvements (i.e., 40-60% performance increase per year, which is often called *Moore's Law*) resulting from adequate research activities (Gray and Szalay [2005], Kurzweil [2005]). In addition, many examples show that typically, the unit cost of a product declines by typically 20-30% each time the cumulative output of that product doubles (this is often called the *Law of Experience*).

These observations strongly indicate that the performance (i.e., number and sensitivity) and price of sensors/stimulators should increase and decrease, respec-

---

<sup>14</sup>As a simple example, even if we can communicate only 2 bits per second per any one mental faculty (e.g., actual or imagined touch, smell, speech, motor movements, etc.), we can achieve 50 bits per second by interacting with only 25 such mental faculties.

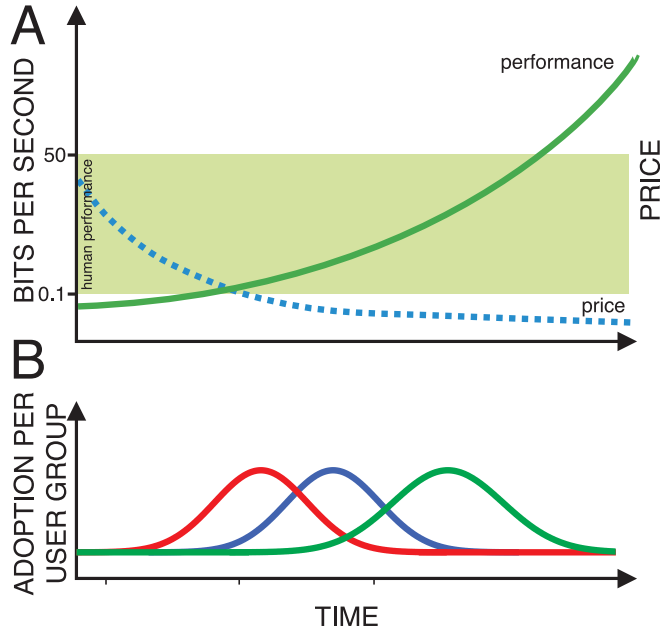


Figure 6.6: Expected performance/price development and associated technology diffusion. Based on historical examples, performance and price of brain-computer interfacing technologies can be expected to improve (A). These devices will begin to be adopted by different user groups as their price and performance makes them attractive to each group (B).

tively (Figure 6.6), assuming that research activities in this area will continue; fortunately, Brain-Computer Interface research has recently experienced large and accelerating research activities (see Figure 6.7).<sup>15</sup>

To further examine the possibilities of even today's technologies, we may visit an example of a hypothetical device that can detect one thousand signals with high fidelity. Such a device could use sensors and electronics patterned on thin films (which allows economical high channel counts) and could be placed on the surface of the brain (where they can detect high-fidelity signals at modest clinical risks (Leuthardt et al. [2004])). Such patterned CMOS electronics have recently been described and used in a number of studies (e.g., Gleskova and Wagner [2003], Lacour et al. [2003], Wagner and Gleskova [2002], Sturm et al. [2001], Wagner et al. [2002]). A small thin film could contain electronics to realize amplification, analog-to-digital

<sup>15</sup>One practical caveat is that the developments in these other areas were accompanied by or even required large up-front investments that drove the price per item (e.g., per transistor, copy of a software program, etc.) down to almost zero, and these large investments are typically only made if the primary target market is large and accessible within a few years.

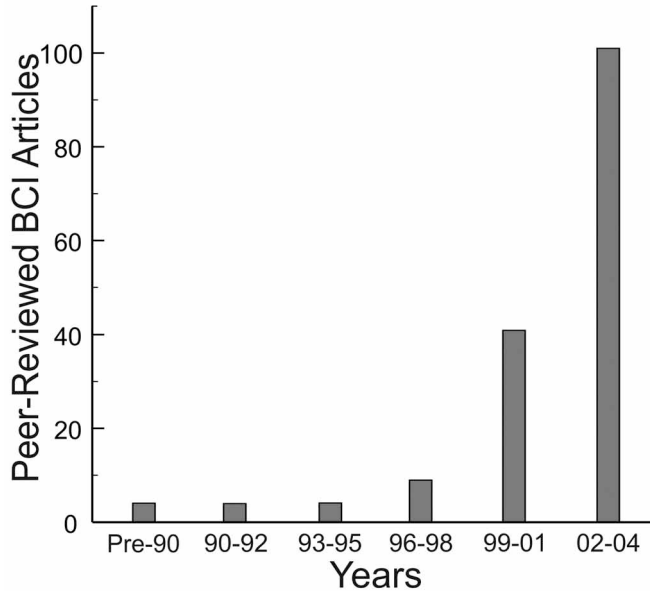


Figure 6.7: Increasing research activity in Brain-Computer Interface (BCI) research. This figure illustrates the exploding increase in research activity over the past 15 years. Results are collected from relevant databases.

conversion, and extraction and wireless transmission of signal features. These signal features could be received by an external computer and converted into device commands (such as the many examples of current brain-computer interfacing technology illustrates). Because even a full-fledged microprocessor with dramatically more transistors can be designed to use only about 1 Watt of power (e.g., Transmeta [2005]), we may use this figure as an upper bound for the necessary power consumption. Rechargeable and implantable Lithium-Ion batteries already exist that could support almost one full day of operation for such a device away from a charging station (e.g., Honda et al. [1997]). The features that are extracted by the electronics may be transmitted to an external computer over a Bluetooth-based wireless link. Class 2 Bluetooth devices consume about 2.5 mW, have a range of about 10 meters, and can transmit up to 125 KBytes per second (see Forret [2005], Wikipedia [2005]). (The recently announced Bluetooth 2.0 standard already provides 3-10 times that bandwidth.) At 1000 channels and 2 bytes per sample, this device could transmit 60 signal samples or signal features per channel per second (without any data compression), which is sufficient to support rapid communication.

In summary, a device that can detect large numbers of brain signals with

high fidelity could be created using current technology given adequate funds; and clearly, the performance and price of this hypothetical device can be expected to dramatically improve over time. In consequence, we have every reason to believe that rapid communication between the brain and the computer is not only a theoretical possibility, but will also become technically possible and practical. Given this expectation, we may begin to elucidate the expected impact of this new technology.

### 6.3.2.3 Expected Adoption and Impact

As any other innovation, brain-computer interfacing technology will begin to be adopted once its value to an individual exceeds the cost to that individual. As the improvements in performance and price described above, this adoption or *technology diffusion* process has been observed and described for many different innovations (Rogers [2003]). Typically, it only takes a modest amount of time until 50% of the market has adopted the new technology, and complete market penetration is achieved after twice that time (Rogers [2003]). For example, using data from radio, television, VHS recorders, cable and satellite TV, DVD players, the Internet, and wireless phones, a recent article (Lawrence [2005]) calculated that it only took an average of 13 years to achieve 50% market penetration. These examples suggest that Brain-Computer Interfacing technology might also be adopted, at least by particular user groups, over a relatively short period of time. I anticipate that this process will eventually proceed in mainly three groups of users (Figure 6.6). Each of these three different user groups will begin to benefit from this new communication capacity as its price and performance improve to a certain point.

With relatively modest improvements, brain-computer interfacing technology will become a practical and safe, albeit simple and slow, communication aid. It will thus soon become of interest to the first group of adopters: handicapped individuals who are currently limited for essentially all tasks by their limited communication capacity. For these people, even the modest rates of communication that will initially be achieved can dramatically improve quality of life.

With further improvements, technology will improve such that it rivals or exceeds some of the conventional human capacities. The second group that I expect to benefit from improved communication abilities are thus healthy individuals for

whom communication is currently a pressing and limiting issue in many of their tasks. For example, limited communication input and output capacity is a serious issue for soldiers in combat. (In absence of the ability to increase these capacities of the brain, the military is currently trying to optimize this communication given our body's constraints.) In consequence, as soon as communication rates between the brain and the computer start to rival those that can currently be achieved with our sensory and motor systems, I expect that this group of users will begin to adopt this new technology.

In the end, brain-computer interfacing technology will become not only safe and affordable, but also will provide capacities that can augment human performance in many ways. It will thus become of interest to many user groups that will use these technologies for a wide variety of purposes. At the same time, this new communication capacity will constitute a radical and disruptive innovation that will not be immediately compatible with existing practice and that will evoke change in many complementary processes. It will thus take some time, perhaps a few decades, until this technology has been fully integrated in human societies (Griliches [1957], Mansfield [1968], Rogers [2003]).

In summary, I expect that, as performance increases and price decreases, Brain-Computer Interfacing technology will become beneficial to an increasing number of individuals, that the direct and indirect effects of its use will become increasingly pervasive, and that the implications on individuals and society will grow in parallel. I thus anticipate that this development of brain-computer interfacing technology will in many ways mirror the development of computers (that addressed the previous bottleneck in human productivity) and of other General-Purpose Technologies (GPTs) (Helpman [1998]). GPTs have been found to have a wide variety of major effects on private and social performance (Indjikian and Siegel [2005]). For example, Information Technology and the Internet have wide applications and productivity-enhancing effects in numerous downstream sectors with high social rates of return that often exceed private rates of return (Mansfield et al. [1977], Tewksbury et al. [1980]), and their dissemination is having a sustained, long-lasting impact on productivity and economic growth. Brain-computer interfacing technology can thus

be expected to have a similar profound impact not only on individual, but also on societal performance.

### 6.3.3 Brain-Computer Symbiosis

To illustrate the anticipated impact of Brain-Computer Interfacing technology, let us visit examples of their applications to the three user groups listed above.

The physically handicapped will primarily benefit from restoration of function. I anticipate that this restoration will initially mainly concern simple communication and control functions and eventually extend into full restoration of movement capacities using existing or artificial limbs. Because there are about 300,000-500,000 individuals with spinal cord injury in the US alone who would benefit tremendously from restored capacities, I anticipate that the commercial application of Brain-Computer Interfacing technology will become a significant driver of progress once system performance improves to the point at which it becomes interesting to this large group of individuals.

As system performance increases, individuals who are often limited by their communication capacity could benefit from this technology in a number of ways. First, direct communication from the brain could entirely eliminate the roughly 150 ms delay that is currently introduced by our nerves and muscles. Second, direct communication from the brain could practically eliminate the constraints imposed by the movement capacities supported by our limbs. Specifically, rather than optimizing interfaces to the static capacities of our body, we could optimize the whole system, human and computer. For example, imagine a jet pilot who currently has to deal with many controls for the many degrees of freedom the airplane supports. Because the number of degrees of freedom of the airplane exceeds the degrees of freedom of our motor system (or at least is very inadequately matched to it), the jet pilot might have to operate specific functions in sequence rather than in parallel. Using direct communication from the brain, the degrees of freedom that the pilot can support could be matched to the degrees of freedom of the airplane, which would transform the airplane from an external tool to a direct extension of the pilot's nervous system, in which different areas of the pilot's motor system would be responsible for controlling movements of the airplane rather than movements of the

pilot's limbs. In addition, sensors in the plane could be connected to the brain's sensory areas such that these measurements can provide the pilot with a picture of the current state of the plane, much in the same way that our bodily sensors give us a picture of the state of our body.

In summary, I anticipate that for these first two groups of users there will be many applications that will prove beneficial and thus will be commercially attractive. At the same time, the full potential of direct brain-to-computer communication will only be realized when this technology can benefit most members of society. As soon as interfaces can be built that can interface safely, economically, and concurrently with most of the major systems in the brain, many applications will emerge that will augment our senses and our communication capacities with others and with computers. It will be then that enhanced communication capacities will pervade the fabric of society with a multitude of side effects on many other technologies and processes.

To many, this vision will be as utopian as J.C.R. Licklider's and Doug Engelbart's outlook on the significant utility of computers almost 50 years ago. However, the foundations of technical innovation and economics have not changed since. Because the present vision depends merely on technological improvements rather than hopeful speculation and because its realization is subject to the same forces that have governed the course of many previous technical developments, it is, in the end, an inevitable next step in our own evolution.

## BIBLIOGRAPHY

- H. Akaike. Information theory and an extension of the maximum likelihood principle. In B. N. Petrov and F. Csaki, editors, *2nd International Symposium on Information Theory, Budapest*, pages 267–281, 1973.
- B. Z. Allison. *P3 or Not P3: Toward a Better P300 BCI*. PhD thesis, University of California, San Diego, April 2003.
- E. O. Altenmueller and C. Gerloff. Psychophysiology and the EEG. In E. Niedermeyer and F.H. Lopes da Silva, editors, *Electroencephalography: Basic Principles, Clinical Applications and Related Fields*, pages 637–655. Williams and Wilkins, Baltimore, 4 edition, 1999.
- B Amirikian and AP Georgopoulos. Directional tuning profiles of motor cortical cells. *Neurosci Res*, 36(1):73–79, 2000.
- P. Anderer, S. Roberts, A. Schloegl, G. Gruber, G. Kloesch, W. Herrmann, R. Rappelesberger, O. Filz, MJ. Barbanoj, G. Dorffner, and Saletu. Artifact processing in computerized analysis of sleep EEG - a review. *Neuropsychobiology*, 1999(40): 150–157, 1999.
- R A Andersen, S Musallam, and B Pesaran. Selecting the signals for a brain-machine interface. *Curr Opin Neurobiol*, 14(6):720–726, Dec 2004. doi: 10.1016/j.conb.2004.10.005.
- C. W. Anderson, E. A. Stoltz, and S. Shamsunder. Multivariate autoregressive models for classification of spontaneous electroencephalographic signals during mental tasks. *IEEE Trans Biomed Eng*, 45:277–286, 1998.
- Hideaki Anno. *Neon Genesis Evangelion (Japanese: Shin Seiki Evangelion) Anime Television Series*. Gainax, 1995.
- F Aoki, E E Fetz, L Shupe, E Lettich, and G A Ojemann. Increased gamma-range

- activity in human sensorimotor cortex during performance of visuomotor tasks. *Clin Neurophysiol*, 110(3):524–537, Mar 1999.
- Neal Asher. *Gridlinked*. Tor Books, 2003.
- B B Averbeck, M V Chafee, D A Crowe, and A P Georgopoulos. Parietal representation of hand velocity in a copy task. *J Neurophysiol*, 93(1):508–518, Jan 2005. doi: 10.1152/jn.00357.2004.
- F. Babiloni, F. Cincotti, L. Lazzarini, J. Millan, J. Mourino, M. Varsta, J Heikkonen, L Bianchi, and M. G. Marciani. Linear classification of low-resolution EEG patterns produced by imagined hand movements. *IEEE Trans Rehabil Eng*, 8(2):186–8, 2000.
- P Baraduc and E Guigon. Population computation of vectorial transformations. *Neural Comput*, 14(4):845–871, 2002.
- J. D. Bayliss. *A Flexible Brain-Computer Interface*. PhD thesis, University of Rochester, Rochester, August 2001. URL <http://www.cs.rochester.edu/trs/robotics-trs.html>.
- H. Berger. Ueber das Electroenkephalogramm des Menschen. *Arch Psychiat Nervenkr*, 87:527–570, 1929.
- C. Biernacki, G. Celeux, and G. Govaert. Choosing starting values for the EM algorithm for getting the highest likelihood in multivariate gaussian mixture models. *Computational Statistics and Data Analysis*, 41:561–575, 2003.
- N. Birbaumer, N. Ghanayim, T. Hinterberger, I. Iversen, B. Kotchoubey, A. Kübler, J. Perelmouter, E. Taub, and H. Flor. A spelling device for the paralysed. *Nature*, 398(6725):297–298, March 1999.
- N. Birbaumer, A. Kübler, N. Ghanayim, T. Hinterberger, J. Perelmouter, J. Kaiser, I. Iversen, B. Kotchoubey, N. Neumann, and H. Flor. The thought translation device (TTD) for completely paralyzed patients. *IEEE Trans Rehabil Eng*, 8(2):190–193, June 2000.

- G. E. Birch and S. G. Mason. Brain-computer interface research at the Neil Squire Foundation. *IEEE Trans Rehabil Eng*, 8(2):193–195, June 2000.
- A. H. Black, G. A. Young, and C. Batenchuk. Avoidance training of hippocampal theta waves in flaxedilized dogs and its relation to skeletal movement. *J Comp Physiol Psychol*, 70:15–24, 1970.
- A.H. Black. The direct control of neural processes by reward and punishment. *Am. Sci.*, 59:236–245, 1971.
- A.H. Black. The operant conditioning of the electrical activity in the brain as a method for controlling neural and mental processes. In *The Psychophysiology of Thinking*, pages 35–68. Academic Press, New York, 1973.
- G. Blanchard and B. Blankertz. BCI competition 2003; data set iia: spatial patterns of self-controlled brain rhythm modulations. *IEEE Trans Biomed Eng*, 51(6):1062–6, 2004.
- B. Blankertz. BCI competition 2003 (web page).  
<http://ida.first.fhg.de/projects/bci/competition>, 2003.
- B. Blankertz, K. R. Müller, G. Curio, T. M. Vaughan, G. Schalk, J. R. Wolpaw, A. Schloegl, C. Neuper, G. Pfurtscheller, T. Hinterberger, M. Schroeder, and N. Birbaumer. The BCI competition 2003: progress and perspectives in detection and discrimination of EEG single trials. *IEEE Trans Biomed Eng*, 51(6):1044–51, 2004.
- Alexander Borst and Frederic E. Theunissen. Information theory and neural coding. *Nat Neurosci*, 2(11):947–957, 1999.
- H. Bozdogan. Model selection and Akaike’s information criterion. *Psychometrika*, 52:345–370, 1974.
- RM Bracewell, P Mazzoni, S Barash, and RA Andersen. Motor intention activity in the macaque’s lateral intraparietal area. ii. changes of motor plan. *J Neurophysiol*, 76(3):1457–1464, 1996.

- E. Oran Brigham. *The Fast Fourier Transform: An Introduction to Its Theory and Application*. Prentice Hall, 1973.
- Selmer Bringsjord and Konstantine Arkoudas. The modal argument for hypercomputing minds. *Theoretical Computer Science*, 317:167–190, 2004.
- L A Bullara, W F Agnew, T G Yuen, S Jacques, and R H Pudenz. Evaluation of electrode array material for neural prostheses. *Neurosurgery*, 5(6):681–686, Dec 1979.
- John Burkardt. GEOMETRY Matlab routines, 2005.
- T. Cacoullos. Estimation of a multi-variate density. *Annals of the Institute of Mathematical Statistics (Tokyo)*, 18(2):179–189, 1966.
- G.T. Carter. Rehabilitation management in neuromuscular disease. *J Neurol Rehabil*, 11:69–80, 1997.
- G. Celeux and G. Govaert. A classification EM algorithm for clustering and two stochastic versions. *Computational Statistics and Data Analysis*, 14:279–416, 1992.
- J. K. Chapin and M. A. Nicolelis. Neural network mechanisms of oscillatory brain states: Characterization using simultaneous multi-single neuron recordings. *Electroenceph Clin Neurophysiol*, 45:113–122, 1996.
- J. K. Chapin and M. A. Nicolelis. Principal component analysis of neuronal ensemble activity reveals multidimensional somatosensory representations. *J Neurosci Meth*, 94:121–140, 1999.
- G. E. Chatrian. The mu rhythm. In *Handbook of Electroencephalography and Clinical Neurophysiology. The EEG of the Waking Adult*, pages 46–69. Elsevier, Amsterdam, 1976.
- Y. L. Chen, F. T. Tang, W. H. Chang, M. K. Wong, Y. Y. Shih, and T. S. Kuo. The new design of an infrared-controlled human-computer interface for the disabled. *IEEE Trans. Rehabil. Eng*, 7:474–481, 1999.

- Arthur C Clarke. *3001 - The Final Odyssey*. Del Rey, 1997.
- Y. E. Cohen and R. A. Andersen. A common reference frame for movement plans in the posterior parietal cortex. *Nature Reviews Neuroscience*, 3:553–562, 2002.
- E. J. Costa and E. F. Cabral. EEG-based discrimination between imagination of left and right hand movements using adaptive gaussian representation. *Med Eng Phys*, 22(5):345–8, 2000.
- RW Cox and JS Hyde. Software for analysis and visualization of functional magnetic resonance neuroimages. *Computers and Biomedical Research*, 10:171–178, 1997.
- S Coyle, T Ward, C Markham, and G McDarby. On the suitability of near-infrared (nir) systems for next-generation brain-computer interfaces. *Physiol Meas*, 25(4):815–822, Aug 2004.
- N E Crone, D L Miglioretti, B Gordon, and R P Lesser. Functional mapping of human sensorimotor cortex with electrocorticographic spectral analysis. ii. event-related synchronization in the gamma band. *Brain*, 121 ( Pt 12):2301–2315, Dec 1998a.
- N E Crone, D L Miglioretti, B Gordon, J M Sieracki, M T Wilson, S Uematsu, and R P Lesser. Functional mapping of human sensorimotor cortex with electrocorticographic spectral analysis. i. alpha and beta event-related desynchronization. *Brain*, 121 ( Pt 12):2271–2299, Dec 1998b.
- N E Crone, L Hao, J Hart, D Boatman, R P Lesser, R Irizarry, and B Gordon. Electrocorticographic gamma activity during word production in spoken and sign language. *Neurology*, 57(11):2045–2053, Dec 2001.
- F. H. Lopes da Silva. Neural mechanisms underlying brain waves: from neural membranes to networks. *Electroenceph Clin Neurophysiol*, 79:81–93, 1991.
- A.M. Dale, Bruce Fischl, and M.I. Sereno. Cortical Surface-Based Analysis I: Segmentation and Surface Reconstruction. *NeuroImage*, 9(2):179–194, 1999.

- A.J. Dalton. Discriminative conditioning of hippocampal electrical activity in curarized dogs. *Comm. Behav. Biol.*, 3:283–287, 1969.
- R. I. Damper, J. W. Burnett, P. W. Gray, L. P. Straus, and R. A. Symes. Handheld text-to-speech device for the non-vocal disabled. *J. Biomed. Eng.*, 9:332–340, 1987.
- F. Darvas and D. Pantazis. Mapping human brain function with MEG and EEG: methods and validation. *NeuroImage*, 23(supplement 1):S289–S299, 2004.
- Peter David. *Spider-Man 2*. Del Rey, 2004.
- P.R. Davidson and D.M. Wolpert. Widespread access to predictive models in the motor system: a short review. *J Neural Eng.*, 2(3):S313–9, 2005.
- Jean Decety and Thierry Chaminade. Neural correlates of feeling sympathy. *Neuropsychologia*, 41:127–138, 2003.
- A. Delorme and S. Makeig. EEGLAB: an open source toolbox for analysis of single-trial EEG dynamics including independent component analysis. *J Neurosci Methods*, 134(1):9–21, Mar 2004. doi: 10.1016/j.jneumeth.2003.10.009.
- A.P. Dempster, N.M. Laird, and D.B. Rubin. Maximum likelihood from incomplete data via the em algorithm. *Journal of Royal Statistical Society B*, 39:1–38, 1977.
- E. Donchin and D. B. Smith. The contingent negative variation and the late positive wave of the average evoked potential. *Electroenceph Clin Neurophysiol*, 29(2):201–203, August 1970.
- E. Donchin, K. M. Spencer, and R. Wijesinghe. The mental prosthesis: assessing the speed of a P300-based brain-computer interface. *IEEE Trans Rehabil Eng*, 8(2):174–179, June 2000.
- JP Donoghue, A Nurmikko, G Fries, and M Black. Development of neuromotor prostheses for humans. *Suppl Clin Neurophysiol*, 57:592–606, 2004.
- R. Duda, P. Hart, and D. Stork. *Pattern Classification*. John Wiley, 2001. 2nd edition, Chapter 2, ISBN: 0-471-05669-3.

- T. Elbert, B. Rockstroh, W. Lutzenberger, and N. Birbaumer. Biofeedback of slow cortical potentials. *Electroenceph Clin Neurophysiol*, 48(3):293–301, March 1980.
- C. Eliasmith. Is the brain analog or digital? *Cognitive Science Quarterly*, 1(2), 2000.
- Douglas C. Engelbart. Augmenting human intellect: A conceptual framework. *AFOSR-3233*, 1962.
- L. A. Farwell and E. Donchin. Talking off the top of your head: toward a mental prosthesis utilizing event-related brain potentials. *Electroenceph Clin Neurophysiol*, 70(6):510–523, December 1988.
- K. A. Ferguson, G. Polando, R. Kobetic, R. J. Triolo, and E. B. Marsolais. Walking with a hybrid orthosis system. *Spinal Cord.*, 37:800–804, 1999.
- E. E. Fetz and D. V. Finocchio. Correlations between activity of motor cortex cells and arm muscles during operantly conditioned response patterns. *Exp Brain Res*, 23:217–240, 1975.
- E. E. Fetz, D. V. Finoccio, M. A. Baker, and M. J. Soso. Sensory and motor responses of precentral cortex cells during compatible passive and active joint movements. *J Neurophysiol*, 43:1070–1089, 1971.
- R.C. Ficke. *Digest of data on persons with disabilities*. U.S. Department of Education, National Institute on Disability and Rehabilitation Research, Washington, DC, 1991.
- B. J. Fisch. *Spehlmann's EEG Primer*. Elsevier, Amsterdam, 2 edition, 1991.
- RA Fisher. The use of multiple measures in taxonomic problems. *Ann. Eugenics*, 1936.
- Paul M. Fitts. The information capacity of the human motor system in controlling the amplitude of movement. *Journal of Experimental Psychology*, 47(6):381–391, 1954.

Peter Forret. Bandwidth chart, 2005. URL [http://www.forret.com/tools/bandwidth\\_chart.asp](http://www.forret.com/tools/bandwidth_chart.asp).

P T Fox, J S Perlmutter, and M E Raichle. A stereotactic method of anatomical localization for positron emission tomography. *J Comput Assist Tomogr*, 9(1):141–153, Jan-Feb 1985.

W. J. Freeman, M. D. Holmes, B. C. Burke, and S. Vanhatalo. Spatial spectra of scalp EEG and EMG from awake humans. *Clin Neurophysiol*, 114:1053–1068, 2003.

N. Friedman and S. Russell. Image segmentation in video sequences: A probabilistic approach. In *IEEE Proceedings, of the Thirteenth Conference on Uncertainty in Artificial Intelligence(UAI), Aug. 1-3*, 1997.

D. Garrett, D. A. Peterson, C. W. Anderson, and M. H. Thaut. Comparison of linear, nonlinear, and feature selection methods for EEG signal classification. *IEEE Trans Rehabil Eng*, 11(2):141–4, 2003.

H. Gastault. Etude electrocorticographique de la reactivite du rythme rolandiques. *Rev Neurol*, 87:176–182, 1952.

A P Georgopoulos and J T Massey. Cognitive spatial-motor processes. 2. information transmitted by the direction of two-dimensional arm movements and by neuronal populations in primate motor cortex and area 5. *Exp Brain Res*, 69(2):315–326, 1988.

A P Georgopoulos, F J Langheim, A C Leuthold, and A N Merkle. Magnetoencephalographic signals predict movement trajectory in space. *Exp Brain Res*, 167(1):132–135, Nov 2005. doi: 10.1007/s00221-005-0028-8.

A.P. Georgopoulos, A.B. Schwartz, and R.E. Kettner. Neuronal population coding of movement direction. *Science*, 233:1416–1419, 1986.

L.A. Gerhardt and R.M. Sabolcik. Eye tracking apparatus and method employing grayscale threshold values. *US patent 5,481,622*, January 1996.

- William Gibson. *Neuromancer (Remembering Tomorrow)*. Ace Books, 1995.
- H. Gleskova and S. Wagner. Fabrication of thin-film transistors on polyimide foils. In K.L. Mittal, editor, *Polymides and Other High Temperature Polymers: Synthesis, Characterization and Applications. Proceedings of the Third International Symposium on Polyimides and Other High Temperature Polymers*, volume 2, pages 459–465, Utrecht, The Netherlands, 2003.
- D.E. Goldberg. *Genetic Algorithms in Search, Optimization and Machine Learning*. Addison-Wesley Longman Publishing Co., 1989.
- Eliyahu M. Goldratt and Jeff Cox. *The Goal*. North River Press, 2004.
- I.I Goncharova, D.J. McFarland, T.M. Vaughan, and J.R. Wolpaw. EMG contamination of EEG: spectral and topographical characteristics. *Electroenceph Clin Neurophysiol*, 114:1580–1593, 2003.
- K. Grauman, M. Betke, J. Gips, and G.R. Bradski. Communication via eye blinks – detection and duration analysis in real time. In *2001 IEEE Computer Society Conference on Computer Vision and Pattern Recognition*, pages 1010–1017. IEEE Computer Society, 2001.
- Jim Gray and Alexander S. Szalay. Where the rubber meets the sky, giving access to science data., 2005. URL <http://research.microsoft.com/\^Gray/>.
- Z. Griliches. Hybrid corn: An exploration in the economics of technological change. *Econometrica*, 25:501–522, 1957.
- E. Gysels, P. Renevey, and P. Celka. SVM-based recursive feature elimination to compare phase synchronization computed from broadband and narrowband EEG signals in brain-computer interfaces. *Signal Processing*, 85(11):2178–89, 2005.
- Mark A. Hall. Correlation-based feature selection for discrete and numeric class machine learning. In *Proc. 17th International Conf. on Machine Learning*, pages 359–366. Morgan Kaufmann, San Francisco, CA, 2000.

- K. D. Harris, D. A. Henze, J. Csicsvari, H. Hirase, and G. Buzsaki. Accuracy of tetrode spike separation as determined by simultaneous intracellular and extracellular measurements. *Journal of Neurophysiology*, 84:401–414, 2000.
- M. Harville, G. Gordon, and J. Woodfill. Foreground segmentation using adaptive mixture models in color and depth. In *IEEE Proceedings, IEEE Workshop on, 8 July 2001*, pages 3–4, 2001.
- S. Haykin. *Adaptive Filter Theory*. Prentice Hall Information and System Sciences Series, 1997.
- S. Haykin. *Neural Networks: A Comprehensive Foundation*. Prentice Hall, 1998.
- Elhanan Helpman, editor. *General Purpose Technologies and Economic Growth*. MIT Press, Cambridge, Massachusetts, 1998.
- Hewlett Packard, Inc. 1.28 terabits per second using hp procure routing switch, 2005. URL [http://www.hp.com/rnd/products/switches/ProCurve\\_Routing-Switch\\_9408sl/overview.htm](http://www.hp.com/rnd/products/switches/ProCurve_Routing-Switch_9408sl/overview.htm).
- T. Hinterberger. *Entwicklung und Optimierung eines Gehirn-Computer-Interfaces mit langsamem Hirnpotentialen*. PhD thesis, Eberhard-Karls-Universitaet Tuebingen, Tuebingen, Germany, 1999.
- B Hjorth. Principles for transformation of scalp eeg from potential field into source distribution. *J Clin Neurophysiol*, 8(4):391–396, Oct 1991.
- L R Hochberg, M D Serruya, G M Friehs, J A Mukand, M Saleh, A H Caplan, A Branner, D Chen, R D Penn, and J P Donoghue. Neuronal ensemble control of prosthetic devices by a human with tetraplegia. *Nature*, 442(7099):164–171, Jul 2006. doi: 10.1038/nature04970.
- J. A. Hoffer, R. B. Stein, M. K. Haugland, T. Sinkjaer, W. K. Durfee, A. B. Schwartz, G. E. Loeb, and C. Kantor. Neural signals for command control and feedback in functional neuromuscular stimulation: a review. *J. Rehabil. Res. Dev.*, 33:145–157, 1996.

- H. Honda, K. Shiba, E. Shu, K. Koshiji, T. Murai, J. Yana, T. Masuzawa, E. Tatsumi, Y. Taenaka, and H. Takano. Study on lithium-ion secondary battery for implantable artificial heart. *Proceedings of the IEEE/EMBS*, pages 2315–2317, 1997.
- N. J. Huan and R. Palaniappan. Neural network classification of autoregressive features from electroencephalogram signals for brain-computer interface design. *J Neural Eng*, 1(3):142–50, 2004.
- JE Huggins, SP Levine, SL BeMent, RK Kushwaha, LA Schuh, EA Passaro, MM Rohde, DA Ross, KV Elisevich, and BJ Smith. Detection of event-related potentials for development of a direct brain interface. *J Clin Neurophysiol*, 16(5):448–455, 1999.
- Rouben Indjikian and Donal Siegel. The impact of investment in it on economic performance: Implications for developing countries. *World Development*, 33(5):681–700, 2005.
- Philip L. Jackson, Andrew N. Meltzoff, and Jean Decety. How do we perceive the pain of others? A window into the neural processes involved in empathy. *Neuroimage*, 24:771–779, 2005.
- M.I. Jordan and R.A. Jacobs. Hierarchical mixtures of experts and the em algorithm. *Neural Computation*, 6:181–214, 1994.
- J. Kaiser, J. Perelmouter, I. H. Iversen, N. Neumann, N. Ghanayim, T. Hinterberger, A. Kübler, B. Kotchoubey, and N. Birbaumer. Self-initiation of eeg-based communication in paralyzed patients. *Clin. Neurophysiol.*, 112:551–554, 2001.
- J F Kalaska and M L Hyde. Area 4 and area 5: differences between the load direction-dependent discharge variability of cells during active postural fixation. *Exp Brain Res*, 59(1):197–202, 1985.
- Laurence M. Katz and Anne Chang, editors. *Magill's Medical Guide*. Salem Press, 2005.

- L Kauhanen, T Nykopp, J Lehtonen, P Jylänki, J Heikkonen, P Rantanen, H Alaranta, and M Sams. Eeg and meg brain-computer interface for tetraplegic patients. *IEEE Trans Neural Syst Rehabil Eng*, 14(2):190–193, Jun 2006.
- Z. A. Keirn and J. I. Aunon. Man-machine communications through brain-wave processing. *IEEE Eng Med Biol*, 9:55–57, 1990.
- J. Kennedy and R. Eberhart. Particle swarm optimization. In *Proceedings to the 1995 IEEE International Conference on Neural Networks*, volume 5, pages 1942–1948, 1995.
- P. R. Kennedy and R. A. Bakay. Restoration of neural output from a paralyzed patient by a direct brain connection. *Neuroreport*, 9:1707–1711, 1998.
- P. R. Kennedy, R. A. Bakay, M. M. Moore, and J. Goldwaith. Direct control of a computer from the human central nervous system. *IEEE Trans Rehabil Eng*, 8 (2):198–202, June 2000.
- RE Kettner, JK Marcario, and MC Clark-Phelps. Control of remembered reaching sequences in monkey. i. activity during movement in motor and premotor cortex. *Exp Brain Res*, 112(3):335–346, 1996.
- K. L. Kilgore, P. H. Peckham, M. W. Keith, G. B. Thrope, K. S. Wuolle, A. M. Bryden, and R. L. Hart. An implanted upper-extremity neuroprosthesis: Follow-up of five patients. *J Bone Joint Surg*, 79-A:533–541, 1997.
- S P Kim, J C Sanchez, Y N Rao, D Erdogmus, J M Carmena, M A Lebedev, M A Nicolelis, and J C Principe. A comparison of optimal mimo linear and nonlinear models for brain-machine interfaces. *J Neural Eng*, 3(2):145–161, Jun 2006. doi: 10.1088/1741-2560/3/2/009.
- Stephen M. Kosslyn. Aspects of a cognitive neuroscience of mental imagery. *Science*, 240:1621–1626, 1988.
- A. Kostov and M. Polak. Parallel man-machine training in development of EEG-based cursor control. *IEEE Trans Rehabil Eng*, 8(2):203–205, 2000.

- B. Kotchoubey, D. Schneider, H. Schleichert, U. Strehl, C. Uhlmann, V. Blankenhorn, W. Froscher, and N. Birbaumer. Self-regulation of slow cortical potentials in epilepsy: a retrial with analysis of influencing factors. *Epilepsy Res*, 25(3):269–276, November 1996.
- J. W. Kozelka and T. A. Pedley. Beta and mu rhythms. *J Clin Neurophysiol*, 7:191–207, 1990.
- D.J. Krusienski, G. Schalk, D.J. McFarland, and J.R. Wolpaw. A mu rhythm matched filter for continuous control of a brain-computer interface. *IEEE Trans Biomed Eng*, page submitted, 2006.
- A. Kübler, B. Kotchoubey, T. Hinterberger, N. Ghanayim, J. Perelmouter, M. Schauer, C. Fritsch, E. Taub, and N. Birbaumer. The Thought Translation Device: a neurophysiological approach to communication in total motor paralysis. *Exp Brain Res*, 124(2):223–232, January 1999.
- M. Kubota, Y. Sakakihara, Y. Uchiyama, A. Nara, T. Nagata, H. Nitta, K. Ishimoto, A. Oka, K. Horio, and M. Yanagisawa. New ocular movement detector system as a communication tool in ventilator-assisted werdnig-hoffmann disease. *Dev. Med. Child Neurol.*, 42:61–64, 2000.
- W. N. Kuhlman. EEG feedback training: Enhancement of somatosensory cortical activity. *Electroenceph Clin Neurophysiol*, 45:290–294, 1978.
- B.C. Kuo, J.M. Yan, and D.A. Landgrebe. Gaussian mixture classifier with regularized covariance estimator for hyperspectral data classification. In *Proceedings IGARSS '03, of the Geoscience and Remote Sensing Symposium*, volume 1, pages 276–278, 2003.
- Ray Kurzweil. *The Age of Spiritual Machines: When Computers Exceed Human Intelligence*. Penguin, 2000.
- Ray Kurzweil. *The Singularity Is Near : When Humans Transcend Biology*. Viking Adult, 2005.

- Stephanie Perichon Lacour, Zhenyu Huang, Zhigang Suo, and Sigurd Wagner. Stretchable gold conductors on elastomeric substrates. *Applied Physics Letters*, 82:2404–2406, 2003.
- J. R. LaCourse and Jr. F. C. Hludik. An eye movement communication-control system for the disabled. *IEEE Trans. Biomed. Eng*, 37:1215–1220, 1990.
- T. N. Lal, M. Schroder, T Hinterberger, J. Weston, M. Bogdan, N. Birbaumer, and B. Scholkopf. Support vector channel selection in BCI. *IEEE Trans Biomed Eng*, 51(6):1003–10, 2004.
- T.N. Lal, M. Schröder, N.J. Hill, H. Preissl, T. Hinterberger, J. Mellinger, M. Bogdan, W. Rosenstiel, T. Hofmann, N. Birbaumer, and B. Schölkopf. A brain computer interface with online feedback based on magnetoencephalography. In *Proceedings of the 22nd International Conference on Machine Learning, Bonn, Germany*, 2005.
- W. Lang, D. Cheyne, P. Hollinger, W. Gerschlager, and G. Lindinger. Electric and magnetic fields of the brain accompanying internal simulation of movement. *Brain Res Cogn Brain Res*, 3:125–129, 1996.
- M. Laubach and J. Wessberg. Cortical ensemble activity increasingly predicts behavior outcomes during learning of a motor task. *Nature*, 405:567–571, 2000.
- Stacy Lawrence. Digital media make their mark. *Technology Review*, 2005.
- J Le and A Gevins. Method to reduce blur distortion from eeg's using a realistic head model. *IEEE Trans Biomed Eng*, 40(6):517–528, Jun 1993.
- M A Lebedev, J M Carmena, J E O'Doherty, M Zackenhouse, C S Henriquez, J C Principe, and M A Nicolelis. Cortical ensemble adaptation to represent velocity of an artificial actuator controlled by a brain-machine interface. *J Neurosci*, 25(19):4681–4693, May 2005. doi: 10.1523/JNEUROSCI.4088-04.2005.
- D.S. Lee. Effective gaussian mixture learning for video background subtraction. *IEEE Trans. Pattern Anal. Mach. Intell.*, 27(5):827–832, 2005.

- EC Leuthardt, G Schalk, JR Wolpaw JR, JG Ojemann, and DW Moran. A brain-computer interface using electrocorticographic signals in humans. *J Neural Eng*, 1(2):63–71, 2004.
- S. P. Levine, J. E. Huggins, S. L. BeMent, R. K. Kushwaha, L. A. Schuh, E. A. Passaro, M. M. Rohde, and D. A. Ross. Identification of electrocorticogram patterns as the basis for a direct brain interface. *J Clin Neurophysiol*, 16:439–447, 1999.
- S. P. Levine, J. E. Huggins, S. L. BeMent, R. K. Kushwaha, L. A. Schuh, M. M. Rohde, E. A. Passaro, D. A. Ross, K. V. Elisevich, and B. J. Smith. A direct brain interface based on event-related potentials. *IEEE Trans Rehabil Eng*, 8(2):180–185, June 2000.
- J. C. R. Licklider. Man-computer symbiosis. *IRE Transactions on Human Factors in Electronics*, 1:4–11, 1960.
- Huan Liu and Lei Yu. Toward integrating feature selection algorithms for classification and clustering. *IEEE Transactions on Knowledge and Data Engineering*, 17(4):491–502, 2005.
- L. Liyuan, W. Huang, I. Yu-Hua Gu, and Q. Tian. Statistical modeling of complex backgrounds for foreground object detection. In *IEEE Transactions, Image Processing*, volume 13, pages 1459–1472, 2004.
- G E Loeb, A E Walker, S Uematsu, and B W Konigsmark. Histological reaction to various conductive and dielectric films chronically implanted in the subdural space. *J Biomed Mater Res*, 11(2):195–210, Mar 1977. doi: 10.1002/jbm.820110206.
- I. Scott MacKenzie. Fitt's law as a research and design tool in human-computer interaction. *Human-Computer Interaction*, 7:91–139, 1992.
- S. Makeig, T.P. Jung, A.J. Bell, and T.J. Sejnowski. Independent component analysis of electroencephalographic data. In *Advances in Neural Information Processing Systems 8*, pages 145–151. MIT Press, Cambridge, MA, 1996.

- S. Makeig, T. P. Jung, A. J. Bell, D. Ghahremani, and T. J. Sejnowski. Blind separation of auditory event-related brain responses into independent components. *Proceedings of the National Academy of Sciences of the United States of America*, 94(20):10979–10984, September 1997.
- E. Mansfield. *Industrial Research and Technological Innovation*. Norton, New York, 1968.
- Edwin Mansfield, John Rapoport, Anthony Romeo, Samuel Wagner, and George Beardsley. Social and private rates of return from industrial innovations. *The Quarterly Journal of Economics*, 91(2):221–240, 1977.
- E Margalit, JD Weiland, RE Clatterbuck, GY Fujii, M Maia, M Tameesh, G Torres, SA D’Anna, S Desai, DV Piyathaisere, A Olivi, E Jr de Juan, and MS Humayun. Visual and electrical evoked response recorded from subdural electrodes implanted above the visual cortex in normal dogs under two methods of anesthesia. *J Neurosci Methods*, 123(2):129–137, 2003.
- S Lawrence Marple. *Digital spectral analysis : with applications*. Prentice-Hall, Englewood Cliffs, 1987.
- Steve Marschner. Simple ray-triangle intersection. Cornell University, 2003.
- S. G. Mason and G. E. Birch. A general framework for brain-computer interface design. *IEEE Trans Neur Syst Rehabil Eng*, 11(1):70–85, 2003.
- P Mazzoni, RM Bracewell, S Barash, and RA Andersen. Motor intention activity in the macaque’s lateral intraparietal area. i. dissociation of motor plan from sensory memory. *J Neurophysiol*, 76(3):1439–1456, 1996.
- D. J. McFarland and J. R. Wolpaw. EEG-based communication and control: speed-accuracy relationships. *Appl Psychophysiol Biofeedback*, 28(3):217–31, September 2003.
- D. J. McFarland, T. Lefkowicz, and J. R. Wolpaw. Design and operation of an EEG-based brain-computer interface (BCI) with digital signal processing technology. *Behav Res Methods Instrum Comput*, 29:337–345, 1997a.

- D. J. McFarland, L. M. McCane, S. V. David, and J. R. Wolpaw. Spatial filter selection for EEG-based communication. *Electroenceph Clin Neurophysiol*, 103(3):386–394, September 1997b.
- D. J. McFarland, L. A. Miner, T. M. Vaughan, and J. R. Wolpaw. Mu and beta rhythm topographies during motor imagery and actual movements. *Brain Topogr*, 12(3):177–186, 2000.
- D. J. McFarland, W. A. Sarnacki, and J. R. Wolpaw. Brain-Computer Interface (BCI) Operation: Optimizing Information Transfer Rates. *Biol Psychol*, 63(3):237–251, July 2003.
- Dennis J. McFarland, G. W. Neat, and J. R. Wolpaw. An EEG-based method for graded cursor control. *Psychobiology*, 21:77–81, 1993.
- D.J. McFarland, Charles W. Anderson, Klaus-Robert Müller, Alois Schlögl, and Dean J. Krusienski. Bci meeting 2005 – workshop on bci signal processing: Feature extraction and translation. *IEEE Trans Neur Syst Rehabil Eng*, 14(2):135–138, 2006.
- C Mehring, J Rickert, E Vaadia, S Cardosa de Oliveira, A Aertsen, and S Rotter. Inference of hand movements from local field potentials in monkey motor cortex. *Nat Neurosci*, 6(12):1253–1254, Dec 2003. doi: 10.1038/nn1158.
- J. Mellinger, G. Schalk, C. Braun, H. Preissl, N. Birbaumer, and A. Kübler. A brain-computer interface (bci) based on magneto-encephalography (meg). In *Society for Psychophysiological Research Annual Meeting Abstract, Lisbon, Portugal*, 2005.
- H Merchant, A Battaglia-Mayer, and A P Georgopoulos. Neural responses during interception of real and apparent circularly moving stimuli in motor cortex and area 7a. *Cereb Cortex*, 14(3):314–331, Mar 2004.
- L. A. Miner, D. J. McFarland, and J. R. Wolpaw. Answering questions with an electroencephalogram-based brain-computer interface. *Arch Phys Med Rehabil*, 79:1029–1033, 1998.

- M. L. Minsky. *The Society of Mind*. Simon and Schuster, New York, 1988.
- M. L. Minsky. *The Emotion Machine: Commonsense Thinking, Artificial Intelligence, and the Future of the Human Mind*. Simon and Schuster, New York, 2006.
- D W Moran and A B Schwartz. Motor cortical activity during drawing movements: population representation during spiral tracing. *J Neurophysiol*, 82(5):2693–2704, Nov 1999a.
- D W Moran and A B Schwartz. Motor cortical representation of speed and direction during reaching. *J Neurophysiol*, 82(5):2676–2692, Nov 1999b.
- D W Moran and A B Schwartz. One motor cortex, two different views. *Nat Neurosci*, 3(10):963–965, Oct 2000. doi: 10.1038/79880.
- Richard Morgan. *Altered Carbon*. Del Rey, 2003.
- S T Morgan, J C Hansen, and S A Hillyard. Selective attention to stimulus location modulates the steady-state visual evoked potential. *Proc Natl Acad Sci U S A*, 93(10):4770–4774, May 1996.
- K. R. Müller, C. W. Anderson, and G. E. Birch. Linear and nonlinear methods for brain-computer interfaces. *IEEE Trans Rehabil Eng*, 11(2):165–9, 2003.
- C.J.L. Murray and A.D. Lopez, editors. *Global Burden of Disease*. Harvard University Press, Boston, 1996.
- N Nathoo, D Nair, M Phillips, and MA Vogelbaum. Mapping prosody: correlation of functional magnetic resonance imaging with intraoperative electrocorticography recordings in a patient with a right-sided temporooccipital glioma. case illustration. *J Neurosurg*, 103(5):930, 2005.
- National Advisory Board on Medical Rehabilitation Research. *Report and Research Plan for the National Center for Medical Rehabilitation Research, National Institute of Child Health and Human Development*. National Institutes of Health, 1992.

- C. Neuper, K.R. Müller, A. Kübler, N. Birbaumer, and G. Pfurtscheller. Clinical application of an EEG-based brain-computer interface: a case study of a patient with severe motor impairment. *Electroenceph Clin Neurophysiol*, 114:399–409, 2003.
- E. Niedermeyer. The normal EEG of the waking adult. In E. Niedermeyer and F. H. Lopes da Silva, editors, *Electroencephalography: basic principles, clinical applications and related fields, 4th edition*, pages 149–173. Williams and Wilkins, Baltimore, MD, 1999.
- D. A. Norman. *Things That Make Us Smart: Defending Human Attributes in the Age of the Machine*. Addison-Wesley, Reading, MA, 1993.
- D. P. Nowles and J. Kamiya. The control of electroencephalographic alpha rhythms through auditory feedback and the associated mental activity. *Psychophysiol*, 6: 476–484, 1970.
- D Nozaki, K Nakazawa, and M Akai. Muscle activity determined by cosine tuning with a nontrivial preferred direction during isometric force exertion by lower limb. *J Neurophysiol*, 93(5):2614–2624, 2005.
- The Editors of Scientific American. *The Scientific American Book of the Brain*, volume 3. Scientific American, New York, 1999.
- L Paninski, M R Fellows, N G Hatsopoulos, and J P Donoghue. Spatiotemporal tuning of motor cortical neurons for hand position and velocity. *J Neurophysiol*, 91(1):515–532, Jan 2004. doi: 10.1152/jn.00587.2002.
- E. Parzen. On estimation of probability density function and mode. *Ann Math Stat*, 33:1065–1073, 1962.
- W. D. Penny, S. J. Roberts, E. A. Curran, and M. J. Stokes. EEG-based communication: a pattern recognition approach. *IEEE Trans Rehabil Eng*, 8:214–215, 2000.
- J. Perelmouter, B. Kotchoubey, A. Kübler, E. Taub, and N. Birbaumer. Language support program for thought-translation-devices. *Automedica*, 18:67–84, 1999.

- F. Pernkopf and D. Bouchaffra. Genetic-based EM algorithm for learning gaussian mixture models. *IEEE Trans. Pattern Anal. Mach. Intell.*, 27(8):1344–1348, 2005.
- G Pfurtscheller. Event-related synchronization (ers): an electrophysiological correlate of cortical areas at rest. *Electroencephalogr Clin Neurophysiol*, 83(1):62–69, Jul 1992.
- G. Pfurtscheller. EEG event-related desynchronization (ERD) and event-related synchronization (ERS). In E. Niedermeyer and F. H. Lopes da Silva, editors, *Electroencephalography: basic principles, clinical applications and related fields, 4th edition*, pages 958–967. Williams and Wilkins, Baltimore, MD, 1999a.
- G. Pfurtscheller. Event-related desynchronization. In F.H. Lopes da Silva and G. Pfurtscheller, editors, *Handbook of Electroencephalography and Clinical Neurophysiology*. Elsevier, Amsterdam, 1999b.
- G Pfurtscheller and A Aranibar. Event-related cortical desynchronization detected by power measurements of scalp eeg. *Electroencephalogr Clin Neurophysiol*, 42(6):817–826, Jun 1977.
- G. Pfurtscheller and A. Berghold. Patterns of cortical activation during planning of voluntary movement. *Electroenceph Clin Neurophysiol*, 72:250–258, 1989.
- G. Pfurtscheller and R. Cooper. Frequency dependence of the transmission of the eeg from cortex to scalp. *Electroenceph Clin Neurophysiol*, 38:93–96, 1975.
- G. Pfurtscheller and C. Neuper. Motor imagery activates primary sensorimotor area in humans. *Neurosci Lett*, 239:65–68, 1997.
- G. Pfurtscheller, D. Flotzinger, and J. Kalcher. Brain-computer interface - a new communication device for handicapped persons. *J. Microcomp. App.*, 16:293–299, 1993.
- G. Pfurtscheller, C. Neuper, D. Flotzinger, and M. Pregenzer. EEG-based discrimination between imagination of right and left hand movement. *Electroencephalogr Clin Neurophysiol*, 103(6):642–51, 1997.

- G. Pfurtscheller, C. Guger, G. Müller, G. Krausz, and C. Neuper. Brain oscillations control hand orthosis in a tetraplegic. *Neurosci Lett*, 292(3):211–214, October 2000a.
- G. Pfurtscheller, C. Neuper, C. Guger, W. Harkam, H. Ramoser, A. Schlögl, B., and M. Pregenzer. Current trends in Graz Brain-Computer Interface (BCI) research. *IEEE Trans Rehabil Eng*, 8(2):216–219, June 2000b.
- G Pfurtscheller, B Graimann, J E Huggins, S P Levine, and L A Schuh. Spatiotemporal patterns of beta desynchronization and gamma synchronization in corticographic data during self-paced movement. *Clin Neurophysiol*, 114(7):1226–1236, Jul 2003.
- WH Pilcher and WG Rusyniak. Complications of epilepsy surgery. *Neurosurg Clin N Am*, 4(2):311–325, 1993.
- R. Pless. Evaluation of local models of dynamic backgrounds. In *IEEE Proceedings, Computer Vision and Pattern Recognition*, volume 2, pages 73–78, 2003.
- M.B. Priestley. *Spectral Analysis and Time Series*. Academic Press, Orlando, Florida, 1981.
- Willard Van Orman Quine. *Word and Object (Studies in Communication)*. MIT Press, 1964.
- R J Radke, S Andra, O Al-Kofahi, and B Roysam. Image change detection algorithms: a systematic survey. *IEEE Trans Image Process*, 14(3):294–307, Mar 2005.
- H. Ramoser, J. R. Wolpaw, and G. Pfurtscheller. EEG-based communication: evaluation of alternative signal prediction methods. *Biomedizinische Technik*, 42(9): 226–233, September 1997.
- H. Ramoser, J. Müller-Gerking, and G. Pfurtscheller. Optimal spatial filtering of single trial EEG during imagined hand movement. *IEEE Trans Rehabil Eng*, 8 (4):441–446, December 2000.

- Raghubeer M. Rao and Ajit S. Bopardikar. *Wavelet Transforms: Introduction to Theory and Applications*. Prentice Hall PTR; 1st edition, 1998.
- Charlotte M. Reed and Nathaniel I. Durlach. Note on information transfer rates in human communication. *Presence*, 7(5):509–518, 1998.
- G A Reina, D W Moran, and A B Schwartz. On the relationship between joint angular velocity and motor cortical discharge during reaching. *J Neurophysiol*, 85(6):2576–2589, Jun 2001.
- K. M. Rice, E. B. Blanchard, and M. Purcell. Biofeedback treatments of generalized anxiety disorder: Preliminary results. *Biofeedback Self Regul*, 18:93–105, 1993.
- J Rickert, S C Oliveira, E Vaadia, A Aertsen, S Rotter, and C Mehring. Encoding of movement direction in different frequency ranges of motor cortical local field potentials. *J Neurosci*, 25(39):8815–8824, Sep 2005. doi: 10.1523/JNEUROSCI.0816-05.2005.
- Fred Rieke, David Warland, Rob deRuytervanStevenick, and William Bialek. *Spikes: Exploring the neural code*. MIT Press, Cambridge, MA, 1999.
- J. Rissanen. Modelling by the shortest data description. *Automatica*, 14:465–471, 1978.
- B. Rockstroh, T. Elbert, A. Canavan, W. Lutzenberger, and N. Birbaumer. *Slow Cortical Potentials and Behavior*. Urban and Schwarzenberg, Baltimore, MD, 2nd edition, 1989.
- Everett M. Rogers. *Diffusion of Innovations*. Free Press, 2003.
- M M Rohde, S L BeMent, J E Huggins, S P Levine, R K Kushwaha, and L A Schuh. Quality estimation of subdurally recorded, event-related potentials based on signal-to-noise ratio. *IEEE Trans Biomed Eng*, 49(1):31–40, Jan 2002.
- U Rokni, O Steinberg, E Vaadia, and H Sompolinsky. Cortical representation of bimanual movements. *J Neurosci*, 23(37):11577–11586, Dec 2003.

- E Salinas and L F Abbott. Vector reconstruction from firing rates. *J Comput Neurosci*, 1(1-2):89–107, Jun 1994.
- Edward Sapir. Communication. *Encyclopaedia of the Social Sciences (New York)*, 4:78–81, 1931.
- G. Schalk, D.J. McFarland, T. Hinterberger, N. Birbaumer, and J.R. Wolpaw. BCI2000: A General-Purpose Brain-Computer Interface (BCI) System. *IEEE Trans Biomed Eng*, 51:1034–1043, 2004.
- A. Schloegl, P. Anderer, M.-J. Barbanoj, G. Dorffner, G. Gruber, G. Kloesch, J.L. Lorenzo, P. Rappelsberger, and G. Pfurtscheller. Artifacts in the sleep EEG - a database for the evaluation of automatedprocessing methods. In *Proceedings Third International Congress, of the World Federation of Sleep Research Societies (WFSRS)*, volume 2, page 586, 1999.
- E. M. Schmidt. Single neuron recording from motor cortex as a possible source of signals for control of external devices. *Ann Biomed Eng*, 8:339–349, 1980.
- A B Schwartz and D W Moran. Motor cortical activity during drawing movements: population representation during lemniscate tracing. *J Neurophysiol*, 82(5):2705–2718, Nov 1999.
- A B Schwartz, D M Taylor, and S I Tillery. Extraction algorithms for cortical control of arm prosthetics. *Curr Opin Neurobiol*, 11(6):701–707, Dec 2001.
- A B Schwartz, D W Moran, and G A Reina. Differential representation of perception and action in the frontal cortex. *Science*, 303(5656):380–383, Jan 2004. doi: 10.1126/science.1087788.
- A.B. Schwartz. Motor cortical activity during drawing movement: population representation during sinusoid tracing. *J Neurophysiol*, 70:28–36, 1993.
- T H Schwartz, C W Bazil, T S Walczak, S Chan, T A Pedley, and R R Goodman. The predictive value of intraoperative electrocorticography in resections for limbic epilepsy associated with mesial temporal sclerosis. *Neurosurgery*, 40(2):302–309, Feb 1997.

- G. Schwarz. Estimating the dimension of a model. *Annals of Statistics*, 6:461–464, 1978.
- E W Sellers and E Donchin. A p300-based brain-computer interface: initial tests by als patients. *Clin Neurophysiol*, 117(3):538–548, Mar 2006. doi: 10.1016/j.clinph.2005.06.027.
- L E Sergio, C Hamel-Pâquet, and J F Kalaska. Motor cortex neural correlates of output kinematics and kinetics during isometric-force and arm-reaching tasks. *J Neurophysiol*, 94(4):2353–2378, Oct 2005. doi: 10.1152/jn.00989.2004.
- MD Serruya, NG Hatsopoulos, L Paninski, MR Fellows, and JP Donoghue. Instant neural control of a movement signal. *Nature*, 416(6877):141–142, 2002.
- W. Shain, L. Spataro, J. Dilgen, K. Haverstick, S. Retterer, M. Isaacson, M. Saltzman, and J.N. Turner. Controlling cellular reactive responses around neural prosthetic devices using peripheral and local intervention strategies. *IEEE Trans Neural Syst Rehabil Eng*, 11:186–188, 2003.
- C. E. Shannon and W. Weaver. *The Mathematical Theory of Communication*. University of Illinois Press, Urbana, 1964.
- Claude E. Shannon. Prediction and entropy of printed English. *The Bell System Technical Journal*, 30(1):50–64, 1951.
- F. Sharbrough, G.E. Chatrian, R.P. Lesser, H. Luders, M. Nuwer, and T.W. Picton. American electroencephalographic society guidelines for standard electrode position nomenclature. *Electroenceph Clin Neurophysiol*, 8:200–202, 1991.
- KV Shenoy, D Meeker, S Cao, SA Kureshi, B Pesaran, CA Buneo, AP Batista, PP Mitra, JW Burdick, and RA Andersen. Neural prosthetic control signals from plan activity. *Neuroreport*, 14(4):591–596, 2003.
- S Shoham, L M Paninski, M R Fellows, N G Hatsopoulos, and Normann RA. Donoghue, J P. Statistical encoding model for a primary motor cortical brain-machine interface. *IEEE Trans Bio-Med Eng*, 52(7):1312–1322, 2005.

- A Sinai, C W Bowers, C M Crainiceanu, D Boatman, B Gordon, R P Lesser, F A Lenz, and N E Crone. Electrocorticographic high gamma activity versus electrical cortical stimulation mapping of naming. *Brain*, 128(Pt 7):1556–1570, Jul 2005. doi: 10.1093/brain/awh491.
- LH Snyder, AP Batista, and RA Andersen. Coding of intention in the posterior parietal cortex. *Nature*, 386(6621):167–170, 1997.
- I. Son and B. Yazici. Near infrared imaging and spectroscopy for brain activity monitoring. In *Advances in Sensing with Security Applications, Il Ciocco, Italy*, 2005.
- R. Srinivasan, P. L. Nunez, and R. B. Silberstein. Spatial filtering and neocortical dynamics: Estimates of EEG coherence. *IEEE Trans Biomed Eng*, 45:814–826, 1998.
- C. Stauffer and W.E.L. Grimson. Evaluation of local models of dynamic backgrounds. In *IEEE Proceedings, Computer Vision and Pattern Recognition*, volume 2, pages 246–252, 1999.
- M. B. Sterman. Basic concepts and clinical findings in the treatment of seizure disorders with EEG operant conditioning. *Clin Electroencephalogr*, 31:45–55, 2000.
- J.C. Sturm, P.I. Hsu, M. Huang, H. Gleskova, S. Miller, A. Darhuber, S. Wagner, Z. Suo, and S. Troian. Technologies for large-area electronics on deformable substrates. In C. L. Claeys, F. Gonzales, J. Murota, and K. Saraswat, editors, *ULSI Process Integration II*, pages 506–517. Proc. Electrochemical Soc. 2001-2, 2001.
- E. E. Sutter. The brain response interface: communication through visually guided electrical brain responses. *J Microcomput Appl*, 15:31–45, 1992.
- S. Sutton, M. Braren, J. Zubin, and E.R. John. Evoked correlates of stimulus uncertainty. *Science*, 150:1187–1188, 1965.
- M Taira, J Boline, N Smyrnis, A P Georgopoulos, and J Ashe. On the relations between single cell activity in the motor cortex and the direction and magnitude

- of three-dimensional static isometric force. *Exp Brain Res*, 109(3):367–376, Jun 1996.
- J. Talairach and P. Tournoux. *Co-Planar Stereotaxic Atlas of the Human Brain*. Thieme Medical Publishers, Inc., New York, 1988.
- D. M. Taylor, S. I Tillery, and A. B. Schwartz. Direct cortical control of 3D neuroprosthetic devices. *Science*, 296:1829–1832, 2002.
- J.G. Tewksbury, M.S. Crandall, and W.E. Crane. Measuring the societal benefits of innovation. *Science*, 209(4457):658–662, 1980.
- C. Thomas. *Firefox*. Holt, Rinehart, and Winston, New York, 1977.
- Henk Tijms. *Understanding Probability: Chance Rules in Everyday Life*. Cambridge University Press, 2004.
- E Todorov. Cosine tuning minimizes motor errors. *Neural Comput*, 14(6):1233–1260, 2002.
- C Toro, C Cox, G Friehs, C Ojakangas, R Maxwell, J R Gates, R J Gumnit, and T J Ebner. 8-12 hz rhythmic oscillations in human motor cortex during two-dimensional arm movements: evidence for representation of kinematic parameters. *Electroencephalogr Clin Neurophysiol*, 93(5):390–403, Oct 1994.
- Philip H. S. Torr. An assessment of information criteria for motion model selection. In *Proceedings CVPR '97, of Conference on Computer Vision and Pattern Recognition*, pages 47–52, 1997.
- K. Toyama, J. Krumm, B. Brumitt, and B. Meyers. Statistical modeling of complex backgrounds for foreground object detection. In *IEEE Proceedings, of the Seventh IEEE International Conference on Computer Vision*, volume 1, pages 20–27, 1999.
- Inc. Transmeta. The transmeta crusoe processor typically operates between several hundred milliwatts and 1-2 watts., 2005. URL <http://www.transmeta.com/crusoe/faq.html>.

- T. A. Travis, C. Y. Kondo, and J. R. Knott. Alpha enhancement research: a review. *Biol Psychiatry*, 10:69–89, 1975.
- J. N. Turner, H. Ancin, D. Becker, D. H. Szarowski, M. Holmes, N. O'Connor, M. Wang, T. J. Holmes, and B. Roysam. Automated image analysis technologies for biological 3-d light microscopy. *International Journal of Imaging Systems and Technology, Special Issue on Microscopy*, 8:240–254, 1997.
- RS Turner, JW Jr Owens, and ME Anderson. Directional variation of spatial and temporal characteristics of limb movements made by monkeys in a two-dimensional work space. *J Neurophysiol*, 74(2):684–697, 1995.
- V. N. Vapnik and A. J. Chervonenkis. Ordered risk minimization (I and II). *Automation and Remote Control*, 34:1226–1235 and 1403–1412, 1974.
- T. M. Vaughan, D. J. McFarland, G. Schalk, W. A. Sarnacki, L. Robinson, and J. R. Wolpaw. EEG-based brain-computer-interface: development of a speller. *Society for Neuroscience Abstracts*, 27(1):167, 2001.
- J. J. Vidal. Real-time detection of brain events in EEG. In *IEEE Proceedings, Special Issue on Biological Signal Processing and Analysis*, volume 65, pages 633–664, 1977.
- Nicolas Wade, editor. *The Science Times Book of the brain*, volume 150. The Lyons Press, New York, 1998.
- Sigurd Wagner and Helena Gleskova. Silicon thin-film transistors on flexible foil substrates. In *Digest of Technical Papers, Korean Information and Display Society*, pages 263–267, Seoul, 2002.
- Sigurd Wagner, Helena Gleskova, I-Chun Cheng, and Ming Wu. Thin-film transistors and flexible electronics. In Ralf B. Bergmann, editor, *Growth, Characterization and Electronic Applications of S-based Thin Films*, pages 1–14. Research Signpost, Trivandrum, 2002.

- W. G. Walter, R. Cooper, V. J. Aldridge, W. C. McCallum, and A. L. Winter. Contingent negative variation: an electric sign of sensorimotor association and expectancy in the human brain. *Nature*, 203:380–384, 1964.
- Darren Weber. Bioelectromagnetism Matlab Toolbox, 2005.
- N Weiskopf, R Veit, M Erb, K Mathiak, W Grodd, R Goebel, and N Birbaumer. Physiological self-regulation of regional brain activity using real-time functional magnetic resonance imaging (fMRI): methodology and exemplary data. *Neuroimage*, 19(3):577–586, Jul 2003.
- N Weiskopf, K Mathiak, S W Bock, F Scharnowski, R Veit, W Grodd, R Goebel, and N Birbaumer. Principles of a brain-computer interface (bci) based on real-time functional magnetic resonance imaging (fMRI). *IEEE Trans Biomed Eng*, 51(6):966–970, Jun 2004.
- J. Wessberg, C. R. Stambaugh, J. D. Kralik, P. D. Beck, M. Laubach, J. K. Chapin, J. Kim, S. J. Biggs, M. A. Srinivasan, and M. A. Nicolelis. Real-time prediction of hand trajectory by ensembles of cortical neurons in primates. *Nature*, 408: 361–365, 2000.
- Wikipedia. List of device bandwidths, 2005. URL [http://en.wikipedia.org/wiki/List\\_of\\_device\\_bandwidths](http://en.wikipedia.org/wiki/List_of_device_bandwidths).
- J. R. Wolpaw and D. J. McFarland. Multichannel EEG-based brain-computer communication. *Electroenceph Clin Neurophysiol*, 90(6):444–449, June 1994.
- J. R. Wolpaw, D. J. McFarland, G. W. Neat, and C. A. Forneris. An EEG-based brain-computer interface for cursor control. *Electroenceph Clin Neurophysiol*, 78 (3):252–259, March 1991.
- J. R. Wolpaw, H. Ramoser, D. J. McFarland, and G. Pfurtscheller. EEG-based communication: Improved accuracy by response verification. *IEEE Trans Rehab Engin*, 6:326–333, 1998.

- J. R. Wolpaw, D. J. McFarland, and T. M. Vaughan. Brain-computer interface research at the Wadsworth Center. *IEEE Trans Rehabil Eng*, 8(2):222–226, June 2000.
- J. R. Wolpaw, N. Birbaumer, D. J. McFarland, G. Pfurtscheller, and T. M. Vaughan. Brain-computer interfaces for communication and control. *Electroenceph Clin Neurophysiol*, 113(6):767–791, June 2002.
- J.R. Wolpaw and D.J. McFarland. Control of a two-dimensional movement signal by a non-invasive brain-computer interface in humans. *Society for Neuroscience Abstracts. In press.*, 2004.
- J.R. Wolpaw, D.J. McFarland, and A.T. Cacace. Preliminary studies for a direct brain-to-computer parallel interface. *Projects for Persons with Disabilities. IBM Technical Symposium*, pages 11–20, 1986.
- J.R. Wolpaw, D. Flotzinger, G. Pfurtscheller, and D.J. McFarland. Timing of EEG-based cursor control. *Electroenceph Clin Neurophysiol*, 14:529–538, 1997.
- JR Wolpaw, DJ McFarland, TM Vaughan, and G Schalk. The wadsworth center brain-computer interface (bci) research and development program. *IEEE Trans Neur Syst Rehabil Eng*, 11(2):204–207, 2003.
- T. H. Wonnacott and R. Wonnacott. *Introductory Statistics*. John Wiley and Sons, New York, 3 edition, 1977.
- A. R. Wyler and K. J. Burchiel. Factors influencing accuracy of operant control of pyramidal tract neurons in monkey. *Brain Res*, 152:418–421, 1978.
- A. R. Wyler, K. J. Burchiel, and C. A. Robbins. Operant control of precentral neurons in monkeys: Evidence against open loop control. *Brain Res*, 171:29–39, 1979.
- W. Wyrwicka and M. B. Sterman. Instrumental conditioning of sensorimotor cortex EEG spindles in the waking cat. *Psychol Behav*, 3:703–707, 1968.

T G Yuen, W F Agnew, and L A Bullara. Tissue response to potential neuroprosthetic materials implanted subdurally. *Biomaterials*, 8(2):138–141, Mar 1987.

## APPENDIX A NOTATION

### Signal:

$f_s$	$f_s \in \mathbb{N}$	sampling frequency
$k$	$k \in \mathbb{N}$	discrete time index of the raw signal
$\vec{s}$	$\vec{s} \in \mathbb{R}^H; \vec{s} = [s_1, s_2, \dots, s_H]^T$	acquired raw signal
$H$	$H \in \mathbb{N}$	number of recorded channels
$h$	$h \in \{1, 2, \dots, H\}$	channel index
$t_x$	$t_x \in T_x \subset \mathbb{R}$	horizontal position of the cursor
$t_y$	$t_y \in T_y \subset \mathbb{R}$	vertical position of the cursor
$t_{rx}$	$t_{rx} \in T_{rx} \subset \mathbb{R}$	horizontal position of the target
$t_{ry}$	$t_{ry} \in T_{ry} \subset \mathbb{R}$	vertical position of the target

### Features:

$a_j$	$a_j \in \mathbb{A}_j$	feature
$\mathbb{A}_j$	$\mathbb{A}_j \subset \mathbb{R}$	feature $a_j$ domain
$\mathcal{A}$	$\mathcal{A} = \{1, 2, \dots, J\}$	feature set
$j$	$j \in \mathcal{A}$	feature index
$J$	$J \in \mathbb{N}$	number of features
$\mathbb{A}$	$\mathbb{A} = \mathbb{A}_1 \times \mathbb{A}_2 \times \dots \times \mathbb{A}_J$	feature space
$\vec{a}$	$\vec{a} \in \mathbb{A}; \vec{a} = [a_1, a_2, \dots, a_J]^T$	feature vector
$\vec{a}'$	$\vec{a}' \in \mathbb{A}; \vec{a}' = [a'_1, a'_2, \dots, a'_J]^T$	transformed feature vector
$\mathcal{A}''$	$\mathcal{A}'' \subset \mathcal{A}$	feature subset
$\mathbb{A}''$	$\mathbb{A}'' \subset \mathbb{A}$	reduced feature space
$\vec{a}''$	$\vec{a}'' \in \mathbb{A}''; \vec{a}'' = [a''_{j''}]^T; j'' \in \mathcal{A}''$	reduced transformed feature vector

**Kinematic Parameters:**

$c_i$	$c_i \in \mathbb{C}_i$	kinematic parameter
$\mathbb{C}_i$	$\mathbb{C}_i \subset \mathbb{R}$	kinematic parameter $c_i$ domain
$i$	$i \in \{1, 2, \dots, I\}$	kinematic parameter index
$I$	$I \in \mathbb{N}$	number of kinematic parameters
$\mathbb{C}$	$\mathbb{C} = \mathbb{C}_1 \times \mathbb{C}_2 \times \dots \times \mathbb{C}_N$	kinematic parameter space
$\vec{c}$	$\vec{c} \in \mathbb{C}; \vec{c} = [c_1, c_2, \dots, c_N]^T$	kinematic parameter vector
$\hat{\vec{c}}$	$\hat{\vec{c}} \in \mathbb{C}; \hat{\vec{c}} = [\hat{c}_1, \hat{c}_2, \dots, \hat{c}_N]^T$	predicted kinematic parameter vector

**Common:**

$n$	$n \in \{1, 2, \dots, N\}$	discrete time index of extracted features
$N$	$N \in \mathbb{N}$	maximal $n$
$\mathbb{M}$	$\mathbb{M} = (m_{ij}) = (\vec{m}_1 \quad \vec{m}_2 \quad \vec{m}_I)^T$	coefficient matrix
$T_1$	$T_1 \in \mathbb{R}$	one revolution of the tracking movement
$p(x)$	$p(x) \in \mathbb{R}$	probability density function

**Operators:**

$\text{corr}$	$\text{corr}(x, y) = \frac{\text{Cov}(x, y)}{\sqrt{\text{Var}(x)\text{Var}(y)}}$	Pearson's correlation
$E$	$E(x) = \int x \cdot p(x) \, dx$	expected value